UNIVERSITY OF ALBERTA

THE EFFECT OF IMMOBILE FLUID SATURATIONS ON CONVECTIVE MIXING IN A POROUS MEDIUM IN MISCIBLE DISPLACEMENT

by

ASHRAF ANWAR BEN KHAYAL

A THESIS

SUBMITTED TO THE FACULTY OF GRADUATE STUDIES AND RESEARCH IN PARTIAL FULFILLMENT OF THE REQUIREMENTS FOR THE DEGREE OF MASTER OF SCIENCE

IN

PETROLEUM ENGINEERING

DEPARTMENT OF MINING, METALURGICAL AND PETROLEUM ENGINEERING

EDMONTON, ALBERTA
FALL, 1996

National Library
of Canada

Acquisitions and
Bibliographic Services Branch

395 Wellington Street
Ottawa, Ontario
K1A 0N4

Bibliothèque nationale
du Canada

Direction des acquisitions et
des services bibliographiques

395, rue Wellington
Ottawa (Ontario)
K1A 0N4

Your file *Votre référence*

Our file *Notre référence*

The author has granted an irrevocable non-exclusive licence allowing the National Library of Canada to reproduce, loan, distribute or sell copies of his/her thesis by any means and in any form or format, making this thesis available to interested persons.

L'auteur a accordé une licence irrévocable et non exclusive permettant à la Bibliothèque nationale du Canada de reproduire, prêter, distribuer ou vendre des copies de sa thèse de quelque manière et sous quelque forme que ce soit pour mettre des exemplaires de cette thèse à la disposition des personnes intéressées.

The author retains ownership of the copyright in his/her thesis. Neither the thesis nor substantial extracts from it may be printed or otherwise reproduced without his/her permission.

L'auteur conserve la propriété du droit d'auteur qui protège sa thèse. Ni la thèse ni des extraits substantiels de celle-ci ne doivent être imprimés ou autrement reproduits sans son autorisation.

ISBN 0-612-18234-7

Canada

UNIVERSITY OF ALBERTA

LIBRARY RELEASE FORM

NAME OF AUTHOR:	Ashraf Anwar Ben Khayal
TITLE OF THESIS:	The Effect of Immobile Fluid Saturations on Convective Mixing in a Porous Medium in Miscible Displacement
DEGREE :	Master of Science
YEAR THIS DEGREE GRANTED:	1996

Permission is hereby granted to the University of Alberta Library to reproduce single copies of this thesis and to lend or sell such copies for private, scholarly, or scientific research purposes only.

The author reserves all other publication and other rights in association with the copyright in the thesis, and except as hereinbefore provided, neither the thesis nor any substantial portion thereof may be printed or otherwise reproduced in any material form whatever without the author's prior written permission.

A. Ben Khayal

Permanent Address:

P.O. Box: 83813
Tripoli, Libya
North Africa

DATED: Oct. 4, 1996

UNIVERSITY OF ALBERTA

FACULTY OF GRADUATE STUDIES AND RESEARCH

The undersigned certify that they have read, and recommend to the Faculty of Graduate Studies and Research for acceptance, a thesis entitled THE EFFECT OF IMMOBILE FLUID SATURATIONS ON CONVECTIVE MIXING IN A POROUS MEDIUM IN MISCIBLE DISPLACEMENT submitted by ASHRAF ANWAR BEN KHAYAL in partial fulfillment of the requirements for the degree of Master of Science in Petroleum Engineering.

Dr. S.M. Farouq Ali (Supervisor)

Dr. Q. Doan (Chairman & Examiner)

Dr. P. Schiavone (External Examiner)

DATED: Sept 30, 96

Abstract

Miscible flooding is a major tertiary recovery method where a solvent is injected into the reservoir to reduce the interfacial tension and the capillary forces. In this case, the solvent (displacing fluid) is mixed with oil on first contact to form a mixing zone where the interfacial tension is eliminated. Under ideal conditions, oil recovery by this method leaves behind minimal residual oil saturation.

There are so many factors affecting the mixing process, this investigation was focused mainly on the study of convective mixing in short unconsolidated porous media in the presence of an immobile phase in various configurations, consisting of irreducible water and residual oil.

Continuous miscible and miscible slug displacements were conducted in glass-bead packs employing a 160 cc/hr (3.84×10^{-3} m^3/day) flow rate. A two-component miscible displacement at a favourable mobility ratio was used to obtain the mixing coefficient through the longitudinal dispersion coefficients. The mixing coefficient was then correlated as a function of type and amount of the immobile phase saturation.

Experiments with an unfavourable mobility ratio were conducted in order to compare the mixing coefficients for favourable mobility against those at unfavourable mobility ratios.

For an oleic miscible displacement fluid system, at a favourable mobility ratio and in the presence of an immobile water phase, the mixing coefficient α was found to increase with an increase in the immobile water saturation. On the other hand, for an aqueous miscible displacement fluid system, at a favourable mobility ratio and in the presence of an immobile oil phase, the mixing coefficient α was found to decrease with an increase in the immobile oil saturation.

The results of this study should find application in the simulation of miscible and miscible-type process, such as micellar flooding.

Acknowledgements

I wish to express my sincere appreciation to my academic supervisor, Dr. S.M. Farouq Ali for suggesting this problem, his guidance, encouragement and long-term support throughout the course of this study.

Mr. Robert W. Smith deserves special thanks for designing and constructing the physical apparatus used for the experiments. I am also grateful to Mr. John Czuroski for his help in obtaining some of the materials used in this study.

My appreciation is also extended to Dr. Quang Doan for his advice and helpful discussions.

Thanks are also due to Dr. Sara Thomas for offering some needed instruments to carry out the experiments and for her continuous help.

Finally, I would like to thank my family, especially my mother and wife for their enduring patience, and full support.

Table of Contents

Chapter 1: Introduction 1

Chapter 2: Review of the Literature 3

2.1 Introduction 3

2.2 Review of Diffusion and Dispersion 4

2.2.1 Molecular Diffusion Coefficient 4

2.2.2 Longitudinal and Transverse Dispersion Coefficients 6

2.3 Factors Affecting Miscible Displacement 9

2.3.1 Effect of Flow Velocity 10

2.3.2 Effect of Pack Diameter, Path length and Model Dimension 12

2.3.3 Effect of Packing and Permeability Heterogeneities 14

2.3.4 Effect of Viscosity Ratio 15

2.3.5 Effect of Density Ratio 16

2.3.6 Effect of Particle Size Distribution and Particle Shape 17

2.3.7 Ratio of Particle Diameter to Column Diameter 18

2.3.8 Effect of an Immobile Phase 18

2.3.8.1 Effect of an Immobile Polymer Phase 19

2.3.8.2 Effect of an Immobile Gas Phase 19

2.3.8.3 Effect of an Immobile Oil Phase 20

2.3.8.4 Effect of an Immobile Water Phase 20

2.4 Miscible Slug Displacement 21

2.5 Other Related Work 22

Chapter 3: The Mathematical Models 26

3.1 Brigham Model 27

3.2 Coats and Smith Model 30

3.3 Porous-Sphere Model 32

3.4 Transverse-Matrix-Diffusion Model 33

Chapter 4: Statement of the Problem 34

Chapter 5: Experimental Fluids, Apparatus and Procedure 35

5.1 Fluids 35

5.2 Porous Medium 37

5.3 Experimental Apparatus 37

5.3.1 Injection System 39

5.3.2 Physical Model 39

5.3.3 Production System 41

5.4 Experimental Design 41

5.4.1 Core Preparation and Packing Procedure 42

5.4.2 Core Saturations 42

5.4.3 Permeability Test 43

5.5 Experimental Procedure 44

5.5.1 Continuous Miscible Displacement 44

5.5.2 Continuous Miscible Displacement in the Presence of an Immobile Saturation 45

5.5.3 The Reduction of the Immobile Saturation 45

5.5.4 Miscible Slug Runs 46

5.6 Sample Analysis 47

Chapter 6: Discussion and Analysis of Results 50

6.1 Presentation of Results 50

6.2 Miscible Displacement and Miscible Slug Runs 51

6.3 Miscible Displacement in the Presence of an Immobile Water Phase 54

6.4 Miscible Displacement in the Presence of an Immobile Oil Phase 58

6.5 Effect of an Immobile Water Phase on the Mixing Coefficient 64

6.6 Effect of an Immobile Oil Phase on the Mixing Coefficient 65

6.7 Effect of Immobile Aqueous and Oleic Phase Saturation on the Mixing Coefficient 65

6.8 Effect of Immobile Aqueous and Oleic Phase Saturation on the Mixing Coefficient in a Miscible Slug Process 66

6.9 Effect of Slug Size on the Mixing Coefficient in the Presence of Various Immobile Aqueous and Oleic Phases 67

6.10 Effect of Mobility Ratio on Miscible Displacement 68

6.10.1 Effect of an Unfavourable Mobility Ratio on the Mixing Coefficient in the Presence of an Immobile Water Phase 68

6.10.2 Effect of an Unfavourable Mobility Ratio on the Mixing Coefficient in the Presence of an Immobile Oil Phase 69

6.10.3 Effect of an Unfavourable Mobility Ratio on the Mixing Coefficient in the Presence of Various Immobile Aqueous and Oleic Phases 69

6.10.4. Effect of an Unfavourable Mobility Ratio on the Mixing Coefficient in the Presence of Various Immobile Aqueous and Oleic Phases for a Miscible Slug Process 70

6.10.5 Effect of Various Slug Sizes on the Mixing Coefficient in the Presence of Various Immobile Aqueous and Oleic Phases at Unfavourable Mobility Ratios 71

6.11 Effect of Favourable Mobility Ratio on the Mixing Coefficient in the Absence of an Immobile Phase Saturation for the Continuous and the Miscible Slug Displacement Process 71

6.12 Effect of Favourable Mobility Ratio on the Mixing Coefficient in the Presence of an Immobile Phase Saturation for the Continuous and the Miscible Slug Displacement Process 72

6.13 Effect of the Type of Mobility Ratio on the Linearity of the Probability Plot 73

6.14 Relative Role of the Type of Immobile Phase on the Mixing Coefficient 75

6.15 Relative Role of the Type of Porous Medium on the Mixing Coefficient 76

6.16 Reproducibility of Results 76

Chapter 7: Summary and Conclusions 79

7.1 Summary 79
7.2 Conclusions 80
References 82
Appendix A 88
Appendix B 94
Appendix C 147

List of Tables

Table 5-1: Fluid Properties 36

Table 5-2: Properties of the Porous Media..... 36

Table 6: Summary of the Short Unconsolidated-Core Miscible Displacement Runs..... 52

Table 6-1: Dispersion and Mixing Coefficients for the Oleic Fluid System Displacements at Zero Immobile Water Saturation in Unconsolidated Core No. 1..... 55

Table 6-2: Dispersion and Mixing Coefficients for the Aqueous Fluid System Displacements at Zero Immobile Oil Saturation in Unconsolidated Core No. 2..... 56

Table 6-3: Dispersion and Mixing Coefficients for the Oleic Fluid System Displacements at 25% Immobile Water Saturation in Unconsolidated Core No. 3..... 57

Table 6-4: Dispersion and Mixing Coefficients for the Oleic Fluid System Displacements at 10% Immobile Water Saturation in Unconsolidated Core No. 5. 59

Table 6-5: Dispersion and Mixing Coefficients for the Oleic Fluid System Displacements at Various Immobile Water Saturations..... 60

Table 6-6: Dispersion and Mixing Coefficients for the Aqueous Fluid System Displacements at 26% Immobile Oil Saturation in Unconsolidated Core No. 4..... 61

Table 6-7: Dispersion and Mixing Coefficients for the Aqueous Fluid System Displacements at 8% Immobile Oil Saturation in Unconsolidated Core No. 6..... 62

Table 6-8: Dispersion and Mixing Coefficients for the Aqueous Fluid System Displacements at Various Immobile Oil Saturations..... 63

Table 6-9: Dispersion and Mixing Coefficients for the Repeated Experimental Runs..... 77

Table 6-10: Summary of the Alpha Values Obtained for the Aqueous and the Oleic Fluid System Runs..... 74

Table C-1: Experimental Effluent Concentration Data for Run 1 148

Table C-1.1: Effluent Data for Figure B-1.1 150

Table C-2: Experimental Effluent Concentration Data for Run 2 149

Table C-2.1: Effluent Data for Figure B-2.1 150

Table C-3: Experimental Effluent Concentration Data for Run 3 151
Table C-4: Experimental Effluent Concentration Data for Run 4 152
Table C-5: Experimental Effluent Concentration Data for Run 5 153
Table C-6: Experimental Effluent Concentration Data for Run 6 154
Table C-7: Experimental Effluent Concentration Data for Run 7 155
Table C-7.1: Effluent Data for Figure B-7.1 157
Table C-8: Experimental Effluent Concentration Data for Run 8 156
Table C-8.1: Effluent Data for Figure B-8.1 157
Table C-9: Experimental Effluent Concentration Data for Run 9 158
Table C-10: Experimental Effluent Concentration Data for Run 10..... 159
Table C-11: Experimental Effluent Concentration Data for Run 11..... 160
Table C-12: Experimental Effluent Concentration Data for Run 12..... 161
Table C-13: Experimental Effluent Concentration Data for Run 13..... 162
Table C-13.1: Effluent Data for Figure B-13.1..... 164
Table C-13R: Effluent Data for Figure B-13R 163
Table C-13R.1: Effluent Data for Figure B-13R.1..... 164
Table C-14: Experimental Effluent Concentration Data for Run 14..... 165
Table C-14.1: Effluent Data for Figure B-14.1..... 166
Table C-15: Experimental Effluent Concentration Data for Run 15..... 167
Table C-16: Experimental Effluent Concentration Data for Run 16..... 168
Table C-17: Experimental Effluent Concentration Data for Run 17..... 169
Table C-18: Experimental Effluent Concentration Data for Run 18..... 170
Table C-19: Experimental Effluent Concentration Data for Run 19..... 171
Table C-19.1: Effluent Data for Figure B-19.1..... 173
Table C-20: Experimental Effluent Concentration Data for Run 20..... 172
Table C-20.1: Effluent Data for Figure B-20.1..... 173

Table C-21: Experimental Effluent Concentration Data for Run 21 174
Table C-21R: Experimental Effluent Concentration Data for Run 21R 175
Table C-22: Experimental Effluent Concentration Data for Run 22 176
Table C-23: Experimental Effluent Concentration Data for Run 23 177
Table C-24: Experimental Effluent Concentration Data for Run 24 178
Table C-25: Experimental Effluent Concentration Data for Run 25 179
Table C-25.1: Effluent Data for Figure B-25.1 181
Table C-26: Experimental Effluent Concentration Data for Run 26 180
Table C-26.1: Effluent Data for Figure B-26.1 181
Table C-27: Experimental Effluent Concentration Data for Run 27 182
Table C-28: Experimental Effluent Concentration Data for Run 28 183
Table C-29: Experimental Effluent Concentration Data for Run 29 184
Table C-30: Experimental Effluent Concentration Data for Run 30 185
Table C-31: Experimental Effluent Concentration Data for Run 31 186
Table C-31.1: Effluent Data for Figure B-31.1 188
Table C-32: Experimental Effluent Concentration Data for Run 32 187
Table C-32.1: Effluent Data for Figure B-32.1 188
Table C-33: Experimental Effluent Concentration Data for Run 33 189
Table C-34: Experimental Effluent Concentration Data for Run 34 190
Table C-35: Experimental Effluent Concentration Data for Run 35 191
Table C-36: Experimental Effluent Concentration Data for Run 36 192
Table C-36R: Experimental Effluent Concentration Data for Run 36R 193

List of Figures

Figure 2-1: Convective Dispersion in Porous Media 7

Figure 2-2: Mixing by Longitudinal and Transverse Dispersion in a Porous Medium 7

Figure 5-1: Schematic Diagram of the Miscible Flood Apparatus..... 38

Figure 5-2: Cross-Sectional View of the Physical Core Holder 40

Figure 5-6.1: Standard Concentration Curve - Refractive Index Versus % Cyclohexane. 48

Figure 5-6.2: Standard Concentration Curve - Refractive Index Versus % 10% Brine 49

Figure B-1: Run 1: Concentration Profile of Cyclohexane Displacing N-hexane in the Presence of Zero Immobile Water Saturation. 95

Figure B-1.1: Effluent Concentration Plotted on Arithmetic Probability Paper for Run 1..... 96

Figure B-2: Run 2: Concentration Profile of N-hexane Displacing Cyclohexane in the Presence of Zero Immobile Water Saturation 97

Figure B-2.1: Effluent Concentration Plotted on Arithmetic Probability Paper for Run 2..... 98

Figure B-3: Run 3: Concentration Profile of N-hexane Displacing a 20% P.V. Slug of Cyclohexane in the Presence of Zero Immobile Water Saturation 99

Figure B-4: Run 4: Concentration Profile of N-hexane Displacing a 30% P.V. Slug of Cyclohexane in the Presence of Zero Immobile Water Saturation 100

Figure B-5: Run 5: Concentration Profile of Cyclohexane Displacing a 20% P.V. Slug of N-hexane in the Presence of Zero Immobile Water Saturation 101

Figure B-6: Run 6: Concentration Profile of Cyclohexane Displacing a 30% P.V. Slug of N-hexane in the Presence of Zero Immobile Water Saturation 102

Figure B-7: Run 7: Concentration Profile of 10% Brine Displacing 2% Brine in the Presence of Zero Immobile Oil Saturation..... 103

Figure B-7.1: Effluent Concentration Plotted on Arithmetic Probability Paper for Run 7..... 104

Figure B-8: Run 8: Concentration Profile of 2% Brine Displacing 10% Brine in the Presence of Zero Immobile Oil Saturation 105

Figure B-8.1: Effluent Concentration Plotted on Arithmetic Probability Paper for Run 8 106

Figure B-9: Run 9: Concentration Profile of 2% Brine Displacing a 20% P.V. Slug of 10% Brine in the Presence of Zero Immobile Oil Saturation 107

Figure B-10: Run 10: Concentration Profile of 2% Brine Displacing a 30% P.V. Slug of 10% Brine in the Presence of Zero Immobile Oil Saturation 108

Figure B-11: Run 11: Concentration Profile of 10% Brine Displacing a 20% P.V. Slug of 2% Brine in the Presence of Zero Immobile Oil Saturation 109

Figure B-12: Run 12: Concentration Profile of 10% Brine Displacing a 30% P.V. Slug of 2% Brine in the Presence of Zero Immobile Oil Saturation 110

Figure B-13: Run 13: Concentration Profile of Cyclohexane Displacing N-hexane in the Presence of 25% Immobile Water Saturation. 111

Figure B-13.1: Effluent Concentration Plotted on Arithmetic Probability Paper for Run 13 112

Figure B-13R: Repeat of Run 13: Concentration Profile of Cyclohexane Displacing N-hexane in the Presence of 25% Immobile Water Saturation 113

Figure B-13R.1: Effluent Concentration Plotted on Arithmetic Probability Paper for Run 13R 114

Figure B-14: Run 14: Concentration Profile of N-hexane Displacing Cyclohexane in the Presence of 25% Immobile Water Saturation. 115

Figure B-14.1: Effluent Concentration Plotted on Arithmetic Probability Paper for Run 14. 116

Figure B-15: Run 15: Concentration Profile of N-hexane Displacing a 20% P.V. Slug of Cyclohexane in the Presence of 25% Immobile Water Saturation 117

Figure B-16: Run 16: Concentration Profile of N-hexane Displacing a 30% P.V. Slug of Cyclohexane in the Presence of 25% Immobile Water Saturation 118

Figure B-17: Run 17: Concentration Profile of Cyclohexane Displacing a 20% P.V. Slug of N-hexane in the Presence of 25% Immobile Water Saturation 119

Figure B-18: Run 18: Concentration Profile of Cyclohexane Displacing a 30% P.V. Slug of N-hexane in the Presence of 25% Immobile Water Saturation 120

Figure B-19: Run 19: Concentration Profile of 10% Brine Displacing 2% Brine in the Presence of 26% Immobile Oil Saturation..... 121

Figure B-19.1: Effluent Concentration Plotted on Arithmetic Probability Paper for Run 19 122

Figure B-20: Run 20: Concentration Profile of 2% Brine Displacing 10% Brine in the Presence of 26% Immobile Oil Saturation..... 123

Figure B-20.1: Effluent Concentration Plotted on Arithmetic Probability Paper for Run 20 124

Figure B-21: Run 21: Concentration Profile of 2% Brine Displacing a 20% P.V. Slug of 10% Brine in the Presence of 26% Immobile Oil Saturation 125

Figure B-21R: Repeat of Run 21: Concentration Profile of 2% Brine Displacing a 20% P.V. Slug of 10% Brine in the Presence of 26% Immobile Oil Saturation 126

Figure B-22: Run 22: Concentration Profile of 2% Brine Displacing a 30% P.V. Slug of 10% Brine in the Presence of 26% Immobile Oil Saturation 127

Figure B-23: Run 23: Concentration Profile of 10% Brine Displacing a 20% P.V. Slug of 2% Brine in the Presence of 26% Immobile Oil Saturation 128

Figure B-24: Run 24: Concentration Profile of 10% Brine Displacing a 30% P.V. Slug of 2% Brine in the Presence of 26% Immobile Oil Saturation 129

Figure B-25: Run 25: Concentration Profile of Cyclohexane Displacing N-hexane in the Presence of 10% Immobile Water Saturation. 130

Figure B-25.1: Effluent Concentration Plotted on Arithmetic Probability Paper for Run 25 131

Figure B-26: Run 26: Concentration Profile of N-hexane Displacing Cyclohexane in the Presence of 10% Immobile Water Saturation. 132

Figure B-26.1: Effluent Concentration Plotted on Arithmetic Probability Paper for Run 26 133

Figure B-27: Run 27: Concentration Profile of N-hexane Displacing a 20% P.V. Slug of Cyclohexane in the Presence of 10% Immobile Water Saturation 134

Figure B-28: Run 28: Concentration Profile of N-hexane Displacing a 30% P.V. Slug of Cyclohexane in the Presence of 10% Immobile Water Saturation 135

Figure B-29: Run 29: Concentration Profile of Cyclohexane Displacing a 20% P.V. Slug of N-hexane in the Presence of 10% Immobile Water Saturation. 136

Figure B-30: Run 30: Concentration Profile of Cyclohexane Displacing a 30% P.V. Slug of N-hexane in the Presence of 10% Immobile Water Saturation. 137

Figure B-31: Run 31: Concentration Profile of 10% Brine Displacing 2% Brine in the Presence of 8% Immobile Oil Saturation 138

Figure B-31.1: Effluent Concentration Plotted on Arithmetic Probability Paper for Run 31 139

Figure B-32: Run 32: Concentration Profile of 2% Brine Displacing 10% Brine in the Presence of 8% Immobile Oil Saturation 140

Figure B-32.1: Effluent Concentration Plotted on Arithmetic Probability Paper for Run 32. 141

Figure B-33: Run 33: Concentration Profile of 2% Brine Displacing a 20% P.V. Slug of 10% Brine in the Presence of 8% Immobile Oil Saturation 142

Figure B-34: Run 34: Concentration Profile of 2% Brine Displacing a 30% P.V. Slug of 10% Brine in the Presence of 8% Immobile Oil Saturation 143

Figure B-35: Run 35: Concentration Profile of 10% Brine Displacing a 20% P.V. Slug of 2% Brine in the Presence of 8% Immobile Oil Saturation 144

Figure B-36: Run 36: Concentration Profile of 2% Brine Displacing a 30% P.V. Slug of 10% Brine in the Presence of 8% Immobile Oil Saturation 145

Figure B-36R: Repeat of Run 36: Concentration Profile of 2% Brine Displacing a 30% P.V. Slug of 10% Brine in the Presence of 8% Immobile Oil Saturation 146

Nomenclature

a	Rate group, $m l / \vartheta$, dimensionless
a_e	Effective mixing coefficient, K/ϑ , cm
A	Cross sectional area for diffusion, cm^2
C	Concentration, volume fraction
C_o	Initial concentration of the slug, cc/cc
C_{max}	Maximum concentration of the slug, cc/cc
C^*	Concentration in stagnant fluid, volume fraction
d_p	Average particle diameter, cm
D_o	Molecular diffusion coefficient, cm^2/sec
erf	Error function
E	Longitudinal dispersion coefficient, cm^2/sec
f	Fraction of pore space occupied by mobile fluid, dimensionless
F	Formation electrical resistivity factor, dimensionless
g	Acceleration due to gravity, cm/sec^2
I	Pore volumes injected, dimensionless
k	Absolute permeability, m^2 or darcy
k_{avg}	Absolute average permeability, m^2 or darcy
k_r	Relative permeability, dimensionless
K	Dispersion coefficient, cm^2/sec
K_e	Effective dispersion coefficient, cm^2/sec
K_l	Total coefficient of longitudinal dispersion, cm^2/sec
K_t	Total coefficient of transverse dispersion, cm^2/sec
l	Core length, cm
L	Length of undiluted slug, cm

m	Rate constant, sec^{-1}
M	Mobility ratio, dimensionless
P_e	Peclet number, dimensionless
q	Flow rate, m^3/day or cc/hr
Q	Quantity of material diffusing across a plane, cm^3
Q_c, $Q_{st.}$	Critical and stable flow rates, respectively, cc/sec
$\bar{r}$	Average radius of sand grains or glass beads, cm
t	time, sec
v_c, $v_{st.}$	Critical and stable velocities, respectively, cm/sec
V_i	Injected volume, cc
V_p	Pore volume, cc
VR	Viscosity ratio, dimensionless
x	Distance, cm
X_{90}, X_{10}	Distance from the initial interface where the composition is 90% and 10%, respectively, of the fluid under consideration, cm
y	Dimensionless distance

Subscript:

ed	Displaced
ing	Displacing

Greek Symbol:

α	Mixing coefficient, cm
β	Empirical constant determined by trial and error, dimensionless
ϑ	Average Darcy velocity, cm/sec
σ	Inhomogeneity factor, dimensionless
ϕ	Porosity, dimensionless

μ	Viscosity, cp
μ_O, μ_S	Oil and solvent viscosities, respectively, gm/cm.sec or cp
λ	Volume modifying function (lambda), dimensionless
$\lambda_{90}, \lambda_{10}$	Values of modified volume function at effluent concentrations of 90% and 10%, respectively, dimensionless
γ	Dimensionless dispersion
ρ_o, ρ_s	Oil and solvent densities, respectively, gm/cc

1. Introduction

Miscible displacement has been the subject of intensive investigations since the early 1950s due to its great potential for oil recovery from depleted reservoirs. It has special significance among the several tertiary recovery techniques, since it enables the recovery of a considerable quantity of oil still remaining within the reservoir after it has been subjected to natural depletion and secondary recovery.

Conventional primary and secondary oil-recovery techniques usually recover less than 50% of the oil initially present in the reservoir. Because of the interface between gas and oil and between water and oil, the oil is not completely displaced from the formation. Miscible displacement is a process which is capable of recovering almost 100% of the oil present in the reservoir.

There are two types of miscible displacement:

- " First-contact miscible " where the displacing fluid mixes directly with the displaced fluid at first contact,
- " Multiple contact " where miscibility between the two fluids is obtained by repeated contacts and mixing.

In this investigation, I will be dealing with "first-contact miscible displacement".

It is known that two fluids are considered to be miscible when they mix in all proportions and there is no interface between them (i.e. when the mixture of the miscible fluids becomes and remains as a single phase). The objective of miscible displacement, therefore, is to reduce the residual oil saturation to its lowest possible value by eliminating the interfacial tension and capillary forces between the oil and the displacing fluid (solvent), and hence permit the recovery of a sizable proportion of the residual oil.

The economic factor, however, does not permit injection of a large quantity of a solvent; and it has not been as widely applicable as waterflooding because of the higher expenditure involved in using chemicals, such as micellar/polymer or light crudes, as displacing fluids, and because of the lack of certainty in displacement efficiency due to an incomplete understanding of the viscous fingering process.

The miscible slug process however, is a partial answer to this problem. In this process, a small quantity of a miscible solvent is injected and then followed by a bank of a less expensive fluid. This process is continued until the slug is dispersed.

Numerous theoretical and supporting laboratory studies lead to the conclusion that the low efficiency of miscible displacement in enhanced oil recovery processes is mainly because of mixing effects. This investigation focuses mainly on the mixing characteristics of miscible fluids in short unconsolidated porous media in the presence of an immobile phase at favourable and unfavourable mobility ratios.

The variation of mixing with the amount of immobile saturation as well as the various configurations, (i.e. immobile oil and water) were investigated. This investigation also accounts for the effect of miscible slug displacement on mixing characteristics in a porous medium.

The "Mixing Coefficient", which is the subject of this investigation, determines the dissipation of a slug of miscible or "almost" miscible material (as in the case of micellar flooding) in a variety of tertiary oil recovery processes.

It is hoped that an understanding of the mixing coefficient, in the presence of various types of immobile saturations, at favourable and unfavourable mobility ratios, would lead to more reliable slug-size selection.

2. Review of the Literature

2.1 Introduction

Enhanced oil recovery methods were developed in an attempt to increase recovery by minimizing or eliminating the effects of interfacial tension and capillary forces. A displacing fluid which is completely miscible with the resident oil under reservoir conditions is injected into the formation. The choice of the solvent used is dictated by economical and operational considerations.

The efficiency of the miscible flooding process depends on two main groups of factors:

1) Flood Instabilities: an unstable miscible front is detrimental to the efficiency of the displacement process. When the displacement front is stable, laboratory miscible displacement experiments may then be interpreted in terms of one-parameter convection-dispersion equation. Factors important to the attainment of a stable front include:

a) The velocity of the front (or the displacement rate).

b) The production rate of fluids from the wellbore.

c) The effect of geological heterogeneities within the porous media.

2) Fluid Mixing: the mixing process is governed by three main mechanisms:

a) molecular diffusion: where the two fluids are immobile and diffuse into each other as a result of the thermal motion of molecules.

b) microscopic convective dispersion: where mixing is due to the movement of the fluid in the pores without channelling. Two types of dispersion may take place in a porous medium; one is longitudinal, which is in the direction of fluid movement, and is described by the longitudinal dispersion coefficient (K_l), and the other is transverse, which is perpendicular to the direction of fluid flow, and it is described by the transverse dispersion coefficient (K_t).

c) macroscopic convective dispersion: where mixing is due to the channelling of the displacing fluid through the porous media, and it results in bypassing the resident fluid in large regions of the medium and can result from:

i) permeability stratification (if the degree of heterogeneity is large).

ii) segregation of fluids by gravity (due to fluids density differences).

iii) viscous fingering (due to an adverse mobility ratio).

2.2 Review of Diffusion and Dispersion

Mixing of two miscible fluids in a porous medium is influenced by diffusion and dispersion phenomena. Molecular diffusion and convective dispersion phenomena are known to have a strong influence, not only on the mixing of solvent with oil in miscible displacements, but also on the efficiency of the displacements.

When two miscible fluids are in contact, they will slowly diffuse into each other due to a concentration gradient and random motion of the molecules of the two fluids (it is well known that molecular diffusion is the dominant mixing process at reservoir conditions of rate, length and pore size), the initially sharp interface between the two fluids will become a transition zone, as time advances, while the concentration changes between the two boundaries from one pure fluid to the other.

When a miscible displacement is conducted in a porous medium, in addition to mixing due to molecular diffusion, considerable additional mixing of the two fluids is caused by microscopic convective dispersion and macroscopic convective dispersion. Because of this mixing, a transition zone, composed of a mixture of solvent and oil, separates 100% solvent from 100% oil.

2.2.1 Molecular Diffusion Coefficient

Mixing caused by molecular diffusion in a porous medium is often represented by the well-known Fick's[1, 14] diffusion equation.

$$\frac{dQ}{dt} = -D_O A \varnothing \frac{\partial C}{\partial x} \qquad (1)$$

where:

Q = the quantity of material diffusing across a plane, (cm^3)

D_o = the molecular diffusion coefficient, (cm^2/sec)

C = concentration, volume fraction

Ø = porosity, fraction

A= cross sectional area for diffusion, (cm^2)

t = time, (sec)

x = distance, (cm)

In the above equation, the molecular diffusion coefficient may be a function of the concentration. It is difficult to solve Equation (1) mathematically especially with a variable molecular diffusion coefficient. An "effective average molecular diffusion coefficient" was introduced by Taylor[2] which is constant and independent of concentration to solve Equation (1). As D_o is now constant, Equation (1) can be integrated to give the fluid concentration as a function of time and distance for a system of miscible fluids mixing by molecular diffusion:

$$C = \frac{1}{2}\left\{1 \pm erf\left(\frac{x}{2\sqrt{D_o t}}\right)\right\} \qquad (2)$$

where:

C = the concentration of the fluid under consideration, (volume fraction)

x = distance measured from the original position of the interface, (cm)

erf = error function

The minus or plus sign of Equation 2 depends on the boundary conditions:

If @ t=0, C=1 for x< 0 and C=0 for x> 0 then use a minus sign.
If @ t=0, C=0 for x< 0 and C=1 for x> 0 then use a plus sign.

$$D_o = \frac{1}{t}\left[\frac{X_{90} - X_{10}}{3.625}\right]^2 \qquad (3)$$

Where:

X_{90}, X_{10} = The distance from the initial interface where the composition is 90% and 10%, respectively, of the fluid under consideration.

With little information available on the molecular diffusion coefficients of reservoir fluids, van der Poel[3] suggested that the molecular diffusion coefficients have the same order of magnitude (10^{-5} cm^2/sec) in both water-glycerine systems and reservoir fluid mixtures.

In the oil industry, the apparent molecular diffusion coefficient in a porous medium must be adjusted to account for the tortuous path for diffusion in the pores of the rock. Many investigators[3, 5, 11] have recognized that there is an analogy between apparent diffusion and electrical conductivity in porous media.

2.2.2 Longitudinal and Transverse Dispersion Coefficients

When fluids flow through a porous medium, more mixing takes place in the direction of the flow and perpendicular to the fluid flow direction than would be expected from molecular diffusion alone. There are two types of dispersion to be considered: longitudinal dispersion and transverse dispersion. Each type of dispersion has two components: one due to diffusion and another due to mechanical mixing.

Considerable effort has been directed to the study of dispersion phenomena in flow through porous media. Brigham et al[5] noticed that mixing zone length increases at very low and very high flow rates, and that the mixing-zone length achieves a minimum value at a particular growth rate. At this velocity, diffusion contributes only a small fraction of the total dispersion coefficient.

In 1954, Morse[6] observed that the length of the mixing zone is dependent on some variables such as rate of displacement, distance traveled, and viscosity ratio of the fluids. In 1965, Kyle and Perrine[7] conducted a series of experiments to measure the growth rate of the mixing zone as a function of the viscosity ratio and average fluid velocity. The experimental results showed that, in the range of flow rates used, mixing zone expansion depended on the amount of solvent injected, and not the displacing rate, for a given viscosity ratio of fluids used.

Perkins and Johnston[8], and Coats and Smith[9] have indicated that both convective dispersion and channeling play a major role in the mixing processes at both the laboratory and field scales. Variations in the interstitial velocity field at microscopic

scales result in a combination of streamlines having markedly different solvent concentrations (Figure 2-1).

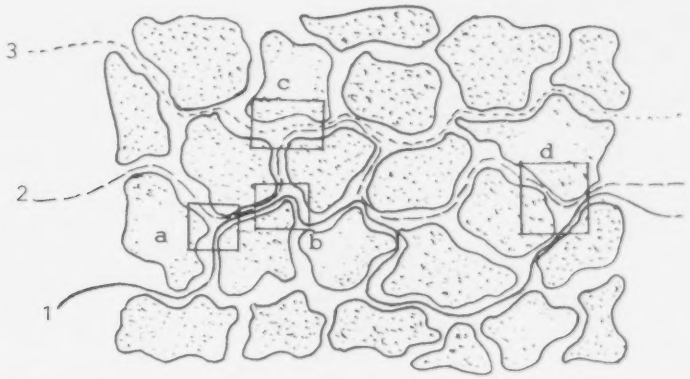

Figure 2-1: Convective Dispersion in Porous Media
(from Stalkup, 1983)

The above figure illustrates the mixing of streamlines 1 and 2 in pore A. The equalized solvent concentration then proceeds to pore C where mixing with streamline 3 takes place. Mixing in the direction of flow is called "longitudinal dispersion", and mixing orthogonal to the direction of flow is called "transverse dispersion" (Figure 2-2).

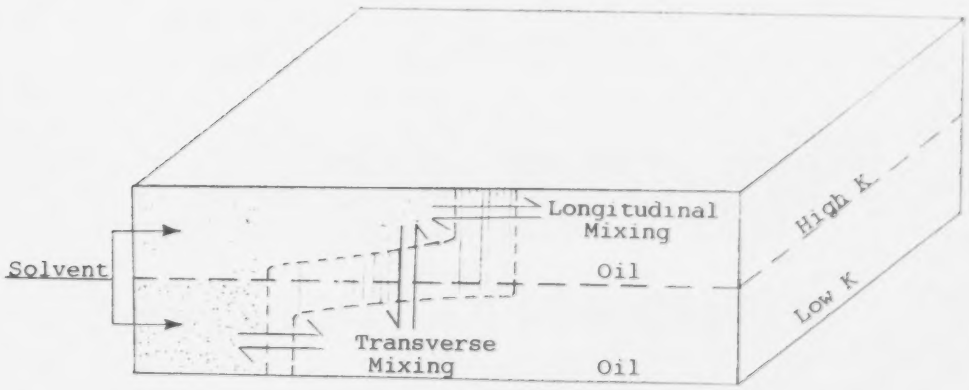

Figure 2-2: Mixing by Longitudinal and Transverse Dispersion in a Porous Medium.
(from Stalkup, 1983)

The mixing of fluids due to microscopic convective dispersion is normally described by a combination of the longitudinal dispersion coefficient (K_l) and the

transverse dispersion coefficient (K_t). For fluid flow at a constant velocity in the x-direction , the overall transport and mixing of fluids can be described by the following diffusion-convection equation:

$$K_l \frac{\partial^2 C}{\partial x^2} + K_t \frac{\partial^2 C}{\partial y^2} + K_t \frac{\partial^2 C}{\partial z^2} - \vartheta \frac{\partial C}{\partial x} = \frac{\partial C}{\partial t} \qquad (4)$$

where:

$K_l = D_o + E$, the total coefficient of longitudinal dispersion, (cm^2/sec)

D_o = molecular diffusion coefficient, (cm^2/sec)

E = longitudinal dispersion coefficient, (cm^2/sec)

and

K_t = the total coefficient of transverse dispersion, (cm^2/sec)

The first term in Equation (4) takes care of the longitudinal dispersion in the x-direction and the second and third terms account for the transverse dispersion in the y and z directions.

Raimondi and Gardener[10] proposed an empirical equation for longitudinal dispersion coefficient. This equation is based on miscible floods using fluids of equal density and viscosity:

$$K_l = D_o \left\{ \frac{1}{F\phi} + 0.50 \frac{\vartheta o d_p}{D_o} \right\} \quad , \qquad P_e<50 \qquad (5)$$

Carman[12] has shown that in a porous medium, fluids move on the average at about 45^0 to the net direction of flow. Thus, there is a perpendicular component of the velocity vector at any point, which results in mixing transverse to the direction of fluid flow. Transverse dispersion plays an important role in miscible displacement at an unfavourable viscosity ratio because, depending on the rate, it controls the longitudinal growth of the viscous fingers.

Blackwell[13] stated that the effects of pore-size distribution and inhomogeneities are almost the same on longitudinal and transverse dispersion. However, the coefficient of transverse dispersion is reported by several investigators to be considerably different from longitudinal dispersion coefficient.

Based upon a review of published data, Perkins and Johnston[8] showed that the transverse dispersion coefficient can be calculated empirically for a miscible flood system of fluids with same density and viscosity:

$$K_t = D_o\left\{\frac{1}{F\phi} + 0.0157\frac{\vartheta\sigma dp}{D_o}\right\}, \qquad P_e<10^4 \qquad (6)$$

where:

ϑ = average Darcy velocity, (cm/sec)

σ = the inhomogeneity factor

dp = average particle diameter, (cm)

P_e= Peclet number, $\frac{\vartheta\sigma dp}{D_o}$, dimensionless

Channeling of solvent through the conduits of increased or decreased permeability is not addressed explicitly in the formulation of Equations (5) and (6) but is implicitly included in most calculation methods used for determining K_l and K_t.

An examination of Equations (5) and (6) suggests that at low fluid velocities the molecular diffusion term will tend to dominate and $K_l \approx K_t$.

Under stable displacement conditions, in the absence of gravity effects K_l will tend to dominate the mixing process with increasing fluid velocity. An examination of the dispersion terms of Equations (5) and (6) indicates that K_l will increase at a rate approximately 30 times that of K_t under these conditions[15].

2.3 Factors Affecting Miscible Displacement

Several factors may affect the recovery efficiency of a miscible displacement process. Laboratory experiments have shown that the longitudinal and transverse dispersion coefficients magnitude are affected by[8]: the displacement rate (or flow velocity), the geometry of the model (such as: pack diameter, length, dimension and shape), porous medium type (such as: packing and permeability heterogeneities),

gravity forces, viscosity ratios, particle size distribution, particle shape, ratio of particle diameter to column diameter, and any immobile fluid saturation.

Because of the very large number of papers in the literature, only major works are reviewed; the effects of these factors are summarized in the following sections.

2.3.1 Effect of Flow Velocity

At non-flow conditions, the only case of mixing should be ordinary molecular (Fick) diffusion, and the dispersion coefficient K_l will be constant. Brigham[5] showed that the dispersion coefficient and the molecular diffusion are related by the following equation:

$$\frac{K_l}{D_o} = \frac{1}{F\phi} \tag{7}$$

where,

F = formation resistivity factor, dimensionless

ϕ = porosity, fraction

D_o = molecular diffusion coefficient, (cm^2/sec)

At high rates of flow, the dispersion coefficient is characterized by the following relation for sandstones and glass bead packs[5]:

$$\frac{K_l}{D_o} = \alpha\left(\frac{\bar{r}\vartheta}{D_o}\right)^{1.2} \tag{8}$$

where,

α = mixing coefficient, (cm)

$\bar{r}$ = average radius of sand grains or glass beads, (cm)

ϑ = average pore velocity, (cm/sec)

The exponent 1.2 is only valid for bead packs and sandstones, while the value of this exponent can be between 1 and 2 for various kinds of pore structures.

The fluid velocity affects the length of the mixing zone. The mixing zone length was found to increase at very low flow rates, as well as at very high flow rates, and there is a velocity at which the mixing zone length was a minimum. However, Hall et al.[28] found that displacement rate does not affect the length of the mixing zone after the mixing zone stabilizes at the initial rate.

It was found that (at reservoir rates in natural reservoir materials) the rate of mixing (as measured by the dispersion coefficient) was considerably higher than that in glass bead packs. The higher mixing rate is caused by the inhomogeneity of reservoir rock as compared to glass beads, and the amount of inhomogeneity is expressed in terms of the mixing coefficient α.

Equation (7) for low rates can be combined with Equation (8) for high rates to give a single equation expressing the dispersion coefficient as a function of velocity and lithology:

$$\frac{K_l}{D_o} = \frac{1}{F\phi} + \alpha\left(\frac{\bar{r}\vartheta}{D_o}\right)^{1.2} \tag{9}$$

Raimondi, Gardner, and Petrick[10] introduced the mixing coefficient α, as:

$$\alpha = \sigma^2 dp \tag{10}$$

where σ^2 is a dimensionless constant determined by velocity distribution in the direction of the flow. Therefore, α is dependent on core lithology and is independent of the fluid properties.

Using equations (5) and (10), Raimondi et al.[10] suggested the following relationship between the longitudinal dispersion coefficient K_l and the mixing coefficient α :

$$K_l = D_o + \alpha\vartheta \tag{11}$$

At high flow rates, parameter D_o is usually neglected.

At moderate flow rates, the porous medium will create a slightly asymmetrical mixed zone (trailing edge stretched out) with the convective dispersion coefficient

approximately proportional to the first power of average fluid velocity (if composition is equalized in pore spaces by diffusion)[8].

Turbulent flow conditions are not likely to be encountered in a petroleum reservoir, but may be encountered in laboratory experiments. Carman[16] has suggested that turbulent eddies develop at selected spots throughout the medium. Actually the amount of turbulence at a given Reynolds number is influenced by particle shape and packing. Longitudinal and transverse dispersion coefficients will be different as in the case of laminar flow.

In the turbulent region, most investigators have reported dispersion coefficients in terms of the "Peclet number". This dimensionless group is defined by the following equation:

$$P_e = \frac{d_p v}{K} \tag{12}$$

where, K= dispersion coefficient

2.3.2 Effect of Pack Diameter, Path Length and Model Dimension

Brigham et al.[5] had found that greater (longer) mixing is achieved in packings with smaller diameters. However, they emphasized on using caution when viewing data acquired from small-diameter packs (less than approximately 3 cm in diameter). Their explanation of this fact is that boundary effects arise when smaller models are considered, or that it is more difficult to achieve uniform packing in a small tubing.

However, Lacey et al.[21] made an opposite observation: that an increase in core diameter causes a drastic increase in the length of the mixing zone, which they explained by postulating an increased variation in permeability for larger diameter cores. As a consequence, they concluded that the transverse dispersion process may stabilize laboratory displacements because disturbances are limited to short "wave lengths", but that they may not stabilize field floods because of the larger cross section of reservoirs.

Farouq Ali and Stahl[17] investigated the effect of core length and diameter on the efficiency of miscible displacement. They showed that an increase in both length and diameter will decrease the effect of viscous fingers as well as the length of the mixing zone, hence, improve the efficiency of displacement.

It is known that the length of the transition zone is inversely proportional to the square root of the length of porous medium[5]. The question arises whether a shorter slug size is needed for sweeping out oil from a longer reservoir. Holm and Csaszar[18] found that the slug size required decreased with increased path length, while Meyer et al.[19] had the opposite findings. Farouq Ali and Stahl's investigations verified Holm and Csaszar's results.

Blackwell et al.[20] studied the effect of model dimensions. They found that recovery depended on the geometry of the model. They presented similar observations as those of Lacey et al., in which they found that breakthrough recovery decreases with decreasing length-to width ratio of the model.

Offeringa et al.[22] noted deviations in the results of miscible displacements using short cores as compared to those using long cores. In the tests reported, results with tubes of 1.60 and 3.0 m in length were in good agreement, whereas those with a 1.03 m tube showed appreciable deviations. The reason for the difference, as they suggested, may possibly be that the diameter of the short tube (6.4 cm) was too small as compared to the grain size of the sand (0.07 cm).

Coskuner and Bentsen[24] extended the small perturbation theory of Chuoke[23] which enables one to describe the effect of length theoretically. The variational analysis from the theory indicated that fingers were more readily formed in a longer system than in a shorter one under similar flow conditions, provided that the transverse dimensions are the same in both systems. They suggested that it is due to the fact that perturbations in the flow direction have wavelengths longer than the length of the porous medium and, therefore, the instability could not manifest itself. As a consequence, the system behaved as if it was stable. However, in a longer porous medium, these perturbations would be felt causing the displacement to be unstable.

2.3.3 Effect of Packing and Permeability Heterogeneities

The effect of packing heterogeneities in "random packs" has been described by several investigators[5, 8, 13].

Blackwell[13] reported that the increase in dispersion coefficient with decreasing sand sizes for sands smaller than 20-30 mesh was noted by van Deemter et al.[25] for longitudinal dispersion. Van Deemter et al. attributed this increase to bridging by the particles and other microscopic packing irregularities which occur more frequently as the sand size decreases or the particle shape becomes more irregular. Ebach[26] found that for 30 mesh or larger particle sizes the longitudinal dispersion coefficients were independent of size.

Dispersion in outcrop rocks has been studied by several investigators. They all found that dispersion was larger than one might have suspected from particle size alone (thus reflecting the increased heterogeneities). Brigham[5] reported that in natural sandstones at reservoir rates, the rate of dispersion was considerably higher than that found in glass bead packs, because natural sandstone was more heterogeneous.

Groboske and Farouq Ali[27] verified Brigham's results. They found that the mixing coefficients calculated for the unconsolidated porous media were substantially lower than those for sandstone cores.

Blackwell[13] found that channeling and bypassing of oil will occur in horizontal reservoirs, even in homogeneous sand. He also concluded that permeability stratification decreased the recovery below that for a homogeneous sand.

Stalkup[1] showed that fingering of miscible solvent into reservoir fluid caused severe reduction to the volumetric sweep efficiency. Furthermore, this phenomenon was investigated by Hewett and Behrens[44] as the heterogeneity of the reservoir was taken into account.

Warren et al.[4] concluded that macroscopic dispersion resulting solely from variations in the permeability of the porous medium were related to the scale of the heterogeneity as well as the distribution function of the permeabilities. They indicated that the macroscopic dispersions determined from laboratory experiments performed on

conventional oil-field cores does not yield a valid measure for reservoir engineering purposes since the scale of heterogeneity for both field and laboratory is incomparable.

Arya et al.[42] examined the interrelationship between the heterogeneity and diffusion. They concluded that dispersivity increased with increasing heterogeneity.

Coats and Smith[9] proposed a capacitance model. It included dispersion and convection in a flowing region of the core and mass transfer between flowing and stagnant regions. By adjusting the parameters included in the model, it was used successfully to match the skewed effluent histories of miscible displacements conducted in homogeneous consolidated cores[9, 29, 30].

Much effort has been also made to develop mathematical models to describe miscible displacements adequately by several other investigators: Houseworth[31], Koval[32] , Dougherty[33], Perrine[34], Deans[35], Nguyen et al.[36], Fayers[37], Vossoughi et al.[38], Udey et al.[39, 40] and Oguztoreli et al.[74].

Walsh and Withjack[41] suggested that Fickian dispersion theory was not valid for miscible displacement in Berea sandstone. The main reason was that the Berea mixing zone growth did not grow proportional to the square root of time as required by Fickian theory; rather, it grew more nearly proportional to time. They argued that the non-Fickian flow behavior can be attributed to very small, yet significant, spatial variations in permeability.

2.3.4 Effect of Viscosity Ratio

Viscosity ratio is defined as the ratio of the viscosity of the displaced fluid to the viscosity of the displacing fluid (i.e., μ_{ed} / μ_{ing}). In miscible displacement the permeability to the displacing fluid is equal to that of displaced fluid. Then, a viscosity ratio less than unity corresponds to the mobility ratio M.

$$M = \frac{\left(k_r / \mu\right)_{ing}}{\left(k_r / \mu\right)_{ed}} \qquad (13)$$

Equation (13) will reduce to the following relationship for miscible displacement:

$$M = VR = \mu_{ed} / \mu_{ing} \qquad (14)$$

For an unfavourable viscosity ratio (i.e., the displacing fluid is less viscous than the displaced fluid), viscous fingers will form. The behaviour of viscous fingers has been the subject of many investigations, and at present a satisfactory theory does not exist.

Various investigators have noted that the dispersion coefficient decreases as the mobility ratio of the miscible fluids becomes more favourable. However, there is a limit to this beneficial effect as the viscosity ratio becomes very favourable, more detailed explanation about this effect is contained in Cashdollar's[43] work.

Perkins and Johnston[8] suggested that a favourable mobility ratio would tend to suppress the effects of packing or permeability heterogeneities. Lacey et al.[21] found that the length of the mixing zone increased as the oil viscosity increases.

Brigham et al.[5] reported that the value of the dispersion coefficient and the rate of dispersion increased with an increase in mobility ratio, and that with an unfavourable mobility ratio, viscous fingering usually occurred and the theoretical error function curve was no longer valid.

Blackwell et al.[20] presented an investigation on the effects of adverse mobility ratios in which they observed that both breakthrough and cumulative recoveries decreased because of increased instability in the displacements.

Habermann[45] found that when a miscible slug was followed by dry gas, the process would be less efficient than expected. In addition to low areal sweep efficiencies encountered for high mobility ratio displacements, the effectiveness of a miscible slug was greatly reduced. This is caused by an accelerated growth of the mixing zone between the driving and the displacing fluids.

2.3.5 Effect of Density Ratio

If fluids of unequal density are used during miscible displacements, then gravity forces may influence dispersion. For vertical displacements, if the denser fluid is placed above the less-dense fluid, then gravity will usually cause redistribution or perhaps gravity "fingers". However, if the denser fluid is on the bottom (favourable gravity forces), then a stable displacement will usually occur.

In some reservoirs with dip, gravity can be used as an advantage to improve sweepout and oil recovery[20]. This is achieved by injecting the solvent up dip and producing the reservoir at a rate low enough for gravity to keep the less dense solvent segregated from the oil, suppressing fingers of solvent as they try to form.

An effect of gravity forces on transverse dispersion was reported by Grane and Gardner[11], and Pozzi and Blackwell[46]. Blackwell et al.[20] found that the effectiveness of gravity segregation in improving the displacement efficiency decreased rapidly after injection rate exceeds the critical rate. Gardner et al[47] investigated gravity segregation of miscible fluids in linear models and presented analytical solutions for horizontal, vertical and inclined positions.

Slobod et al.[48] studied the effect of density differences of miscible fluids on the observed efficiency of the displacement process. They found that gravity segregation could act to shorten the mixing zone when the displacing material was the less dense phase, and lengthen the zone for unfavourable density differences. They also found that the length of the mixing zone was dependent upon the ratio of the viscous forces to the gravity forces.

Farouq Ali and Stahl[17] suggested that the little investigated gravity effects may have considerably influenced the mechanism of alcohol slug displacements in Berea sandstone cores. Nielsen[61] and Niko[62] support the same view.

2.3.6 Effect of Particle Size Distribution and Particle Shape

Raimondi et al.[10] and Orlob and Radhakrishna[49] as referred to in Perkins and Johnston[8], and Bretz et al.[50] investigated the effect of particle size distribution on dispersion. They indicated that wide particle size distributions would lead to increased dispersion.

Furthermore, Raimondi et al.[10] concluded that the mixing coefficient (α) for packings of uniform size particles was directly proportional to the particle diameter, and that for mixtures of different size particles: (a) at constant permeability, α increased with an increasing distribution of particle sizes; (b) at constant particle size distribution

(homologus packings), α increased almost linearly with the square root of the permeability.

Blackwell[13] found that flow channel junctures in unconsolidated sand packs will occur at distances approximately equal to the diameter of the sand grains. Bretz et al.[50] indicated that the evidence concerning wide pore-size distributions and preferential flow paths could be obtained easily from measurements of pore size and pore-size spatial correlation made with thin-sections.

The effect of particle shape on dispersion was studied by Bernard and Wilhelm[51], Carberry[52], Ebach and White[53], among others. These investigators studied spheres, cubes, rings, saddles, crushed granular material, etc. It was generally found that packs of non spherical particles lead to greater dispersion than do packs of spherical particles of about the same size.

2.3.7 Ratio of Particle Diameter to Column Diameter

If spherical particles are packed into a cylinder, there would be packing irregularities near the container walls. Packing irregularities of this type will no doubt have an effect on both the longitudinal and transverse dispersion.

Several investigators including Latinen[54], Fahien and Smith[55], and Singer and Wilhelm[56] have experimentally investigated the "wall effect" on transverse dispersion for turbulent flow. Their experimental data suggested that the increase in transverse dispersion in the laminar region will be, roughly, the same order of magnitude as in the turbulent region.

2.3.8 Effect of an Immobile Phase

In the absence of any immobile phase in the porous medium, mixing in miscible displacement is governed by the properties of the porous medium, such as permeability, pore size distribution, and by the molecular properties of the miscible fluids; (while) in the presence of an immiscible fluid, such as gas or immobile phase, mixing is also influenced by the quantity and the distribution of the immobile phase.

2.3.8.1 Effect of an Immobile Polymer Phase

Groboske and Farouq Ali[27] investigated the effect of an immobile polymer phase on the mixing characteristics in both consolidated and unconsolidated porous media. They observed that the pore-size distribution was more uniform in the sandstone core in the presence of an immobile polymer phase. Thus, the mixing coefficient was smaller as compared to the other immobile liquid phases employed. The same result was reported for unconsolidated cores; however, there was no definite trend observed for this case.

2.3.8.2 Effect of an Immobile Gas Phase

The effect of an immobile gas phase on dispersion and mixing was studied by Orlob and Radhakrishna[49]. They observed a considerable reduction in the volume of the liquid bypassed in the system. This led them to the conclusion that entrapment of a small quantity of gas within the pore space may trap some of the liquid and keep it from the flow current. They found that the volume of trapped liquid varied considerably with each individual set-up, ranging up to about 5 percent and averaging about 2.5 percent of the total pore volume.

They also found that dispersion in the liquid phase was influenced by gas entrapment. The structure of the porous medium and the location of gas bubbles indicated the extent to which the dispersion was influenced by a residual gas phase.

Entrapment of gas bubbles in the larger pore spaces would cause greater uniformity in pore-size distribution and, hence, would reduce the amount of dispersion. In general, they believed that the more nearly uniform the medium, the less would be the influence of trapped gas.

They also reported that a small amount of trapped gas (say, less than 5 percent of the total pore volume) had little effect on dispersion.

2.3.8.3 Effect of an Immobile Oil Phase

Kasraie[57] investigated the effect of an immobile oil saturation on the mixing coefficient in Berea sandstone cores. She observed that the mixing coefficient tends to increase in the case of a non-wetting (oil or gas) immobile saturation, as compared to displacement in the absence of an immobile phase. She also noticed that the mixing coefficient increased with an increase in the immobile saturation, but registered a decrease for the largest value of the saturation.

2.3.8.4 Effect of an Immobile Water Phase

Raimondi et al.[10] found that oil was trapped by water at high water saturations and this oil was recovered only by means of continuous solvent injection.

Thomas, Countryman and Fatt[59] investigated the effect of an immobile water phase on the mixing characteristics. They reported that the pore size distribution was different in the presence of an immiscible fluid, as compared to that in the absence of any immobile phase. They also stated that at high water saturations some of the oil was trapped in the dead-end pores and was not recovered by injection of a solvent.

Stalkup[60] also reported similar findings and stated that this entrapped oil was only recoverable by molecular diffusion.

Raimondi, Torcaso and Henderson[58] carried out an intensive investigation on miscible displacement in the presence of an immobile water phase in Berea sandstone cores. They found that the mixing coefficients (α) of the wetting phase were between 0.16 and 3.4 cm for a wide range of saturation conditions. These values indicated a very efficient miscible displacement of the wetting phase.

They reported that the mixing coefficient of the non-wetting phase decreased in the presence of an irreducible wetting phase saturation, while when the water saturation was increased above the irreducible saturation, the displacement of oil was less efficient and as a result a longer mixing zone was observed.

They noticed that all of the non-wetting phase was recoverable by miscible displacement even when its saturation was very low and regardless of whether it was

established by drainage or imbibition. They also observed that water phase was stationary for irreducible water saturations, while above the irreducible water saturations, there was simultaneous flow of both oil and water phase.

2.4 Miscible Slug Displacement

In the miscible slug process a small quantity of oil-miscible solvent followed by a bank of another fluid is injected into the oil reservoir. This process will efficiently sweep out oil from the reservoir.

Koch and Slobod[63] investigated the miscible slug process where they injected slugs of propane or LPG into long cores prior to gas injection. Their laboratory experiments indicated that the high recoveries associated with miscible phase displacements was achieved by injecting a small band or slug (2 to 3 percent of the total pore volume) of propane or LPG prior to gas injection.

They studied several factors controlling the slug size selection, but the most important and striking discovery of their laboratory work which included displacements from cores up to 123 ft. in length was that relatively small slugs of propane or LPG were effective over reservoir distances in the miscible displacement of oil. Thus, the process may be commercially applicable. They also found that the miscible slug process achieved a miscible phase displacement at relatively lower pressures (around 1200 psi compared to above 3000 psi for a miscible-type high pressure gas injection operation).

Craig and Owens[64] reviewed laboratory results of miscible slug flooding; they emphasized on the general conclusions of the laboratory studies as applied to field application of miscible flooding. They studied the factors which resulted in inefficient sweep of LPG slug flooding, and proposed methods for improving the sweep efficiency.

Raimondi et al.[10] explained that at a fixed distance traveled by the center of slug X, and for negligible molecular diffusion, the maximum concentration is as follows:

$$\frac{C_{max}}{C_o} = erf\left(\frac{L}{4\sqrt{a_e X}}\right) \qquad (15)$$

where:

L = length of the undiluted slug, (cm)

a_e = effective mixing coefficient, (cm)

C_o = initial concentration of the slug, (cm^3/cm^3)

C_{max} = maximum concentration of the slug, (cm^3/cm^3)

and

$$a_e = \alpha + \frac{D}{\vartheta} = \frac{K}{\vartheta} \qquad (16)$$

For small values of the argument, Equation (15) is simplified to the following form:

$$\frac{C_{max}}{C_o} = \frac{L}{\sqrt{4\pi a_e X}} \qquad (17)$$

Equation (17) indicates that the maximum concentration (C_{max}) depends on the slug size and distance traveled and may be used to determine the coefficient of longitudinal dispersion (K_l).

2.5 Other Related Work

A large amount of research has been conducted in the area of liquid-liquid miscible displacement at the University of Alberta and the Pennsylvania State University, as well as at many other institutions and research centers. However, yet, it is still not fully understood; therefore, it is still under intensive investigation.

Many researchers[15, 17, 19, 23, 43, 57 -58, 62, 65 -72] carried out intensive investigations in this area. Some selected research will be briefly discussed in this section.

Giesbrecht[15] studied the possibility of using the fractal dimension of permeability to describe heterogeneity for a variety of rock types. The study was undertaken by comparing the effluent concentration profiles of first contact miscible displacements in various rock types to the fractal dimension calculated for permeability, porosity and mean pore throat size.

He concluded that the more homogeneous the rock type, the greater the effect of convective dispersion on the recovery. Displacement tests done with carbonate rocks yielded higher dispersion coefficients than those obtained with sandstones. Finally, he found that there was no good correlation between permeability, porosity or mean pore throat size and the dispersion coefficient.

Zhang[65] investigated the effect of the core length on miscible displacement; she found that the length of the porous medium played an important role in the mixing process of miscible fluids. She concluded that the longer the system, the earlier the breakthrough occurred and that the displacement was stable in a short bead-packed core but not in a long one.

She also found that both the longitudinal dispersion coefficient and the stable mixing zone length were dependent on core length. The dependence of the dispersion on core length was more pronounced as the fluid velocity became larger. Her study led to a conclusion that the theoretical error function curve in the Brigham model may still be valid in the unstable displacement case provided that a properly defined longitudinal dispersion coefficient was used.

Le[66] investigated the effect of core length and injection rate on the longitudinal dispersion coefficient. She concluded that the dispersion coefficient depended on both core length and fluid velocity. The dispersion coefficient increased with increasing velocity. The effect was minor in the short core, but became more significant in the longer cores.

She found that the dispersion coefficient increased with increasing core length. However, as the velocity increased, the dispersion coefficient appeared to be independent of length. She noticed that laboratory dispersion in Berea sandstone was not Fickian, as the predicted and the experimental concentration profiles did not match

in every test; she believed that Brigham's model failed to match the predicted and experimental results in this case because the model did not take into account the heterogeneity of the consolidated core.

Tan[67] developed a new mathematical model for one-dimensional miscible displacement (based on Darcy's law, Fick's dispersion law and the continuity equation). He explicitly included the effect of the viscosity ratio and the heterogeneity factor in the main equation. In addition to that, he found an approximate analytical solution to his model when he demonstrated the relationship between transition zone growth with time through an entire miscible displacement process.

He conducted some miscible displacements in a sand pack, using fluids with different viscosities to test his model. He concluded that the new model has successfully matched effluent curves and transition zone length data published in the literature and the effluent histories of the miscible displacements conducted in his study.

The approximate analytical solution to his model demonstrated that the transition zone for a miscible displacement grew with the square root of time at early stages when the concentration gradient was the greatest. The transition zone growth increased linearly with time when dispersion became negligible.

Kasraie[57] investigated the effect of three different injection rates and various immobile fluid saturations on convective mixing in consolidated porous media (Berea sandstone cores). She found that the mixing coefficient tended to decrease in the case of wetting immobile phase, as compared to displacement in the absence of an immobile phase.

She also found that the mixing coefficient tended to increase in the case of a non-wetting (oil or gas) immobile saturation, as compared to displacement in the absence of an immobile phase. In the case of a wetting immobile phase, the mixing coefficient at first decreased, then increased with an increase in the immobile water saturation. However, in the case of a non-wetting (oil) immobile phase, the mixing coefficient increased with an increase in the immobile saturation, but registered a decrease for the largest value of the saturation. An immobile gas saturation followed a similar trend.

Finally, she concluded that the mixing coefficient in all cases tended to decrease both with an increase or decrease in rate, showing a maximum value at an intermediate rate. Exceptions occurred depending on the type of the immobile saturation and its magnitude.

3. The Mathematical Models

There are basically three types of mathematical models. The first one is the standard theory which is a combination of Fick's law and the continuity equation. While this model is valid only for matched miscible fluids and homogeneous porous media as reported by Aris and Amundson[72], some other mathematical models have been proposed, which are capable of taking into account unmatched densities, viscosities and the non-uniform properties of the porous medium (these other models have been referred to in the previous chapter); however, they are not finally conclusive due to some other limitations.

Based on the standard theory, the transition zone length grows with the square root of time. However, some recent miscible displacement experiments by Walsh and Withjack[41] in Berea sandstone cores showed that this is not always true. Furthermore, Pickens and Grisak[73] reported that the value of the dispersion coefficient needed by a simulation to match an actual field scale miscible displacement is usually much larger than that obtained from the breakthrough curves of core flooding in the laboratory. Therefore, the dispersion is apparently scale dependent.

The second approach is to use immiscible two-phase flow theory for miscible displacement, which means that the dispersion is totally neglected. Based on this theory, the transition zone length grows linearly with time. Obviously, this theory approaches the correct solution only when the flow rate is great enough or other variables such as heterogeneity of the porous medium and the properties of the fluids make convection dominate the process. In fact, Blackwell et al.[20] indicated that dispersion plays a very important role during miscible displacement.

Finally, the third approach is to combine the effects of dispersion and convection. Tan[67] used this approach to derive a mathematical model for miscible displacement; he included the viscosity ratio of the fluids and the heterogeneity of the porous medium explicitly in the model. The model was then used to match the experimental data with the one published in the literature.

In view of the very large number of papers in the literature, only major works are reviewed in this chapter.

3.1 Brigham Model

Several investigators have examined the "diffusion equation" for longitudinal dispersion. Brigham[75] used the solution to the convective dispersion equation to match an effluent concentration profile obtained from a miscible displacement experiment.

This model is based on one dimensional flow of incompressible fluid, dispersion occurs only in the direction of flow, first contact miscibility, gravity-stable displacement, a favourable mobility ratio and a homogeneous porous medium system.

Then the displacement process can be described by the following convection-dispersion equation:

$$K_l \frac{\partial^2 C}{\partial x^2} - \vartheta \frac{\partial C}{\partial x} = \frac{\partial C}{\partial t} \qquad (18)$$

where

K_l = the longitudinal dispersion coefficient, (cm^2/sec)

x = the distance from the inlet end of the core, (cm)

C = the in-situ solvent concentration, (cm^3/cm^3)

t = time, (sec)

and

ϑ = the pore velocity, (cm/sec)

Brigham[75] presented several solutions of Equation (18) which differ in form according to the different boundary conditions imposed. To solve Equation (18), the boundary conditions must be defined since each set of boundary conditions yields a different solution. For a miscible displacement where the mixing zone was large compared to the porous medium, the boundary conditions affects the solution significantly.

The solutions generally include an error function term and some other terms from the asymptotic expansion. However, the results calculated from different solutions, as Brigham has shown, became identical when the porous medium was long compared with the length of the mixed zone.

Consider the infinite medium case where the boundary conditions are chosen as:

$$\text{as } x \rightarrow +\infty \qquad C(x,t) \rightarrow 0$$

and

$$\text{at } x = \vartheta t \qquad C(x,t) = 1/2$$

then the solution to Equation (18) is:

$$C = \frac{1}{2} erfc\left(\frac{x - \vartheta t}{2\sqrt{kt}}\right) \tag{19}$$

where

erfc = error function

In a laboratory experiment, one measures the effluent concentration at the outlet end of the core. This concentration is called the flowing concentration, C', and is defined as:

$$C' = \frac{q}{\vartheta A \phi} = C - \frac{K}{\vartheta}\left(\frac{\partial C}{\partial x}\right) \tag{20}$$

where

q = flow rate of displacing fluid, (cm^3/sec)

A = cross-sectional area, (cm^2)

ϕ = porosity, dimensionless

and

K = dispersion coefficient, (cm^2/sec)

Taking the derivative of Equation (19) and substituting the results into Equation (20), the flowing concentration becomes:

$$C' = \frac{1}{2} erfc\left(\frac{x - \vartheta t}{2\sqrt{Kt}}\right) + \left(\frac{K}{\vartheta}\right)\frac{1}{2\sqrt{\pi K t}} e^{\left(\frac{x-\vartheta t}{2\sqrt{Kt}}\right)^2} \tag{21}$$

Then by setting x=L, core length, and by introducing the dimensionless dispersion[24], $\gamma = \vartheta L / K$, Equation (21) becomes the well known solution of Equation (18) for predicting effluent flowing (instead of in-situ) concentration; and it is given by:

$$C = \frac{1}{2} erfc\left(\frac{1-I}{2\sqrt{I/\gamma}}\right) + \frac{1}{2\sqrt{\pi\gamma I}} e^{-\left(\frac{1-I}{2\sqrt{I/\gamma}}\right)^2} \qquad (22)$$

where

I = pore volumes injected, V_i / V_p or $\vartheta t / L$

V_i = injected volume, (cm^3)

V_p = pore volume, (cm^3)

Brigham[75] also introduced a simple method to determine the effective dispersion coefficient, K_e, using the experimental effluent concentration of the displacing fluid via a volume modifying function (lambda), λ, which is defined as:

$$\lambda = \frac{(Vi/Vp)-1}{\sqrt{Vi/Vp}} = \frac{I-1}{\sqrt{I}} \qquad (23)$$

A plot of the volume modifying function versus effluent concentration on an arithmetic probability paper should yield a straight line, if the model is applicable. The value of γ in Equation (22) can be calculated as:

$$\gamma = \left(\frac{2.380}{\lambda_{80} - \lambda_{20}}\right)^2 = \left(\frac{3.625}{\lambda_{90} - \lambda_{10}}\right)^2 = \left(\frac{4.650}{\lambda_{95} - \lambda_{5}}\right)^2 \qquad (24)$$

where the constant that one uses depends on the range used in the λ function, these constants are available in standard tables of error function.

Also, λ_{90} *and* λ_{10}= values of modified volume function at effluent concentrations of

90% and 10%, respectively.

The effective dispersion coefficient is then calculated as:

$$K_e = \frac{\vartheta\, l}{\gamma} = \vartheta\, l \left(\frac{\lambda_{90} - \lambda_{10}}{3.625} \right)^2 \qquad (25)$$

where

K_e = effective dispersion coefficient, $cm^2/sec.$

ϑ = pore velocity, cm/sec.

and

l = core length, cm.

The convective-dispersion equation which was used by Brigham to determine the effective dispersion coefficient has the disadvantage of not accounting for dead-end pore volume in the porous medium and also does not address the problem of scale dependence in convective dispersion.

Baker[29] introduced a more sophisticated approach to deal with cases where a significant portion of the pore space consists of dead-end pores.

3.2 Coats and Smith Model

A more sophisticated approach to the modelling of effluent concentration profiles was proposed by Coats and Smith[9]. In this model, resident oil is assumed to be trapped in dead-end or occluded pore space. This dead-end pore space is only accessible to the flowing solvent at a single point with mass transfer occurring by diffusional processes only.

The Coats and Smith model is a modification of the convective-dispersion (C-D) model in which terms accounting for a stagnant volume are added (i.e. it took into account the additional effect the diffusion of residual oil trapped in the dead-end pore space had on the overall dispersion coefficient).

All assumptions implicit in the development of the convective-dispersion model also apply to the Coats and Smith model. By defining (1-f) as the fraction of the total

volume that was stagnant and C^* as the average concentration in these pores, the displacement can be represented by the following equation:

$$K\frac{\partial^2 C}{\partial x^2} - \vartheta\frac{\partial C}{\partial x} = f\left(\frac{\partial C}{\partial t}\right) + (1-f)\frac{\partial C^*}{\partial t} \qquad (26)$$

and

$$(1-f)\frac{\partial C^*}{\partial t} = m\left(C - C^*\right) \qquad (27)$$

or in dimensionless terms as:

$$\frac{1}{\gamma}\frac{\partial^2 C}{\partial y^2} - \frac{\partial C}{\partial y} = f\left(\frac{\partial C}{\partial I}\right) + (1-f)\frac{\partial C^*}{\partial I} \qquad (28)$$

and

$$(1-f)\frac{\partial C^*}{\partial I} = a\left(C - C^*\right) \qquad (29)$$

where

f = fraction of pore space occupied by mobile fluid

C = concentration of injected fluid

C^* = concentration in stagnant fluid

I = pore volumes injected, $\vartheta t / l$

$\gamma = \vartheta l / K$, dimensionless dispersion

$y = x / l$, dimensionless distance

and

$a = m l / \vartheta$, rate group

At low flow rates, where the fluid moves with sufficiently small velocity, the rate group, $m l / \vartheta$, is large; so the mass transfer between the flowing fluid and the fluid trapped in the stagnant space is almost instantaneous. The model reduces to the simple diffusion model proposed by Brigham[75]. In this case the solution to Equation (28) is as follows:

$$\frac{C}{C_o} = \frac{1}{2} erfc\left(\frac{\sqrt{\gamma}}{2} \cdot \frac{y-I}{\sqrt{I}}\right) - \frac{\sqrt{I}}{\sqrt{\pi\gamma}(y+I)} e^{-\gamma(y-I)^2/4I} \cdot \left(1 - 2\frac{I}{1+I}\right) \qquad (30)$$

where

C_0 is the feed concentration

At high flow rates, the rate group becomes very small and can be neglected. Again, the model degenerates to the diffusion model. However, in this case, the solution to Equation (28) is in the same form as Equation (30) with the I replaced by J = (1/f).

The dispersion coefficient is normally determined from the results of miscible displacement tests conducted in the laboratory. In such cases, the fluid velocity , ϑ, is always larger and the core length is smaller than the actual field conditions. Therefore, the rate group, m l / ϑ, may be sufficiently small so the mixing by capacitance effect is almost negligible.

In the field, where l is many times greater and ϑ is much smaller, the rate group becomes important and significantly affects the mixing process. Hence, to apply the laboratory miscible displacement test results to field-case mixing requires the inclusion of both the convective dispersion mechanism and the capacitance mechanism.

The Coats and Smith[9] model is a more accurate model to use in cases where the existence of a stagnant volume is important because it takes into account the mass transfer from the dead-end pore space by diffusion mechanism. Giesbrecht[15] found that the Coats and Smith model worked very well in the case of miscible displacement tests conducted with a Golden Spike limestone core.

3.3 Porous-Sphere Model

A more complex model, the Porous-Sphere (P-S) model, was presented by Bretz and Orr[30] . In addition to taking convection and the longitudinal dispersion in the flowing fraction into consideration, diffusive interchange of material in the pore spheres with fluid flowing past them is included as well. In the P-S model, flow occurs between spheres, which are themselves porous.

The model is quite similar to the C-S model except that there is an explicit representation of the length scale of the low-permeability (stagnant) regions. Furthermore, the P-S model also depends on three parameters which are the fractional flow, the Peclet number associated with convection and dispersion in the flowing stream, and a second Peclet number which is defined as a ratio of characteristic times for diffusion in the spheres to that for the flow through the core.

However, the P-S model has the same limitations for miscible fluids, as it requires matched viscosities and densities. Furthermore, as Bretz and Orr[30] observed, the theoretical prediction using the P-S model for slower displacements agrees well with the experimental data; at higher velocities, however, it is not as good. Neither the prediction of the P-S model nor the best fit of the C-S model fits the experimental observations at higher velocities, which may be explained as effects of instability.

3.4 Transverse-Matrix-Diffusion Model

A similar approach to that of the P-S model was taken by Grisak and Pickens[76]; that is, convection and longitudinal dispersion are considered in the flowing fraction, and transverse diffusion is taken into account between the flowing and stagnant fractions.

Correa et al.[77] used simplified solutions to the Coats and Smith, porous-sphere and transverse-matrix-diffusion models to interpret effluent concentration profiles from heterogeneous cores. Using simplified solutions in Laplace space, they developed a means of estimating a unique set of parameters which apply to any of the three parameter models they studied.

Correa et al.[78] used an efficient numerical inverter to invert the model solutions from Laplace space to real-time space. They suggested that the transverse-matrix-diffusion model is suitable for describing reservoir miscible performance, provided that the parameters are determined from laboratory displacements.

4. Statement of the Problem

The main objective of this research was to study first contact liquid-liquid miscible displacement in a short unconsolidated porous medium, in the presence of an immobile phase at favourable and unfavourable mobility ratios. Specifically, it was desired to investigate:

(1) The effect of an immobile aqueous phase on the mixing coefficient.

(2) The variation of the mixing coefficient in the presence of an immobile oleic phase.

(3) The effect of various immobile aqueous and oleic phase saturations on the mixing coefficient.

(4) The variation of the average mixing coefficient for a slug-type displacement in the presence of various immobile aqueous and oleic phase saturations.

(5) The effect of various slug sizes on the mixing coefficient in the presence of various immobile aqueous and oleic phase saturations.

(6) The effect of mobility ratio on all of the above-mentioned cases (1, 2, 3, 4, and 5).

It should be clearly noted that no attempt was made to simulate an actual reservoir. The results, therefore, are illustrative only of the fundamental behaviour of the miscible displacement process in a porous medium.

5. Experimental Fluids, Apparatus and Procedure

The purpose of this research was to study first contact liquid-liquid miscible displacement in a short unconsolidated porous medium, in the presence of an immobile phase at favourable and unfavourable mobility ratios. The study involved a series of miscible flood experiments using n-hexane as the resident oil and cyclohexane as the solvent (for the case of the oleic fluid system), 2% and 10% by weight calcium chloride brines were used as the resident fluid and the solvent, respectively (for the case of the aqueous fluid system).

N-hexane was also used as the immobile oil phase for the experiments performed with the aqueous fluid system (2% and 10% by weight brines), while the 2% by weight calcium chloride brine was used as the immobile water phase for the experiments performed with the oleic fluid system (n-hexane and cyclohexane).

Isopropyl alcohol (IPA) was used to lower the saturations of both the immobile oil phase and the immobile water phase.

5.1 Fluids

The fluids used in these experiments were: n-hexane, cyclohexane, 2% by weight calcium chloride brine, 10% by weight calcium chloride brine and isopropyl alcohol (IPA). The properties of these fluids are given in Table 5-1.

The fluids used for the two-component first-contact miscible displacements had to satisfy the following requirements:

1) First-contact miscibility at standard temperature and pressure conditions.

2) A large difference in refractive index between the components.

3) A small difference in density between the components.

The choice of both, the oleic and the aqueous fluid systems, were found to satisfy the first two requirements. However, the density difference between the two

Table 5-1: Fluid Properties

Fluid Type	Viscosity, cp (@ 21 ^{o}C)	Density, gm/cc (@ 25 ^{o}C)	Refractive Index (@ 25 ^{o}C)
n-hexane (C_6H_{14}) (Oil)	0.3291	0.6683	1.376
Cyclohexane (C_6H_{12}) (Solvent)	0.9865	0.7792	1.425
Isopropyl Alcohol (IPA)	2.1	0.783	1.3759
2% $CaCl_2$ Brine	1.0127	1.0082	1.3362
10% $CaCl_2$ Brine	1.0606	1.1706	1.3482

Table 5-2: Properties of the Porous Media

Core no.	Type	Pore Volume, (cc)	Porosity	Permeability, (darcy)
1	Unconsolidated	390	0.32	7.65
2	Unconsolidated	400	0.33	7.82
3	Unconsolidated	420	0.35	10.13
4	Unconsolidated	435	0.36	8.08
5	Unconsolidated	430	0.35	7.03
6	Unconsolidated	400	0.33	7.82

components (in each fluid system) is significant and may result in gravity segregation and a resulting reduction in recovery efficiency.

This possibility was addressed by injecting the heavier solvent from the bottom of the core and conducting the displacement upward at a rate low enough for the density difference between the solvent and the oil to overcome the tendency for solvent fingers to protrude into the oil [79] and it was considered as a gravity stable displacement; this was the case for the favourable mobility ratio.

For the unfavourable mobility ratio case, where viscous-fingering was observed, the process was reversed. The density difference between oil and the solvent was exploited by injecting the less dense oil at the top of the core and conducting the displacement downward at a rate as in the above mentioned case. This ensured a gravity stable displacement.

5.2 Porous Medium

The experiments were carried out employing six short unconsolidated cores, using Rotair glass beads (size # 9, US mesh size 80-120) as the porous media. Each core was 60.72 cm (23.9 in) in length and 5.05 cm (1.99 in) in diameter. Other properties of these cores are given in Table 5-2. Wet sieve analysis was performed for three glass bead samples and the mean particle diameter (d_p) was found to be 0.128 mm (127.7 micron).

5.3 Experimental Apparatus

Figure 5-1 shows a schematic diagram of the experimental apparatus which consists of the following:

- a double cylinder Ruska pump

- a set of stainless steel cylinders

- a stand with a coreholder unit

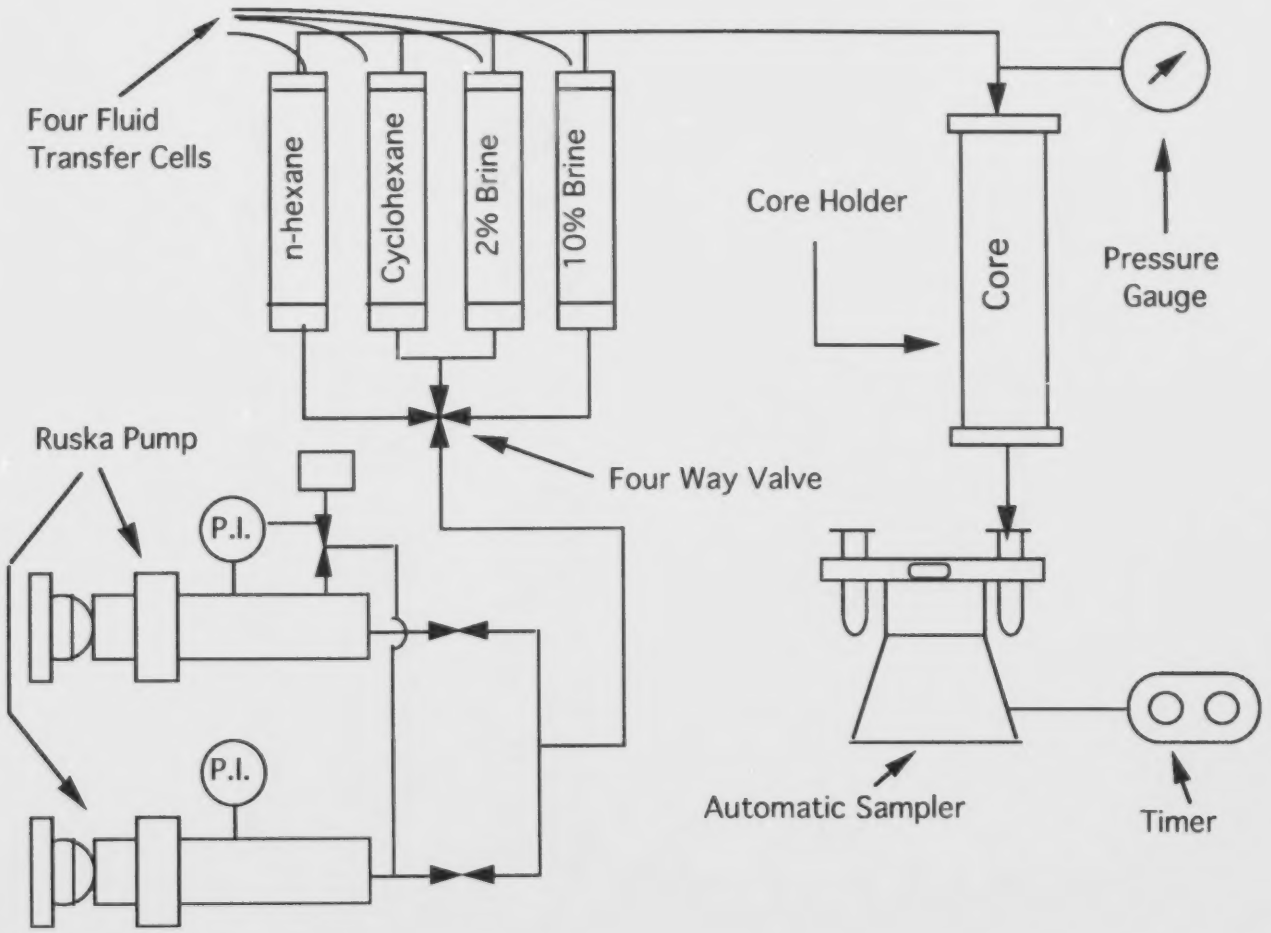

Figure 5-1: Schematic Diagram of the Miscible Flood Apparatus

- a pressure gauge at the inlet end of the core

- a sample collection unit with timer

- a refractometer

5.3.1 Injection System

The injection system consisted of a Ruska positive displacement pump with a quick change transmission, a set of four stainless steel cylinders and a pressure gauge at the inlet end of the core. The pump was used to keep the flow rate constant at any desired value with no pulsation. The pump had two 500 ml capacity cylinders and could be operated to a maximum pressure of 82.7 MPa (12,000 psig). Each cylinder had a discharge rate from 2.5 to 560 cm^3/hr (6×10^{-5} *to* 134.4×10^{-5} m^3/day). The injection rate could be varied by changing the gear on the pump transmission system. The two pump cylinders could be operated together or separately.

The pump was connected to the four-cylinder set by a high pressure stainless-steel flexible hose. The fluids cylinder set had the capacity of two litres per cylinder. The core holder inlet was connected to the cylinders by another high pressure stainless steel flexible hose. A 10 psig pressure gauge was installed at the inlet of the core holder.

The four-cylinder set contained n-hexane, cyclohexane, 2% by weight brine and 10% by weight brine, respectively. By using a four-way valve at the bottom of the set, a specific fluid was selected for injection as required.

5.3.2 Physical Model

The physical model (coreholder) used in this work consisted of a stainless steel cylinder, 60.72 cm (23.9 in) in length by 5.05 cm (1.99 in) in diameter as shown in Figure 5-2. Endcaps with o-ring type seals were then bolted to each end of the

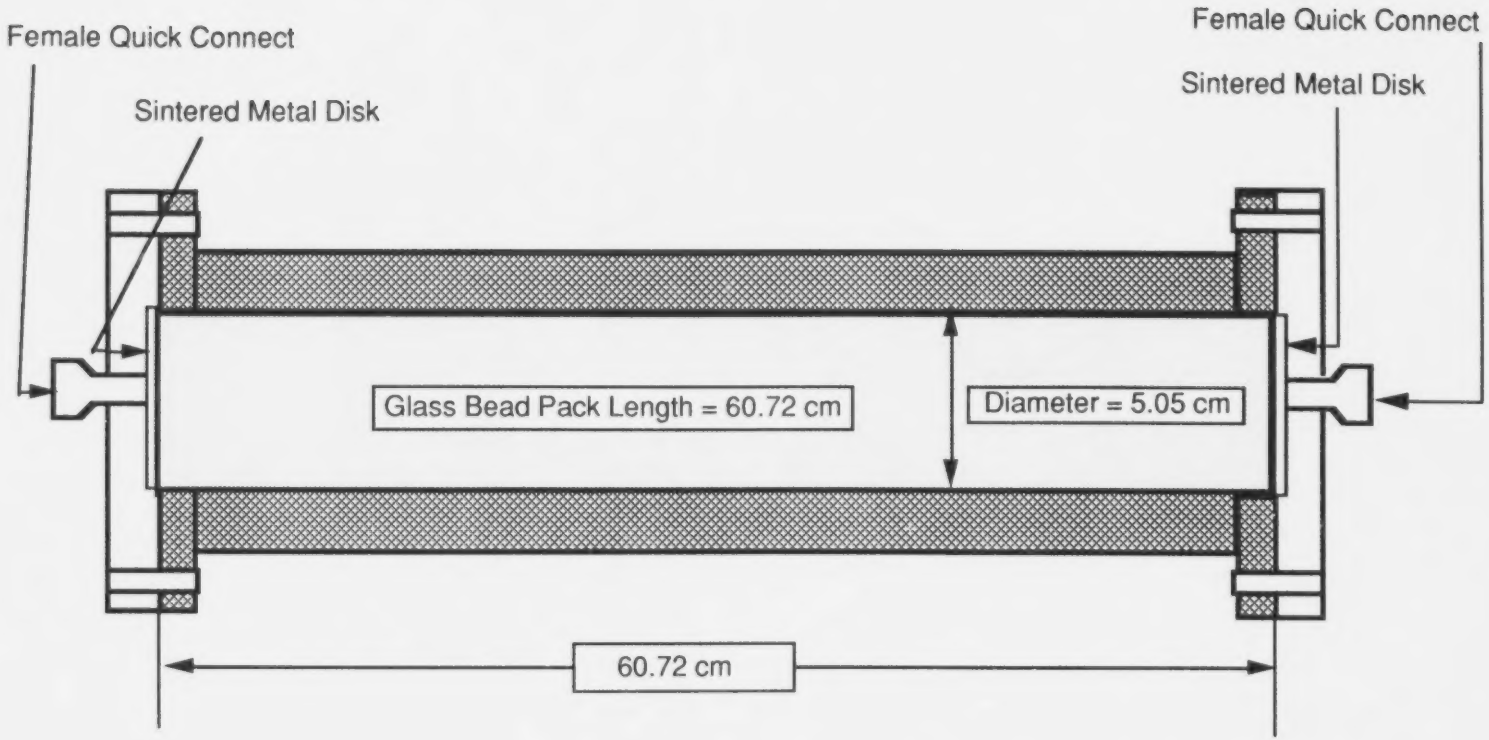

Figure 5-2: Cross-Sectional View of the Physical Core Holder

coreholder. The endcaps used a sintered metal screen to evenly distribute the injected and produced fluids across the inlet and outlet faces of each core.

5.3.3 Production System

The collection system consisted of a small tube end fitted on the down-stream end cap, a rotating sample collection tray with timer and a refractometer. The rotating sample collection tray contained a series of 50 ml graduated centrifuge tubes. The resulting coreflood effluent was collected in the centrifuge tubes at atmospheric pressure and then analyzed for refractive index, using an Abbe Model A303 refractometer.

5.4 Experimental Design

Prior to the experimental work, and in order to calculate the critical fluid velocity using Dumore's method[79], the densities and the viscosities of the oleic fluid, and the aqueous fluid systems were measured, as well as the densities and the viscosities of mixtures of each fluid system as a function of solvent volumetric concentration at room temperature, using a density meter and a Cannon-Fenske SR-50-314 viscometer, respectively.

Using Dumore's method[79], the critical flow rate for the oleic fluid system was calculated and found to be 912.8 cm^3/hr (2.19×10^{-2} m^3/day) and the stable flow rate was 379.1 cm^3/hr (9.1×10^{-3} m^3/day), while the critical and the stable rates for the aqueous fluid system were 1835.7 cm^3/hr (4.4×10^{-2} m^3/day) and 761.5 cm^3/hr (1.8×10^{-2} m^3/day), respectively. Therefore, a flow rate of 160 cm^3/hr (3.84×10^{-3} m^3/day) was selected as the optimum rate for these experiments.

The objective of setting and selecting the injection rate was to minimize the effect of molecular diffusion on the process; in addition to that, the rate must be selected to be lower than the critical rate in order to maintain a steady stable displacement.

The Abbe refractometer was checked out for calibration prior to the start of each experiment. Distilled water was used for calibration and its refractive index ranged from 1.3310 to 1.3315, depending on room temperature.

5.4.1 Core Preparation and Packing Procedure

The core holder was placed vertically on the stand in preparation for packing. The dry packing method was used in all experiments in this study. The packing process started with the core holder mounted vertically, with the injection end pointing upwards and the production end pointing downwards.

A mechanical vibrator was strapped onto the core. Then a transparent extension was attached to the inlet end. The extension acted to extend the core length, and as a result maintained a more consistent packing throughout the core and ensured that the glass bead pack level flush with the top end flange. The glass beads were loaded into the core holder while vibrating, to ensure even and uniform distribution (the core continued to vibrate for 8 hours overnight).

5.4.2 Core Saturation

After vibration, the top-extension was removed and a top end flange was bolted. The pack was then subjected to a vacuum (to remove the air from the pore space). The drawing of a vacuum was conducted by connecting the core to a vacuum pump for at least six hours with the core in the vertical position. The core was connected to the vacuum pump at one end and to a vacuum gauge at the other end. This allowed the quality of the vacuum to be monitored during the time the vacuum was being drawn.

After vacuuming, the vacuum pump and the gauge were removed. N-hexane (oil) was allowed to imbibe into the glass bead core from the bottom end. At this stage, the core was 100% saturated with n-hexane. The amount of imbibed n-hexane was then taken to be the pore volume of the glass bead pack. Porosity was then determined by dividing the pore volume by the bulk volume calculated from the inside core dimensions.

5.4.3 Permeability Test

At this stage, the core was 100% saturated with n-hexane (oil). N-hexane was then injected into the core at a specific pressure, left to stabilize, volume and time were then recorded, and subsequently the corresponding flow rate was determined. The same process was again repeated for at least eight different pressures.

Darcy's law for linear flow was then used to calculate the absolute permeability for each experiment,

$$q = k\left(\frac{A\,\Delta P}{\mu\,L}\right)$$

Given that

L = 0.6072 m (length of the glass bead pack)

μ = measured fluid viscosity at room temperature, Pa.sec

ΔP = pressure difference, Pa

A = 0.002003 m^2 (cross-sectional area of the glass bead pack)

q = fluid flow rate, m^3/sec

k = absolute permeability, m^2

The permeability was calculated for each of the eight runs, and then an average absolute permeability was calculated:

$$k_{avg} = \frac{\sum k_n}{no.\ of\ runs}$$

where

$\sum k_n$ = summation of all calculated permeabilities, m^2

k_{avg} = absolute average permeability, m^2

The same process was repeated for each of the six core packs used in this investigation.

5.5 Experimental Procedure

5.5.1 Continuous Miscible Displacement

After the absolute permeability was measured, and once the core was ready for test, the Ruska pump was set to inject cyclohexane (solvent) into the core from the bottom end, at a flow rate of 160 cm^3/hr ($3.84 \times 10^{-3}\ m^3/day$) with a favourable mobility ratio of 0.33.

The effluent was collected in a series of centrifuge tubes mounted on a rotating collection tray from the top production end of the core. Each effluent sample contained approximately 0.05 PV, and the refractive index of each sample was then measured and the process continued until 2 PVs of cyclohexane (solvent) were injected into the core.

It was found that an amount of about 2 PVs of cyclohexane (solvent) had to be injected into the system to completely remove the n-hexane (oil) and to make sure that the core was saturated with 100% cyclohexane. The test now had cyclohexane (solvent) as the displaced fluid and n-hexane (oil) as the displacing fluid, that was the case for an unfavourable mobility ratio (M=3.0) and the displacement was reversed by injecting n-hexane (oil) from top downwards to displace cyclohexane (solvent), to ensure a gravity stable displacement.

However, the displacement was unstable, and as a result of the adverse mobility ratio, viscous fingering took place. It was found that at least 3 PVs of n-hexane had to be injected into the system to completely remove the cyclohexane, and to make sure that the core was again saturated with 100% n-hexane.

The above-mentioned experimental procedure describes the miscible displacement of the oleic fluid system at favourable and unfavourable mobility ratios with no immobile water phase present. The same description could be applied to the aqueous fluid system in a new glass bead pack by replacing n-hexane (oil) with 2% (by weight) calcium chloride brine, and cyclohexane (solvent) with 10% (by weight) calcium chloride brine. However, the experimental runs were conducted with no immobile oil phase present in this case.

5.5.2 Continuous Miscible Displacement in the Presence of an Immobile Saturation

For the case of an oleic fluid system miscible displacement, at favourable and unfavourable mobility ratios in the presence of an immobile water saturation, the newly prepared and vacuumed glass bead pack was imbibed with 2% (by weight) brine from the bottom end. The porosity and the permeability of the glass bead pack were then determined using the same previous steps. At this stage, the core was 100% saturated with 2% (by weight) brine.

In order to obtain an immobile water (2% by weight brine) saturation, n-hexane (oil) was injected continuously into the pack from the top end. The quantity of 2% by weight brine which was not displaced was determined by material balance and used to calculate the saturation of the immobile water phase. The immobile water phase was found to be 25% PV. Afterwards, cyclohexane (solvent) was employed as the displacing phase. Following this, two-component miscible displacements (six runs) were carried out at favourable (M=0.33) and unfavourable (M=3.0) mobility ratios in the presence of 25% PV immobile water saturation (the process is the same as explained before).

5.5.3 The Reduction of the Immobile Saturation

In order to reduce the immobile water saturation below the residual value for a newly prepared glass bead pack, the above-mentioned procedure was again employed. At this point, n-hexane was injected continuously into the pack from the top end, until no more 2% brine was expelled from the pack. The quantity of 2% by weight brine which was not displaced was determined by material balance and found to be 29% PV.

After determining the immobile water saturation by material balance (29% PV), a 5% PV slug of isopropyl alcohol (IPA) was injected into the pack, followed by a large volume of n-hexane (oil). Additional quantity of 2% brine was expelled from the pack. Following this, similar two-component miscible displacements (six runs) were carried out. The reduced immobile water saturation was found to be 10% PV.

In order to obtain an immobile oil (n-hexane) saturation in a newly prepared glass bead pack for an aqueous fluid system displacements, the exact same process was

employed, by replacing n-hexane (oil) with 2% (by weight) brine and cyclohexane (solvent) with 10% (by weight) brine.

At this point, the pack was fully saturated with n-hexane. 2% brine was injected continuously into the pack from the bottom end, until no more n-hexane was expelled from the pack. The quantity of n-hexane which was not displaced was determined by material balance and found to be 26% PV. Here, again, the immobile oil saturation was reduced by injecting 5% PV slug of isopropyl alcohol (IPA) followed by a large volume of 2% brine. Additional quantity of n-hexane was expelled from the pack and the immobile oil saturation was reduced to 8% PV. Following this, similar two-component miscible displacements were carried out for the aqueous fluid system.

5.5.4 Miscible Slug Runs

In this part, the miscible slug-type displacements will be discussed. The miscible slug process consisted of two different slug sizes (20% & 30% PVs, respectively) used in each glass bead pack.

For each run (for both the oleic and the aqueous fluid systems), a 20% PV slug of the displacing fluid was injected and followed by the injection of 2 PV of the original saturating fluid. The same process was repeated again by injecting 30% PV of the displacing fluid, followed by the injection of 2 PV of the original saturating fluid (for the favourable mobility ratio case). For an unfavourable mobility ratio case, the displaced fluid becomes the displacing fluid, and vice versa. Again, 20% and 30% PV slug sizes were used and the process was repeated.

In the slug runs, two fronts were present. The analysis carried out in this work gives the average mixing coefficient for the two fronts. Miscible slug displacements were carried out in all of the six glass bead packs (for both the oleic and the aqueous fluid systems) using 20% & 30% PV slug sizes at favourable and unfavourable mobility ratios in the presence of various immobile fluid saturations, as well as when no immobile fluid saturations were present.

5.6 Sample Analysis

For each run performed, effluent samples were collected in the centrifuge tubes. The refractive index of each sample was then measured using the Abbe A303 refractometer.

A concentration profile on the basis of displacing liquid concentration in the effluent was obtained (Figures 5-6.1 & 5-6.2). This was used to determine the mixing coefficient.

Appendices A, B and C contain the calculation procedure, the effluent concentration profiles for all experiments, the lambda-function plots on probability paper for the continuous miscible displacement runs, as well as all the data tables for these plots.

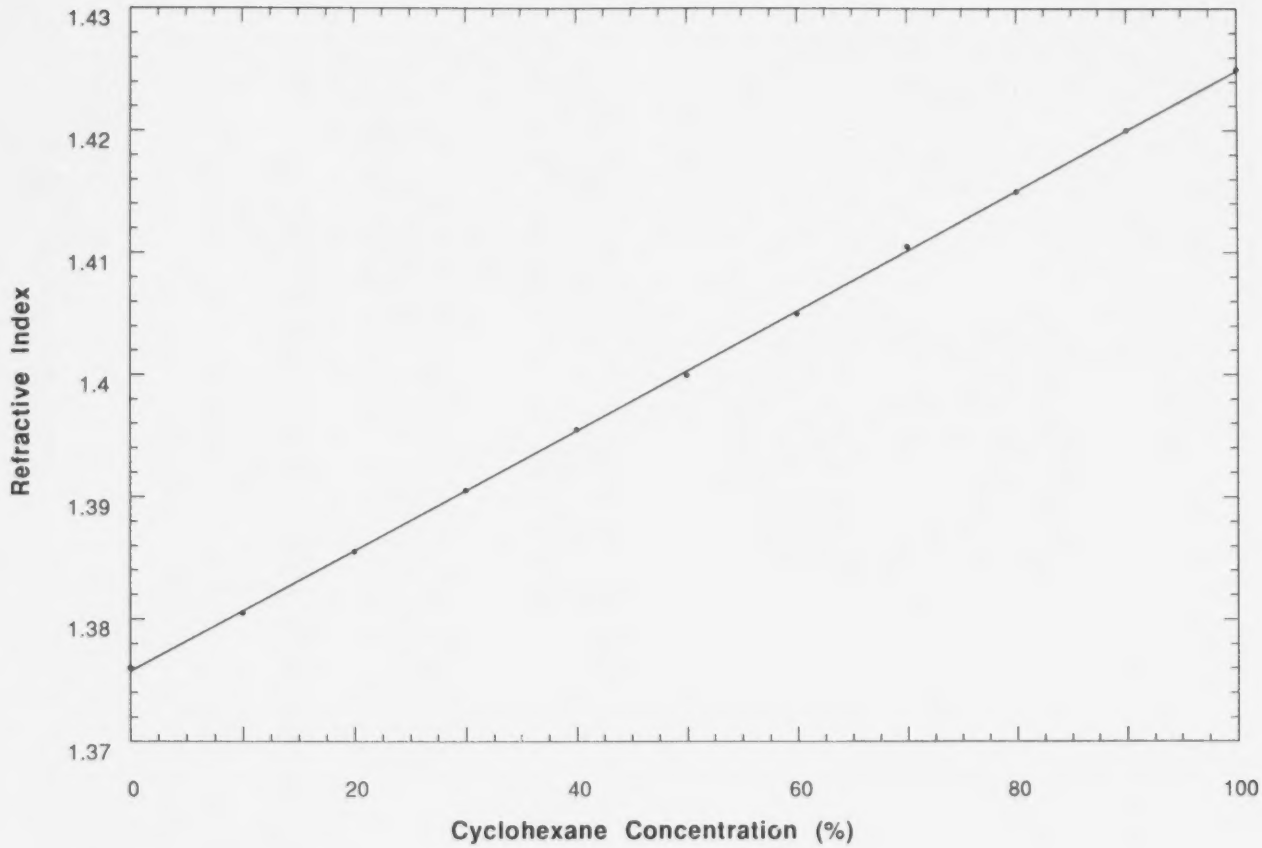

Figure 5-6.1: Standard Concentration Curve
Refractive Index Versus % Cyclohexane

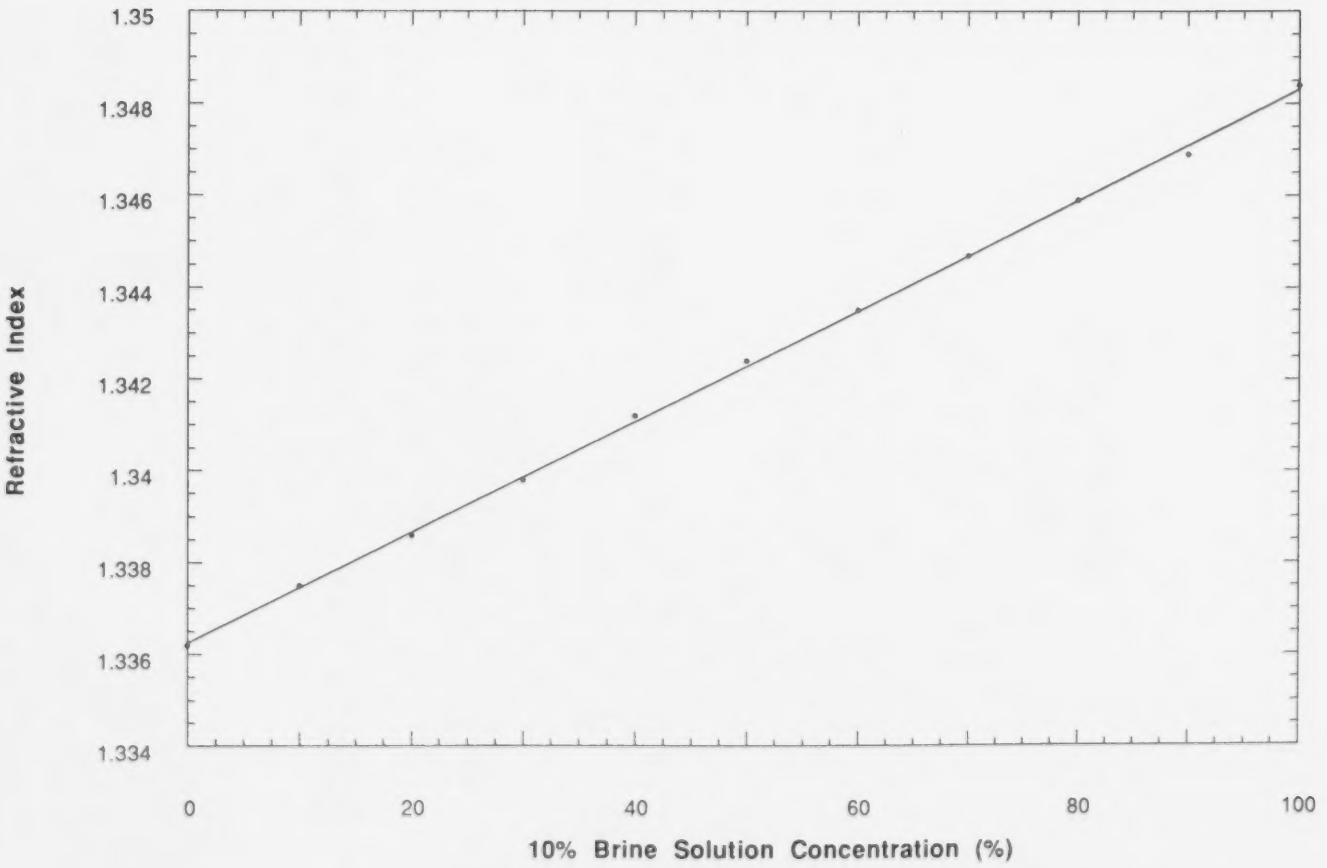

Figure 5-6.2: Standard Concentration Curve
Refractive Index Versus % 10% Brine

6. Discussion and Analysis of Results

This chapter presents the results of the experimental work conducted to investigate some of the mixing characteristics of miscible fluids in porous media. The research was aimed at investigating one of the important factors (effect of an immobile phase) that affect mixing of fluids in a porous medium. Effort was directed toward studying the effect of various immobile fluid saturations at favourable and unfavourable mobility ratios on fluids mixing in porous media while keeping the other factors constant within experimental limitations.

6.1 Presentation of Results

A total of thirty-six experimental runs were carried out in this investigation. Six short glass bead packs were employed for this purpose. Runs 1 to 6 were conducted in Core No.1 where continuous miscible displacements and miscible slug runs were carried out for the oleic fluid system at favourable and unfavourable mobility ratios in the absence of an immobile saturation. Runs 7 to 12 were conducted in Core No.2 where continuous miscible displacements and miscible slug runs were carried out for the aqueous fluid system at favourable and unfavourable mobility ratios in the absence of an immobile saturation. Runs 13 to 18 were conducted in Core No.3 where continuous miscible displacements and miscible slug runs were carried out for the oleic fluid system at favourable and unfavourable mobility ratios in the presence of 25% PV immobile saturation. Runs 19 to 24 were conducted in Core No.4 where continuous miscible displacements and miscible slug runs were carried out for the aqueous fluid system at favourable and unfavourable mobility ratios in the presence of 26% PV immobile saturation. Runs 25 to 30 were conducted in Core No.5 where continuous miscible displacements and miscible slug runs were carried out for the oleic fluid system at favourable and unfavourable mobility ratios in the presence of 10% PV immobile saturation. Core No.6 was used for Runs 31 to 36 where continuous miscible displacements and miscible slug runs were carried out for the aqueous fluid system at favourable and unfavourable mobility ratios in the presence of 8% PV immobile saturation. One flow rate 160 cm^3/hr ($3.84 \times 10^{-3}\ m^3/day$) was used in this investigation.

A complete tabulation of the data obtained from the thirty-six runs made in this study appears in Table 6.

In the runs consisting of oil-phase displacements, both favourable and unfavourable mobility ratios were employed. In the favourable mobility ratio displacement, cyclohexane (solvent) was used as the displacing fluid, while n-hexane (oil) was employed as the displaced fluid. On the other hand, at an unfavourable mobility ratio, n-hexane (oil) was injected into the core to displace cyclohexane (solvent).

Similarly, in those runs where water-phase displacements were conducted for both favourable and unfavourable mobility ratios, 10% (by weight) calcium chloride brine was used as the displacing fluid, while 2% (by weight) calcium chloride brine was employed as the displaced fluid for the favourable mobility ratio case. However, at an unfavourable mobility ratio, 2% (by weight) brine was used to displace 10% (by weight) brine.

6.2 Miscible Displacement and Miscible Slug Runs

Runs 1 and 2 consisted of miscible displacements in the oil phase with zero immobile saturation, using n-hexane and cyclohexane. The runs were conducted at 160 cm^3/hr (3.84×10^{-3} m^3/day)for both favourable and unfavourable mobility ratios.

Run 2 was carried out to compare oil displacement at an unfavourable mobility ratio with Run 1. These runs were designed to show the basic displacement of oil with no immobile phase present. The results are summarized in Table 6-1.

Runs 3, 4, 5 and 6 consisted of slug-type runs. In this regard, when the core contained n-hexane, a 20% PV slug of cyclohexane, followed by 2 PVs of n-hexane, was injected into the core. For Run 4, the process was repeated by injecting 30% PV slug of cyclohexane, followed by the injection of 2 PVs of n-hexane (Runs 3 and 4 were conducted at unfavourable mobility ratios with two different slug sizes).

In Run 5, n-hexane was displaced by the injection of 2 PVs of cyclohexane, then a 20% PV slug of n-hexane, followed by 2 PVs of cyclohexane. Again, for Run 6, the process was repeated by injecting 30% PV slug of n-hexane, followed by the

Table 6: SUMMARY OF THE SHORT UNCONSOLIDATED-CORE MISCIBLE DISPLACEMENT RUNS

Test #	Test Description	Displacement Rate (cc/hr)	Fluid Velocity (m/day)	Permeability (darcy)	Porosity	Displaced Fluid Viscosity (cp)	Displacing Fluid Viscosity (cp)	Mobility Ratio (M)	Mobility Ratio Type	Type of Immobile Fluid	Immobile Fluid Saturation (% PV)	Slug Type	Slug Size (% PV)	Dispersion Coefficient Ke (cm^2/sec)	Mixing Coefficient α (cm)
1	Cyclohexane (solvent) displacing n-hexane (oil)	160	1.92	7.65	0.32	0.329	0.987	0.334	Favourable	N/A	0	N/A	0	1.84E-04	0.083
2	N-hexane displacing cyclohexane	160	1.92	7.65	0.32	0.987	0.329	2.998	Unfavourable	N/A	0	N/A	0	1.44E-02	6.467
3	N-hexane displacing 20% PV slug of cyclchexane	160	1.92	7.65	0.32	0.987	0.329	2.998	Unfavourable*	N/A	0	Cyclohexane	20	4.23E-03	1.906
4	N-hexane displacing 30% PV slug of cyclohexane	160	1.92	7.65	0.32	0.987	0.329	2.998	Unfavourable*	N/A	0	Cyclohexane	30	5.50E-03	2.477
5	Cyclohexane displacing 20% PV slug of n-hexane	160	1.92	7.65	0.32	0.329	0.987	0.334	Favourable*	N/A	0	N-hexane	20	7.14E-04	0.322
6	Cyclohexane displacing 30% PV slug of n-hexane	160	1.92	7.65	0.32	0.329	0.987	0.334	Favourable*	N/A	0	N-hexane	30	1.10E-03	0.494
7	10% brine displacing 2% brine	160	1.92	7.82	0.33	1.013	1.171	0.865	Favourable	N/A	0	N/A	0	3.39E-03	1.525
8	2% brine displacing 10% brine	160	1.92	7.82	0.33	1.171	1.013	1.156	Unfavourable	N/A	0	N/A	0	1.26E-03	0.566
9	2% brine displacing 20% PV slug of 10% brine	160	1.92	7.82	0.33	1.171	1.013	1.156	Unfavourable*	N/A	0	10% Brine	20	5.88E-04	0.265
10	2% brine displacing 30% PV slug of 10% brine	160	1.92	7.82	0.33	1.171	1.013	1.156	Unfavourable*	N/A	0	10% Brine	30	1.21E-03	0.546
11	10% brine displacing 20% PV slug of 2% brine	160	1.92	7.82	0.33	1.013	1.171	0.865	Favourable*	N/A	0	2% Brine	20	8.16E-04	0.368
12	10% brine displacing 30% PV slug of 2% brine	160	1.92	7.82	0.33	1.013	1.171	0.865	Favourable*	N/A	0	2% Brine	30	1.23E-03	0.552
13	Cyclohexane displacing n-hexane	160	1.92	10.13	0.35	0.329	0.987	0.334	Favourable	2% Brine	25	N/A	0	3.39E-03	1.525
14	N-hexane displacing cyclohexane	160	1.92	10.13	0.35	0.987	0.329	2.998	Unfavourable	2% Brine	25	N/A	0	3.37E-03	1.52
15	N-hexane displacing 20% PV slug of cyclohexane	160	1.92	10.13	0.35	0.987	0.329	2.998	Unfavourable*	2% Brine	25	Cyclohexane	20	8.98E-04	0.404
16	N-hexane displacing 30% PV slug of cyclohexane	160	1.92	10.13	0.35	0.987	0.329	2.998	Unfavourable*	2% Brine	25	Cyclohexane	30	1.58E-03	0.71
17	Cyclohexane displacing 20% PV slug of n-hexane	160	1.92	10.13	0.35	0.329	0.987	0.334	Favourable*	2% Brine	25	N-hexane	20	9.94E-04	0.448
18	Cyclohexane displacing 30% PV slug of n-hexane	160	1.92	10.13	0.35	0.329	0.987	0.334	Favourable*	2% Brine	25	N-hexane	30	1.66E-03	0.747

* Mobility ratio at the second front for a miscible slug run

Table 6-CONTINUED/ SUMMARY OF THE SHORT UNCONSOLIDATED-CORE MISCIBLE DISPLACEMENT RUNS

Test #	Test Description	Displacement Rate (cc/hr)	Fluid Velocity (cm/hr)	Permeability (darcy)	Porosity	Displaced Fluid Viscosity (cp)	Displacing Fluid Viscosity (cp)	Mobility Ratio (M)	Mobility Ratio Type	Type of Immobile Fluid	Immobile Fluid Saturation (% PV)	Slug Type	Slug Size (% PV)	Dispersion Coefficient Ke (cm^2/sec)	Mixing Coefficient α (cm)
19	10% brine displacing 2% brine	160	1.92	8.08	0.36	1.013	1.171	0.865	Favourable	N-hexane	26	N/A	0	2.68E-03	1.205
20	2% brine displacing 10% brine	160	1.92	8.08	0.36	1.171	1.013	1.156	Unfavourable	N-hexane	26	N/A	0	5.12E-04	0.231
21	2% brine displacing 20% PV slug of 10% brine	160	1.92	8.08	0.36	1.171	1.013	1.156	Unfavourable*	N-hexane	26	10% Brine	20	6.10E-04	0.275
22	2% brine displacing 30% PV slug of 10% brine	160	1.92	8.08	0.36	1.171	1.013	1.156	Unfavourable*	N-hexane	26	10% Brine	30	1.16E-03	0.522
23	10% brine displacing 20% PV slug of 2% brine	160	1.92	8.08	0.36	1.013	1.171	0.865	Favourable*	N-hexane	26	2% Brine	20	7.36E-04	0.332
24	10% brine displacing 30% PV slug of 2% brine	160	1.92	8.08	0.36	1.013	1.171	0.865	Favourable*	N-hexane	26	2% Brine	30	1.14E-03	0.513
25	Cyclohexane (solvent) displacing n-hexane (oil)	160	1.92	7.03	0.35	0.329	0.987	0.334	Favourable	2% Brine	10	N/A	0	3.39E-03	1.525
26	N-hexane displacing cyclohexane	160	1.92	7.03	0.35	0.987	0.329	2.998	Unfavourable	2% Brine	10	N/A	0	4.41E-03	1.984
27	N-hexane displacing 20% PV slug of cyclohexane	160	1.92	7.03	0.35	0.987	0.329	2.998	Unfavourable*	2% Brine	10	Cyclohexane	20	1.22E-03	0.548
28	N-hexane displacing 30% PV slug of cyclohexane	160	1.92	7.03	0.35	0.987	0.329	2.998	Unfavourable*	2% Brine	10	Cyclohexane	30	1.20E-03	0.538
29	Cyclohexane displacing 20% PV slug of n-hexane	160	1.92	7.03	0.35	0.329	0.987	0.334	Favourable*	2% Brine	10	N-hexane	20	1.70E-03	0.767
30	Cyclohexane displacing 30% PV slug of n-hexane	160	1.92	7.03	0.35	0.329	0.987	0.334	Favourable*	2% Brine	10	N-hexane	30	1.88E-03	0.847
31	10% brine displacing 2% brine	160	1.92	7.82	0.33	1.013	1.171	0.865	Favourable	N-hexane	8	N/A	0	2.67E-03	1.205
32	2% brine displacing 10% brine	160	1.92	7.82	0.33	1.171	1.013	1.156	Unfavourable	N-hexane	8	N/A	0	7.47E-04	0.337
33	2% brine displacing 20% PV slug of 10% brine	160	1.92	7.82	0.33	1.171	1.013	1.156	Unfavourable*	N-hexane	8	10% Brine	20	5.45E-04	0.245
34	2% brine displacing 30% PV slug of 10% brine	160	1.92	7.82	0.33	1.171	1.013	1.156	Unfavourable*	N-hexane	8	10% Brine	30	1.07E-03	0.481
35	10% brine displacing 20% PV slug of 2% brine	160	1.92	7.82	0.33	1.013	1.171	0.865	Favourable*	N-hexane	8	2% Brine	20	6.71E-04	0.302
36	10% brine displacing 30% PV slug of 2% brine	160	1.92	7.82	0.33	1.013	1.171	0.865	Favourable*	N-hexane	8	2% Brine	30	1.23E-03	0.552

* Mobility ratio at the second front for a miscible slug run

injection of 2 PVs of cyclohexane (Runs 5 and 6 were conducted at favourable mobility ratios with two different slug sizes).

These slug-type runs were designed to give the average values of the mixing coefficient which were compared with the two corresponding values obtained for the favourable and the unfavourable mobility ratios in Runs 1 and 2. The results are given in Table 6-1.

Similarly, Runs 7 - 12 consisted of miscible displacements (Runs 7 and 8) and miscible slug displacements (Runs 9, - 12) with zero immobile saturation at favourable and unfavourable mobility ratios, using 2% and 10% (by weight) brines. Runs 7 - 12 were conducted in the exact same sequence as in Runs 1 - 6; however, n-hexane and cyclohexane were replaced by 2% and 10% (by weight) brines, respectively.

Again, the slug-type runs (Runs 9 - 12) were designed to give the average values of the mixing coefficient which were compared with the two corresponding values obtained for the favourable and the unfavourable mobility ratios in Runs 7 and 8. The results are given in Table 6-2.

6.3 Miscible Displacement in the Presence of an Immobile Water Phase

In order to carry out miscible oil displacements in the presence of an immobile water phase, n-hexane was injected into the core that contained 2% (by weight) brine until an immobile saturation was obtained (25% pore volume). Then, cyclohexane was used as the displacing fluid. Runs 13 - 18 were carried out at this water saturation to study the effect of an immobile water phase on displacement of the oil phase. The same experimental runs sequence was carried out for this set of runs as in Runs 1 - 6. The results of these runs are given in Table 6-3.

It was also desired to carry out runs similar to Runs 13 - 18, at a lower water saturation, in order to investigate the effect of various immobile saturations on miscible displacement. Therefore, a 5% PV slug of isopropyl alcohol (IPA) was injected into a newly prepared glass bead pack (with a known immobile water saturation) to reduce water saturation, and subsequently a large quantity of n-hexane was injected, until no

Table 6-1: Dispersion and Mixing Coefficients for the Oleic Fluid System Displacements at Zero Immobile Water Saturation in Unconsolidated Core No. 1

Run No.	Test Description	Displacement Rate (cc/hr)	Fluid Velocity (m/day)	Displaced Fluid Viscosity (cp)	Displacing Fluid Viscosity (cp)	Mobility Ratio (M)	Mobility Ratio Type	Immobile Water Saturation (% PV)	Slug Type	Slug Size (% PV)	Dispersion Coefficient* $K_e \times 10^{-3}$ (cm^2/sec)	Mixing Coefficient** α (cm)
1	Cyclohexane (solvent) displacing n-hexane (oil)	160	1.92	0.329	0.987	0.334	Favourable	0	N/A	0	0.18	0.083
2	N-hexane displacing cyclohexane	160	1.92	0.987	0.329	2.998	Unfavourable	0	N/A	0	14.4	6.467
3	N-hexane displacing 20% PV slug of cyclohexane	160	1.92	0.987	0.329	2.998	Unfavourable#	0	Cyclohexane	20	4.23	1.906
4	N-hexane displacing 30% PV slug of cyclohexane	160	1.92	0.987	0.329	2.998	Unfavourable#	0	Cyclohexane	30	5.5	2.477
5	Cyclohexane displacing 20% PV slug of n-hexane	160	1.92	0.329	0.987	0.334	Favourable#	0	N-hexane	20	0.71	0.322
6	Cyclohexane displacing 30% PV slug of n-hexane	160	1.92	0.329	0.987	0.334	Favourable#	0	N-hexane	30	1.10	0.494

* Average dispersion coefficient (10%-90%) concentration basis.

** Average mixing coefficient (10%-90%) concentration basis.

Mobility ratio at the second front for a miscible slug run.

Table 6-2: Dispersion and Mixing Coefficients for the Aqueous Fluid System Displacements at Zero Immobile Oil Saturation in Unconsolidated Core No. 2

Run No.	Test Description	Displacement Rate (cc/hr)	Fluid Velocity (m/day)	Displaced Fluid Viscosity (cp)	Displacing Fluid Viscosity (cp)	Mobility Ratio (M)	Mobility Ratio Type	Immobile Oil Saturation (% PV)	Slug Type	Slug Size (% PV)	Dispersion Coefficient* $K_e \times 10^{-3}$ (cm^2/sec)	Mixing Coefficient** α (cm)
7	10% brine displacing 2% brine	160	1.92	1.013	1.171	0.865	Favourable	0	N/A	0	3.39	1.525
8	2% brine displacing 10% brine	160	1.92	1.171	1.013	1.156	Unfavourable	0	N/A	0	1.26	0.566
9	2% brine displacing 20% PV slug of 10% brine	160	1.92	1.171	1.013	1.156	Unfavourable#	0	10% Brine	20	0.59	0.265
10	2% brine displacing 30% PV slug of 10% brine	160	1.92	1.171	1.013	1.156	Unfavourable#	0	10% Brine	30	1.21	0.546
11	10% brine displacing 20% PV slug of 2% brine	160	1.92	1.013	1.171	0.865	Favourable#	0	2% Brine	20	0.82	0.368
12	10% brine displacing 30% PV slug of 2% brine	160	1.92	1.013	1.171	0.865	Favourable#	0	2% Brine	30	1.23	0.552

* Average dispersion coefficient (10%-90%) concentration basis.

** Average mixing coefficient (10%-90%) concentration basis.

Mobility ratio at the second front for a miscible slug run.

Table 6-3: Dispersion and Mixing Coefficients for the Oleic Fluid System Displacements at 25% Immobile Water Saturation in Unconsolidated Core No. 3

Run No.	Test Description	Displacement Rate (cc/hr)	Fluid Velocity (m/day)	Displaced Fluid Viscosity (cp)	Displacing Fluid Viscosity (cp)	Mobility Ratio (M)	Mobility Ratio Type	Immobile Water Saturation (% PV)	Slug Type	Slug Size (% PV)	Dispersion Coefficient* $K_e \times 10^{-3}$ (cm^2/sec)	Mixing Coefficient** α (cm)
13	Cyclohexane (solvent) displacing n-hexane (oil)	160	1.92	0.329	0.987	0.334	Favourable	25	N/A	0	3.39	1.525
14	N-hexane displacing cyclohexane	160	1.92	0.987	0.329	2.998	Unfavourable	25	N/A	0	3.37	1.52
15	N-hexane displacing 20% PV slug of cyclohexane	160	1.92	0.987	0.329	2.998	Unfavourable#	25	Cyclohexane	20	0.90	0.404
16	N-hexane displacing 30% PV slug of cyclohexane	160	1.92	0.987	0.329	2.998	Unfavourable#	25	Cyclohexane	30	1.58	0.71
17	Cyclohexane displacing 20% PV slug of n-hexane	160	1.92	0.329	0.987	0.334	Favourable#	25	N-hexane	20	0.99	0.448
18	Cyclohexane displacing 30% PV slug of n-hexane	160	1.92	0.329	0.987	0.334	Favourable#	25	N-hexane	30	1.66	0.747

* Average dispersion coefficient (10%-90%) concentration basis.

** Average mixing coefficient (10%-90%) concentration basis.

Mobility ratio at the second front for a miscible slug run.

more brine was expelled from the core. At this point, the water saturation was 10% pore volume.

Runs 25 - 30, similar to Runs 13 - 18, were conducted at 10% immobile water saturation. The results are given in Table 6-4.

Runs 13 - 18 and Runs 25 - 30 were correspondingly compared with Runs 1 - 6, at favourable and unfavourable mobility ratios, with and without an immobile phase presence. The results of this series of runs are summarized in Table 6-5.

6.4 Miscible Displacement in the Presence of an Immobile Oil Phase

At this point, a newly prepared glass bead core was ready to conduct miscible brine displacements in the presence of an immobile oil phase. In these runs, n-hexane was used to saturate the core. A large volume of 2% (by weight) brine was then injected into the core until the quantity of n-hexane in the produced brine was less than 1% by volume.

Experimental Runs 19 - 24 were conducted in the presence of 26% immobile oil saturation. The results are given in Table 6-6.

Again, in order to carry out experiments at a lower oil saturation, 5% PV isopropyl alcohol was injected into a newly prepared glass bead core (with a known immobile oil saturation) to reduce oil saturation, followed by a large volume of 2% (by weight) brine. As a result, an immobile oil saturation of 8% PV was obtained.

Experimental Runs 31 - 36, similar to Runs 19 - 24 were carried out at the mean immobile oil saturation of 8% PV. The results are shown in Table 6-7.

Runs 19 - 24 and Runs 31 - 36 were correspondingly compared with Runs 7 - 12, at favourable and unfavourable mobility ratios, with and without immobile phase present. The results of this series of tests are given in Table 6-8.

Table 6-4: Dispersion and Mixing Coefficients for the Oleic Fluid System Displacements at 10% Immobile Water Saturation in Unconsolidated Core No. 5

Run No.	Test Description	Displacement Rate (cc/hr)	Fluid Velocity (m/day)	Displaced Fluid Viscosity (cp)	Displacing Fluid Viscosity (cp)	Mobility Ratio (M)	Mobility Ratio Type	Immobile Water Saturation (% PV)	Slug Type	Slug Size (% PV)	Dispersion Coefficient* $K_e \times 10^{-3}$ (cm^2/sec)	Mixing Coefficient** α (cm)
25	Cyclohexane (solvent) displacing n-hexane (oil)	160	1.92	0.329	0.987	0.334	Favourable	10	N/A	0	3.39	1.525
26	N-hexane displacing cyclohexane	160	1.92	0.987	0.329	2.998	Unfavourable	10	N/A	0	4.41	1.984
27	N-hexane displacing 20% PV slug of cyclohexane	160	1.92	0.987	0.329	2.998	Unfavourable#	10	Cyclohexane	20	1.22	0.548
28	N-hexane displacing 30% PV slug of cyclohexane	160	1.92	0.987	0.329	2.998	Unfavourable#	10	Cyclohexane	30	1.20	0.538
29	Cyclohexane displacing 20% PV slug of n-hexane	160	1.92	0.329	0.987	0.334	Favourable#	10	N-hexane	20	1.70	0.767
30	Cyclohexane displacing 30% PV slug of n-hexane	160	1.92	0.329	0.987	0.334	Favourable#	10	N-hexane	30	1.88	0.847

* Average dispersion coefficient (10%-90%) concentration basis.

** Average mixing coefficient (10%-90%) concentration basis.

\# Mobility ratio at the second front for a miscible slug run.

Table 6-5: Dispersion and Mixing Coefficients for the Oleic Fluid System Displacements at Various Immobile Water Saturations.

Run No.	Test Description	Displacement Rate (cc/hr)	Fluid Velocity (m/day)	Displaced Fluid Viscosity (cp)	Displacing Fluid Viscosity (cp)	Mobility Ratio (M)	Mobility Ratio Type	Immobile Water Saturation (% PV)	Slug Type	Slug Size (% PV)	Dispersion Coefficient* $K_d \times 10^{-3}$ (cm^2/sec)	Mixing Coefficient** α (cm)
1	Cyclohexane (solvent) displacing n-hexane (oil)	160	1.92	0.329	0.987	0.334	Favourable	0	N/A	0	0.18	0.083
2	N-hexane displacing cyclohexane	160	1.92	0.987	0.329	2.998	Unfavourable	0	N/A	0	14.4	6.467
3	N-hexane displacing 20% PV slug of cyclohexane	160	1.92	0.987	0.329	2.998	Unfavourable	0	Cyclohexane	20	4.23	1.906
4	N-hexane displacing 30% PV slug of cyclohexane	160	1.92	0.987	0.329	2.998	Unfavourable	0	Cyclohexane	30	5.5	2.477
5	Cyclohexane displacing 20% PV slug of n-hexane	160	1.92	0.329	0.987	0.334	Favourable	0	N-hexane	20	0.71	0.322
6	Cyclohexane displacing 30% PV slug of n-hexane	160	1.92	0.329	0.987	0.334	Favourable	0	N-hexane	30	1.10	0.494
13	Cyclohexane (solvent) displacing n-hexane (oil)	160	1.92	0.329	0.987	0.334	Favourable	25	N/A	0	3.39	1.525
14	N-hexane displacing cyclohexane	160	1.92	0.987	0.329	2.998	Unfavourable	25	N/A	0	3.37	1.52
15	N-hexane displacing 20% PV slug of cyclohexane	160	1.92	0.987	0.329	2.998	Unfavourable	25	Cyclohexane	20	0.90	0.404
16	N-hexane displacing 30% PV slug of cyclohexane	160	1.92	0.987	0.329	2.998	Unfavourable	25	Cyclohexane	30	1.58	0.71
17	Cyclohexane displacing 20% PV slug of n-hexane	160	1.92	0.329	0.987	0.334	Favourable	25	N-hexane	20	0.99	0.448
18	Cyclohexane displacing 30% PV slug of n-hexane	160	1.92	0.329	0.987	0.334	Favourable	25	N-hexane	30	1.66	0.747
25	Cyclohexane (solvent) displacing n-hexane (oil)	160	1.92	0.329	0.987	0.334	Favourable	10	N/A	0	3.39	1.525
26	N-hexane displacing cyclohexane	160	1.92	0.987	0.329	2.998	Unfavourable	10	N/A	0	4.41	1.984
27	N-hexane displacing 20% PV slug of cyclohexane	160	1.92	0.987	0.329	2.998	Unfavourable	10	Cyclohexane	20	1.22	0.548
28	N-hexane displacing 30% PV slug of cyclohexane	160	1.92	0.987	0.329	2.998	Unfavourable	10	Cyclohexane	30	1.20	0.538
29	Cyclohexane displacing 20% PV slug of n-hexane	160	1.92	0.329	0.987	0.334	Favourable	10	N-hexane	20	1.70	0.767
30	Cyclohexane displacing 30% PV slug of n-hexane	160	1.92	0.329	0.987	0.334	Favourable	10	N-hexane	30	1.88	0.847

Table 6-6: Dispersion and Mixing Coefficients for the Aqueous Fluid System Displacements at 26% Immobile Oil Saturation in Unconsolidated Core No. 4

Run No.	Test Description	Displacement Rate (cc/hr)	Fluid Velocity (m/day)	Displaced Fluid Viscosity (cp)	Displacing Fluid Viscosity (cp)	Mobility Ratio (M)	Mobility Ratio Type	Immobile Oil Saturation (% PV)	Slug Type	Slug Size (% PV)	Dispersion Coefficient* $K_e \times 10^{-3}$ (cm^2/sec)	Mixing Coefficient** α (cm)
19	10% brine displacing 2% brine	160	1.92	1.013	1.171	0.865	Favourable	26	N/A	0	2.68	1.205
20	2% brine displacing 10% brine	160	1.92	1.171	1.013	1.156	Unfavourable	26	N/A	0	0.51	0.231
21	2% brine displacing 20% PV slug of 10% brine	160	1.92	1.171	1.013	1.156	Unfavourable#	26	10% Brine	20	0.61	0.275
22	2% brine displacing 30% PV slug of 10% brine	160	1.92	1.171	1.013	1.156	Unfavourable#	26	10% Brine	30	1.16	0.522
23	10% brine displacing 20% PV slug of 2% brine	160	1.92	1.013	1.171	0.865	Favourable#	26	2% Brine	20	0.74	0.332
24	10% brine displacing 30% PV slug of 2% brine	160	1.92	1.013	1.171	0.865	Favourable#	26	2% Brine	30	1.14	0.513

* Average dispersion coefficient (10%-90%) concentration basis.

** Average mixing coefficient (10%-90%) concentration basis.

Mobility ratio at the second front for a miscible slug run.

Table 6-7: Dispersion and Mixing Coefficients for the Aqueous Fluid System Displacements at 8% Immobile Oil Saturation in Unconsolidated Core No. 6

Run No.	Test Description	Displacement Rate (cc/hr)	Fluid Velocity (m/day)	Displaced Fluid Viscosity (cp)	Displacing Fluid Viscosity (cp)	Mobility Ratio (M)	Mobility Ratio Type	Immobile Oil Saturation (% PV)	Slug Type	Slug Size (% PV)	Dispersion Coefficient* $K_d \times 10^{-3}$ (cm^2/sec)	Mixing Coefficient** α (cm)
31	10% brine displacing 2% brine	160	1.92	1.013	1.171	0.865	Favourable	8	N/A	0	2.67	1.205
32	2% brine displacing 10% brine	160	1.92	1.171	1.013	1.156	Unfavourable	8	N/A	0	0.75	0.337
33	2% brine displacing 20% PV slug of 10% brine	160	1.92	1.171	1.013	1.156	Unfavourable#	8	10% Brine	20	0.55	0.245
34	2% brine displacing 30% PV slug of 10% brine	160	1.92	1.171	1.013	1.156	Unfavourable#	8	10% Brine	30	1.07	0.481
35	10% brine displacing 20% PV slug of 2% brine	160	1.92	1.013	1.171	0.865	Favourable#	8	2% Brine	20	0.67	0.302
36	10% brine displacing 30% PV slug of 2% brine	160	1.92	1.013	1.171	0.865	Favourable#	8	2% Brine	30	1.23	0.552

* Average dispersion coefficient (10%-90%) concentration basis.

** Average mixing coefficient (10%-90%) concentration basis.

Mobility ratio at the second front for a miscible slug run.

Table 6-8: Dispersion and Mixing Coefficients for the Aqueous Fluid System Displacements at Various Immobile Oil Saturations.

Run No.	Test Description	Rate (cc/hr)	Velocity (m/day)	Viscosity (cp)	Viscosity (cp)	Ratio (M)	Type	Saturation (% PV)	Type	Size (% PV)	$K_g \times 10^{-3}$ (cm^3/sec)	α (cm)
7	10% brine displacing 2% brine	160	1.92	1.013	1.171	0.865	Favourable	0	N/A	0	3.39	1.525
8	2% brine displacing 10% brine	160	1.92	1.171	1.013	1.156	Unfavourable	0	N/A	0	1.26	0.566
9	2% brine displacing 20% PV slug of 10% brine	160	1.92	1.171	1.013	1.156	Unfavourable	0	10% Brine	20	0.59	0.265
10	2% brine displacing 30% PV slug of 10% brine	160	1.92	1.171	1.013	1.156	Unfavourable	0	10% Brine	30	1.21	0.546
11	10% brine displacing 20% PV slug of 2% brine	160	1.92	1.013	1.171	0.865	Favourable	0	2% Brine	20	0.82	0.368
12	10% brine displacing 30% PV slug of 2% brine	160	1.92	1.013	1.171	0.865	Favourable	0	2% Brine	30	1.23	0.552
19	10% brine displacing 2% brine	160	1.92	1.013	1.171	0.865	Favourable	26	N/A	0	2.68	1.205
20	2% brine displacing 10% brine	160	1.92	1.171	1.013	1.156	Unfavourable	26	N/A	0	0.51	0.231
21	2% brine displacing 20% PV slug of 10% brine	160	1.92	1.171	1.013	1.156	Unfavourable	26	10% Brine	20	0.61	0.275
22	2% brine displacing 30% PV slug of 10% brine	160	1.92	1.171	1.013	1.156	Unfavourable	26	10% Brine	30	1.16	0.522
23	10% brine displacing 20% PV slug of 2% brine	160	1.92	1.013	1.171	0.865	Favourable	26	2% Brine	20	0.74	0.332
24	10% brine displacing 30% PV slug of 2% brine	160	1.92	1.013	1.171	0.865	Favourable	26	2% Brine	30	1.14	0.513
31	10% brine displacing 2% brine	160	1.92	1.013	1.171	0.865	Favourable	8	N/A	0	2.67	1.205
32	2% brine displacing 10% brine	160	1.92	1.171	1.013	1.156	Unfavourable	8	N/A	0	0.75	0.337
33	2% brine displacing 20% PV slug of 10% brine	160	1.92	1.171	1.013	1.156	Unfavourable	8	10% Brine	20	0.55	0.245
34	2% brine displacing 30% PV slug of 10% brine	160	1.92	1.171	1.013	1.156	Unfavourable	8	10% Brine	30	1.07	0.481
35	10% brine displacing 20% PV slug of 2% brine	160	1.92	1.013	1.171	0.865	Favourable	8	2% Brine	20	0.67	0.302
36	10% brine displacing 30% PV slug of 2% brine	160	1.92	1.013	1.171	0.865	Favourable	8	2% Brine	30	1.23	0.552

6.5 Effect of an Immobile Water Phase on the Mixing Coefficient

The effect of any water saturation at an irreducible level or at a level below the irreducible, in a water-wet porous medium, is to decrease the mixing coefficient in the oil phase. This is due to the fact that water will tend to be localized within the smallest pores and at the core matrix surface in a way that it becomes part of the core matrix. This will considerably decrease the displacement pore volume and at the same time provide a more uniform pore space.

Raimondi et al.[58] indicated that the mixing coefficient will appreciably decrease only in the region of irreducible water, whereas above irreducible water the coefficient of mixing will tend to increase.

From Runs 1, 25 and 13 (0%, 10% and 25%, respectively), it is clearly seen that the mixing coefficient α increases when an immobile water phase is present (0.083, 1.525 and 1.525, respectively, i.e. when the mixing coefficient increases, the mixing zone becomes longer and consequently, the displacement becomes less efficient). However, the mixing coefficient α was found to be the same for both 10% and 25% immobile water saturations (1.525 for both).

For the 20% PV miscible slug Runs 5, 29 and 17 were compared. It was again evident that the mixing coefficient α (0.322, 0.767 and 0.448, respectively) increased when immobile water saturations were present. However, the mixing coefficient α registers the highest increase when 10% immobile water saturation was present.

Similarly, for the 30% PV miscible slug Runs 6, 30 and 18 were compared and the result showed that as the immobile water saturation increases, the mixing coefficient α (0.494, 0.847 and 1.525, respectively) also increases.

In general, it is concluded that the mixing coefficient α will tend to increase as the immobile water phase increases and this would lead to a less efficient displacement process.

6.6 Effect of an Immobile Oil Phase Saturation on the Mixing Coefficient

The case of a residual oil saturation is more complex than that of a immobile water saturation. This is due to the fact that any residual oil in a water-wet porous medium will be confined to the central portion of the pore spaces. Some of the oil may occupy the larger pores. When the oil droplets occur in the central part of the pores, the effective pore diameter will decrease in a rather unpredictable manner.

For the continuous miscible displacement Runs 7, 31 and 19, the mixing coefficient α (1.525, 1.205 and 1.205, respectively) was found to decrease in the presence of an immobile oil saturation (0%, 8% and 26%, respectively). However, the mixing coefficient α (1.205) was found to be the same for both 8% and 26% immobile oil saturations.

For the 20% PV miscible slug Runs 11, 35 and 23 were compared. The result showed that as the immobile oil saturation increases (0%, 8% and 26%, respectively), the mixing coefficient α (0.368, 0.302 and 0.275, respectively) decreases.

Similarly, for the 30% PV miscible slug Runs 12, 36 and 24 were compared, noticing that as the immobile oil saturation increases (0%, 8% and 26%, respectively), the mixing coefficient α (0.552, 0.552 and 0.513, respectively) decreases; however, it was noticed that when 8% immobile oil saturation was present and for the case where no immobile oil phase was present, the mixing coefficient α (0.552) did not change.

Generally, it is noticed that the mixing coefficient α decreases as the immobile oil saturation increases. This finding is the opposite to that for displacements in the presence of immobile water saturations.

6.7 Effect of Immobile Aqueous and Oleic Phase Saturation on the Mixing Coefficient

Continuous miscible displacement Runs 25 and 13, where 10% and 25% immobile water saturations were present, respectively, were conducted for comparison

with Run 1 which was conducted in the presence of zero immobile water saturation. The results showed that when an immobile water phase was present, the mixing coefficient α (1.525, 1.525 and 0.083, respectively) increased. However, the mixing coefficient α remained the same (1.525) the immobile water saturation was decreased from 25% to 10% PV.

In the case of miscible displacements conducted in the presence of various immobile oil saturations as in Runs 31 and 19, where 8% and 26% immobile oil saturations were present, respectively, the mixing coefficient α (1.205, 1.205 and 1.525, respectively) was found to decrease when compared with Run 7 conducted when no immobile oil saturation was present. Here, again, the mixing coefficient α (1.205) remained the same as the immobile oil saturation was decreased from 26% to 8% PV.

From the above findings, we clearly see that a trend exists between the two different fluid systems when an immobile saturation was present in each case. This trend was found when comparing Runs 25 and 13, where 10% and 25% immobile water saturations were present, respectively, with Runs 31 and 19, where 8% and 26% immobile oil saturations were present, respectively. When the immobile water saturation was reduced from 25% as in Run 13 to 10% as in Run 25, the mixing coefficient α did not change (1.525 for both), meanwhile, when the immobile oil saturation was reduced from 26% as in Run 31 to 8% as in Run 19, the mixing coefficient α again did not change (1.205 for both).

6.8 Effect of Immobile Aqueous and Oleic Phase Saturation on the Mixing Coefficient in a Miscible Slug Process

For the 20% PV miscible slug Runs 5, 29 and 17 (where zero, 10% and 25% immobile water saturations were present, respectively), it was evident that the mixing coefficient α (0.322, 0.767 and 0.448, respectively) increases when immobile water saturations were present. However, the mixing coefficient α registered the highest increase (0.767) when 10% immobile water saturation was present.

Similarly, 30% PV miscible slug Runs 6, 30 and 18 were compared and the results showed that as the immobile water saturation increases, the mixing coefficient

α (0.494, 0.847 and 1.525, respectively) also increases. In general, it is concluded that the mixing coefficient α will tend to increase as the immobile water phase increases for miscible slug runs.

However, for the case of miscible slug runs conducted in the presence of various immobile oil saturations, the results were different. The 20% PV miscible slug Runs 11, 35 and 23 were compared and the results showed that as the immobile oil saturation increases (0%, 8% and 26%, respectively), the mixing coefficient α (0.368, 0.302 and 0.275, respectively) decreases.

Similarly, for the 30% PV miscible slug Runs 12, 36 and 24 were compared; it was found that as the immobile oil saturation increases (0%, 8% and 26%, respectively), the mixing coefficient α (0.552, 0.552 and 0.513, respectively) decreases; however, it was noticed that when zero or 8% immobile oil saturation was present, the mixing coefficient α did not change. It is concluded that in general the mixing coefficient α will tend to decrease as the immobile oil phase increases for miscible slug runs.

6.9 Effect of Slug Size on the Mixing Coefficient in the Presence of Various Immobile Aqueous and Oleic Phases

Two different slug sizes, 20% and 30% PVs were employed in these experimental runs. The objective of these runs was to investigate the effect of slug size on the mixing coefficient in the presence of various immobile aqueous and oleic phases.

The mixing coefficients α (0.322, 0.767 and 0.448, respectively) for the 20% PV miscible slug Runs 5, 29 and 17 which were conducted in the presence of zero, 10% and 25% immobile water saturations, respectively, were compared with the mixing coefficients α (0.494, 0.847 and 1.525, respectively) obtained from the 30% PV miscible slug Runs 6, 30 and 18, respectively. The mixing coefficient α was found to increase as the slug size increased.

Similarly, the mixing coefficients α (0.368, 0.302 and 0.275, respectively) for the 20% PV miscible slug Runs 11, 35 and 23 which were conducted in the presence of zero, 8% and 26% immobile oil saturations, respectively, were compared with the

mixing coefficients α (0.552, 0.552 and 0.513, respectively) obtained from the 30% PV miscible slug Runs 12, 36 and 24, respectively. The mixing coefficient α was again found to increase as the slug size increased.

In general, it is concluded that the mixing coefficient α will tend to increase as the slug size increases, regardless of whether an immobile oil or water saturation is present.

6.10 Effect of Mobility Ratio on Miscible Displacement

A total of thirty-six experimental runs were conducted in this investigation, one-half of which were conducted at an unfavourable mobility ratio. In the previous sections, full discussions and analysis for various factors and variables were carried out for experiments conducted at favourable mobility ratios only.

These experiments were analyzed by employing the Brigham[75] method which is based on the standard convective-diffusion equation, utilizing Fick's law, and accounting only for favourable mobility ratios.

However, since there are no analytical models that account for the effect of the unfavourable mobility ratio on a miscible displacement process, and in order to carry out the investigation of the effect of an unfavourable mobility ratio on the mixing coefficient α under various conditions, the Brigham model was again used, even though the standard convective-diffusion approach to miscible displacement does not hold for unfavourable mobility ratios.

6.10.1 Effect of an Unfavourable Mobility Ratio on the Mixing Coefficient in the Presence of an Immobile Water Phase

Runs 2, 26 and 14 were continuous miscible displacements conducted in the presence of zero, 10% and 25% immobile water saturations, respectively, at unfavourable mobility ratios (M=3.0). The result clearly indicates that the mixing coefficient α (6.467, 1.984 and 1.52, respectively) decreases significantly as the immobile water saturation increases.

Figures B-2.1, B-14.1 and B-26.1 were compared and the results showed that as the immobile water saturation increased, the tendency of the probability plot to become non-linear increased, and this was quite evident in the calculation of the mixing coefficients.

6.10.2 Effect of an Unfavourable Mobility Ratio on the Mixing Coefficient in the Presence of an Immobile Oil Phase

The mixing coefficients α (0.566, 0.337 and 0.231, respectively) for the continuous miscible displacement Runs 8, 32 and 20 which were conducted in the presence of zero, 8% and 26% immobile oil saturations, respectively, at unfavourable mobility ratios (M=1.156) will tend to decrease as the immobile oil saturation increases.

Figures B-8.1, B-20.1 and B-32.1 were compared and the results showed that as the immobile oil saturation increased, the tendency of the probability plot to become non-linear increased. However, the tendency of becoming non-linear was less pronounced when compared with Figures B-2.1, B-14.1 and B-26.1.

6.10.3 Effect of an Unfavourable Mobility Ratio on the Mixing Coefficient in the Presence of Various Immobile Aqueous and Oleic Phases

Continuous miscible displacement Runs 26 and 14, where 10% and 25% immobile water saturations were present, respectively, were conducted for comparison with Run 2 which was conducted in the presence of zero immobile water saturation. The result showed that when an immobile water phase was present, the mixing coefficient α (1.984, 1.52 and 6.467, respectively) decreased. Furthermore, as the immobile water saturation was increased, the mixing coefficient α decreased again.

In the case of miscible displacements conducted in the presence of various immobile oil saturations as in Runs 32 and 20, where 8% and 26% immobile oil saturations were present, respectively, the mixing coefficient α (0.337 and 0.231,

respectively) was found to decrease constantly as the immobile oil saturation was increased.

6.10.4 Effect of an Unfavourable Mobility Ratio on the Mixing Coefficient in the Presence of Various Immobile Aqueous and Oleic Phases for a Miscible Slug Process

For the 20% PV miscible slug Runs 3, 27 and 15 were carried out (where zero, 10% and 25% immobile water saturations were present, respectively). It was quite evident that the mixing coefficient α (1.906, 0.548 and 0.404, respectively) decreased when an immobile water saturation was present. As the immobile water saturation was increased, the mixing coefficient α decreased again.

Similarly, for 30% PV miscible slug Runs 4, 28 and 16 were compared, and the results showed that as the immobile water saturation increased (0%, 10% and 25%, respectively), the mixing coefficient α (2.477, 0.538 and 0.71, respectively) decreased; however, the mixing coefficient α registered the highest decrease when 10% immobile water saturation was present.

Miscible slug Runs 9, 33 and 21, where 20% PV slugs were employed, were conducted in the presence of zero, 8% and 26% immobile oil saturations, respectively. These runs were then compared and the results showed that as the immobile oil saturation was increased to 8% PV, the mixing coefficient α (0.265 and 0.245, respectively) decreased. However, it was noticed that when the immobile oil saturation was increased to 26% PV, the process was reversed and the mixing coefficient α (0.275) increased to a value higher than the one obtained from Run 9, when zero immobile oil saturation was present.

Similarly, for 30% PV miscible slug Runs 10, 34 and 22 were compared; it was noted that as the immobile oil saturation increased (0%, 8% and 26%, respectively), the mixing coefficient α (0.546, 0.481 and 0.522, respectively) decreased; however, the mixing coefficient α registered the highest decrease (0.481) when 8% immobile oil saturation was present.

6.10.5 Effect of Various Slug Sizes on the Mixing Coefficient in the Presence of Various Immobile Aqueous and Oleic Phases at Unfavourable Mobility Ratios

Again, 20% and 30% PV slug sizes were employed to investigate the effect of slug size on the mixing coefficient, in the presence of various immobile aqueous and oleic phases at unfavourable mobility ratios.

For the 20% PV miscible slug Runs 3, 27 and 15 (which were conducted in the presence of zero, 10% and 25% immobile water saturations, respectively) were compared with the 30% PV miscible slug Runs 4, 28 and 16, respectively. The mixing coefficient α was found to increase for the zero (from 1.906 to 2.477, respectively), and the 25% (from 0.404 to 0.71, respectively) immobile water saturation runs as the slug size increased, however, it registered a decrease for the 10% immobile water saturation (from 0.548 to 0.538, respectively).

Similarly, for the 20% PV miscible slug Runs 9, 33 and 21 (which were conducted in the presence of zero, 8% and 26% immobile oil saturations, respectively) were compared with the 30% PV miscible slug Runs 10, 34 and 22, respectively. The mixing coefficient α was again found to increase as the slug size increased (from 0.265 to 0.546, from 0.245 to 0.481 and from 0.275 to 0.522, respectively).

In general, it is concluded that the mixing coefficient α will tend to increase as the slug size increases, regardless of whether an immobile oil or water saturations is present.

6.11 Effect of Favourable Mobility Ratio on the Mixing Coefficient in the Absence of an Immobile Phase Saturation for the Continuous and the Miscible Slug Displacement Process

Runs 1, 5 and 6 were conducted at a favourable mobility ratio (M=0.334) employing the oleic fluid system; they were compared, and the results showed that the mixing coefficient α (0.083, 0.322 and 0.494, respectively) increased as the slug size

increased from 20% PV to 30% PV; however, for Run 1, where a continuous miscible displacement was conducted, a very sharp decrease was registered (0.083) for the mixing coefficient α.

Similarly, Runs 12, 11 and 7 were conducted at a favourable mobility ratio (M=0.865), employing the aqueous fluid system; they were compared, and the results showed that the mixing coefficient α (0.368, 0.552, and 1.525, respectively) increased as the slug size increased from 20% PV to 30% PV. The mixing coefficient α registered the highest increase in Run 7 (1.525), where a continuous miscible displacement was conducted.

6.12 Effect of Favourable Mobility Ratio on the Mixing Coefficient in the Presence of an Immobile Phase Saturation for the Continuous and the Miscible Slug Displacement Process

Runs 30, 29 and 25 were conducted at a favourable mobility ratio (M=0.334), employing the oleic fluid system at an immobile water saturation of 10%; they were compared, and the results showed that the mixing coefficient α (0.767, 0.847 and 1.525, respectively) increased as the slug size increased from 20% PV to 30% PV. Again, for Run 25, where a continuous miscible displacement was conducted, the mixing coefficient α registered its highest value at (1.525).

Similarly, Runs 35, 36 and 31 were conducted at a favourable mobility ratio (M=0.865), employing the aqueous fluid system at an immobile oil saturation of 8%; they were compared, and the results showed that the mixing coefficient α (0.302, 0.552 and 1.205, respectively) increased as the slug size increased from 20% PV to 30% PV. The mixing coefficient α registered the highest increase in Run 31 (1.205), where a continuous miscible displacement was conducted.

Runs 17, 18 and 13 were conducted at a favourable mobility ratio (M=0.334), employing the oleic fluid system at an immobile water saturation of 25%; they were compared, and the results showed that the mixing coefficient α (0.448, 1.525 and 1.525, respectively) increased as the slug size increased from 20% PV to 30% PV; however, it did not change (1.525) for the continuous miscible displacement Run 13.

Similarly, Runs 23, 24 and 19 were conducted at a favourable mobility ratio (M=0.865) employing the aqueous fluid system at an immobile oil saturation of 26%; they were compared, and the results showed that the mixing coefficient α (0.275, 0.513 and 1.205, respectively) increased as the slug size increased from 20% PV to 30% PV. The mixing coefficient α registered the highest increase in Run 13 (1.205), where a continuous miscible displacement was conducted.

In general, it is concluded that the mixing coefficient α will tend to increase as the slug size increased, regardless of whether an immobile oil or water saturations is present at favourable mobility ratios. Table 6-10 summarizes the α values for various runs at favourable and unfavourable mobility ratios, and different immobile saturations.

6.13 Effect of the Type of Mobility Ratio on the Linearity of the Probability Plot

Effluent concentration plots on arithmetic probability papers were compared for both fluid systems (oleic and aqueous) at favourable and unfavourable mobility ratios.

Runs 7, 31 and 19 were conducted at a favourable mobility ratio (M=0.865), in the presence of 0%, 8% and 26% immobile oil saturations, respectively. These runs were compared, and their plots showed that as the immobile oil saturation decreased, the more linear the plots became. The best plot in terms of linearity was for Run 7 where no immobile oil was present. Runs 8, 32 and 20 were conducted at unfavourable mobility ratio (M=1.156), in the presence of 0%, 8% and 26% immobile oil saturations, respectively. These runs were compared, and their plots showed that as the immobile oil saturation increased, the more linear the plots became; again, it was noticed that the best plot was for Run 8 where no immobile oil was present.

Plots for Runs 7, 31 and 19 at favourable mobility ratio (M=0.865) were correspondingly compared with Runs 8, 32 and 20 at unfavourable mobility ratio (M=1.156), respectively. Results showed that the plots for Runs 7, 31 and 19 at favourable mobility ratio were much more linear than those for the unfavourable mobility ratio.

Tabe 6-10: Summary of the Alpha Values Obtained for the Aqueous and Oleic Fluid System Runs

Test Description	Run #	α (cm)	Immobile Water Saturation
Cyclohexane (solvent) displacing n-hexane (oil) (Fav. M)	1	0.083	0%
Cyclohexane (solvent) displacing n-hexane (oil) (Fav. M)	25	1.525	10%
Cyclohexane (solvent) displacing n-hexane (oil) (Fav. M)	13	1.525	25%
Cyclohexane displacing 20% PV slug of n-hexane (Fav. M)	5	0.322	0%
Cyclohexane displacing 20% PV slug of n-hexane (Fav. M)	29	0.767	10%
Cyclohexane displacing 20% PV slug of n-hexane (Fav. M)	17	0.448	25%
Cyclohexane displacing 30% PV slug of n-hexane (Fav. M)	6	0.494	0%
Cyclohexane displacing 30% PV slug of n-hexane (Fav. M)	30	0.847	10%
Cyclohexane displacing 30% PV slug of n-hexane (Fav. M)	18	1.525	25%
N-hexane displacing cyclohexane (Unfavourable M)	2	6.467	0%
N-hexane displacing cyclohexane (Unfavourable M)	26	1.984	10%
N-hexane displacing cyclohexane (Unfavourable M)	14	1.52	25%
N-hexane displacing 20% PV slug of cyclohexane (Unfav. M)	3	1.906	0%
N-hexane displacing 20% PV slug of cyclohexane (Unfav. M)	27	0.548	10%
N-hexane displacing 20% PV slug of cyclohexane (Unfav. M)	15	0.404	25%
N-hexane displacing 30% PV slug of cyclohexane (Unfav. M)	4	2.477	0%
N-hexane displacing 30% PV slug of cyclohexane (Unfav. M)	28	0.538	10%
N-hexane displacing 30% PV slug of cyclohexane (Unfav. M)	16	0.71	25%

Alpha Values for the Oleic Fluid System Runs

Test Description	Run #	α (cm)	Immobile Oil Saturation
10% brine displacing 2% brine (Favourable M)	7	1.525	0%
10% brine displacing 2% brine (Favourable M)	31	1.205	8%
10% brine displacing 2% brine (Favourable M)	19	1.205	26%
10% brine displacing 20% PV slug of 2% brine (Fav M)	11	0.368	0%
10% brine displacing 20% PV slug of 2% brine (Fav M)	35	0.302	8%
10% brine displacing 20% PV slug of 2% brine (Fav M)	23	0.275	26%
10% brine displacing 30% PV slug of 2% brine (Fav M)	12	0.552	0%
10% brine displacing 30% PV slug of 2% brine (Fav M)	36	0.552	8%
10% brine displacing 30% PV slug of 2% brine (Fav M)	24	0.513	26%
2% brine displacing 10% brine (Unfavourable M)	8	0.566	0%
2% brine displacing 10% brine (Unfavourable M)	32	0.337	8%
2% brine displacing 10% brine (Unfavourable M)	20	0.231	26%
2% brine displacing 20% PV slug of 10% brine (Unfav M)	9	0.265	0%
2% brine displacing 20% PV slug of 10% brine (Unfav M)	33	0.245	8%
2% brine displacing 20% PV slug of 10% brine (Unfav M)	21	0.275	26%
2% brine displacing 30% PV slug of 10% brine (Unfav M)	10	0.546	0%
2% brine displacing 30% PV slug of 10% brine (Unfav M)	34	0.481	8%
2% brine displacing 30% PV slug of 10% brine (Unfav M)	22	0.522	26%

Alpha Values for the Aqueous Fluid System Runs

Similarly, Runs 1, 25 and 13 were conducted at a favourable mobility ratio (M=0.334), in the presence of 0%, 10% and 25% immobile water saturations, respectively. These runs were compared, and their plots showed that the best linear fit was for Run 1 where no immobile water was present; however, Run 13 showed better fit than that for Run 25.

Runs 2, 26 and 14 were conducted at unfavourable mobility ratio (M=3.0), in the presence of 0%, 10% and 25% immobile water saturations, respectively. These runs were compared, and their plots showed that the best linear fit was for Run 2 where no immobile water was present; however, Run 14 showed better fit than that for Run 26.

Plots for Runs 1, 25 and 13 at favourable mobility ratio (M=0.334) were correspondingly compared with Runs 2, 26 and 14 at unfavourable mobility ratio (M=3.0), respectively. Results showed that the plots for Runs 2, 26 and 14 at unfavourable mobility ratio were much more linear than those for the favourable mobility ratio.

6.14 Relative Role of the Type of Immobile Phase on the Mixing Coefficient

From the previous discussions, based on the results of this experimental investigation, the mixing coefficient α decreased in the presence of immobile water saturations (8% and 26%), as compared to displacement in the absence of an immobile water phase (from 1.525 to 1.205, respectively).

On the other hand, the mixing coefficient α increased in the presence of immobile oil saturations (10% and 25%), as compared to displacement in the absence of an immobile oil phase (from 0.083 to 1.525).

6.15 Relative Role of the Type of Porous Medium on the Mixing Coefficient

This experimental investigation was carried out in unconsolidated, homogeneous porous media. Another type of inhomogeneity that is of great interest is that in cemented outcrop or reservoir rocks. Part of the inhomogeneity is of a small geometric scale (from pore to pore). However, there are larger scale inhomogeneities in natural sandstones. That is, the average permeability of the rock varies over distances of few inches or feet.

Dispersion and mixing in sandstone rocks were studied by several investigators[57, 58] in the presence of an immobile phase. They all found that dispersion is larger than one might have suspected from particle size alone (thus reflecting the increased heterogeneity). Perkins and Johnston[8] reported an average value of about σd_p = 0.36 cm. They indicated that this value can be used to approximate the behaviour of several sandstone cores studied.

The σd_p values calculated in this study ranged between 0.033 and 0.29 cm for the various runs conducted at favourable and unfavourable mobility ratios in the presence of various immobile fluid saturations (thus reflecting a decrease in mixing and dispersion when compared to those runs conducted in heterogeneous consolidated sandstones). These values are quite different from that calculated for sandstone cores. This difference gives rise to the different trends of the mixing coefficient α in the presence of an immobile phase between the two studies.

6.16 Reproducibility of Results

Several runs were carried out to test experimental reproducibility. Results are shown in Table 6-9 for Runs 13R (repeat of Run 13), 21R (repeat of Run 21) and 36R (repeat of Run 36), respectively. For Run 13R, the result showed that continuous miscible displacement experiments conducted in the presence of 25% immobile water saturation could be repeated with no change in the result.

However, for the miscible slug process Run 21R that was conducted in the presence of 26% immobile oil saturation at unfavourable mobility ratio, the result was found to change by a value of ±8.7%; the lack of reproducibility in this case may be due to the adverse mobility ratio and the presence of a high immobile oil saturation.

Table 6-9: Dispersion and Mixing Coefficients for the Repeated Experimental Runs.

Run No.	Test Description	Displacement Rate (cc/hr)	Fluid Velocity (m/day)	Displaced Fluid Viscosity (cp)	Displacing Fluid Viscosity (cp)	Mobility Ratio (M)	Mobility Ratio Type	Immobile Water Saturation (% PV)	Slug Type	Slug Size (% PV)	Dispersion Coefficient* $K_d \times 10^{-3}$ (cm^2/sec)	Mixing Coefficient** α (cm)
13	Cyclohexane (solvent) displacing n-hexane (oil)	160	1.92	0.329	0.987	0.334	Favourable	25	N/A	0	3.39	1.525
13 R	Cyclohexane (solvent) displacing n-hexane (oil)	160	1.92	0.329	0.987	0.334	Favourable	25	N/A	0	3.39	1.525
21	2% brine displacing 20% PV slug of 10% brine	160	1.92	1.171	1.013	1.156	Unfavourable#	26	10% Brine	20	0.61	0.275
21 R	2% brine displacing 20% PV slug of 10% brine	160	1.92	1.171	1.013	1.156	Unfavourable#	26	10% Brine	20	0.56	0.251
36	10% brine displacing 30% PV slug of 2% brine	160	1.92	1.013	1.171	0.865	Favourable#	8	2% Brine	30	1.23	0.552
36 R	10% brine displacing 30% PV slug of 2% brine	160	1.92	1.013	1.171	0.865	Favourable#	8	2% Brine	30	1.18	0.531

* Average dispersion coefficient (10%-90%) concentration basis.

** Average mixing coefficient (10%-90%) concentration basis.

Mobility ratio at the second front for a miscible slug run.

Run 36R, however, was reproduced within ±3.8% when compared with Run 36, indicating good reproducibility.

The percentage values refers to the change in mixing coefficients when compared to the original runs.

7. Summary and Conclusions

7.1 Summary

In this study, a total of thirty-six experiments were conducted to investigate convective mixing in unconsolidated porous medium in the presence of both water and oil immobile phases at favourable and unfavourable mobility ratios. Continuous miscible and miscible slug-type displacements were carried out in glass bead packs..

The miscible displacement in the case of an immobile water phase employed cyclohexane and n-hexane as the displacing and the displaced fluids, respectively, giving a favourable mobility ratio (M=0.334). However, fluids were reversed for the case of unfavourable mobility ratio (M=3.0) runs.

Similarly, for the case of an immobile oil phase, two brines of two different concentrations (10% and 2%, by weight, calcium chloride brines, respectively) were employed as the displacing and the displaced fluids, respectively, giving a favourable mobility ratio (M=0.865). Again, these fluids were reversed for the unfavourable mobility ratio (M=1.156) runs.

Three different immobile phase (water and oil) saturations were employed in these runs (0%, 10% and 25% immobile water saturations, 0%, 8% and 26% immobile oil saturations, respectively) for the continuous miscible and miscible slug-type displacements at favourable and unfavourable mobility ratios.

A total of eighteen experimental runs for the continuous miscible and miscible slug-type displacements were carried out at favourable mobility ratios, the rest were conducted at unfavourable mobility ratios for comparison purposes.

Both the water and oil saturations were lowered below the usual minimum values by the injection of 5% PV alcohol slugs. One stable flood advance rate 160 cc/hr (1.92 m/day) was used throughout this experimental investigation.

The concentration profiles obtained in the displacements were analyzed using Brigham's[75] method, from which, the dispersion coefficients were calculated. Then, Raimondi et al.[10] equations were used to compute the mixing coefficients α, which

were then correlated with the amount and type of the immobile saturation, slug size (for miscible slug-type displacements), and the type of mobility ratio.

7.2 Conclusions

The following conclusions are based on the experimental results obtained in this study:

1) For an oleic miscible displacement fluid system, at a favourable mobility ratio and in the presence of an immobile water phase (brine), the mixing coefficient α was found to increase with an increase in the immobile water saturation; however, it remained unchanged for both 10% and 25% immobile water saturations.

2) For an aqueous miscible displacement fluid system, at a favourable mobility ratio and in the presence of an immobile oil phase (n-hexane), the mixing coefficient α was found to decrease with an increase in the immobile oil saturation; however, it remained unchanged for both 8% and 26% immobile oil saturations.

3)a) For the various miscible-slug runs conducted in the presence of various immobile water saturations, the mixing coefficient α was found to increase as the immobile water saturation increased, however, the highest increase was registered when 10% immobile water saturation was present.

b) For the various miscible-slug runs conducted in the presence of various immobile oil saturations, the mixing coefficient α was found to decrease as the immobile oil saturation increased; however, the mixing coefficient α did not change for the case when both zero and 8% immobile oil were present.

4)a) For continuous miscible displacement runs at unfavourable mobility ratios, the mixing coefficient α decreased as the immobile water and oil saturations increased.

b) For miscible-slug displacement runs at unfavourable mobility ratios, the mixing coefficient α decreased as the immobile water and oil saturations increased.

c) The mixing coefficient α tends to increase as the slug size increases, regardless of the presence of any immobile fluid (oil or water) phase for both, favourable and unfavourable mobility ratio runs.

5) The type of porous medium is of great importance to convective mixing in miscible displacement. The more homogeneous the rock type, the more pronounced the effect of convective mixing in the presence of an immobile phase saturation becomes.

References

1. Stalkup,F.I., Jr.: "Miscible Displacement"; Henry L. Doherty Series, SPE, 1984, Monograph Vol.8.

2. Taylor, G.I.: "Dispersion of Soluble Matter in Solvent Flowing Slowly Through a Tube"; Proc. Roy.Soc.(1953), Vol.219, p186.

3. van der Poel, C.: "Effect of Lateral Diffusivity on Miscible Displacement in Horizontal Reservoirs"; Soc. Pet. Eng. Jour. (Dec.1962), p317.

4. Warren,J.E. and Skiba, F.F.: " Macroscopic Dispersion"; Soc. Pet. Eng. Jour. (Sept. 1964), Trans. AIME, Vol.231, p215-30.

5. Brigham, W.E., Read, P.W. and Dew, J.N.: "Experiments on Mixing During Miscible Displacements in Porous Media"; Soc. Pet. Eng. Jour. (March 1961), Trans. AIME, Vol.225, p1-8.

6. Morse, R.A.: "Discussion"; Trans. AIME (1954), Vol.6, p283.

7. Kyle, C.R. and Perrine, R.L.: "Experimental Studies of Miscible Displacement Instability"; Soc. Pet. Eng. Jour. (Sept. 1965), Trans. AIME, Vol.234, p189-95.

8. Perkins, T.K. and Johnston, O.C.: " A Review of Diffusion and Dispersion in Porous Media"; Soc. Pet. Eng. Jour. (March 1963), p70-79.

9. Coats, K.H. and Smith, B.D.: "Dead-End Pore Volume and Dispersion in Porous Media"; Soc. Pet. Eng. Jour. (March 1964), Trans. AIME, Vol.231, p78-84.

10. Raimondi, P., Gardner, G.H.F. and Petrick, C.B.: "Effect of Pore Structure and Molecular Diffusion on the Mixing of Miscible Liquids Flowing in Porous Media"; Preprint 43 Presented at AIChE-SPE Joint Symposium (Dec. 6-9, 1959), San Fransisco, California.

11. Crane, F.E. and Gardner, G.H.F.: "Measurements of Transverse Dispersion in Granular Media"; Jour. Chem. Eng. Data (1961), Vol.6, p283.

12. Carman, P.C.: "Permeability of Saturated Sands, Soils and Clays"; Jour. Agri. Sci. (1939), Vol.29, p262.

13. Blackwell, R.J.: "Laboratory Studies of Microscopic Dispersion Phenomena"; Soc. Pet. Eng. Jour. (March 1962), p1.

14. Collins, R.E.: "Flow of Fluids through Porous Media"; Reinhold Publishing Co., New York (1957).

15. Giesbrecht, D: "A Fractal Analysis of Heterogeneity in Miscible Displacement"; MSc. Dissertation, University of Alberta, June 1990.

16. Carman, P.C.: "Fluid Flow through Granular Beds"; Trans. Insti. of Chem. Eng., London (1937), Vol.15, p150.

17. Farouq Ali, S.M. and Stahl, C.D.: "Miscible and Alcohol Slug Displacements in Long Sandstone Cores"; Producers Monthly, (1965),Vol.29, p25.

18. Holm, L.M. and Csaszar, A.K.: "Oil Recovery by Solvents Mutually Soluble in Oil and Water"; Trans. AIME (1962), Vol.225, p189.

19. Meyer, W.K., Taber, J.J. and Reed, R.L.: "Alcohol Displacement of Oil from Long Consolidated Sandstone Cores"; Min. Ind. Circular No.61, The Pennsylvania State University (1961), p164.

20. Blackwell, R.J., Rayne,W.M.and Terry, W.M.: "Factors Influencing the Efficiency of Miscible Displacement"; Trans. AIME (1959), Vol.216, p1-8.

21. Lacey, J.W., Draper, A.L. and Binder, G.G., Jr.: "Miscible Fluid Displacement in Porous Media"; Trans. AIME (1958), Vol.213, p76-81.

22. Offeringa, J. and van der Poel, C.: "Displacement of Oil from Porous Media by Miscible Liquids"; Trans. AIME (1954), Vol. 201, p310.

23. Coskuner, G.: "A new Approach to the Onset of Instability for Miscible Displacement"; PhD. Dissertation, University of Alberta, Dec.1986.

24. Coskuner, G. and Bentsen, R.G.: "Effect of Length on Unstable Miscible Displacements"; JCPT (Jul.-Aug., 1989), No.4, Vol.28, p34-44.

25. van Deemter, J.J., Bralder and Lawrence: "Fluid Displacement in Capillaries"; Chem. Eng. Sci. (1956), Vol.5, p271.

26. Ebach, E.A.: "The Mixing of Liquids Flowing through Beds of Porous Solids"; PhD. Dissertation, University of Michigan (1957).

27. Groboske, D.L. and Farouq Ali,S.M.: "Effect of an Immobile Polymer Phase on Dispersive Mixing in a Porous Medium"; Paper 47a, Symp. on Transport Phenomena in Porous Media, AIChE, Feb. 20-23, 1972.

28. Hall, H.N.and Geffen, T.M.: "A Laboratory Study of Solvent Flooding"; Trans. AIME (1957), Vol.210, p48-57.

29. Baker, L.E.: " Effects of Dispersion and Dead-End Pore Volume in Miscible Flooding"; Soc. Pet. Eng. Jour., No.6 (1977), p219.

30. Bretz, R.E. and Orr, F.M., Jr.: "Interpretation of Miscible Displacements in Laboratory Cores"; SPE RE, No. 11 (1987), p492-500.

31. Houseworth, J.E.: "Characterizing Permeability Heterogeneity in Core Samples from Standard Miscible Displacement Experiments"; SPE FE, No. 6 (1993), p112.

32. Koval, E.J.: "A Method for Predicting the Performance of Unstable Miscible Displacement in Heterogeneous Media"; Soc. Pet. Eng. Jour., No.6 (1963), p145.

33. Dougherty, E.L.: "Mathematical Model of an Unstable Miscible Displacement"; Soc. Pet. Eng. Jour., No.6 (1963), p155.

34. Perrine, R.L.: "A Unified Theory for Stable and Unstable Miscible Displacement"; Soc. Pet. Eng. Jour., No.9 (1963), p205.

35. Deans, H.A.: "A Mathematical Model for Dispersion in the Direction of Flow in Porous Media"; Soc. Pet. Eng. Jour., No.3 (1963), p49.

36. Nguyen, H.H. and Bagster, D.F.: "Unstable Miscible Liquid-Liquid Displacement in Porous Media: A New Model for Predicting Displacement Performance in Homogeneous Beds"; The Chemical Engineering Journal, No.18 (1979), p103.

37. Fayers, F.J.: "An Approximate Model with Physically Interpretable Parameters for Representing Miscible Viscous Fingering"; SPE Paper No. 13166 Presented at the 59th Annual Technical Conference and Exhibition (1984), Houston, TX.

38. Vossoughi, S., Smith, J.E., Green, D.W. and Willhite, G.P.: "A New Method to Simulate the Effects of Viscous Fingering on Miscible Displacement Process in Porous Media"; Soc. Pet. Eng. Jour., No.2 (1984), p56.

39. Udey, N. and Spanos, T.J.T.: "A New Approach to Predicting Miscible Flood Performance"; Paper No.91-5 Presented at the CIM/AOSTRA Technical Conference in Banff, Alberta, April 21-24, 1991.

40. Udey, N. and Spanos, T.J.T.: "The Equations of Miscible Flow with Negligible Molecular Diffusion"; Transport in Porous Media, No.10 (1993), p1.

41. Walsh, M.P. and Withjack, E.M.: "On Some Remarkable Observations of Laboratory Dispersion Based on Computed Tomography (CT)"; Paper No. CIM 93-22 Presented at the CIM Annual Technical Conference in Calgary, Alberta, May 9-12, 1993.

42. Arya, A., Hewett, T.A., Carson, R.G. and Lake, L.W.: "Dispersion and Reservoir Heterogeneity"; SPE RE (March 1988), p139-148.

43. Cashdollar, B.H.: "The Effect of Viscosity Ratio and Path Length on Miscible Displacement in Porous Media"; MSc. Thesis, The Pennsylvania State University, 1959.

44. Hewett, T.A. and Behrens, R.A.: "Considerations Affecting The Scaling of Displacements in Heterogeneous Permeability Distributions"; SPE FE, No.12 (1993), p258.

45. Habermann, B.: "The Efficiencies of Miscible Displacement as a Function of Mobility Ratio"; Trans. AIME, Vol.219, p264; Miscible Process Printing Series, SPE, Dallas (Aug.1965), p205-214.

46. Pozzi, A.L. and Blackwell, R.J.: "Design of Laboratory Models for Study of Miscible Displacement"; Soc. Pet. Eng. Jour., (March 1963).

47. Gardner, G.H.F, Downie, J. and Kendall, H.A.: "Gravity Segregation of Miscible Fluids in Linear Models"; Soc. Pet. Eng. Jour., (June 1962), Trans. AIME, Vol.225, p95-104.

48. Slobod, R.L and Howellett, W.E.: "The Effects of Gravity Segregation in Laboratory Studies of Miscible Displacement in Vertical Unconsolidated Porous Media"; Soc. Pet. Eng. Jour., (March 1964), p1-8.

49. Orlob, G.T. and Radhakrishna, G.N.: "The Effects of Entrapped Gases on the Hydraulic Characteristics of Porous Media"; Trans. AGU, No.4 (Aug. 1958), Vol.39, p648.

50. Bretz, R.E., Specter, R.M. and Orr, F.M.: "Effect of Pore Structure on Miscible Displacement in Laboratory Cores"; SPE RE (Aug. 1988), p857-866.

51. Bernard, R.A. and Wilhelm, R.H.: "Turbulent Diffusion in Fixed Beds of Packed Solids"; Chem. Eng. Prog. (1950), Vol.46, p233.

52. Carberry, J.J.: "Axial Dispersion of Mass in Flow Through Fixed Beds"; PhD. Dissertation, Yale University, 1957.

53. Ebach, E.A. and White, R.R.: "Mixing of Fluids Through Beds of Packed Solids"; AIChE Jour. (1958), Vol.6, p161.

54. Latinen, G.A.: "Mechanism of Fluid Phase Mixing of Fixed and Fluidized Beds of Uniformly Sized Spherical Particles"; PhD. Dissertation, Princeton University, 1951.

55. Fahien, R.W. and Smith, J.M.: "Mass Transfer in Packed Beds"; AIChE Jour. (1955), Vol.1, p28.

56. Singer, E. and Wilhelm, R.H.: "Heat Transfer in Packed Beds; Analytical Solution and Design Method; Fluid Flow, Solids Flow and Chemical Reaction"; Chem. Eng. Prog. (1950), Vol.46, p343.

57. Kasraie, M.: "Influence of Rate and Various Immobile Fluid Saturations on Convective Mixing in a Porous Medium"; MSc. Dissertation, The Pennsylvania State University, August 1979.

58. Raimondi, P., Torcaso, M.A. and Henderson, J.H.: "The Effect of Interstitial Water on the Mixing of Hydrocarbons During a Miscible Displacement Process"; Min. Ind. Expt. Station, Circular No.61, The Pennsylvania State University, (Oct. 1961), p1.

59. Thomas, G.H., Countryman, G.R. and Fatt, I.: "Miscible Displacement in a Multiphase System"; Soc. Pet. Eng. Jour., No.3 (Sept. 1963), Vol.3, p189.

60. Stalkup, F.I.: "Displacement of Oil by Solvent at High Water Saturation"; Soc. Pet. Eng. Jour., No.4 (Dec. 1970), Vol.10, p337.

61. Nielsen, R.F.: Private Communication.

62. Niko, H.: "Effect of Rate and Gravity Segregation on the Displacement of Oil and Water by Alcohol Slugs in a Sandstone Core"; MSc. Thesis, The Pennsylvania State University, 1963.

63. Koch, H.A. and Slobod, R.L.: "Miscible Slug Process"; Trans. AIME (1957), Vol.210, p40.

64. Graig, F.F. and Owens, W.W.: "Miscible Slug Flooding-A Review"; Journal of Petroleum Technology, (April 1960), p11-15.

65. Zhang, X.: "The Effect of Core Length on the Instability of Miscible Displacement"; MSc. Dissertation, University of Alberta, May 1993.

66. Le, T.H.: "The Effect of Flow Rate and Core Length on the Longitudinal Dispersion Coefficient"; MSc. Dissertation, University of Alberta, January 1995.

67. Tan, J.: "A New Mathematical Model for One-Dimensional Miscible Displacement"; MSc. Dissertation, University of Alberta, October 1995.

68. Bentsen, R.G.: " A Study of Plane Radial Miscible Displacement in a Consolidated Porous Medium"; MSc. Dissertation, The Pennsylvania State University, June 1964.

69. Crago, D.H.: "Effect of Core Diameter on the Efficiency of Miscible Displacement in Porous Media"; MSc. Thesis, The Pennsylvania State University, 1959.

70. Kravik, G.D.: "A Study of Mixing During Gaseous Displacement at Low Flow Rates in a Consolidated Porous Medium"; MSc. Thesis, The Pennsylvania State University, 1963.

71. Donohue, D.A.T.: "A Mathematical Model to Simulate the Recovery of Oil and Water from Porous Media by the Injection of Solvents"; PhD. Thesis, The Pennsylvania State University, 1963.

72. Aris, R. and Amundson, N.R.: "Some Remarks on Longitudinal Mixing or Diffusion in Fixed Beds"; AIChE Jour., Vol.3 (1957), p280.

73. Pickens, J.F. and Grisak, G.E.: "Scale-Dependent Dispersion in a Stratified Granular Aquifer"; Water Resources Res., Vol.17 (1981), p1191.

74. Oguztoreli, M. and Farouq Ali, S.M.: "Mathematical Treatment of the Miscible Displacement from Porous Media"; AIChE Jour., Vol.2 (1), (1984), p55.

75. Brigham, W.E.: "Mixing Equations in Short Laboratory Cores"; Soc. Pet. Eng. Jour., (Feb. 1974), p91.

76. Grisak, G.E. and Pickens, J.F.: " An Analytical Solution for Solute Transport through Fractured Media with Matrix Diffusion"; Jour. Hydrol. (1981), Vol.52, p47-57.

77. Correa, A.C., Pande, K.K., Ramey Jr., H.J. and Brigham, W.E.: "Prediction and Interpretation of Miscible Displacement Performance Using a Transverse Matrix Dispersion Model"; Paper 16704 Presented at the SPE 62nd Annual Technical Conference and Exhibition, Dallas,TX., Sept. 27-30, 1987.

78. Correa, A.C., Pande, K.K., Ramey, H.J. and Brigham, W.E.: "Computation and Interpretation of Miscible Displacement Performance in Heterogeneous Porous Media"; SPE RE (Feb. 1990), p69-78.

79. Dumore, J.M.: "Stability Considerations in Downward Miscible Displacements"; Soc. Pet. Eng. Jour., (Dec. 1963), Trans. AIME, Vol.231, p356.

Appendix A

APPENDIX A

Calculation of the Results

The dispersion coefficient and the mixing coefficient which are the subjects of this investigation were calculated for both, the first contact miscible displacement process and the miscible slug process.

1. Calculation of the Dispersion and Mixing Coefficients Based on a First Contact Miscible Displacement Process:

The effective dispersion coefficient was calculated using the following formula (from Brigham's[75] method):

$$K_e = \vartheta L \left(\frac{\lambda_{90} - \lambda_{10}}{3.625} \right)^2$$

where:

K_e = *effective dispersion coefficient* (cm^2/sec)

$Q = 160\ cm^3/\ hr$

$r = 2.525\ cm$

$A = \pi r^2$

$Q = A \times \vartheta$

ϑ = *pore velocity* $= 2.22 \times 10^{-3}$ (*cm*/sec)

L = *core length* $= 60.72\ cm$

λ_{90} = *Lambda function value at* X_{90}

λ_{10} = *Lambda function value at* X_{10}

The mixing coefficient was then calculated as follows:

$$K_e = D_o + \alpha\vartheta$$

But since D_o is very small, it can be neglected.

$$\therefore \alpha = \frac{K_e}{\vartheta} \quad (cm)$$

Where

α = the mixing coefficient in cm.

2. Calculation of the Dispersion and Mixing Coefficients Based on a Miscible Slug Process:

The effective dispersion coefficient was determined by using the following equation (from Raimondi et al.[10]):

$$\frac{C_{max}}{C_o} = \frac{L}{\sqrt{4\pi\alpha X}}$$

or

$$\frac{C_{max}}{C_o} = \frac{L}{\sqrt{4\pi\left(\frac{K_e}{\vartheta}\right)X}}$$

where:

C_{max} = maximum concentration of the slug, ($cm^3./cm^3$)

C_o = initial concentration of the slug, .($cm^3./cm^3$)

L = length of undiluted slug, (cm)

X = fixed distance traveled by the center of slug X, (cm)

3. Calculation of the Critical and Stable Flow Rates:

The critical and stable velocities were calculated for both, the oleic and the aqueous fluid systems using Dumore's[79] equations:

$$v_c = \frac{\Delta\rho}{\Delta\mu}Kg = \frac{\rho_o - \rho_s}{\mu_o - \mu_s}Kg \quad and \quad Q_c = v_c \times A$$

$$v_{st} = \frac{\beta(\rho_o - \rho_s)}{\mu_o(\ln\mu_o - \ln\mu_s)}Kg \quad and \quad Q_{st} = v_{st} \times A$$

where

ρ_o, ρ_s = *oil and solvent densities respectively,* (gm/cm^3)

μ_o, μ_s = *oil and solvent viscosities respectively,* $(gm/cm.sec)$

K = permeability, (cm^2)

g = acceleration due to gravity, (cm/sec^2)

A = *area,* (cm^2)

Q_c, Q_{st} = *critical and stable rates respectively,* (cm^3/sec)

β = *empirical constant determined by trial and error for each fluid system,* (β *for the oleic fluid system was found to be* = 0.8644)

4. The Determination of the Dispersion and The Mixing Coefficients

a) Calculation Example for the Continuous Miscible Displacement:

Example: Run # 7: from figure B-7.I

$\lambda_{90} = 0.2021$ *and* $\lambda_{10} = -0.3723$

$$K_e = \vartheta L\left(\frac{\lambda_{90} - \lambda_{10}}{3.625}\right)^2 \qquad \text{(a)}$$

$$\because \vartheta = \frac{Q(cm^3/\sec)}{A(cm^2)} = \frac{0.0444}{20.03} = 2.22\times10^{-3} cm/\sec \ , \qquad \text{L=60.72 cm}$$

Substituting all the values in Eqn. (a) $\rightarrow \therefore K_e = 3.39\times10^{-3} cm^2/\sec$

The mixing coefficient α is then calculated as follows:

$K_e = D_o + \alpha\vartheta$

But since D_o *is very small, it can be neglected.*

$$\therefore \alpha = \frac{K_e}{\vartheta} \quad (cm)$$

Where

α = *the mixing coefficient in cm.*

$$\therefore \alpha = \frac{K_e}{\vartheta} = \frac{3.39 \times 10^{-3}\ (cm^2/\text{sec})}{2.22 \times 10^{-3} (cm/\text{sec})} = 1.525\ cm$$

b) Calculation Example for the Miscible-Slug Process:

Example: Run # 27: From Table C-27, C_{max}= 59.37% , C_o= 100%

Length of the undiluted slug (i.e. 20% PV)= 12.144 cm ,

X = length of the core holder = 60.72 cm

Using the following Eqns.:

$$\frac{C_{max}}{C_o} = \frac{L}{\sqrt{4\pi\alpha X}} \qquad (b)$$

or

$$\frac{C_{max}}{C_o} = \frac{L}{\sqrt{4\pi\left(\frac{K_e}{\vartheta}\right)X}} \qquad (c)$$

$$\therefore K_e = 1.217 \times 10^{-3} \quad cm^2/\text{sec}$$

$$\therefore \alpha = \frac{K_e}{\vartheta} = \frac{1.217 \times 10^{-3}}{2.22 \times 10^{-3}} = 0.548\ cm$$

5. Determination of the Inhomogeneity Factor:

Run # 29: The mixing coefficient α was calculated and found to be = 0.767 cm

Given the average particle diameter (d_p) from the wet sieve analysis = 0.0128 cm

Using Raimondi et al's.[10] Equation (10) in Chapter 2:

$$\alpha = \sigma^2 dp$$

$$\sigma^2 = \frac{\alpha}{d_p} = \frac{0.767}{0.0128} = 59.92$$

$$\sigma = 7.74$$

$$\therefore \sigma\, d_p = 0.099\ cm$$

- The mixing coefficients α calculated in this experimental investigation ranged between 0.083 and 6.467 cm at favourable and unfavourable mobility ratios, and the $\sigma\, d_p$ values ranged between 0.033 and 0.29 cm.

Appendix B

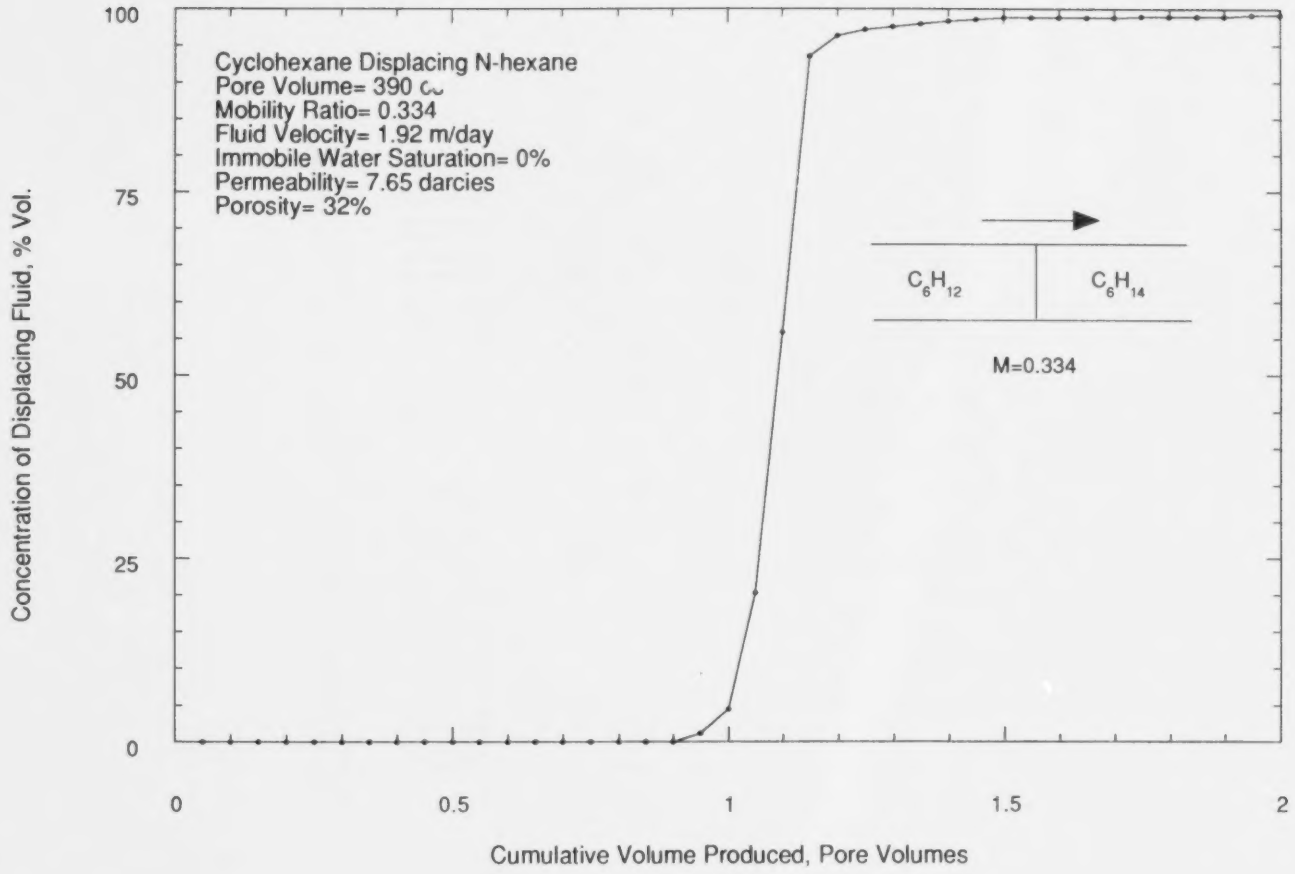

Figure B-1: Run 1: Concentration Profile of Cyclohexane Displacing N-hexane in the Presence of 0% Immobile Water Saturation.

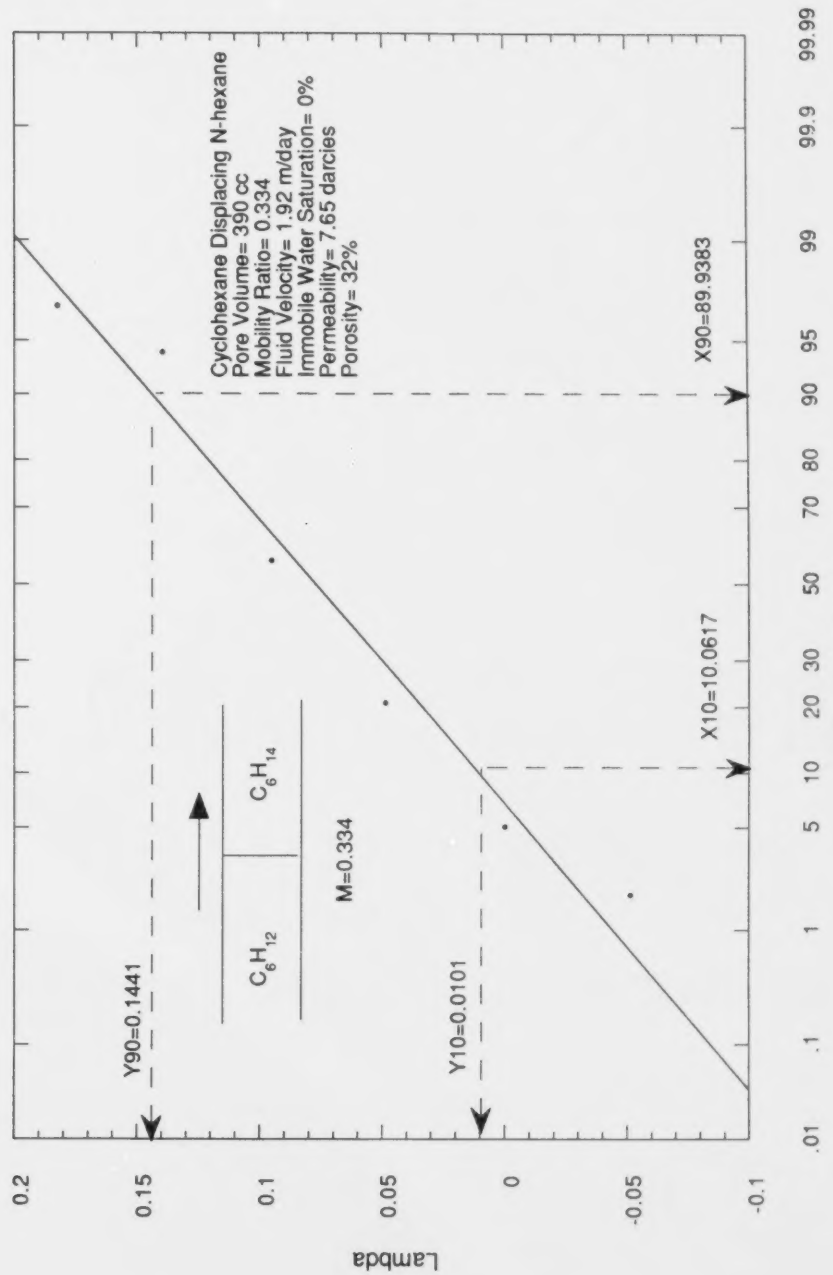

Figure B-1.1: Effluent Concentration Plotted on Arithmetic Probability Paper for Run 1.

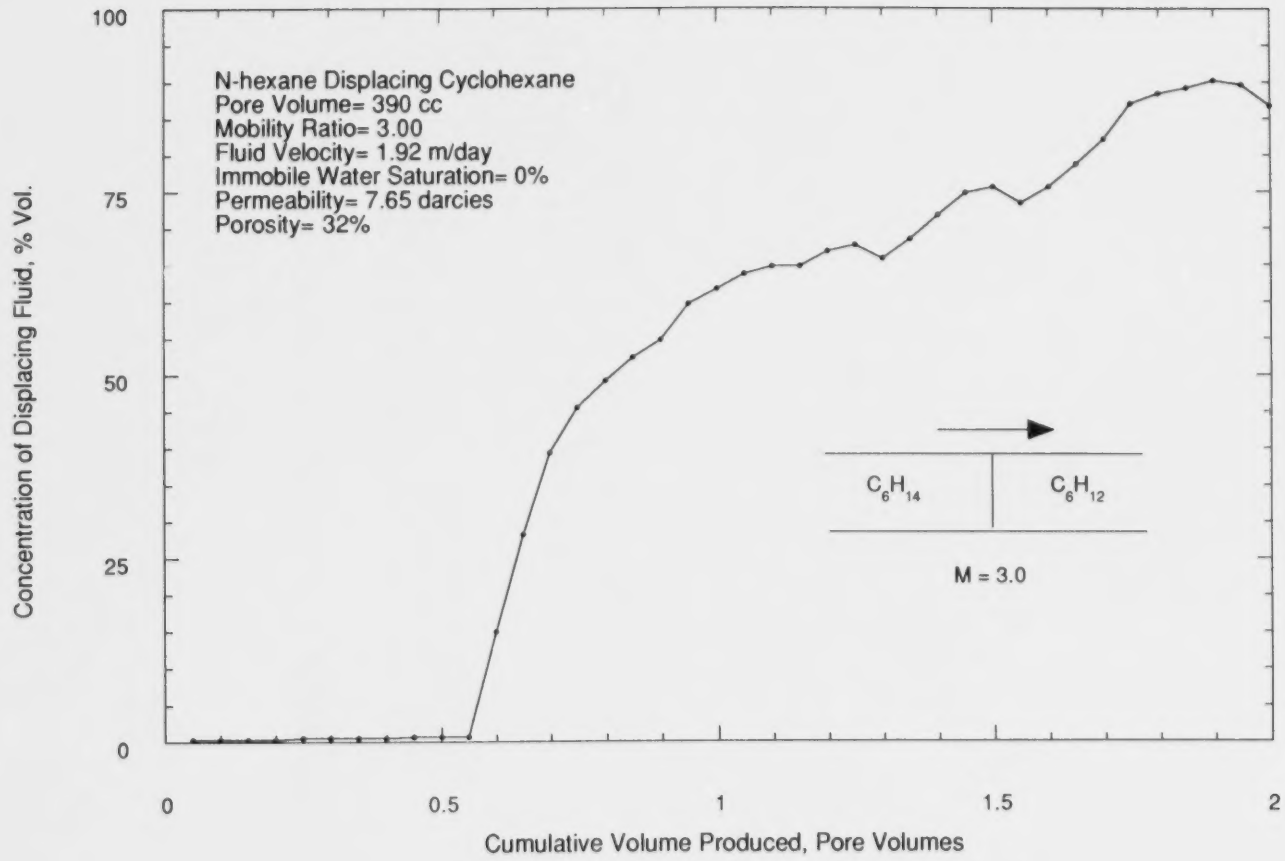

Figure B-2: Run 2: Concentration Profile of N-hexane Displacing Cyclohexane in the Presence of 0% Immobile Water Saturation.

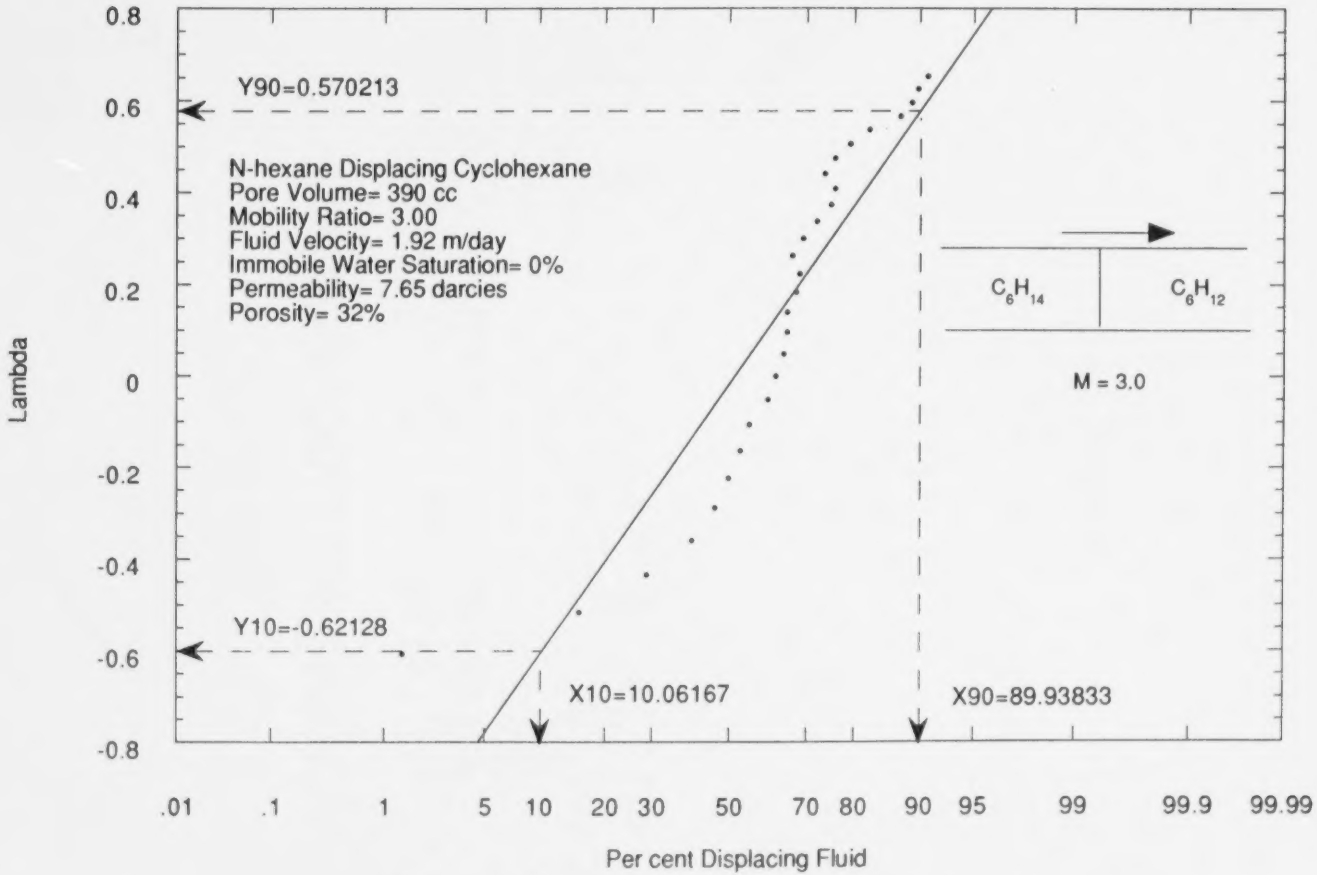

Figure B-2.1: Effluent Concentration Plotted on Arithmetic Probability Paper for Run 2.

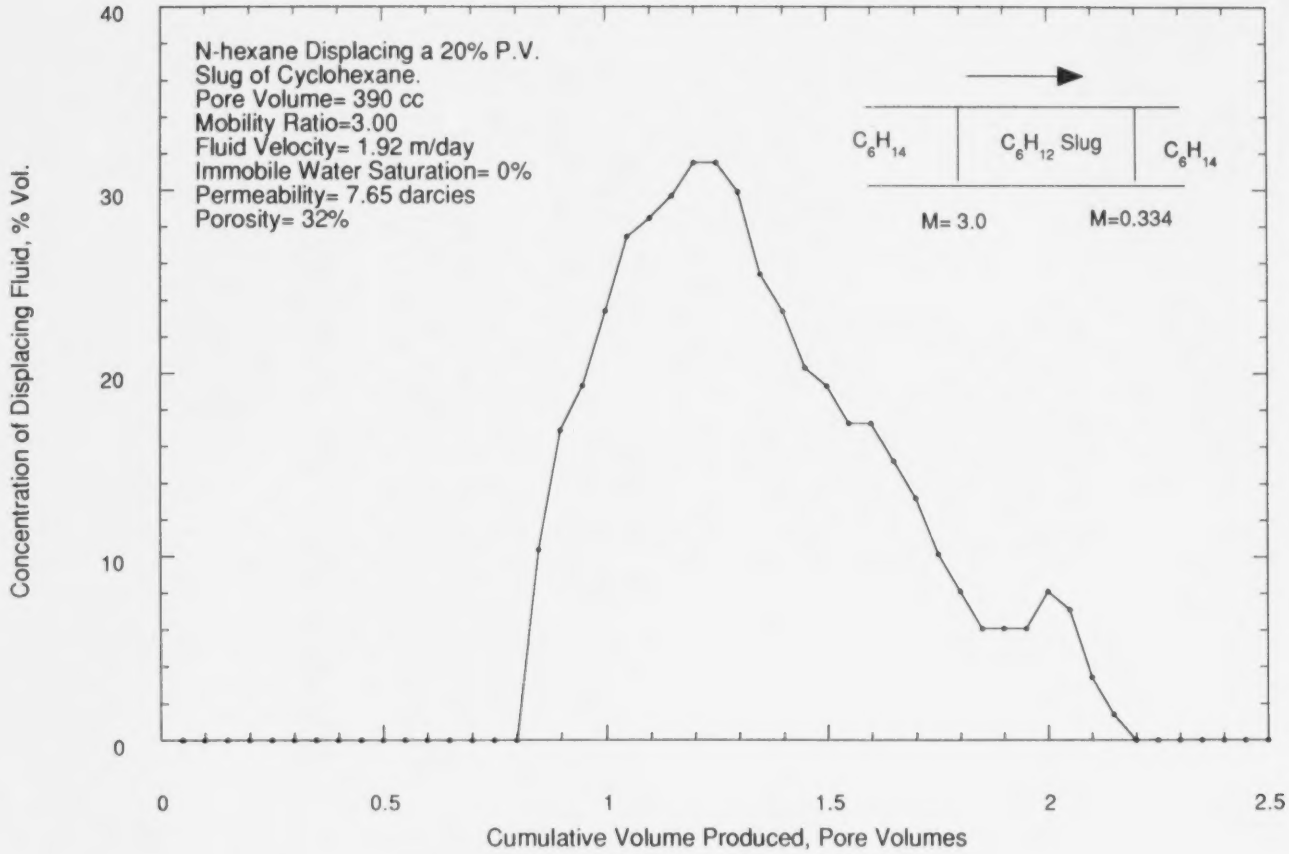

Figure B-3: Run 3: Concentration Profile of N-hexane Displacing a 20% P.V. Slug of Cyclohexane in the Presence of 0% Immobile Water Saturation.

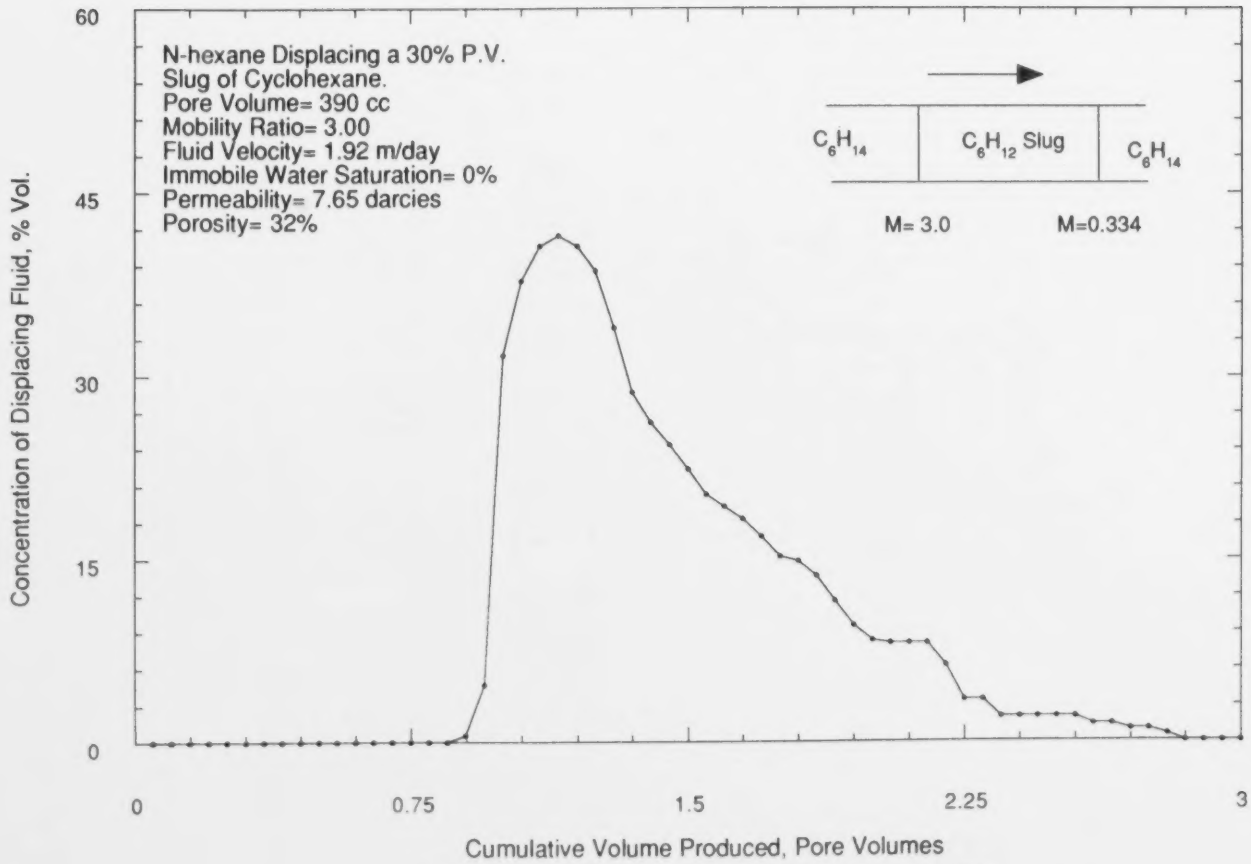

Figure B-4: Run 4: Concentration Profile of N-hexane Displacing a 30% P.V. Slug of Cyclohexane in the Presence of 0% Immobile Water Saturation.

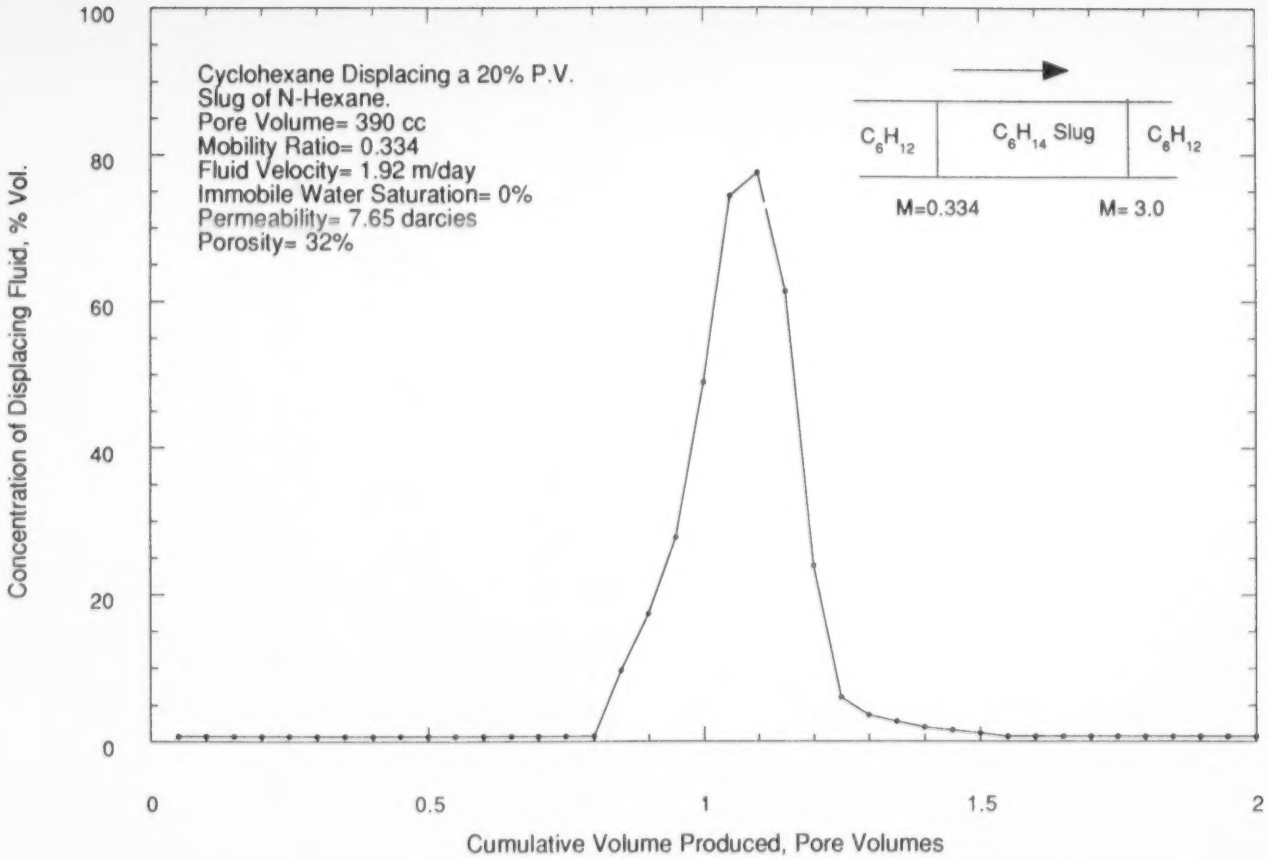

Figure B-5: Run 5: Concentration Profile of Cyclohexane Displacing a 20% P.V. Slug of N-hexane in the Presence of 0% Immobile Water Saturation.

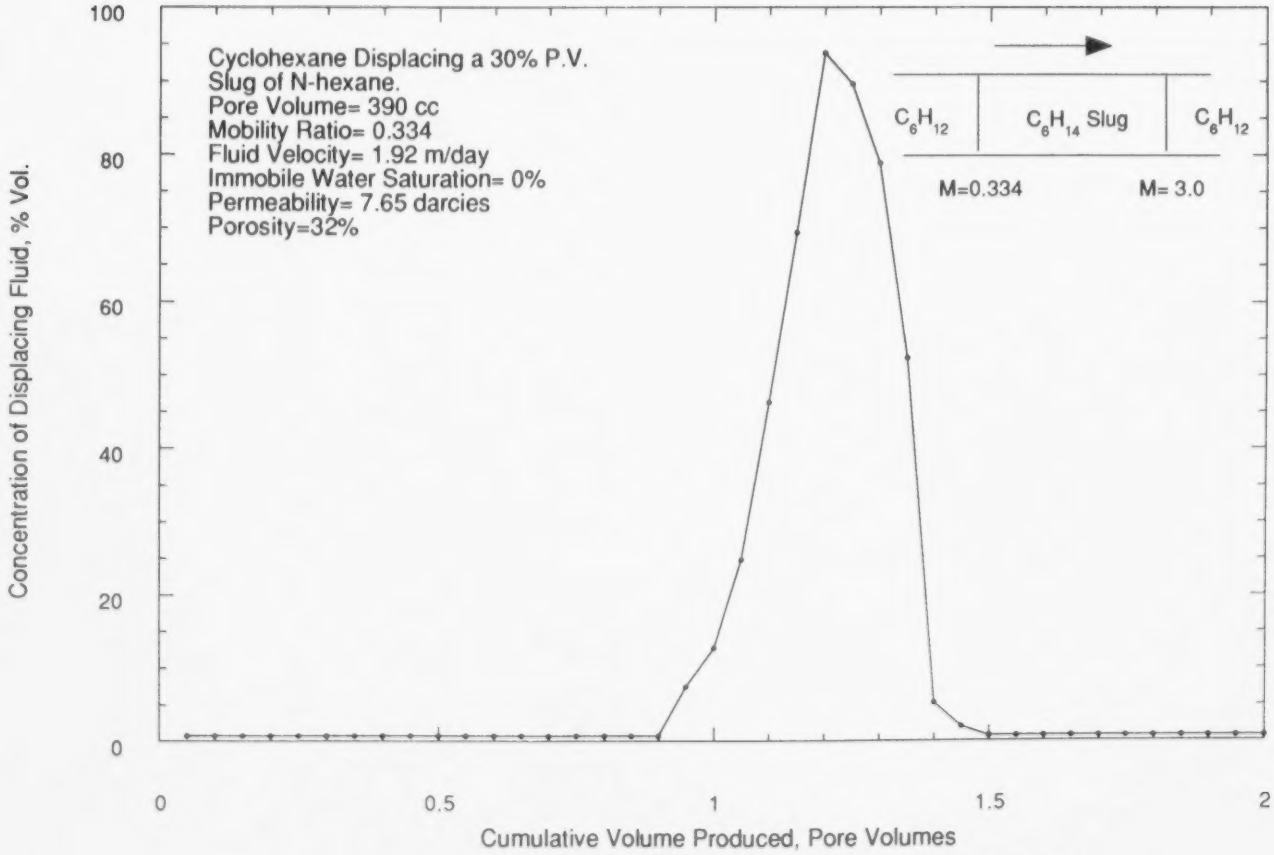

Figure B-6: Run 6: Concentration Profile of Cyclohexane Displacing a 30% P.V. Slug of N-hexane in the Presence of 0% Immobile Water Saturation.

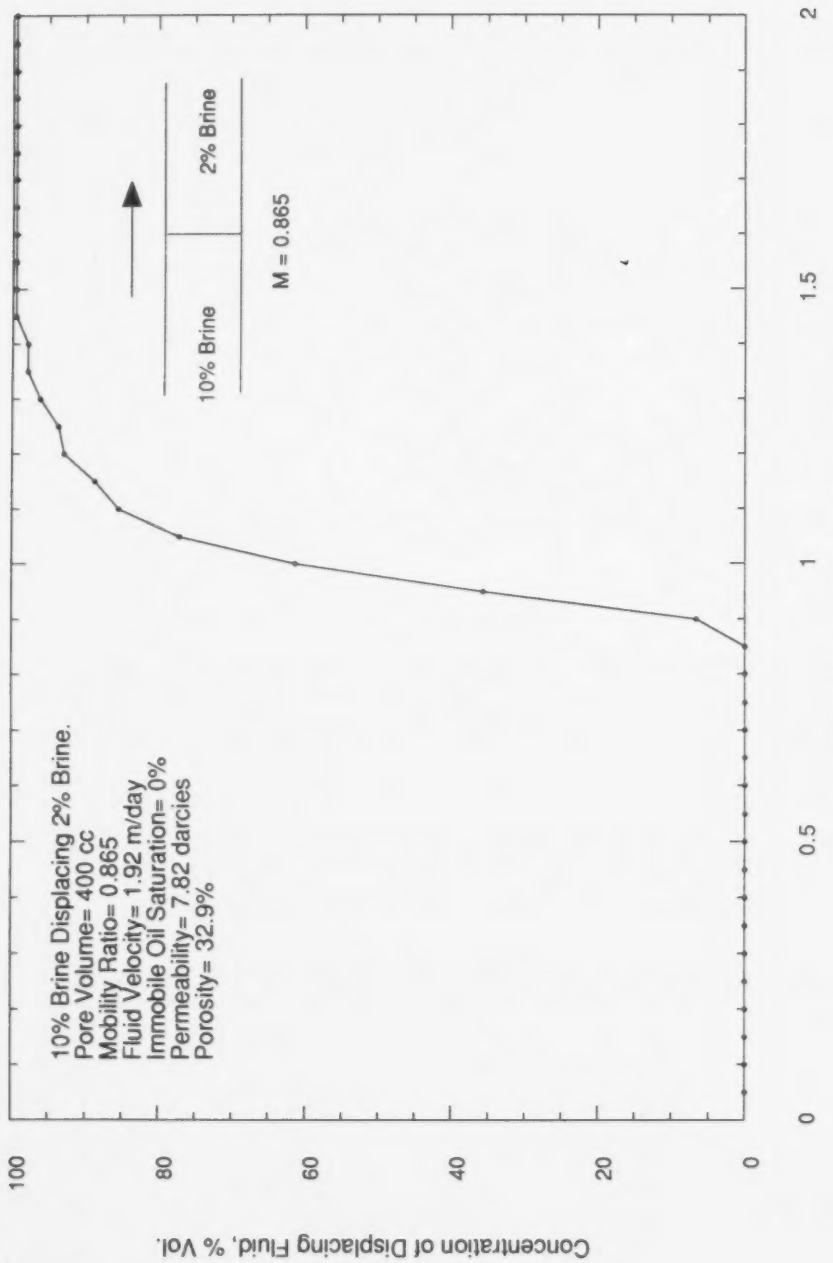

Figure B-7: Run 7: Concentration Profile of 10% Brine Displacing 2% Brine in the Presence of 0% Immobile Oil Saturation.

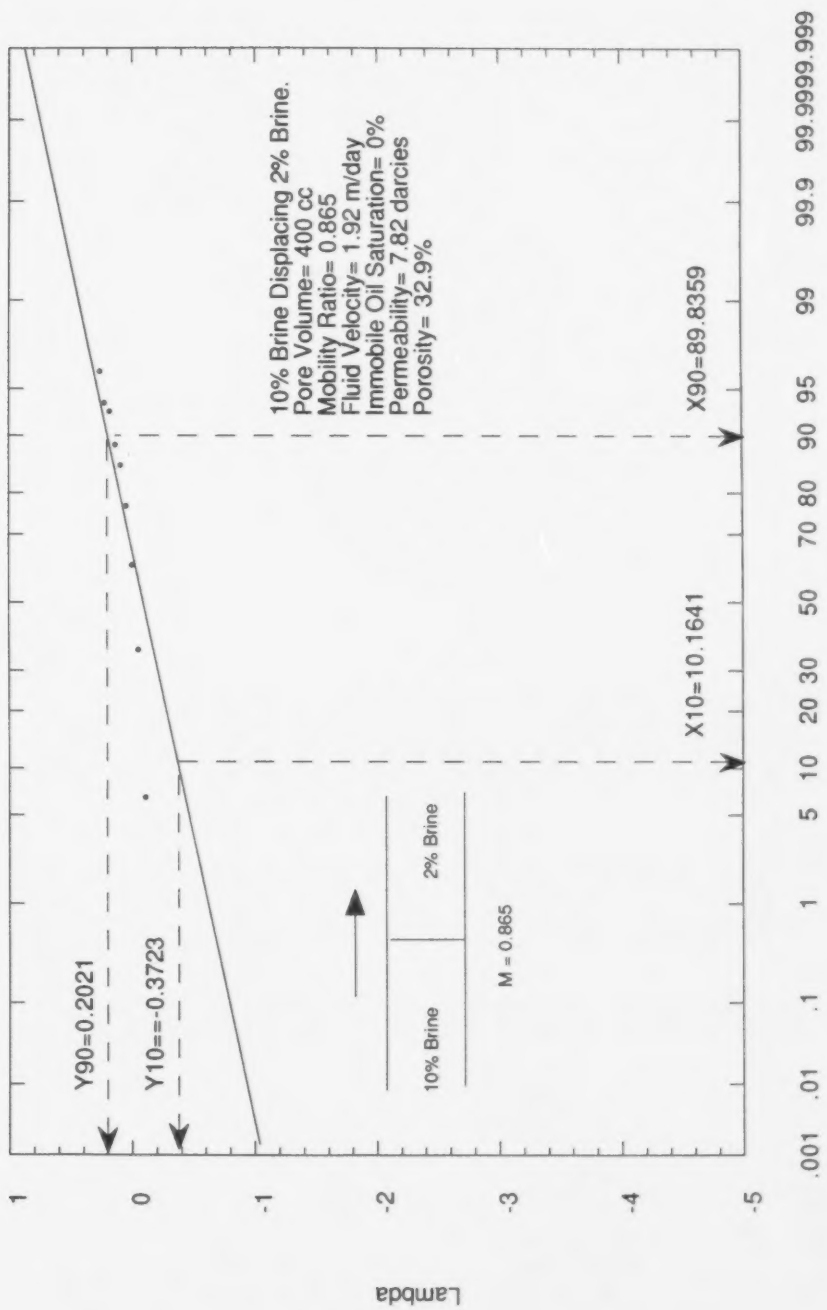

Figure B-7.1: Effluent Concentration Plotted on Arithmetic Probability Paper for Run 7.

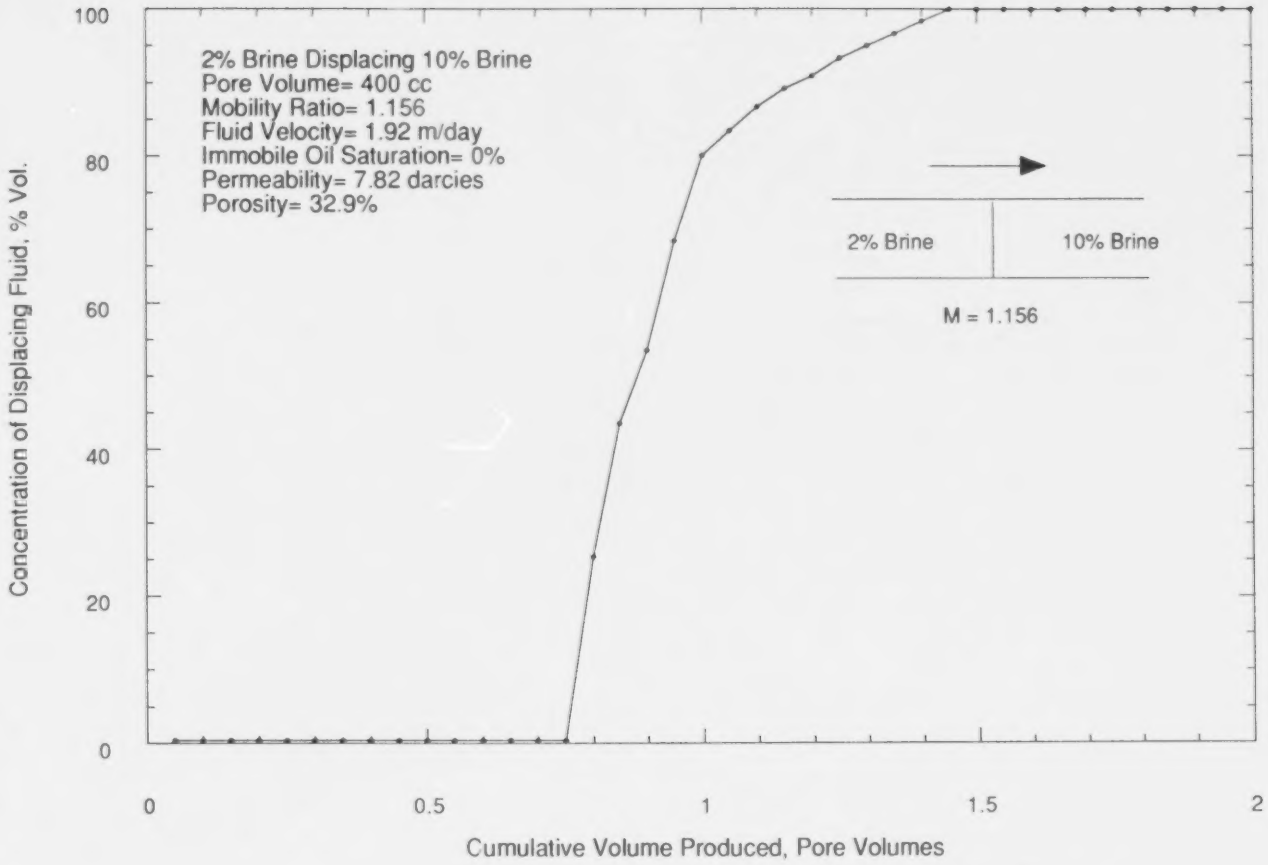

Figure B-8: Run 8: Concentration Profile of 2% Brine Displacing 10% Brine in the Presence of 0% Immobile Oil Saturation.

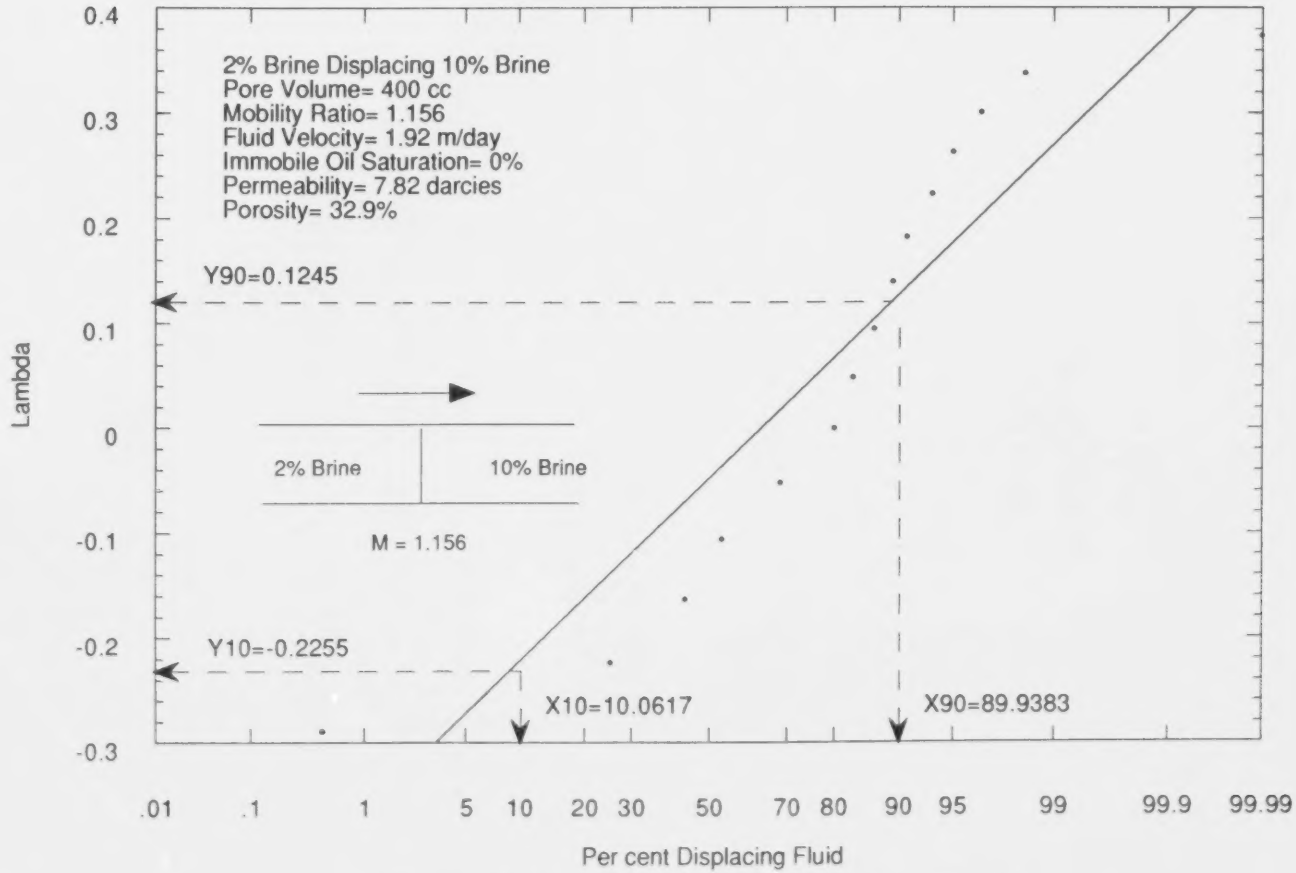

Figure B-8.1: Effluent Concentration Plotted on Arithmetic Probability Paper for Run 8.

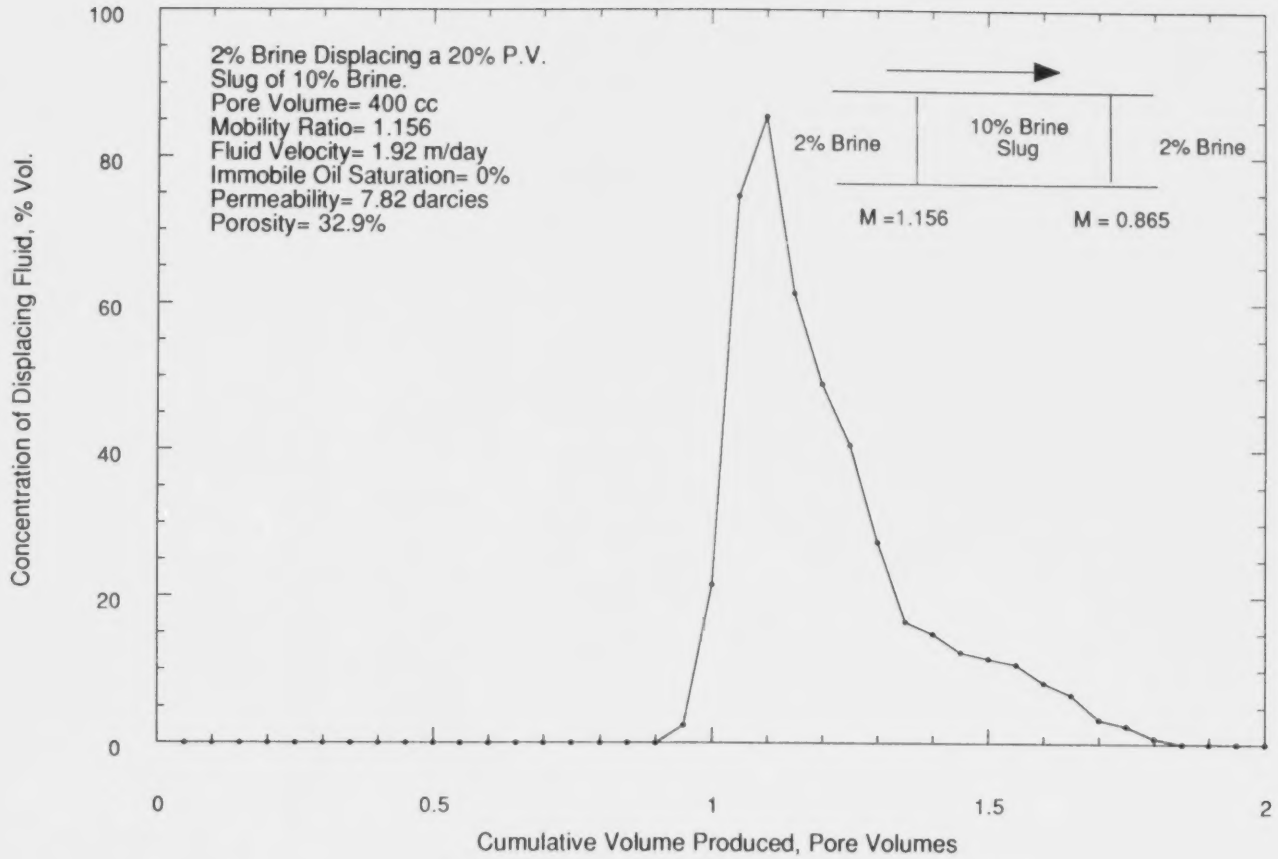

Figure B-9: Run 9: Concentration Profile of 2% Brine Displacing a 20% P.V. Slug of 10% Brine in the Presence of 0% Immobile Oil Saturation.

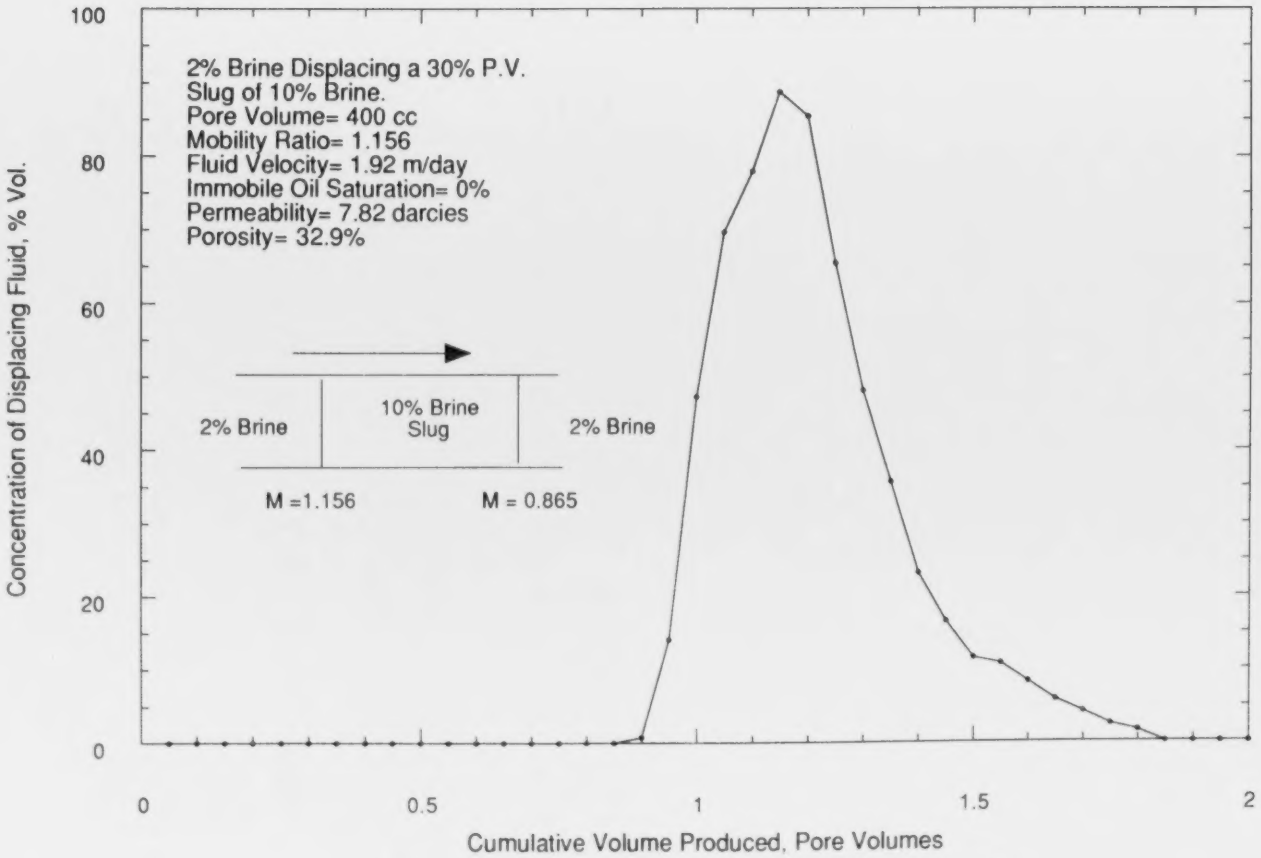

Figure B-10: Run 10: Concentration Profile of 2% Brine Displacing a 30% P.V. Slug of 10% Brine in the Presence of 0% Immobile Oil Saturation.

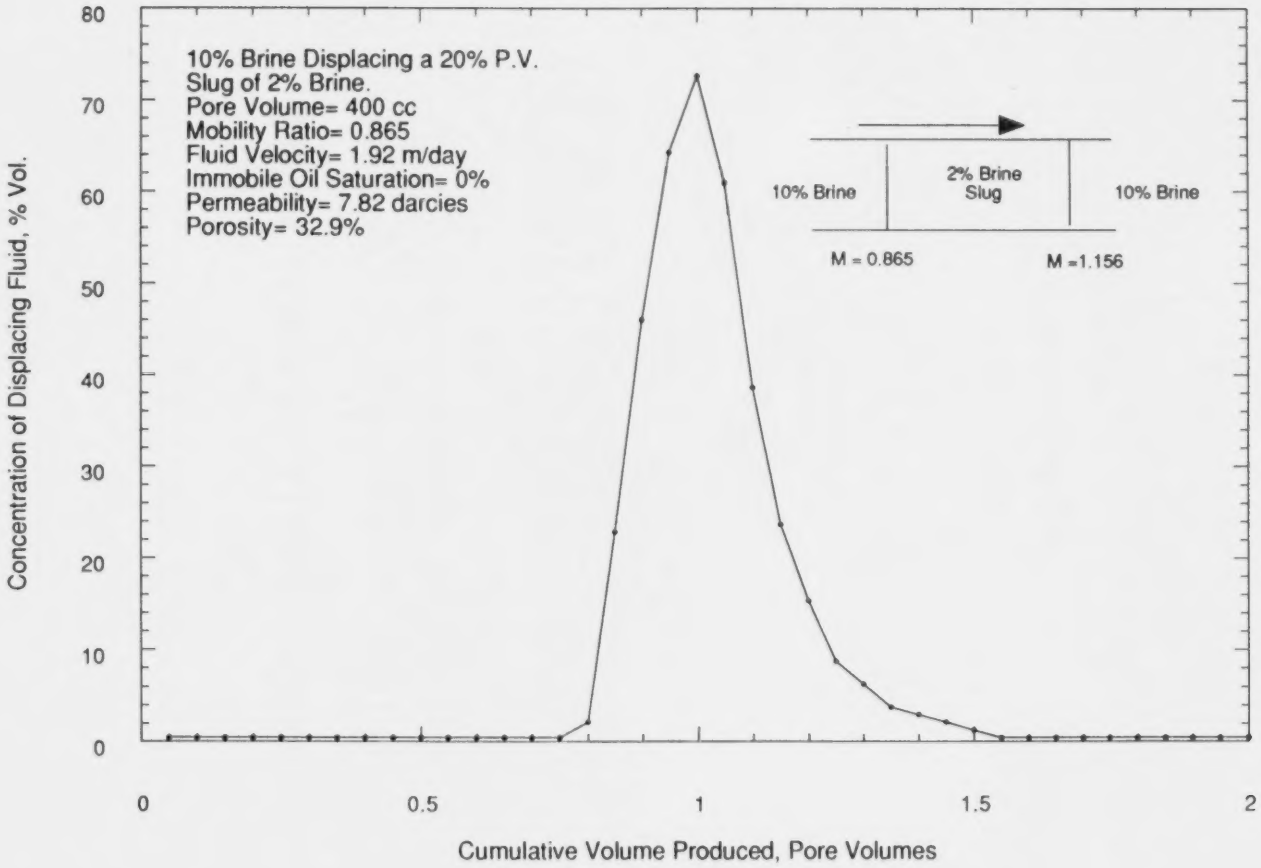

Figure B-11: Run 11: Concentration Profile of 10% Brine Displacing a 20% P.V. Slug of 2% Brine in the Presence of 0% Immobile Oil Saturation.

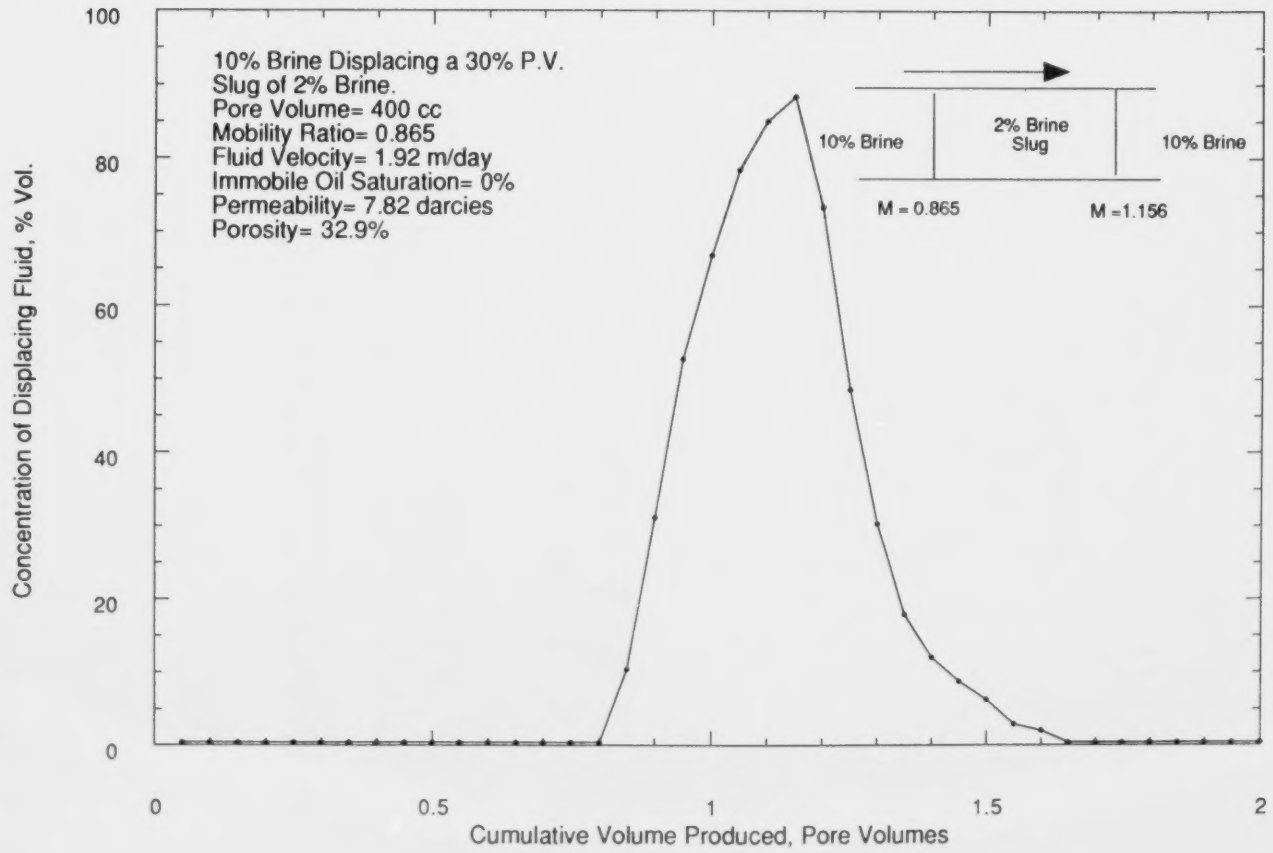

Figure B-12: Run 12: Concentration Profile of 10% Brine Displacing a 30% P.V. Slug of 2% Brine in the Presence of 0% Immobile Oil Saturation.

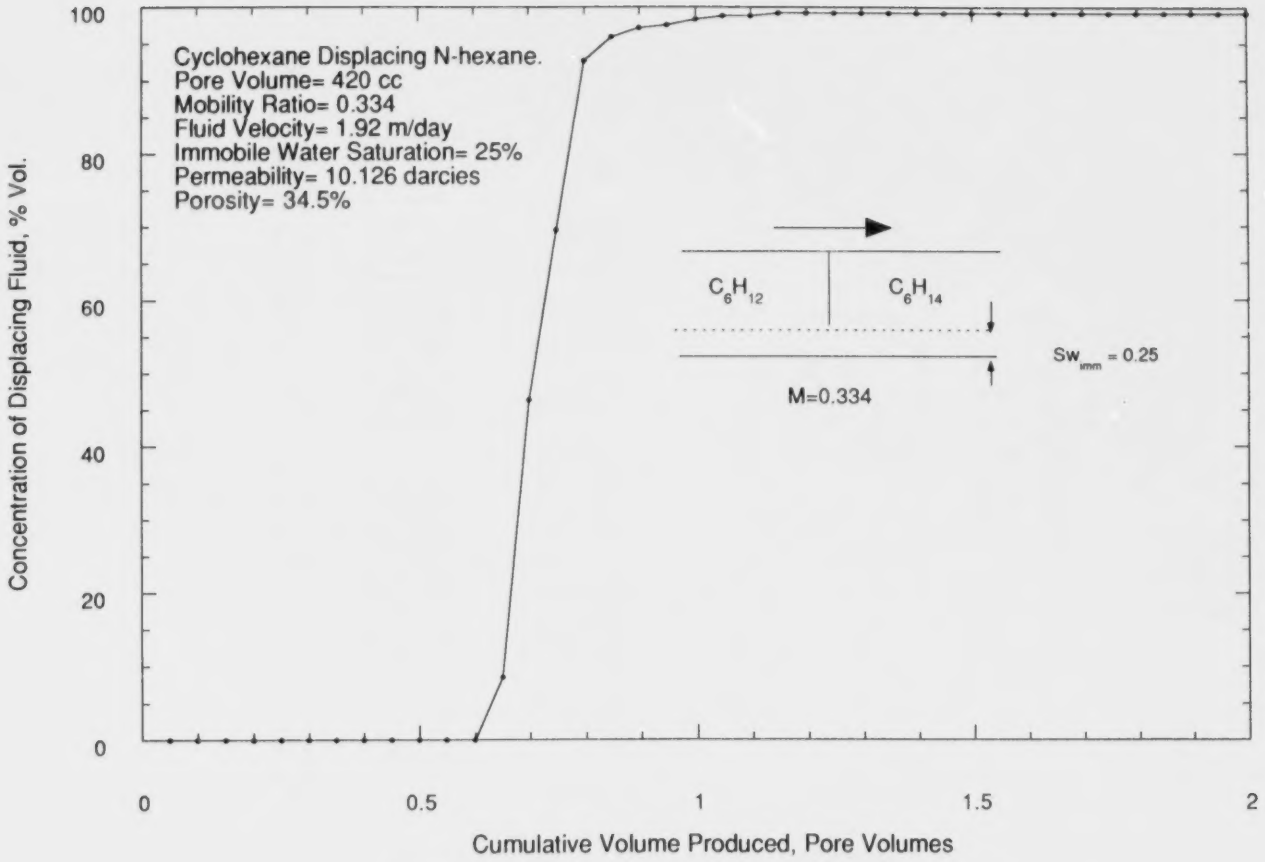

Figure B-13: Run 13: Concentration Profile of Cyclohexane Displacing N-hexane in the Presence of 25% Immobile Water Saturation.

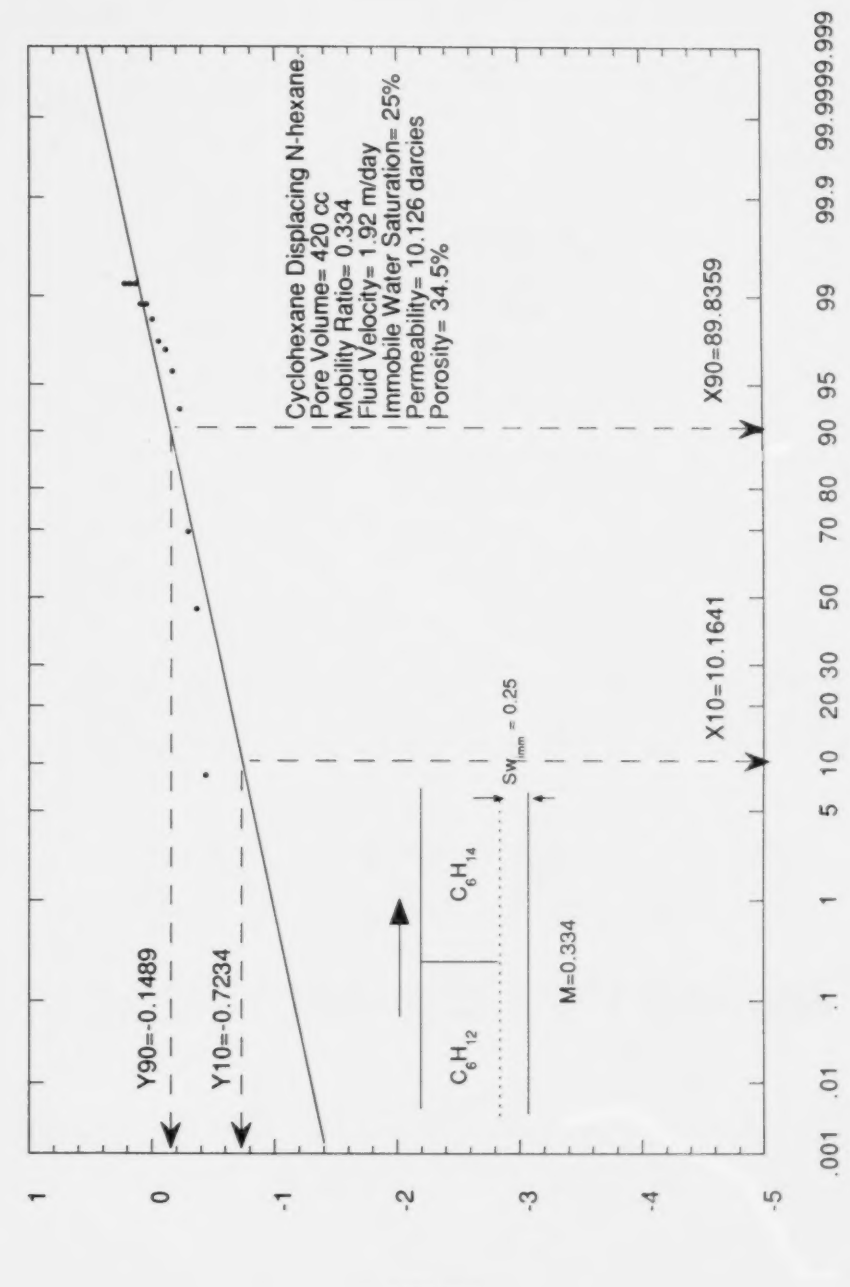

Figure B-13.1: Effluent Concentration Plotted on Arithmetic Probability Paper for Run 13.

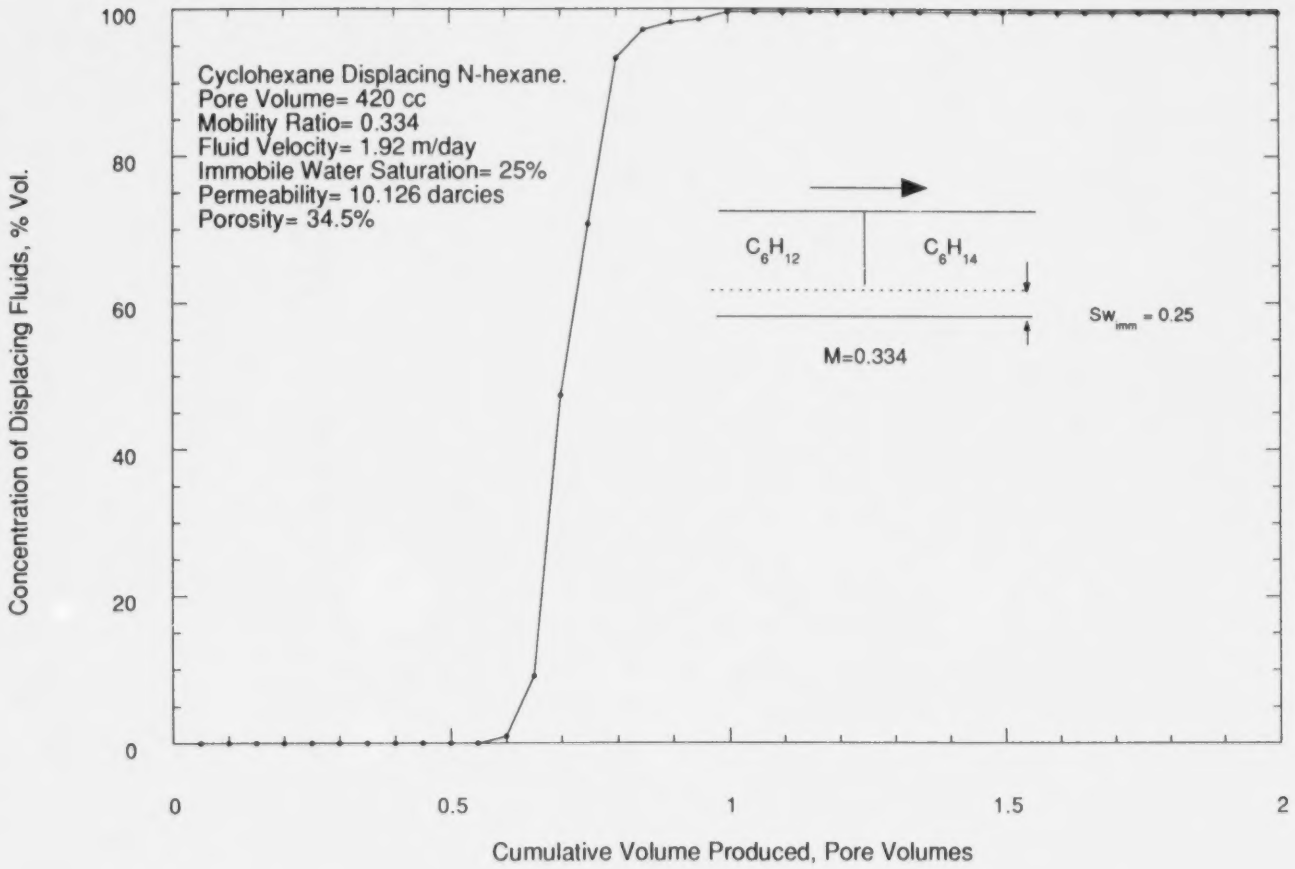

Figure B-13R: Run 13R: Concentration Profile of Cyclohexane Displacing N-hexane in the Presence of 25% Immobile Water Saturation.

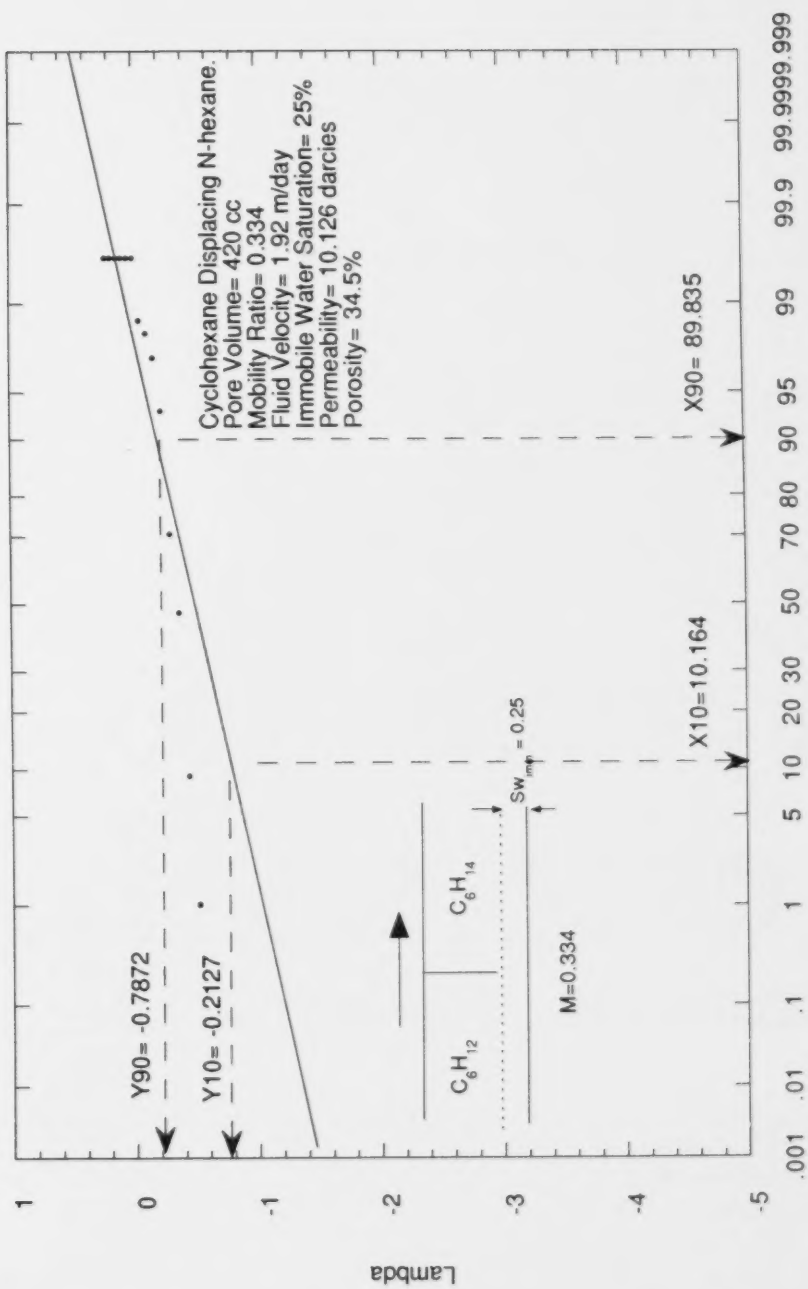

Figure B-13R.1: Effluent Concentration Plotted on Arithmetic Probability Paper for Run 13R.

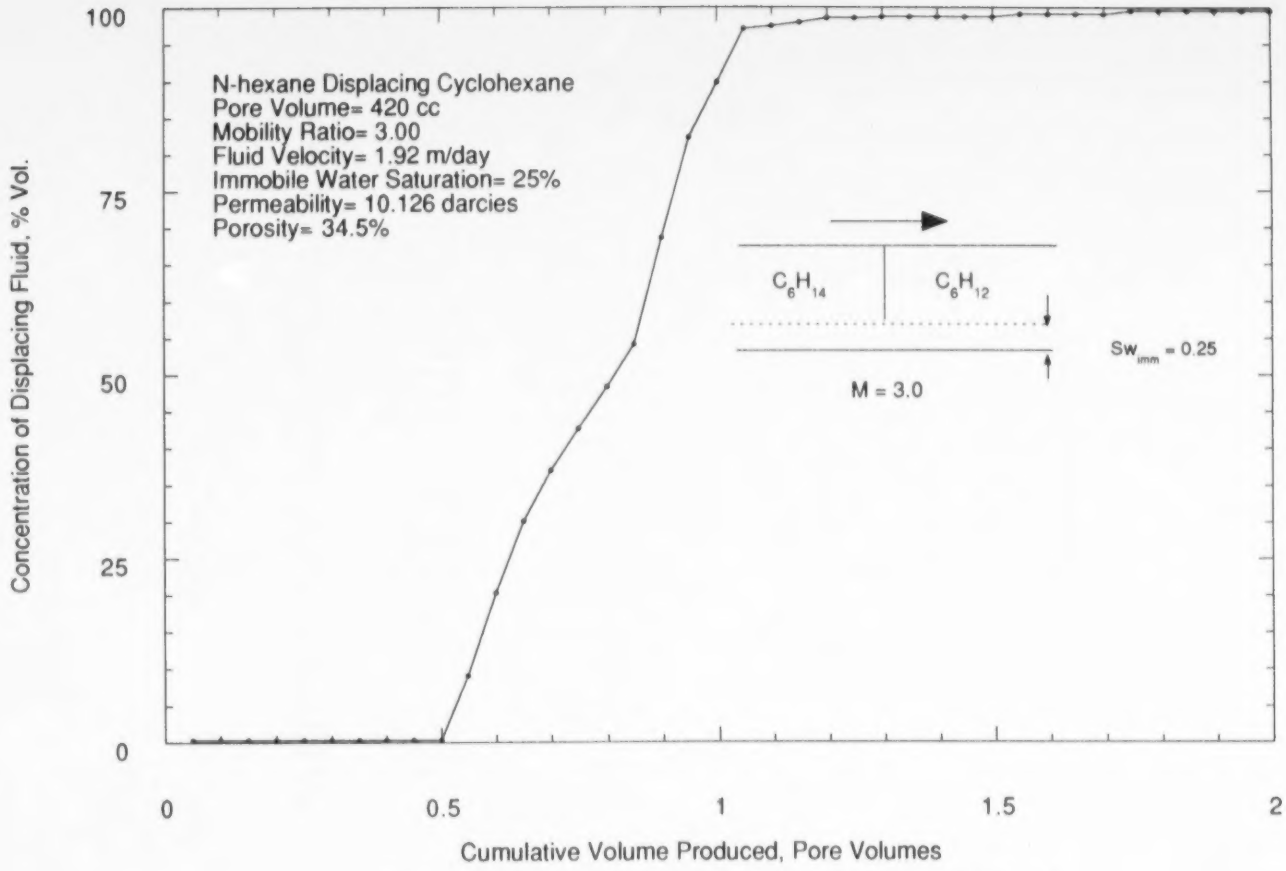

Figure B-14: Run 14: Concentration Profile of N-hexane Displacing Cyclohexane in the Presence of 25% Immobile Water Saturation.

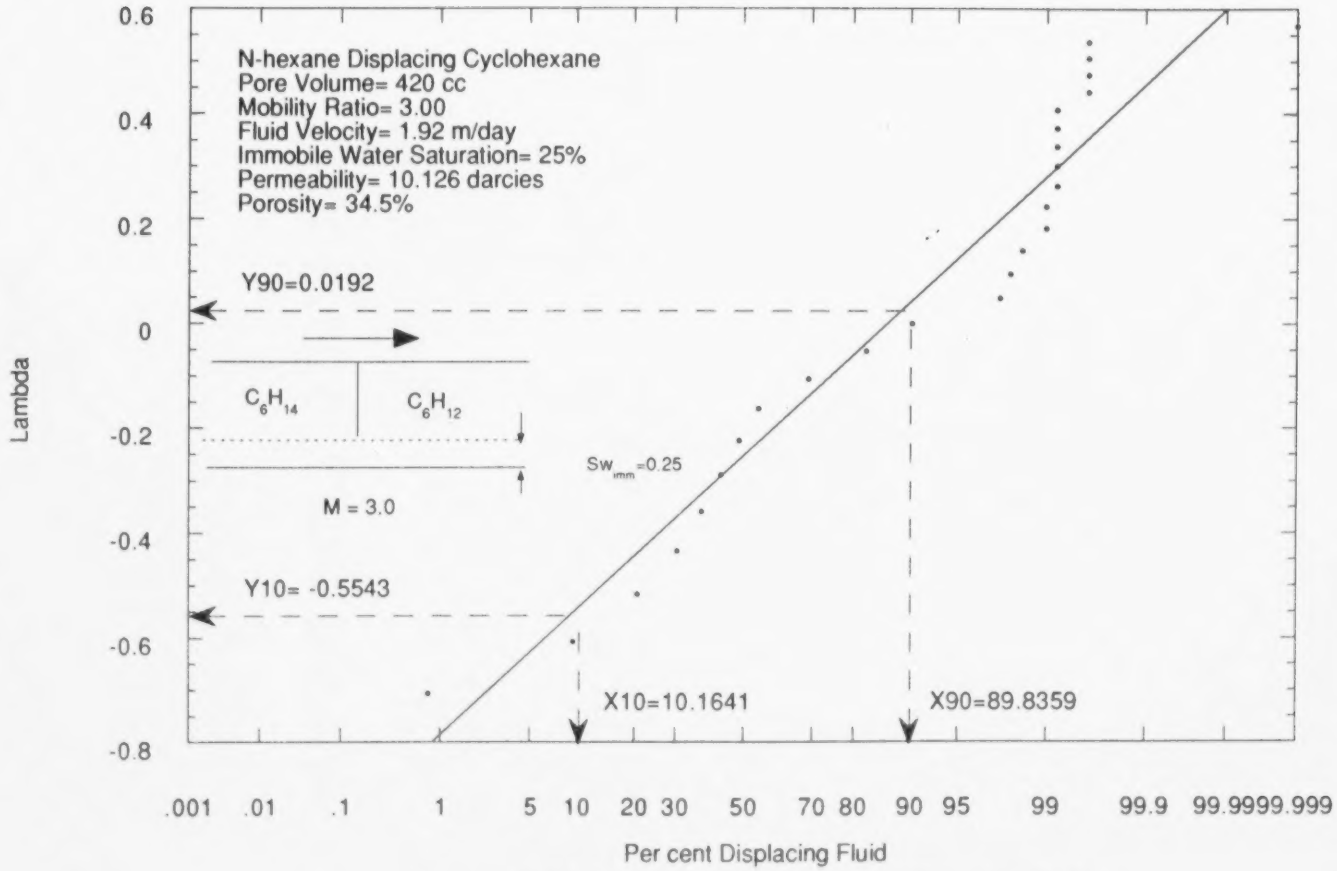

Figure B-14.1: Effluent Concentration Plotted on Arithmetic Probability Paper for Run 14

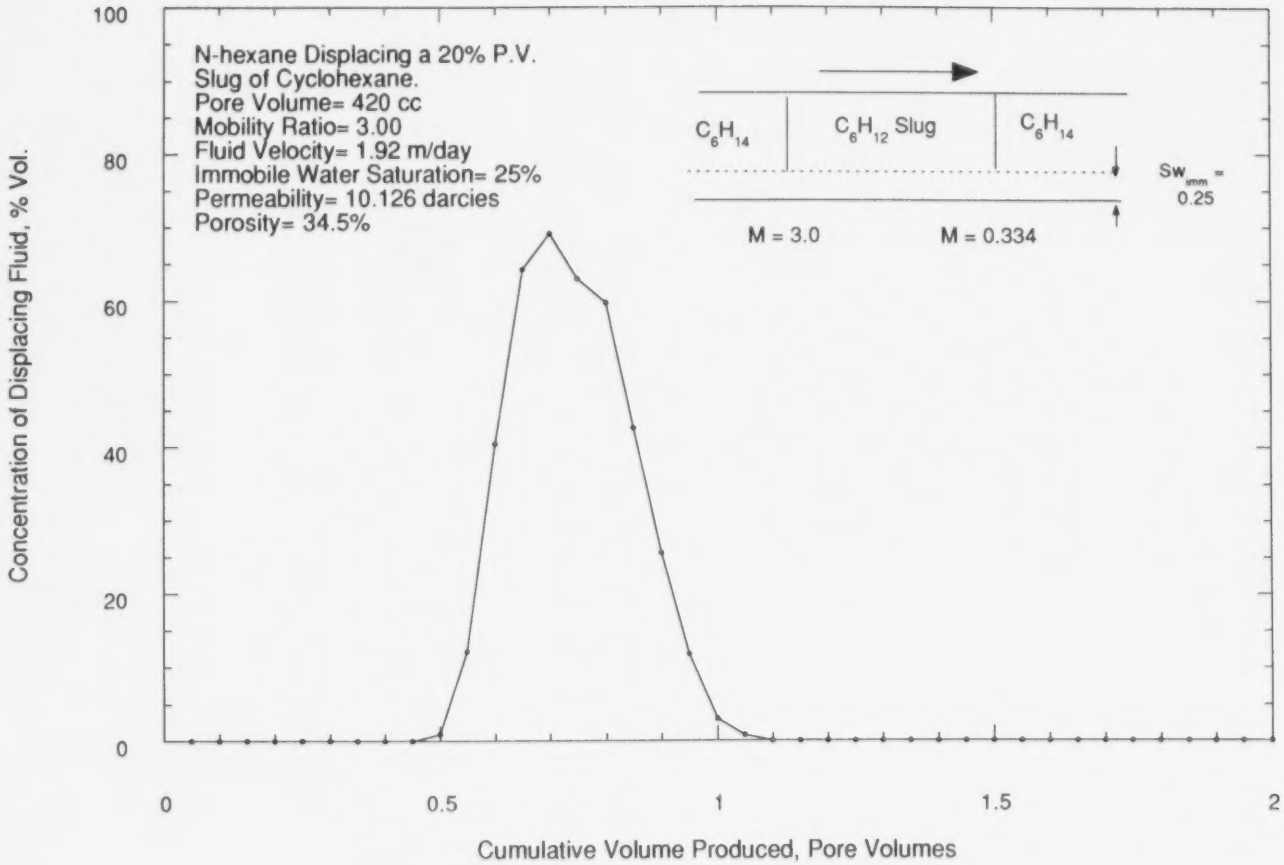

Figure B-15: Run 15: Concentration Profile of N-hexane Displacing a 20% P.V. Slug of Cyclohexane in the Presence of 25% Immobile Water Saturation.

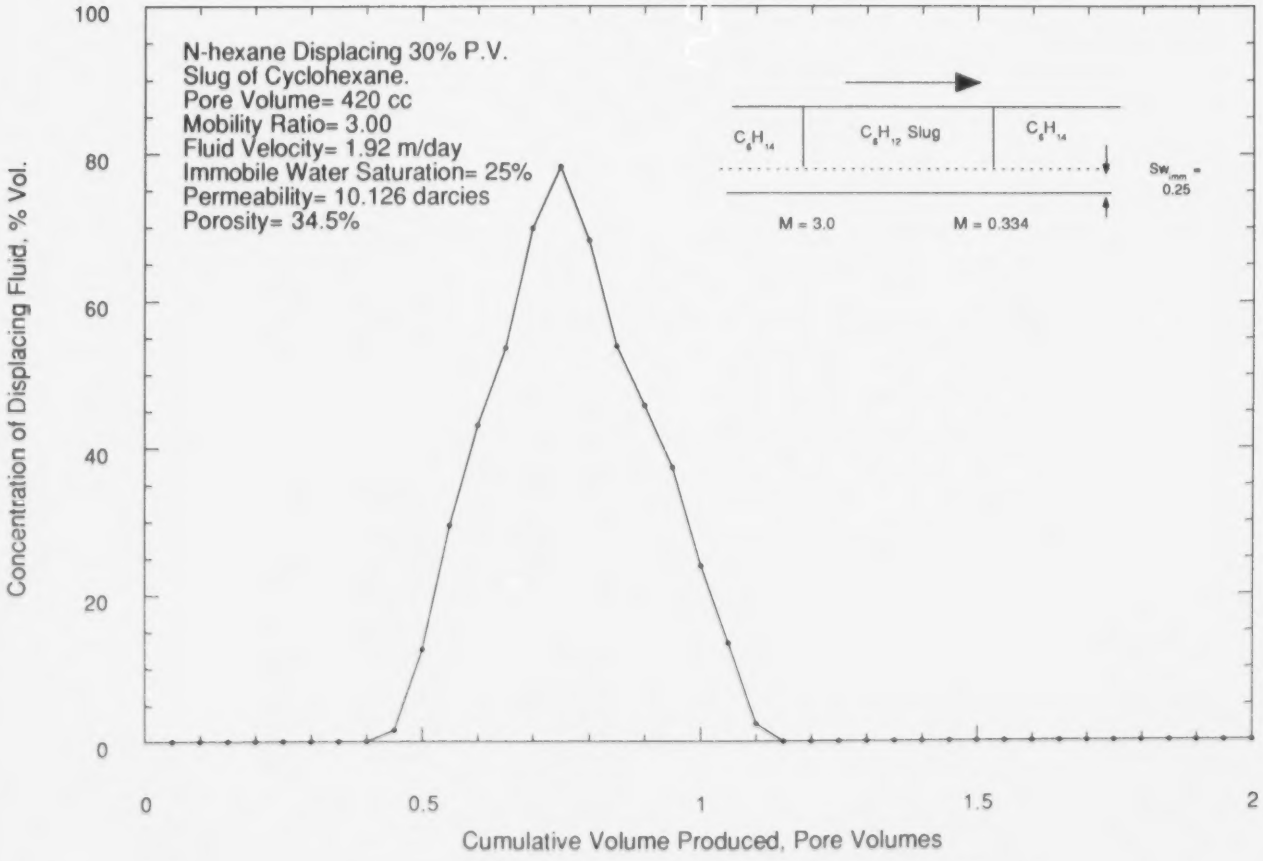

Figure B-16: Run 16: Concentration Profile of N-hexane Displacing a 30% P.V. Slug of Cyclohexane in the Presence of 25% Immobile Water Saturation.

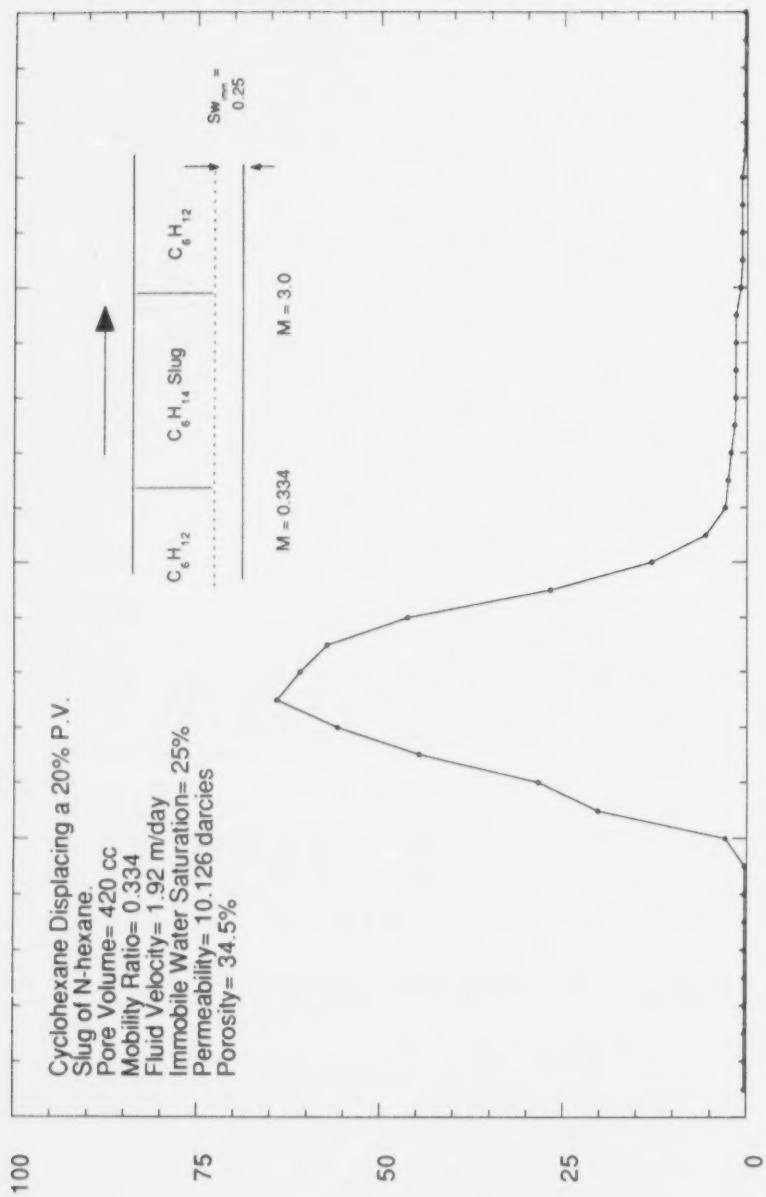

Figure B-17: Run 17: Concentration Profile of Cyclohexane Displacing a 20% P.V. Slug of N-hexane in the Presence of 25% Immobile Water Saturation.

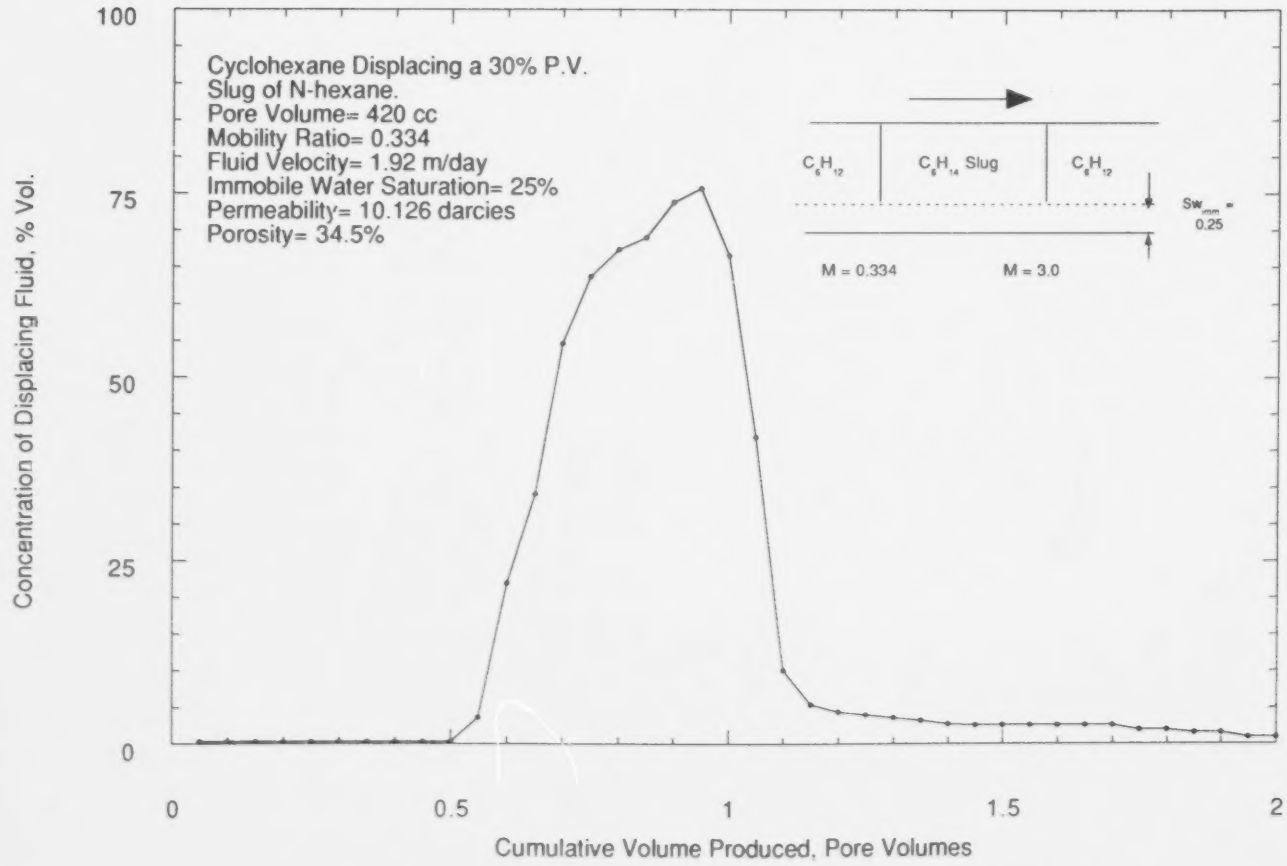

Figure B-18: Run 18: Concentration Profile of Cyclohexane Displacing a 30% P.V. Slug of N-hexane in the Presence of 25% Immobile Water Saturation.

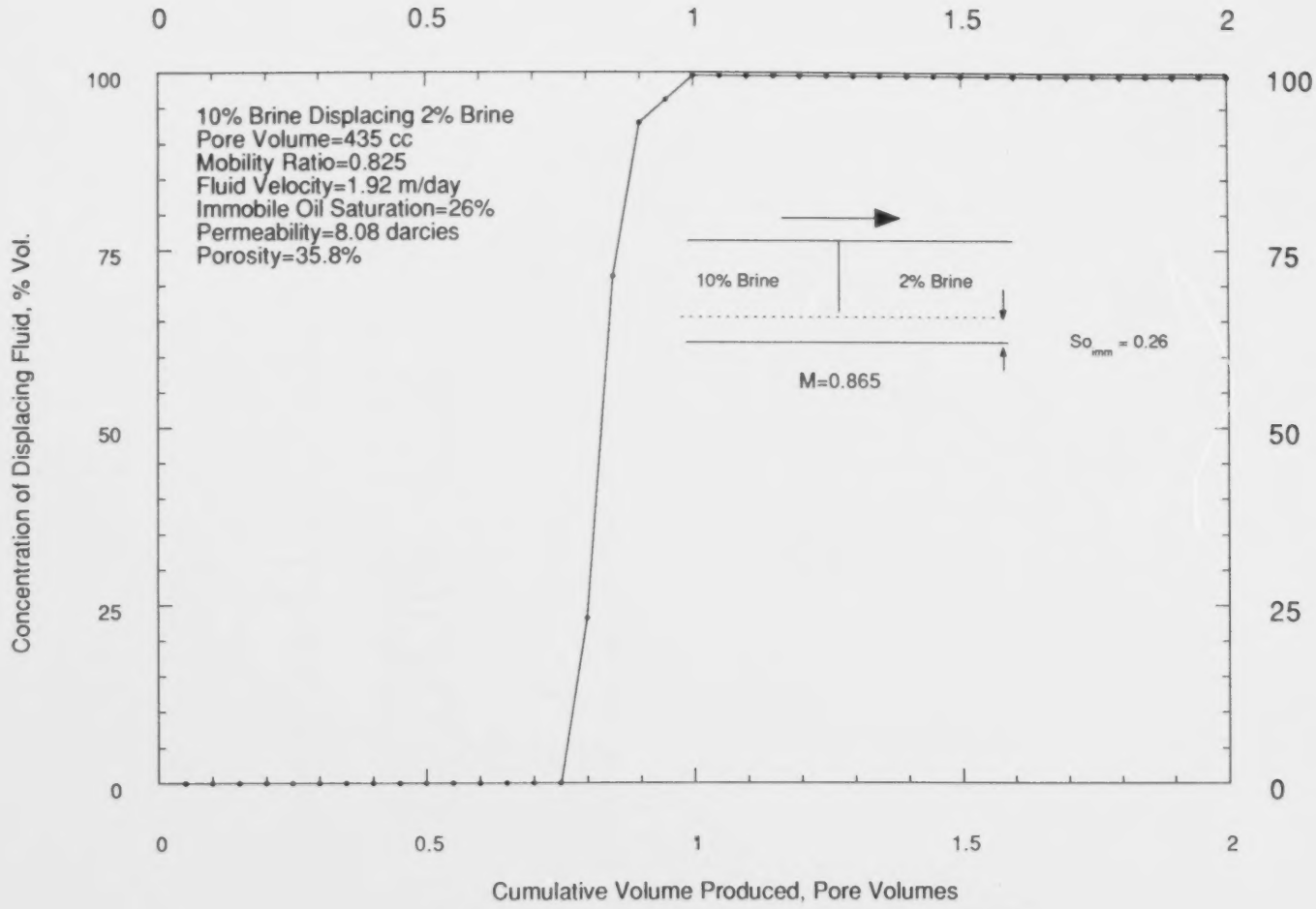

Figure B-19: Run 19: Concentration Profile of 10% Brine Displacing 2% Brine in the Presence of 26% Immobile Oil Saturation.

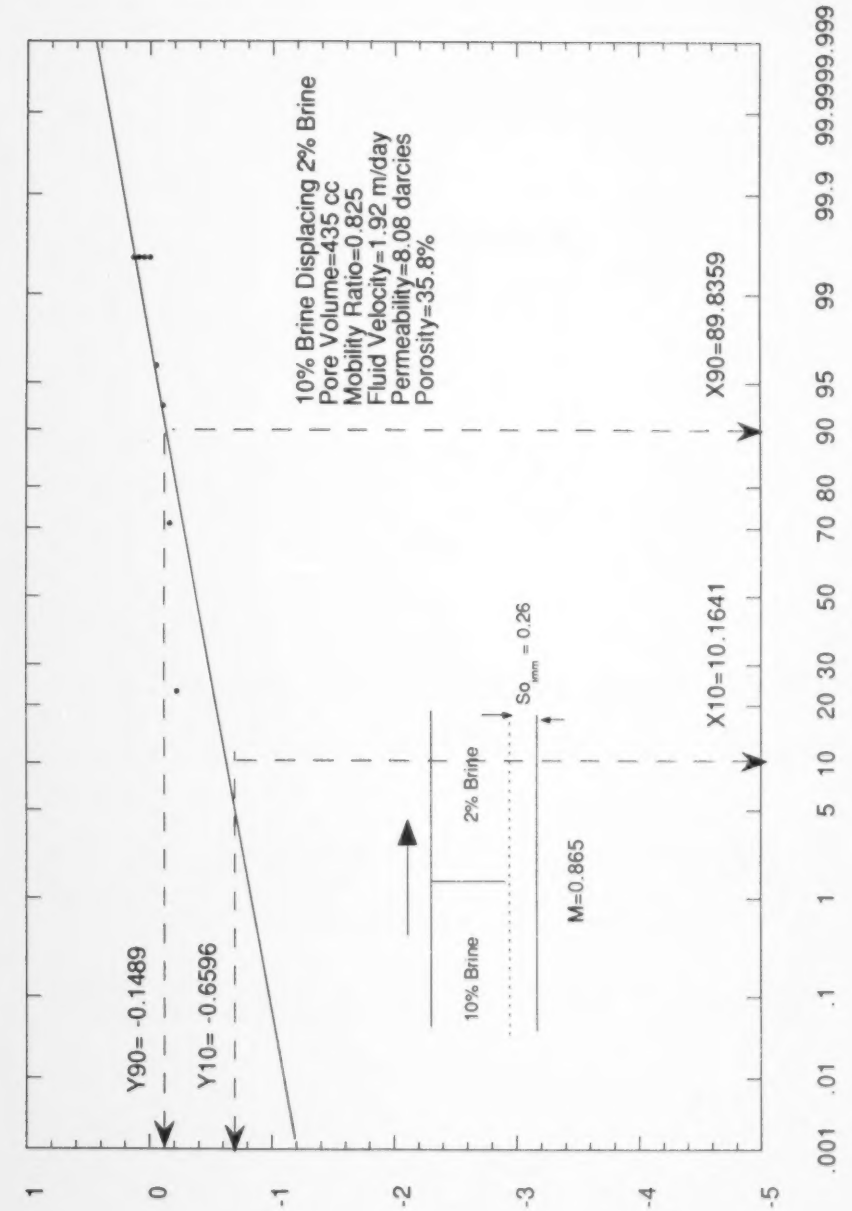

Figure B-19.1: Effluent Concentration Plotted on Arithmetic Probability Paper for Run 19.

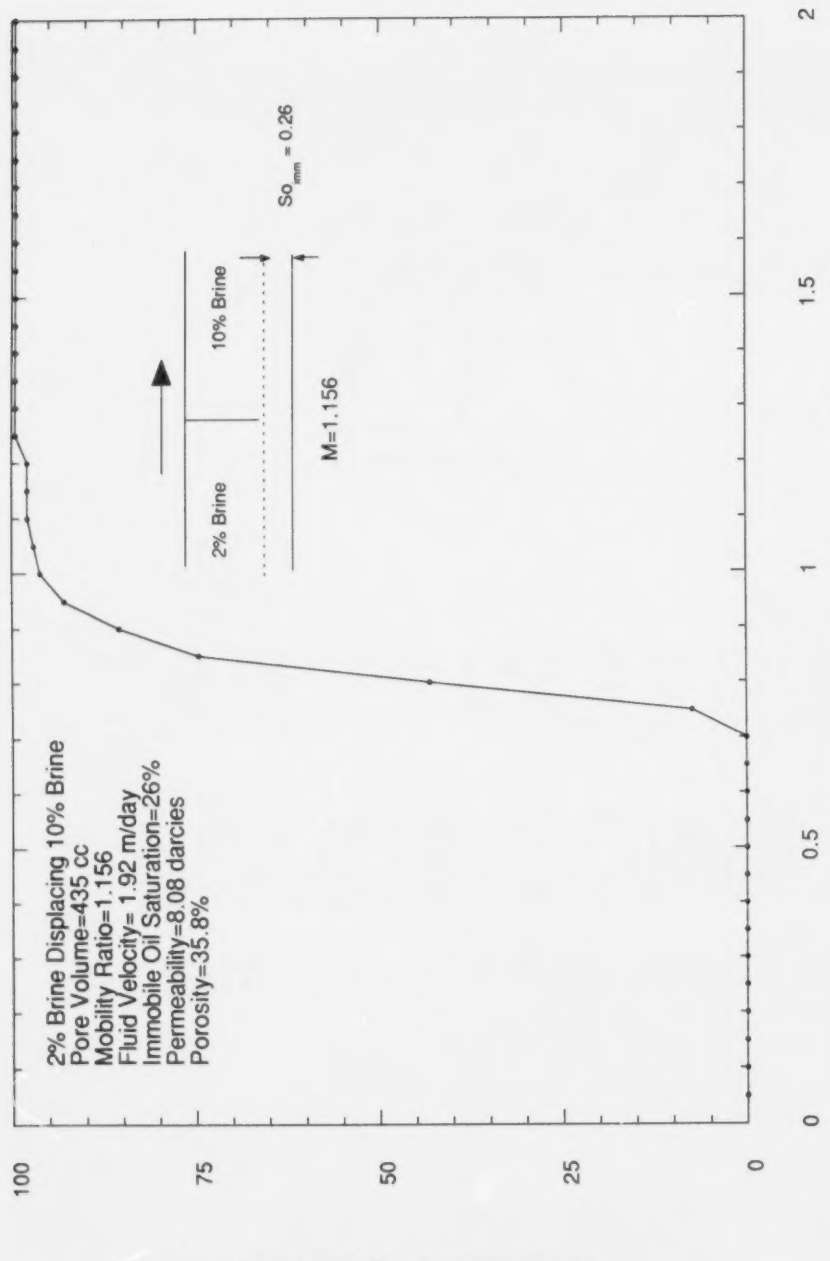

Figure B-20: Run 20: Concentration Profile of 2% Brine Displacing 10% Brine in the Presence of 26% Immobile Oil Saturation.

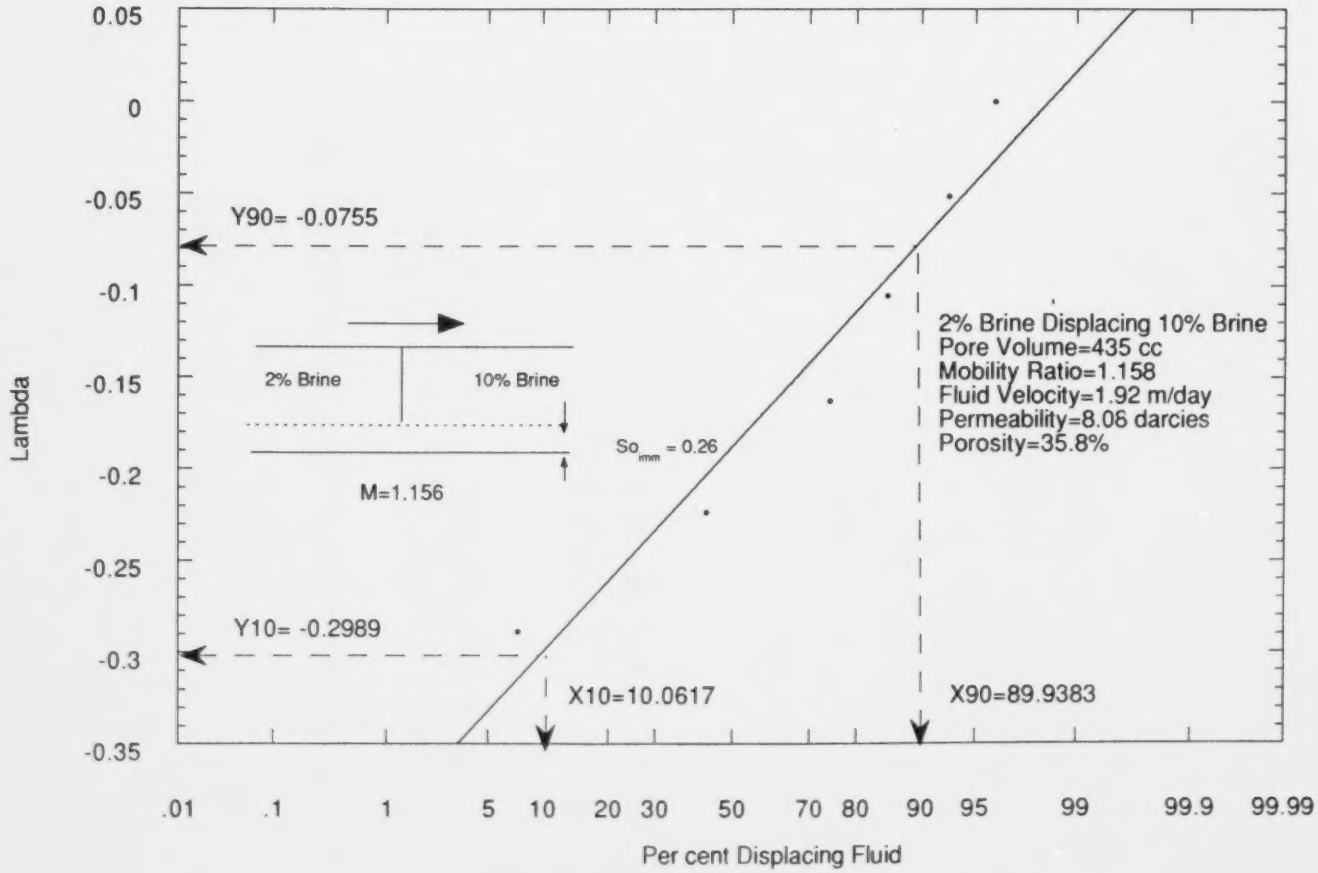

Figure B-20.1: Effluent Concentration Plotted on Arithmetic Probability Paper for Run 20.

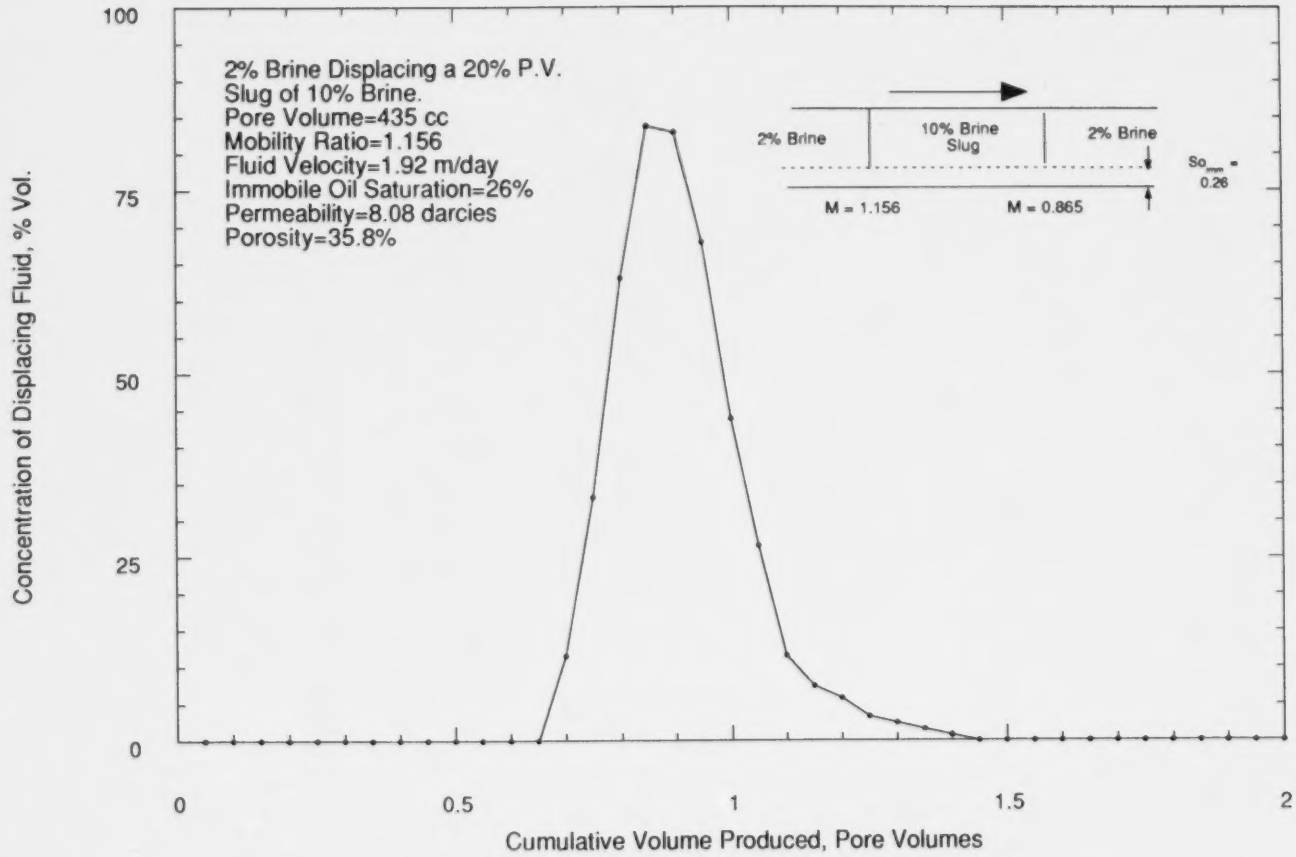

Figure B-21: Run 21: Concentration Profile of 2% Brine Displacing a 20% P.V. Slug of 10% Brine in the Presence of 26% Immobile Oil Saturation.

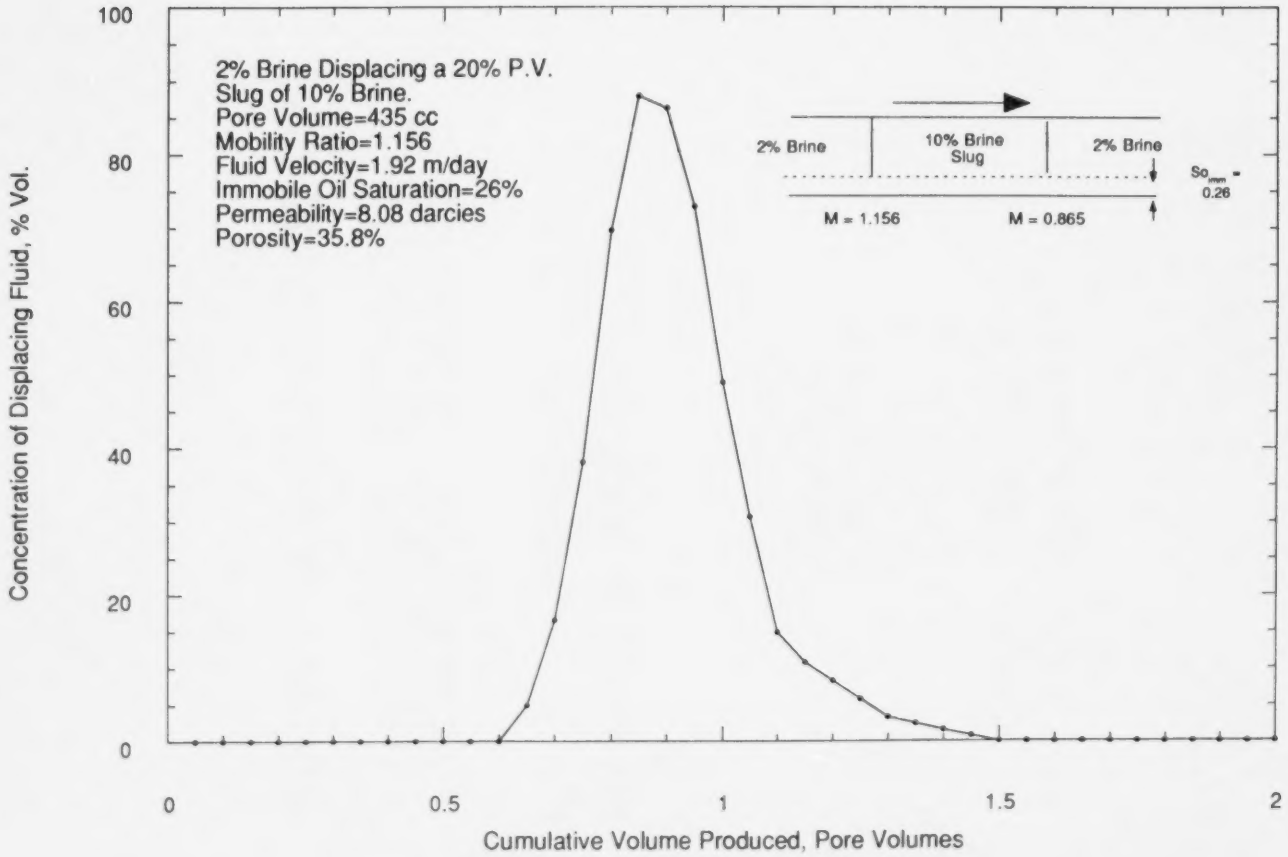

Figure B-21R : Run 21R: Concentration Profile of 2% Brine Displacing a 20% P.V. Slug of 10% Brine in the Presence of 26% Immobile Oil Saturation.

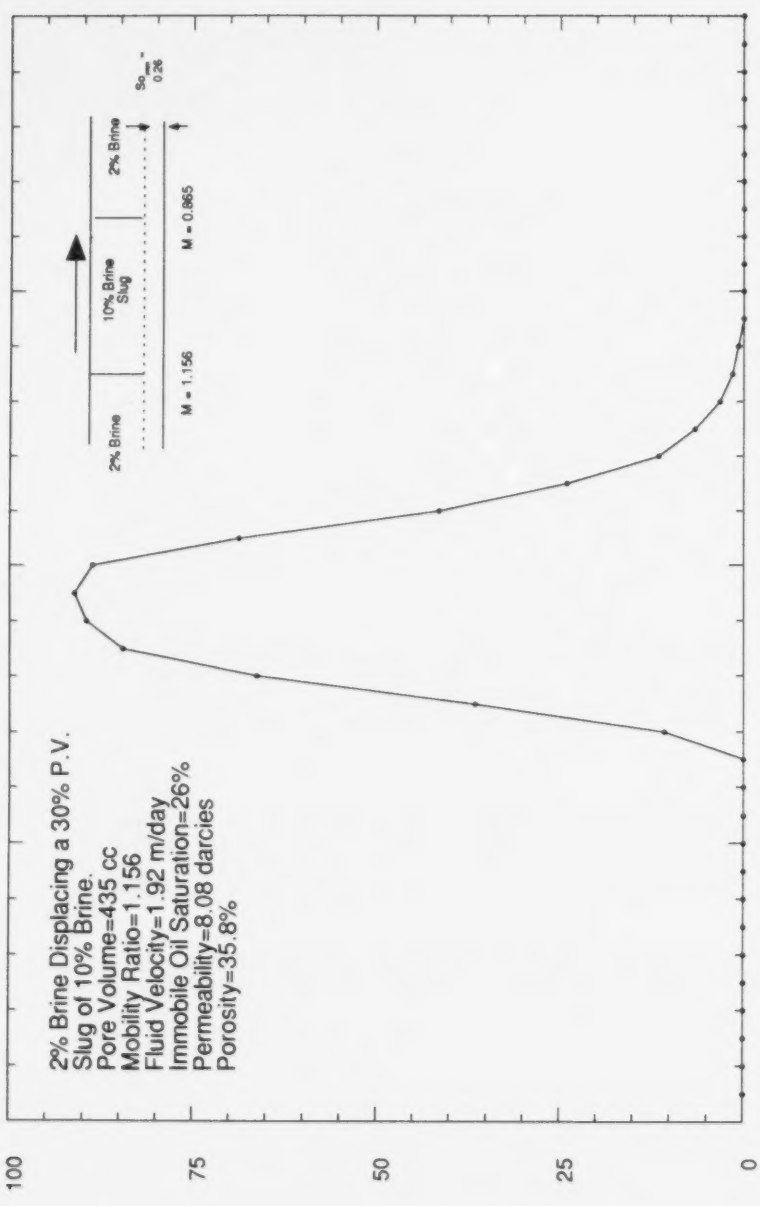

Figure B-22: Run 22: Concentration Profile of 2% Brine Displacing a 30% P.V. Slug of 10% Brine in the Presence of 26% Immobile Oil Saturation.

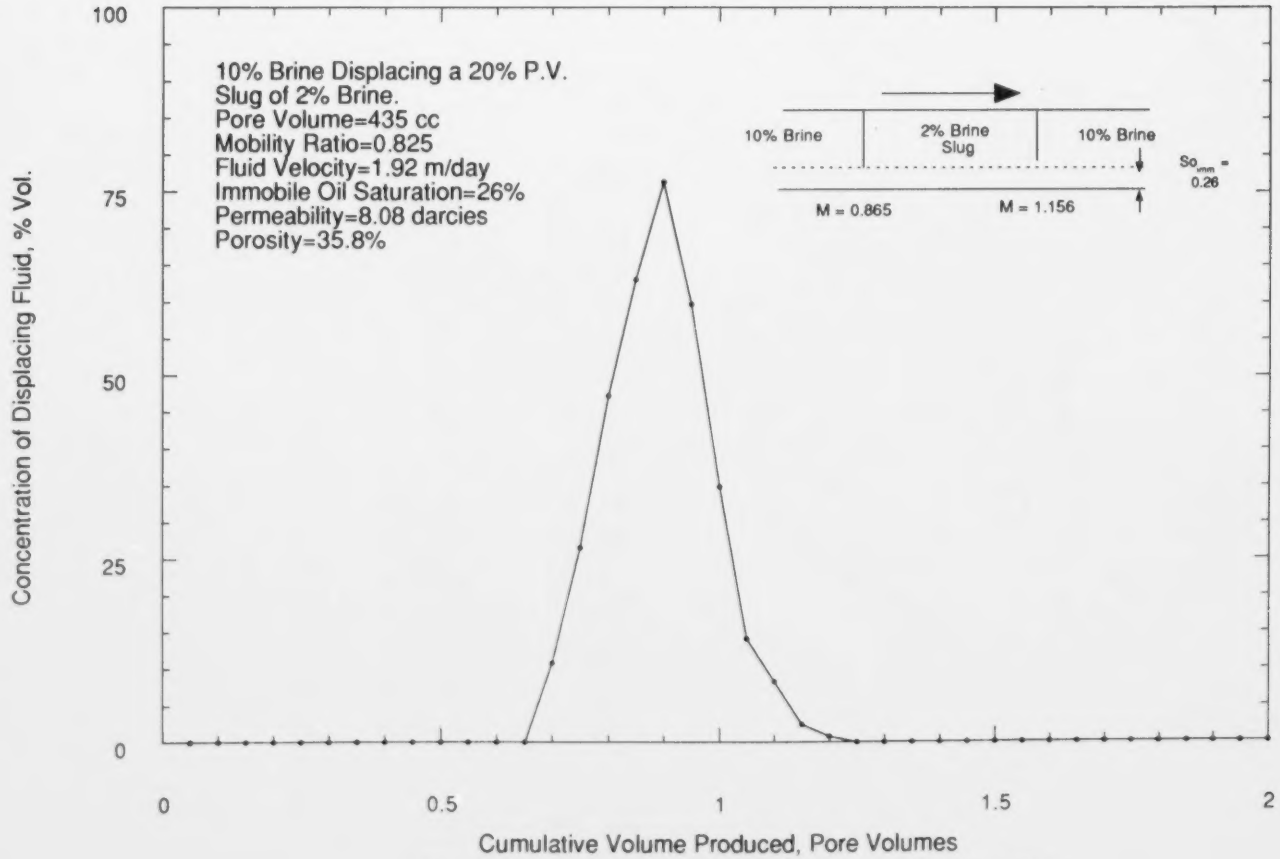

Figure B-23: Run 23: Concentration Profile of 10% Brine Displacing a 20% P.V. Slug of 2% Brine in the Presence of 26% Immobile Oil Saturation.

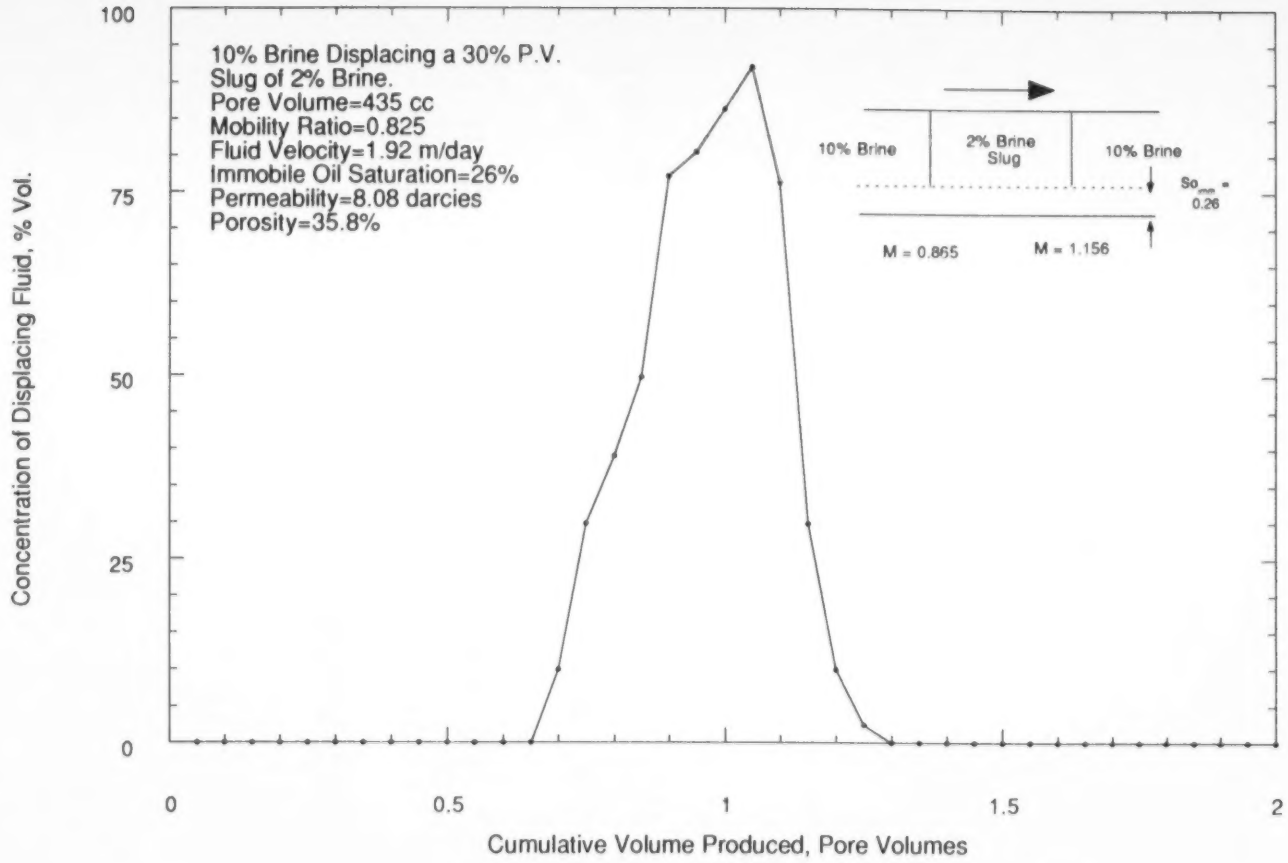

Figure B-24: Run 24: Concentration Profile of 10% Brine Displacing a 30% P.V. Slug of 2% Brine in the Presence of 26% Immobile Oil Saturation.

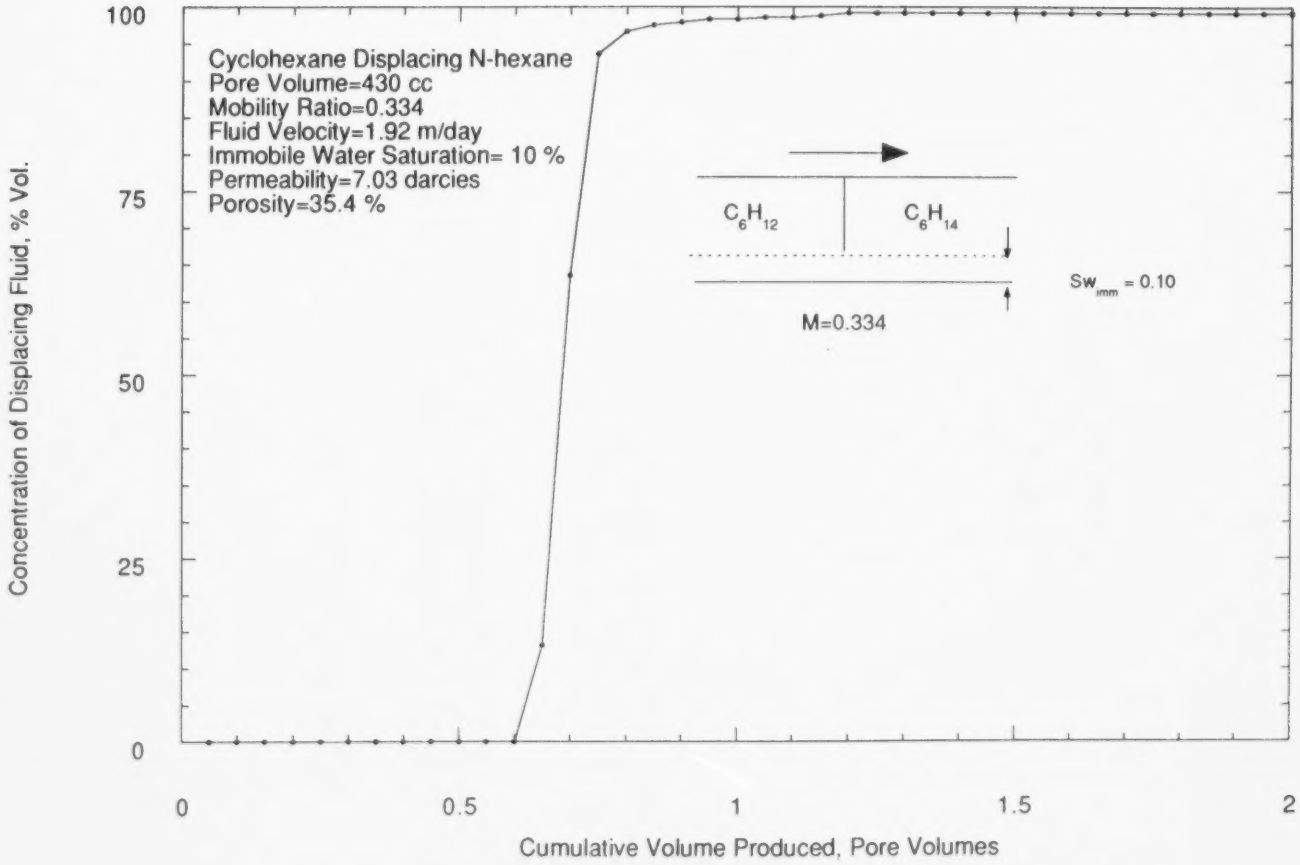

Figure B-25: Run 25: Concentration Profile of Cyclohexane Displacing N-hexane in the Presence of 10 % Immobile Water Saturation.

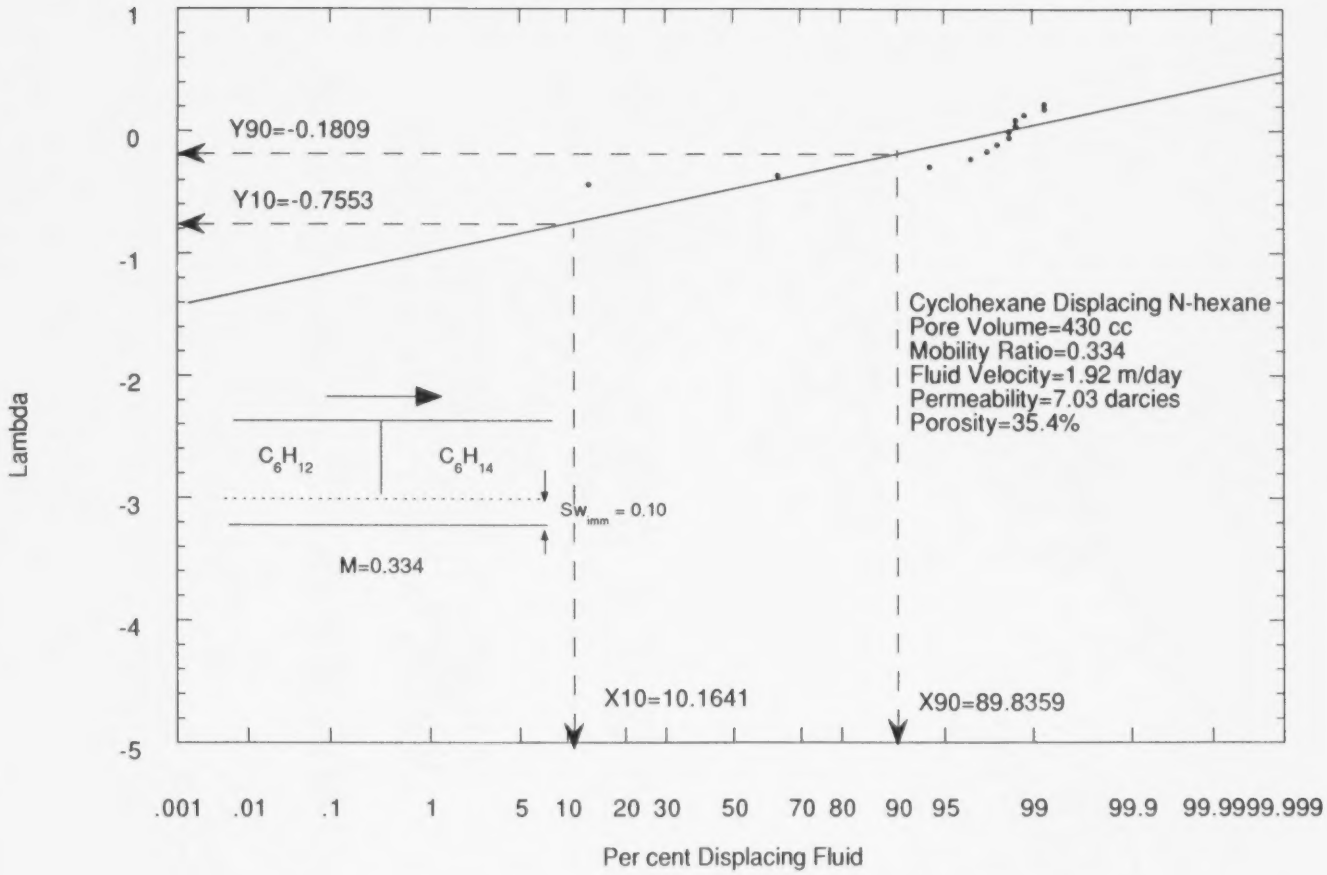

Figure B-25.1: Effluent Concentration Plotted on Arithmetic Probability Paper for Run 25.

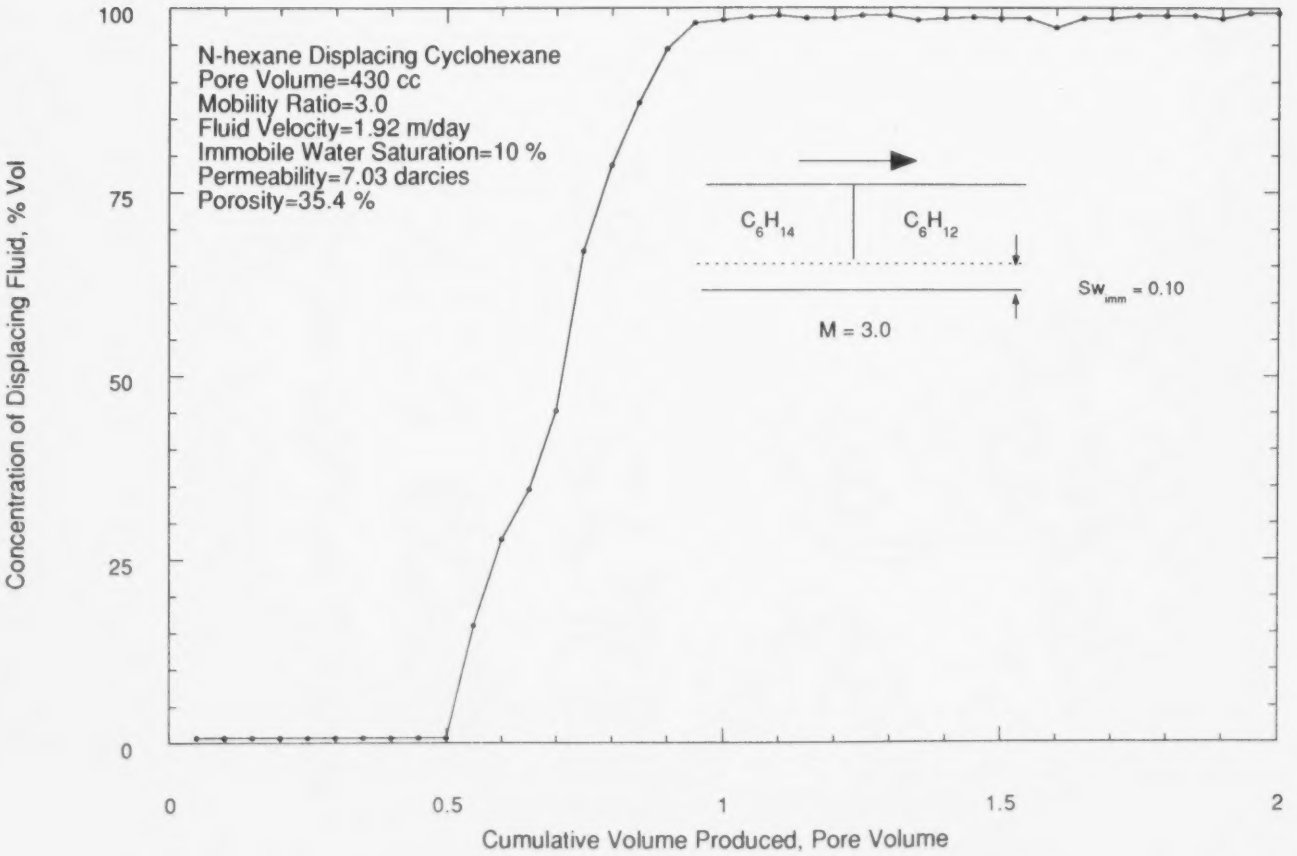

Figure B-26: Run 26: Concentration Profile of N-hexane Displacing Cyclohexane in the Presence of 10 % Immobile Water Saturation.

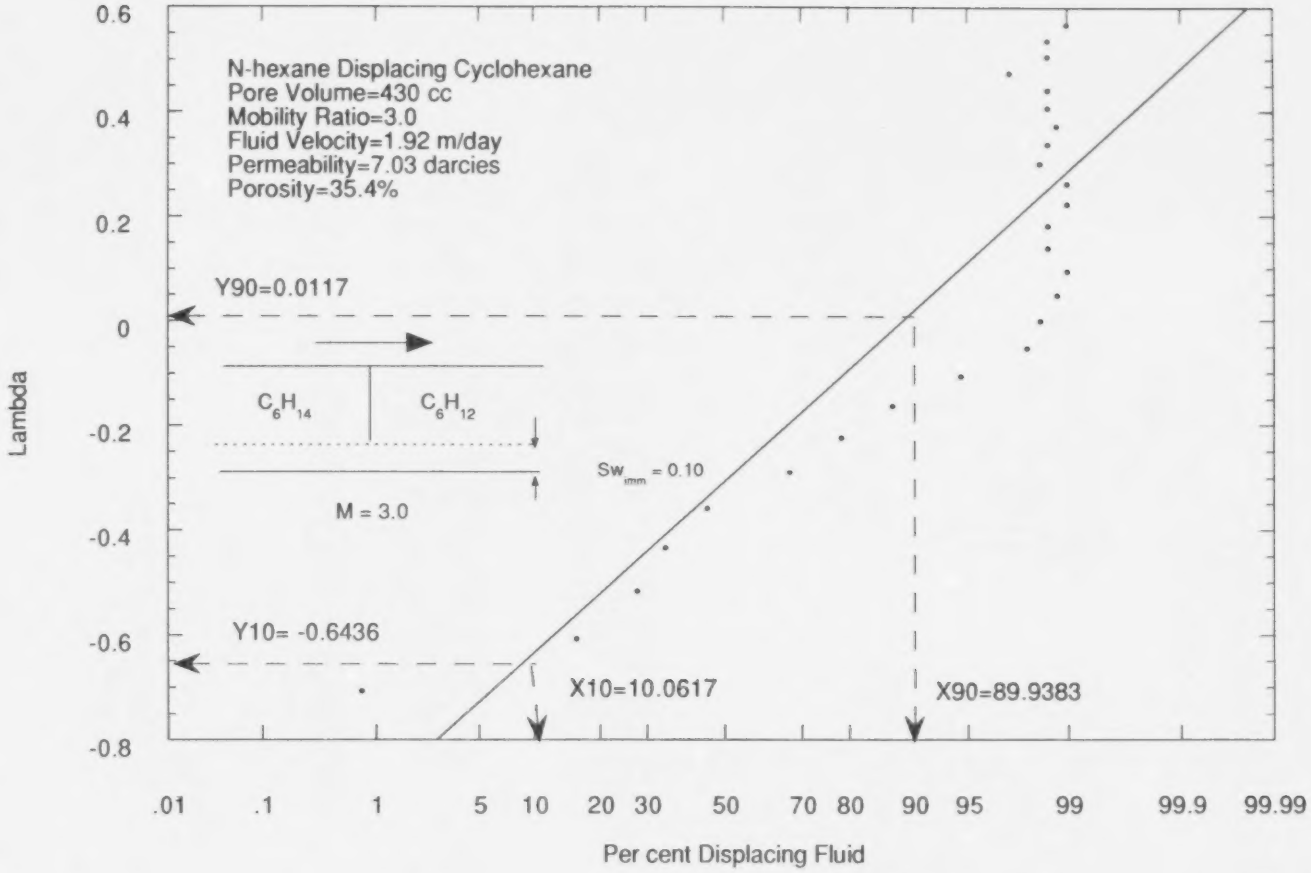

Figure B-26.1: Effluent Concentration Plotted on Arithmetic Probability Paper for Run 26.

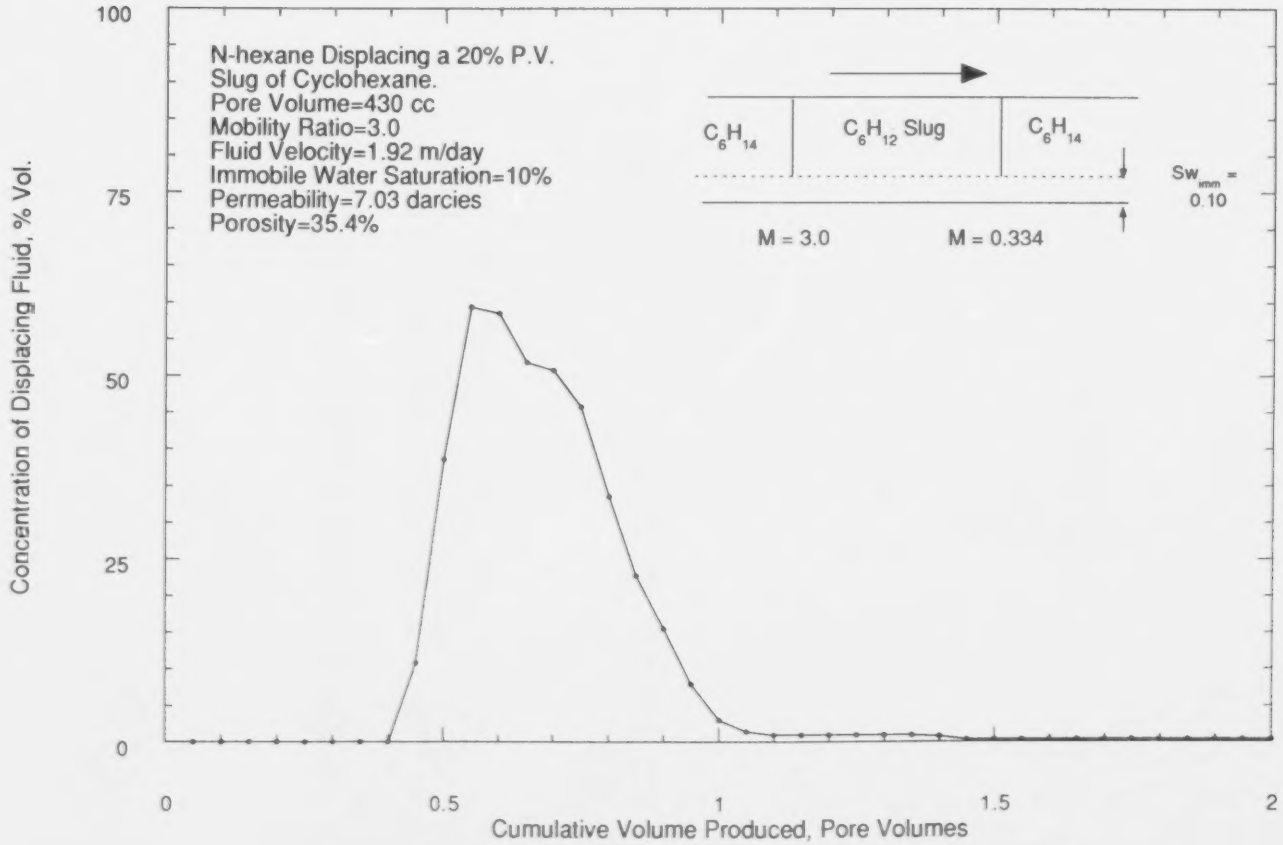

Figure B-27: Run 27: Concentration Profile of N-hexane Displacing a 20% P.V. Slug of Cyclohexane in the Presence of 10% Immobile Water Saturation.

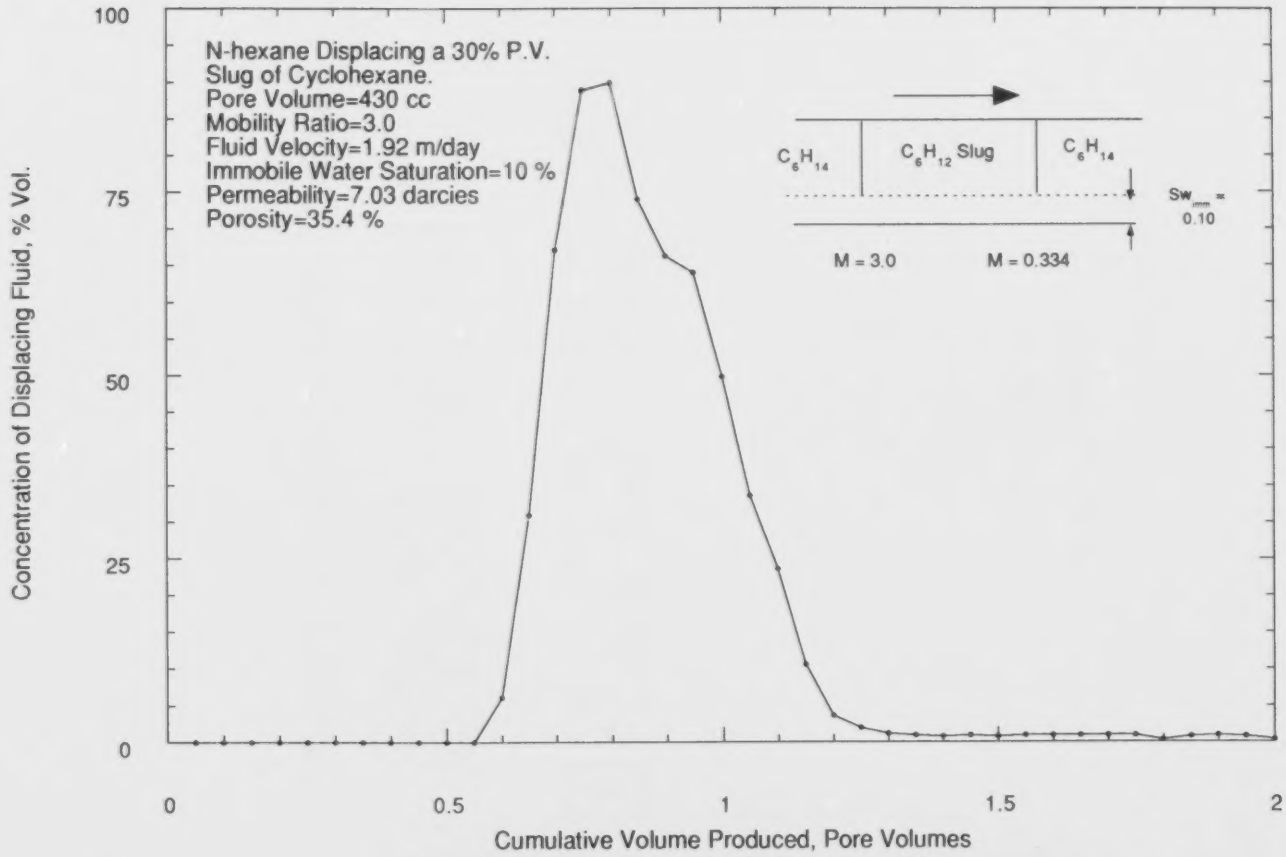

Figure B-28: Run 28: Concentration Profile of N-hexane Displacing a 30% P.V. Slug of Cyclohexane in the Presence of 10 % Immobile Water Saturation.

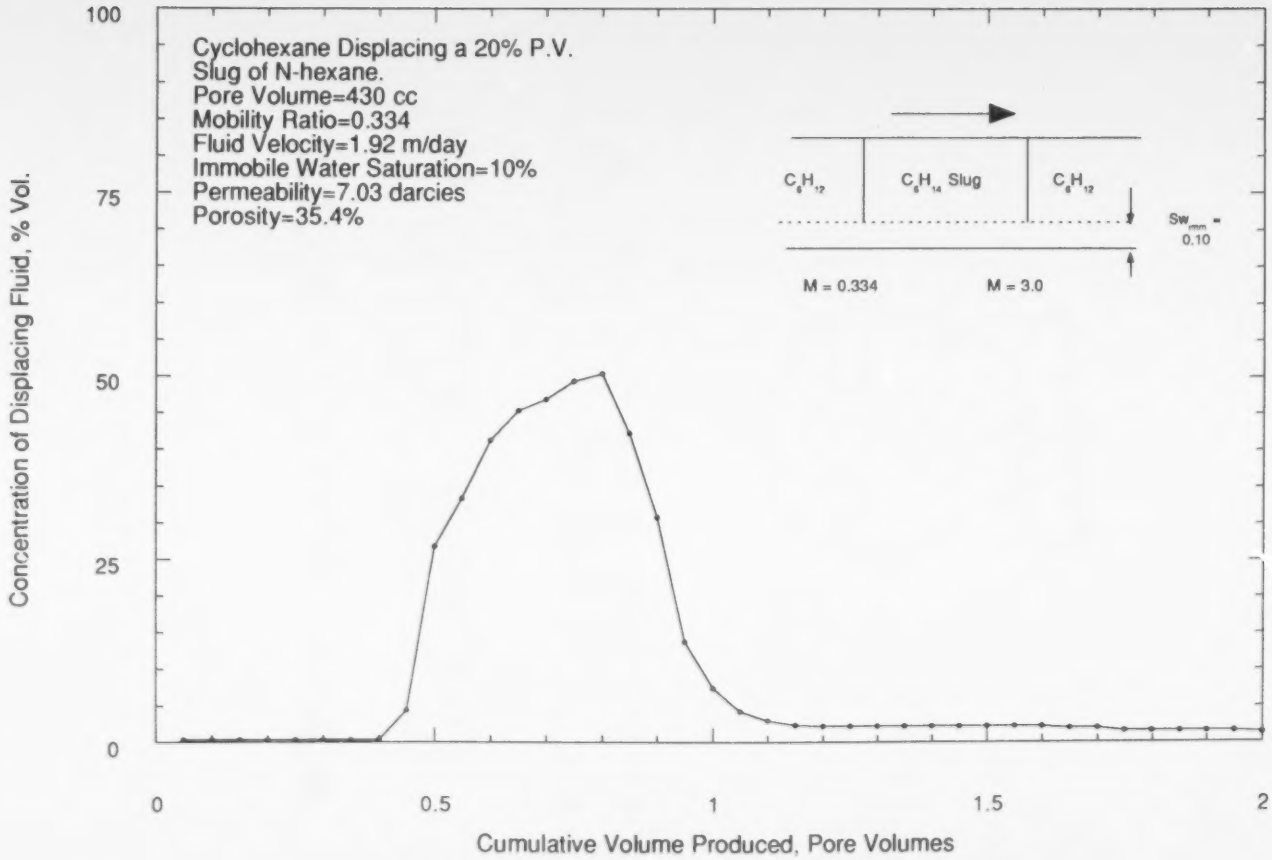

Figure B-29: Run 29: Concentration Profile of Cyclohexane Displacing a 20% P.V. Slug of N-hexane in the Presence of 10% Immobile Water Saturation.

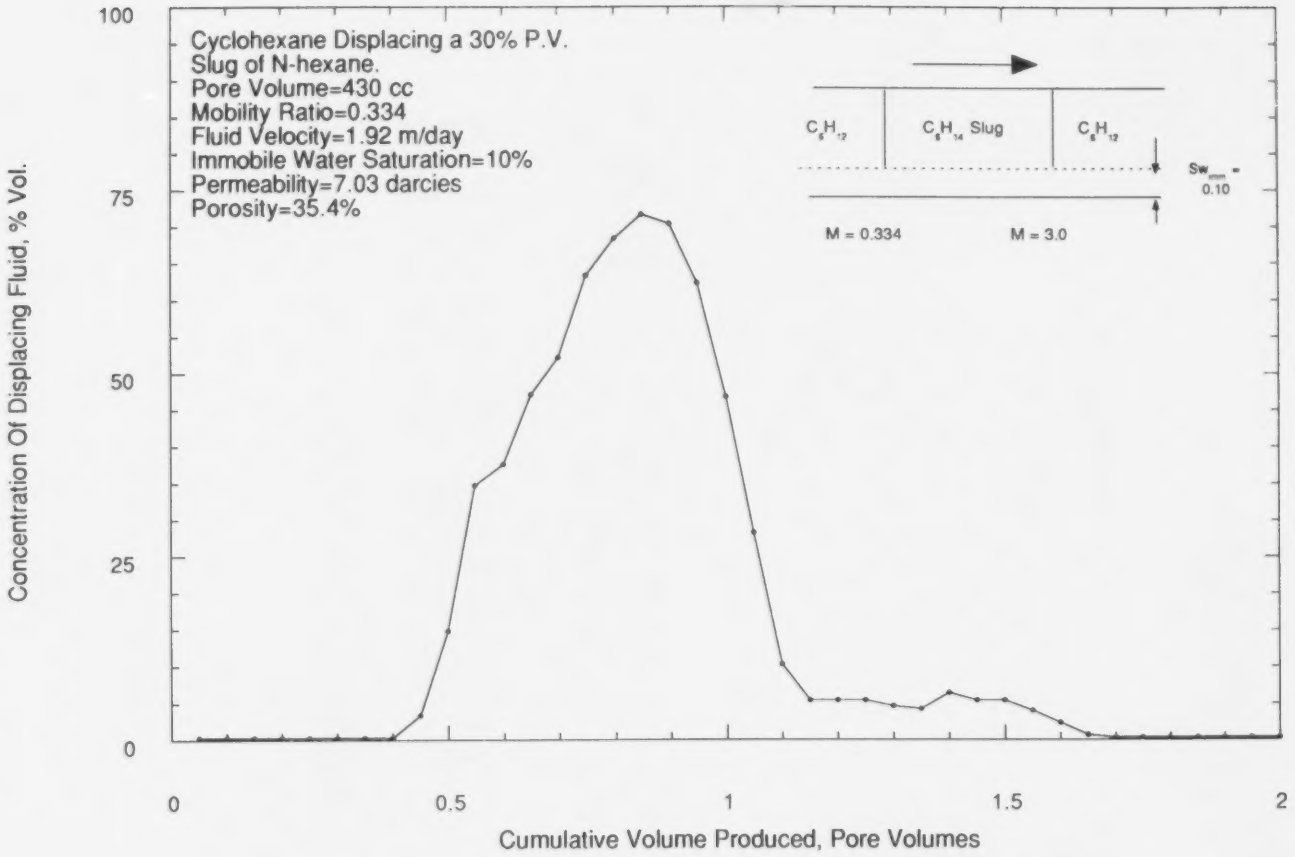

Figure B-30: Run 30: Concentration Profile of Cyclohexane Displacing a 30% P.V. Slug of N-hexane in the Presence of 10% Immobile Water Saturation.

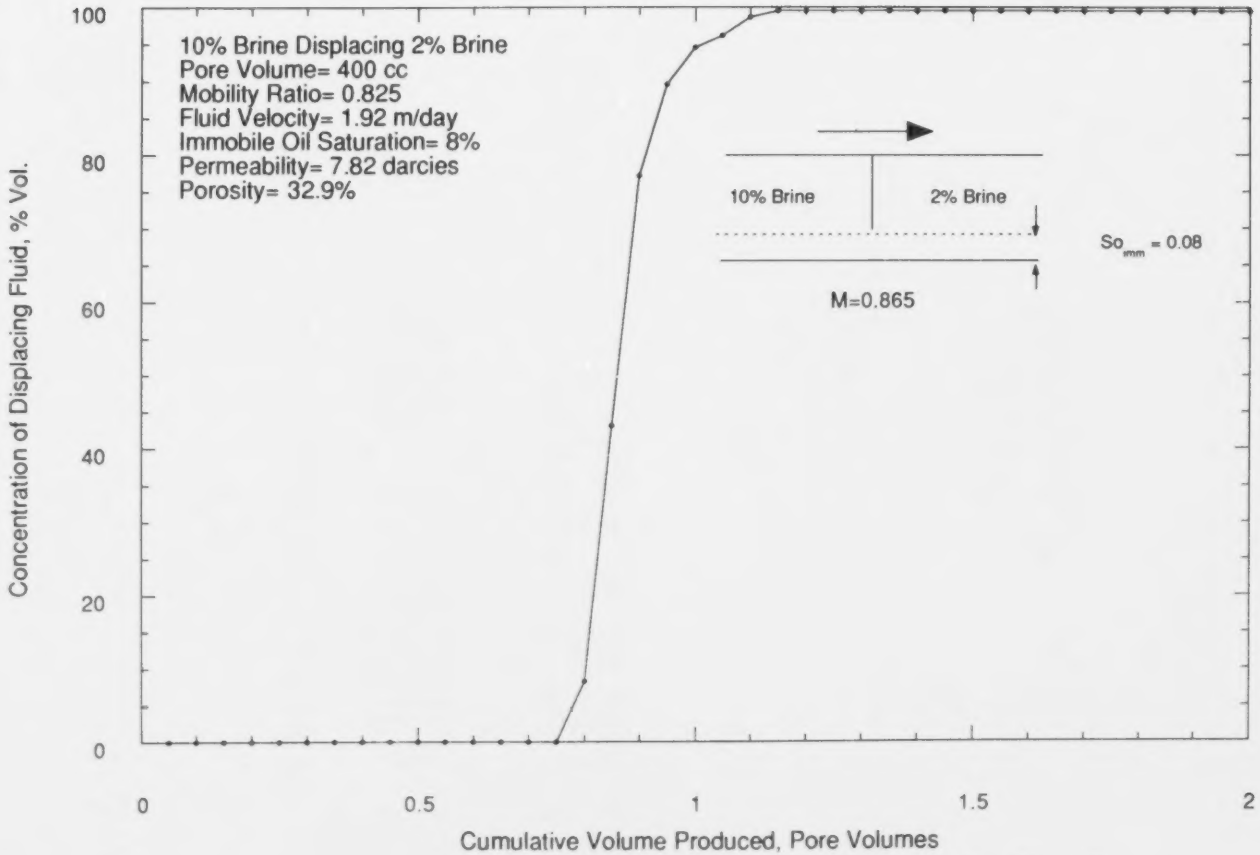

Figure B-31: Run 31: Concentration Profile of 10% Brine Displacing 2% Brine in the Presence of 8% Immobile Oil Saturation.

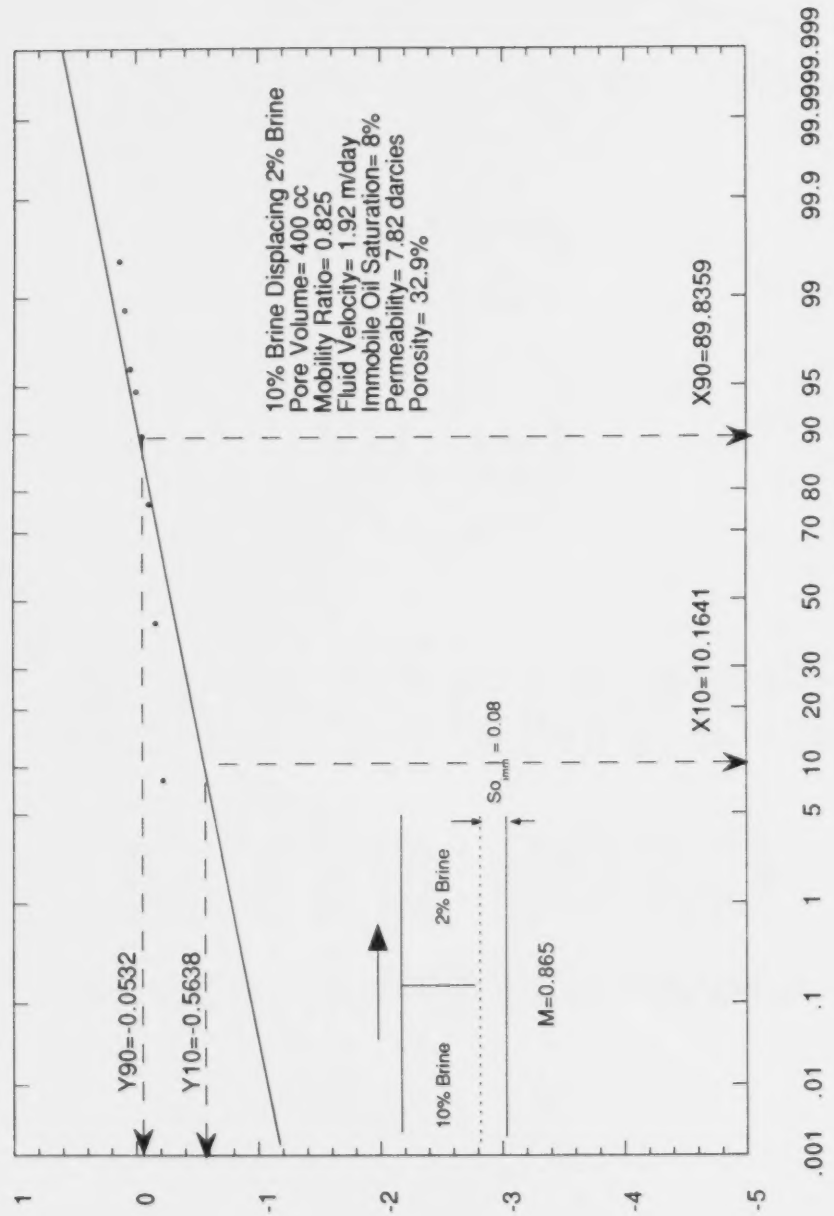

Figure B-31.1: Effluent Conncentration Plotted on Arithmetic Probability Paper for Run 31

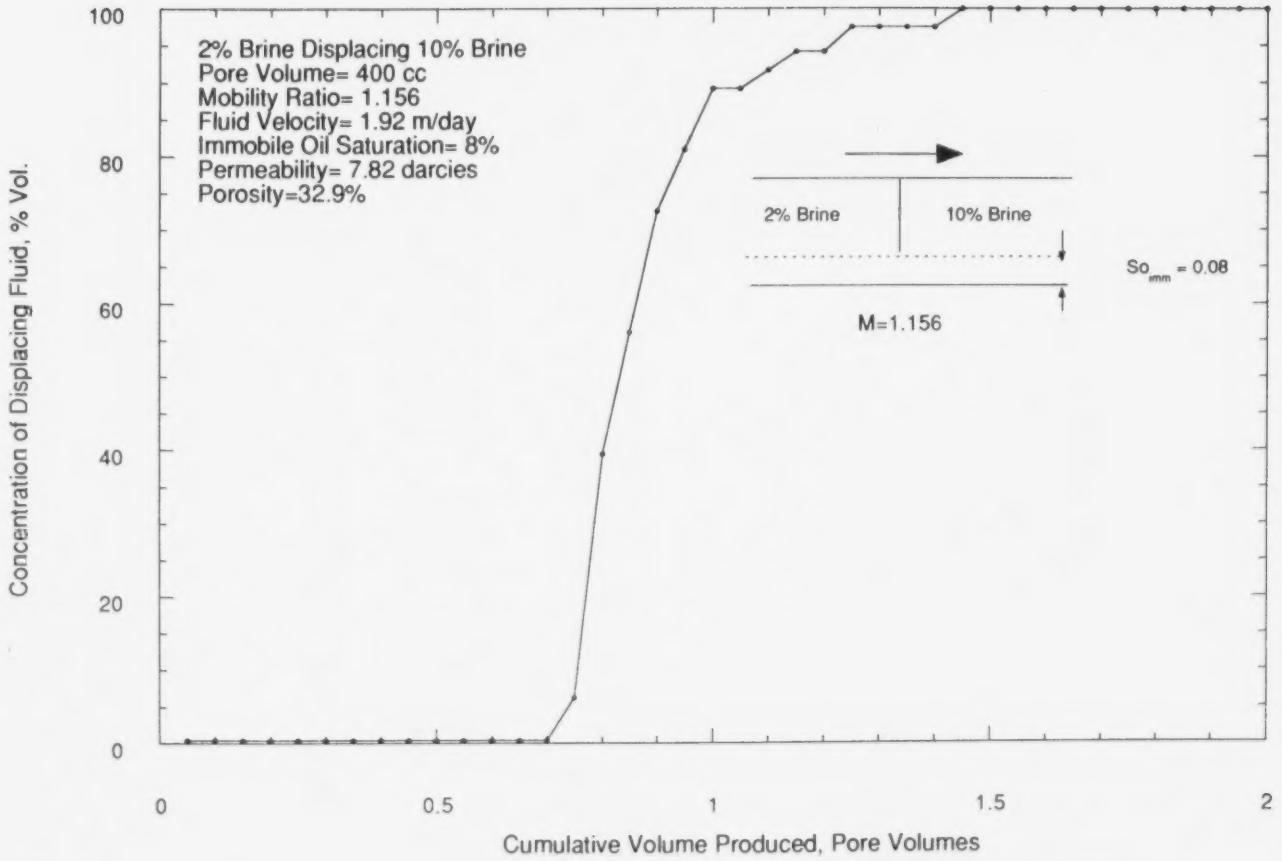

Figure B-32: Run 32: Concentration Profile of 2% Brine Displacing 10% Brine in the Presence of 8% Immobile Oil Saturation.

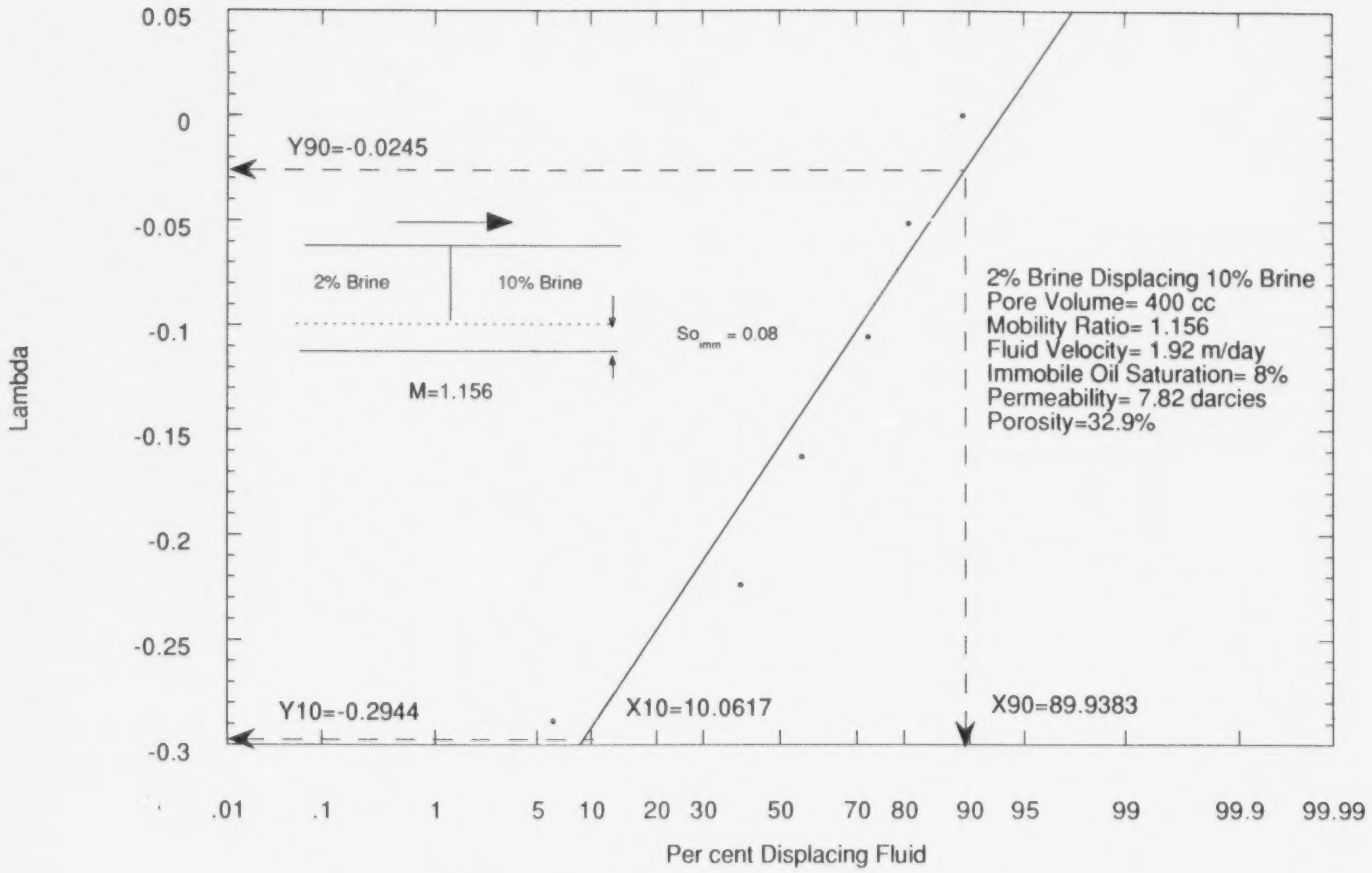

Figure B-32.1: Effluent Concentration Plotted on Arithmetic Probability Paper for Run 32.

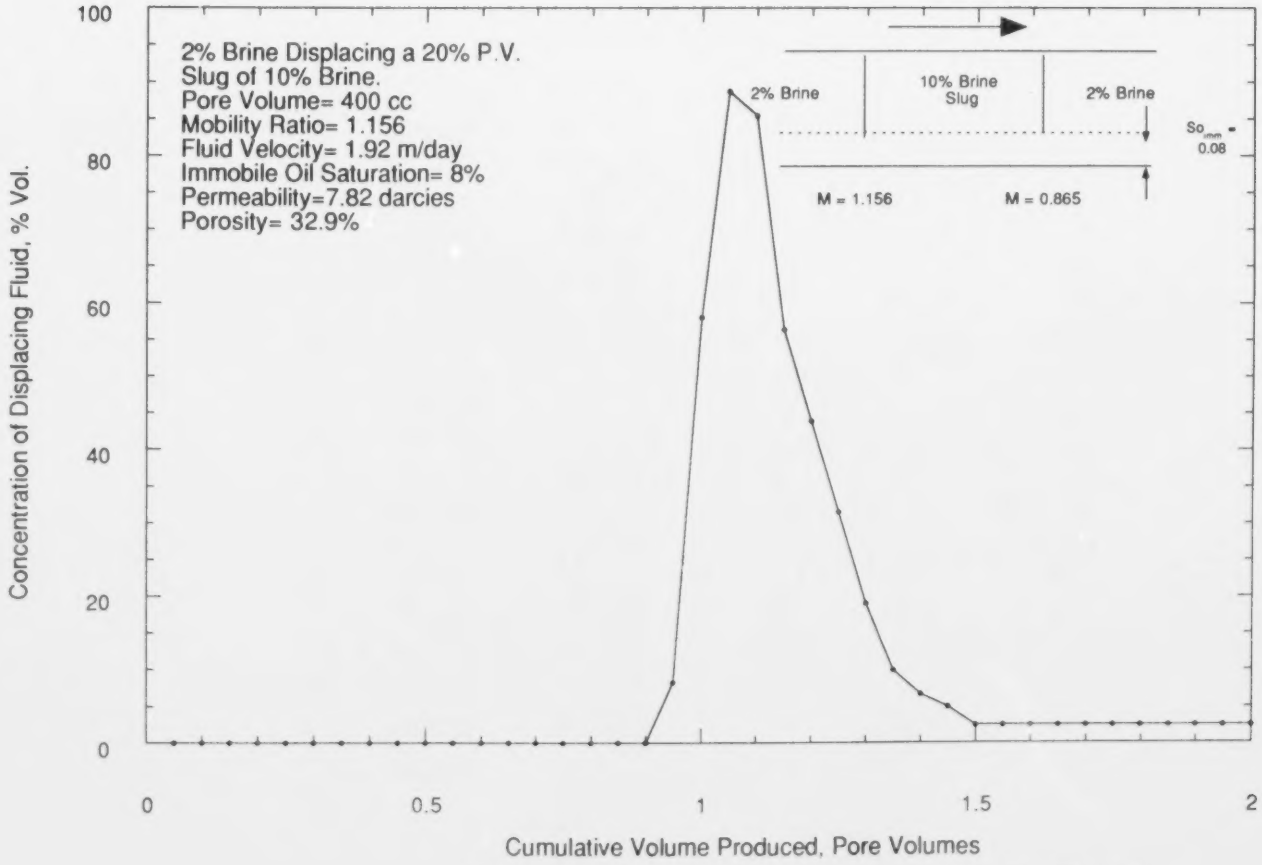

Figure B-33: Run 33: Concentration Profile of 2% Brine Displacing a 20% P.V. Slug of 10% Brine in the Presence 8% Immobile Oil Saturation.

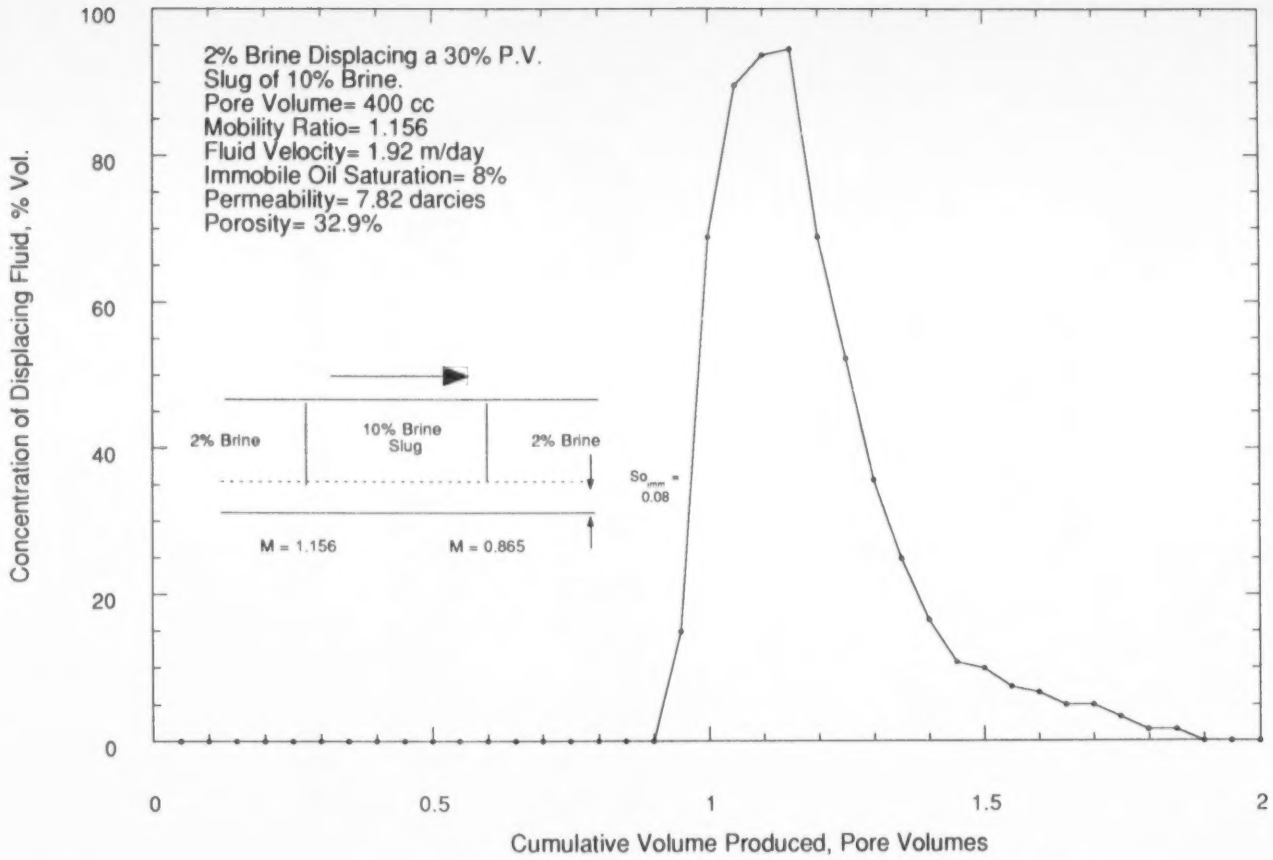

Figure B-34: Run 34: Concentration Profile of 2% Brine Displacing a 30% P.V. Slug of 10% Brine in the Presence of 8% Immobile Oil Saturation.

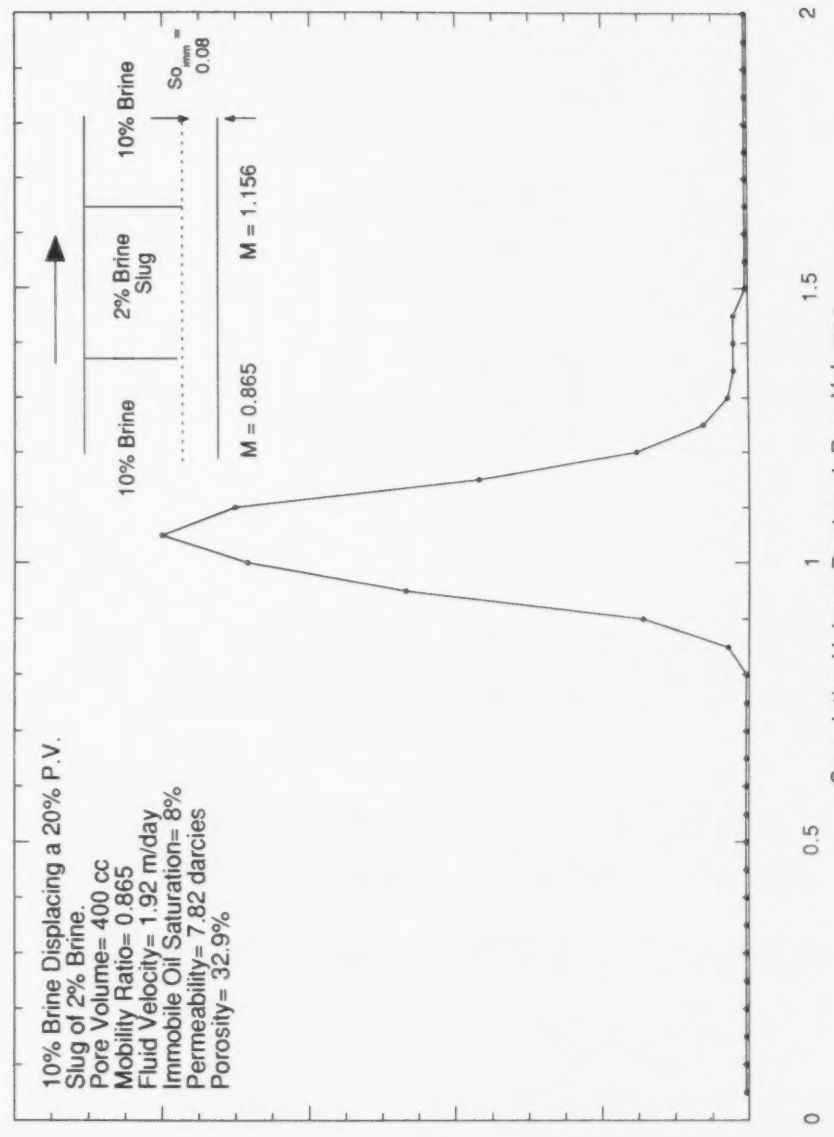

Figure B-35: Run 35: Concentration Profile of 10% Brine Displacing a 20% P.V. Slug of 2% Brine in the Presence of 8% Immobile Oil Saturation.

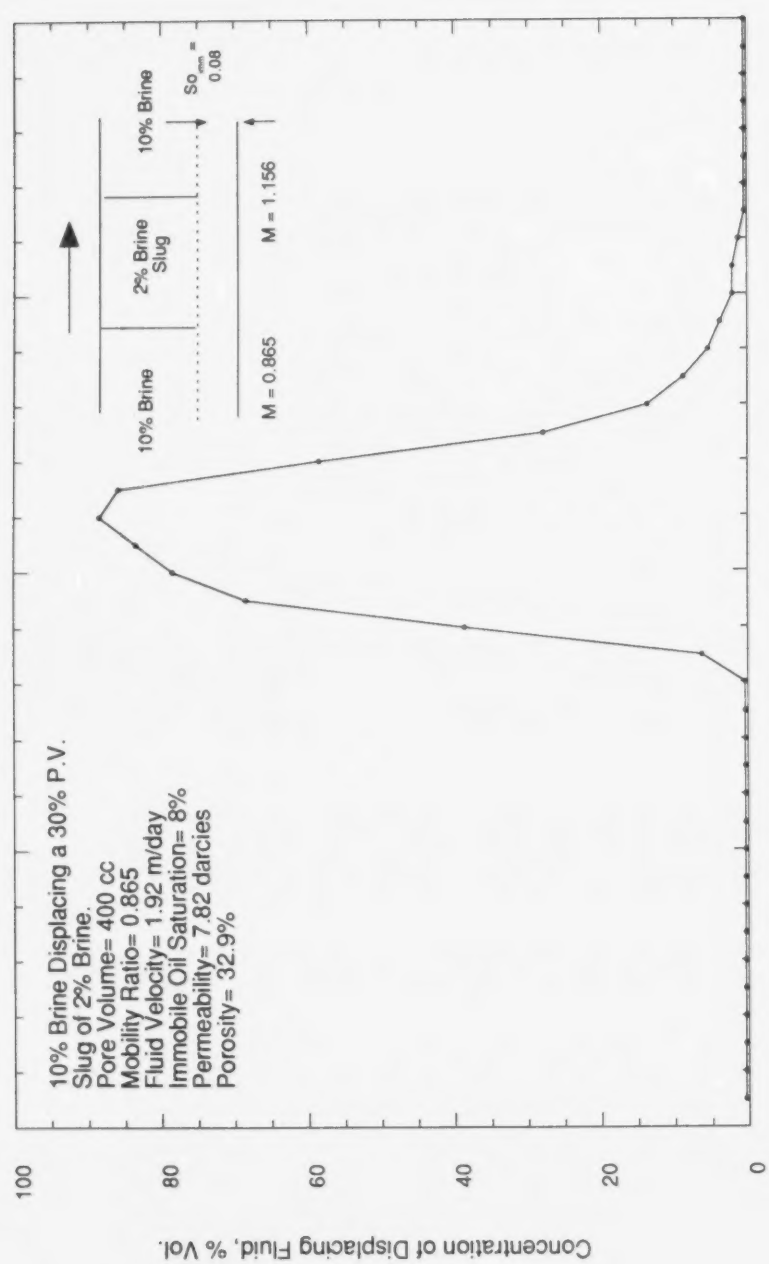

Figure B-36: Run 36: Concentration Profile of 10% Brine Displacing a 30% P.V. Slug of 2% Brine in the Presence of 8% Immobile Oil Saturation.

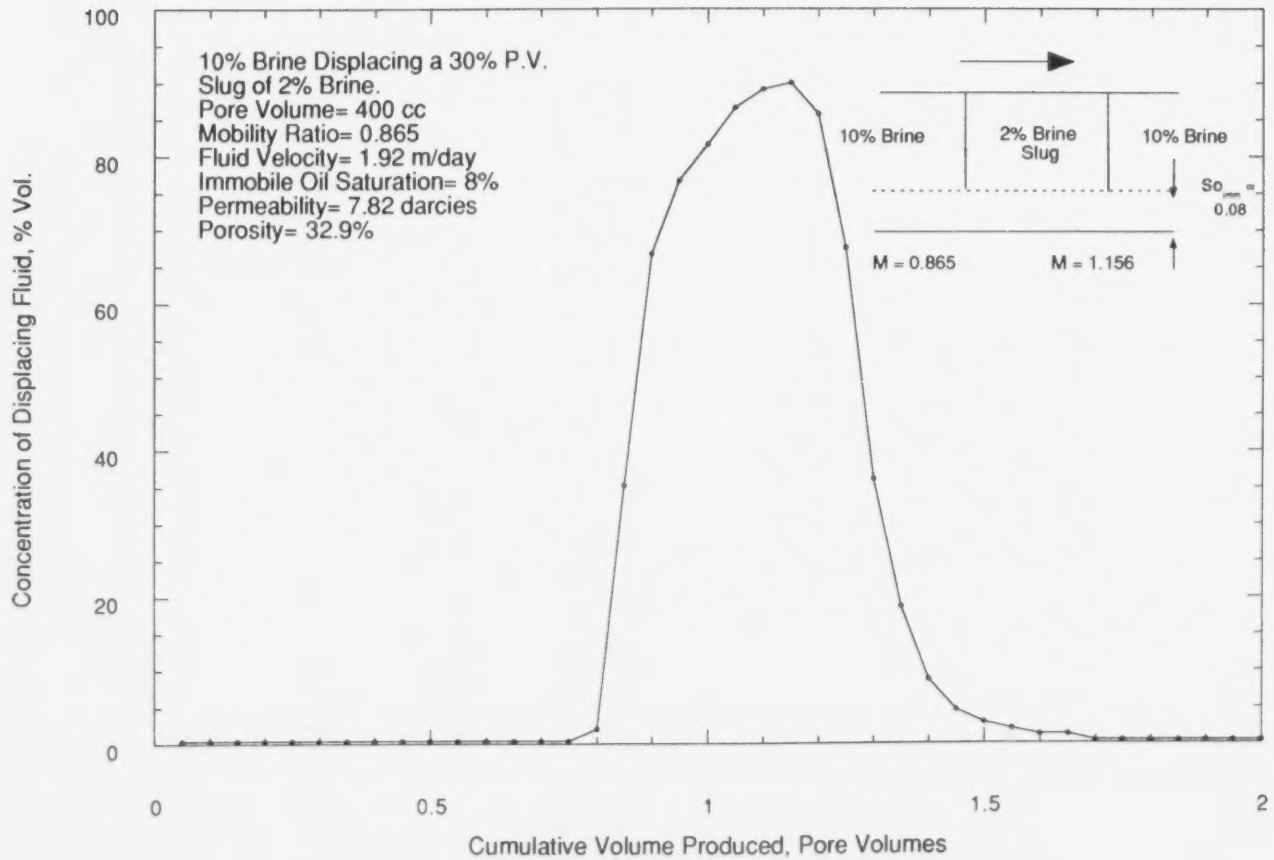

Figure B-36R: Run 36R: Concentration Profile of 10% Brine Displacing a 30% P.V. Slug of 2% Brine in the Presence of 8% Immobile Oil Saturation.

Appendix C

Table C-1: Experimental Effluent Concentration Data for Run 1

Pore Volume Injected	Refractive Index	Cyclohexane Concentration, %	Cumulative P.V. Injected, cc	Lambda	N-Hexane Concentration, %
0.05	1.3760	0.000	19.5	-4.249	100.000
0.10	1.3760	0.000	39	-2.846	100.000
0.15	1.3760	0.000	58.5	-2.195	100.000
0.20	1.3760	0.000	78	-1.789	100.000
0.25	1.3760	0.000	97.5	-1.500	100.000
0.30	1.3760	0.000	117	-1.278	100.000
0.35	1.3760	0.000	136.5	-1.099	100.000
0.40	1.3760	0.000	156	-0.949	100.000
0.45	1.3760	0.000	175.5	-0.820	100.000
0.50	1.3760	0.000	195	-0.707	100.000
0.55	1.3760	0.000	214.5	-0.607	100.000
0.60	1.3760	0.000	234	-0.516	100.000
0.65	1.3760	0.000	253.5	-0.434	100.000
0.70	1.3760	0.000	273	-0.359	100.000
0.75	1.3760	0.000	292.5	-0.289	100.000
0.80	1.3760	0.000	312	-0.224	100.000
0.85	1.3760	0.000	331.5	-0.163	100.000
0.90	1.3760	0.000	351	-0.105	100.000
0.95	1.3766	1.220	370.5	-0.051	98.780
1.00	1.3782	4.473	390	0.000	95.527
1.05	1.3860	20.333	409.5	0.049	79.667
1.10	1.4035	55.915	429	0.095	44.085
1.15	1.4220	93.530	448.5	0.140	6.470
1.20	1.4234	96.377	468	0.183	3.623
1.25	1.4238	97.190	487.5	0.224	2.810
1.30	1.4240	97.597	507	0.263	2.403
1.35	1.4242	98.003	526.5	0.301	1.997
1.40	1.4244	98.410	546	0.338	1.590
1.45	1.4245	98.613	565.5	0.374	1.387
1.50	1.4246	98.817	585	0.408	1.183
1.55	1.4246	98.817	604.5	0.442	1.183
1.60	1.4246	98.817	624	0.474	1.183
1.65	1.4246	98.817	643.5	0.506	1.183
1.70	1.4246	98.817	663	0.537	1.183
1.75	1.4247	99.020	682.5	0.567	0.980
1.80	1.4247	99.020	702	0.596	0.980
1.85	1.4247	99.020	721.5	0.625	0.980
1.90	1.4247	99.020	741	0.653	0.980
1.95	1.4248	99.223	760.5	0.680	0.777
2.00	1.4248	99.223	780	0.707	0.777

Table C-2: Experimental Effluent Concentration Data for Run 2

Pore Volume Injected	Refractive Index	Cyclohexane Concentration, %	Cumulative P.V. Injected, cc	Lambda	N-Hexane Concentration, %
0.05	1.4250	99.630	19.5	-4.249	0.370
0.10	1.4250	99.630	39	-2.846	0.370
0.15	1.4250	99.630	58.5	-2.195	0.370
0.20	1.4250	99.630	78	-1.789	0.370
0.25	1.4249	99.427	97.5	-1.500	0.573
0.30	1.4249	99.427	117	-1.278	0.573
0.35	1.4249	99.427	136.5	-1.099	0.573
0.40	1.4249	99.427	156	-0.949	0.573
0.45	1.4248	99.223	175.5	-0.820	0.777
0.50	1.4248	99.223	195	-0.707	0.777
0.55	1.4248	99.223	214.5	-0.607	0.777
0.60	1.4178	84.990	234	-0.516	15.010
0.65	1.4113	71.774	253.5	-0.434	28.226
0.70	1.4058	60.591	273	-0.359	39.409
0.75	1.4028	54.491	292.5	-0.289	45.509
0.80	1.4010	50.832	312	-0.224	49.168
0.85	1.3994	47.578	331.5	-0.163	52.422
0.90	1.3982	45.138	351	-0.105	54.862
0.95	1.3958	40.259	370.5	-0.051	59.741
1.00	1.3948	38.225	390	0.000	61.775
1.05	1.3938	36.192	409.5	0.049	63.808
1.10	1.3933	35.175	429	0.095	64.825
1.15	1.3933	35.175	448.5	0.140	64.825
1.20	1.3923	33.142	468	0.183	66.858
1.25	1.3919	32.329	487.5	0.224	67.671
1.30	1.3928	34.159	507	0.263	65.841
1.35	1.3915	31.516	526.5	0.301	68.484
1.40	1.3899	28.262	546	0.338	71.738
1.45	1.3884	25.212	565.5	0.374	74.788
1.50	1.3880	24.399	585	0.408	75.601
1.55	1.3891	26.636	604.5	0.442	73.364
1.60	1.3880	24.399	624	0.474	75.601
1.65	1.3865	21.349	643.5	0.506	78.651
1.70	1.3848	17.893	663	0.537	82.107
1.75	1.3824	13.013	682.5	0.567	86.987
1.80	1.3817	11.590	702	0.596	88.410
1.85	1.3813	10.776	721.5	0.625	89.224
1.90	1.3808	9.760	741	0.653	90.240
1.95	1.3811	10.370	760.5	0.680	89.630
2.00	1.3825	13.216	780	0.707	86.784

Table C-1.1: Effluent Data for Plot B-1.1

Pore Volume Injected	Refractive Index	Cyclohexane Concentration, %	Cumulative P.V. Injected, cc	Lambda	N-Hexane Concentration, %
0.95	1.3766	1.220	370.5	-0.051	98.780
1.00	1.3782	4.473	390.0	0.000	95.530
1.05	1.3860	20.330	409.5	0.049	79.670
1.10	1.4035	55.910	429.0	0.095	44.090
1.15	1.4220	93.530	448.5	0.140	6.470
1.20	1.4234	96.380	468.0	0.183	3.623

Table C-2.1: Effluent Data for Plot B-2.1

Pore Volume Injected	Refractive Index	Cyclohexane Concentration, %	Cumulative P.V. Injected, cc	Lambda	N-Hexane Concentration, %
0.55	1.4245	98.610	214.5	-0.607	1.390
0.60	1.4175	84.380	234.0	-0.516	15.600
0.65	1.4110	71.160	253.5	-0.434	28.800
0.70	1.4055	59.980	273.0	-0.359	40.000
0.75	1.4025	53.880	292.5	-0.289	46.100
0.80	1.4007	50.220	312.0	-0.224	49.800
0.85	1.3991	46.970	331.5	-0.163	53.000
0.90	1.3979	44.530	351.0	-0.105	55.500
0.95	1.3955	39.650	370.5	-0.051	60.400
1.00	1.3945	37.620	390.0	0.000	62.400
1.05	1.3935	35.580	409.5	0.049	64.400
1.10	1.3930	34.570	429.0	0.095	65.400
1.15	1.3930	34.570	448.5	0.140	65.400
1.20	1.3920	32.530	468.0	0.183	67.500
1.25	1.3916	31.720	487.5	0.224	68.300
1.30	1.3925	33.550	507.0	0.263	66.500
1.35	1.3912	30.910	526.5	0.301	69.100
1.40	1.3896	27.650	546.0	0.338	72.300
1.45	1.3881	24.600	565.5	0.374	75.400
1.50	1.3877	23.790	585.0	0.408	76.200
1.55	1.3888	26.030	604.5	0.442	74.000
1.60	1.3877	23.790	624.0	0.474	76.200
1.65	1.3862	20.740	643.5	0.506	79.300
1.70	1.3845	17.280	663.0	0.537	82.700
1.75	1.3821	12.400	682.5	0.567	87.600
1.80	1.3814	10.980	702.0	0.596	89.000
1.85	1.3810	10.170	721.5	0.625	89.800
1.90	1.3805	9.150	741.0	0.653	90.900

Table C-3: Experimental Effluent Concentration Data for Run 3

Pore Volume Injected	Refractive Index	Cyclohexane Concentration, %	Cumulative P.V. Injected, cc	Lambda	N-Hexane Concentration, %
0.05	1.3760	0.000	19.5	-4.249	100.000
0.10	1.3760	0.000	39	-2.846	100.000
0.15	1.3760	0.000	58.5	-2.195	100.000
0.20	1.3760	0.000	78	-1.789	100.000
0.25	1.3760	0.000	97.5	-1.500	100.000
0.30	1.3760	0.000	117	-1.278	100.000
0.35	1.3760	0.000	136.5	-1.099	100.000
0.40	1.3760	0.000	156	-0.949	100.000
0.45	1.3760	0.000	175.5	-0.820	100.000
0.50	1.3760	0.000	195	-0.707	100.000
0.55	1.3760	0.000	214.5	-0.607	100.000
0.60	1.3760	0.000	234	-0.516	100.000
0.65	1.3760	0.000	253.5	-0.434	100.000
0.70	1.3760	0.000	273	-0.359	100.000
0.75	1.3760	0.000	292.5	-0.289	100.000
0.80	1.3760	0.000	312	-0.224	100.000
0.85	1.3811	10.370	331.5	-0.163	89.630
0.90	1.3843	16.876	351	-0.105	83.124
0.95	1.3855	19.316	370.5	-0.051	80.684
1.00	1.3875	23.383	390	0.000	76.617
1.05	1.3895	27.449	409.5	0.049	72.551
1.10	1.3900	28.466	429	0.095	71.534
1.15	1.3906	29.686	448.5	0.140	70.314
1.20	1.3915	31.516	468	0.183	68.484
1.25	1.3915	31.516	487.5	0.224	68.484
1.30	1.3907	29.889	507	0.263	70.111
1.35	1.3885	25.416	526.5	0.301	74.584
1.40	1.3875	23.383	546	0.338	76.617
1.45	1.3860	20.333	565.5	0.374	79.667
1.50	1.3855	19.316	585	0.408	80.684
1.55	1.3845	17.283	604.5	0.442	82.717
1.60	1.3845	17.283	624	0.474	82.717
1.65	1.3835	15.249	643.5	0.506	84.751
1.70	1.3825	13.216	663	0.537	86.784
1.75	1.3810	10.166	682.5	0.567	89.834
1.80	1.3800	8.133	702	0.596	91.867
1.85	1.3790	6.100	721.5	0.625	93.900
1.90	1.3790	6.100	741	0.653	93.900
1.95	1.3790	6.100	760.5	0.680	93.900
2.00	1.3800	8.133	780	0.707	91.867
2.05	1.3795	7.116	799.5	0.733	92.884
2.1	1.3777	3.457	819	0.759	96.543
2.15	1.3767	1.423	838.5	0.784	98.577
2.2	1.3760	0.000	858	0.809	100.000
2.25	1.3760	0.000	877.5	0.833	100.000
2.3	1.3760	0.000	897	0.857	100.000
2.35	1.3760	0.000	916.5	0.881	100.000
2.4	1.3760	0.000	936	0.904	100.000
2.45	1.3760	0.000	955.5	0.926	100.000
2.5	1.3760	0.000	975	0.949	100.000

Table C-4: Experimental Effluent Concentration Data for Run 4

Pore Volume Injected	Refractive Index	Cyclohexane Concentration, %	Cumulative P.V. Injected, cc	Lambda	N-Hexane Concentration, %
0.05	1.3760	0.000	21	-4.249	100.000
0.10	1.3760	0.000	42	-2.846	100.000
0.15	1.3760	0.000	63	-2.195	100.000
0.20	1.3760	0.000	84	-1.789	100.000
0.25	1.3760	0.000	105	-1.500	100.000
0.30	1.3760	0.000	126	-1.278	100.000
0.35	1.3760	0.000	147	-1.099	100.000
0.40	1.3760	0.000	168	-0.949	100.000
0.45	1.3760	0.000	189	-0.820	100.000
0.50	1.3760	0.000	210	-0.707	100.000
0.55	1.3760	0.000	231	-0.607	100.000
0.60	1.3760	0.000	252	-0.516	100.000
0.65	1.3760	0.000	273	-0.434	100.000
0.70	1.3760	0.000	294	-0.359	100.000
0.75	1.3760	0.000	315	-0.289	100.000
0.80	1.3760	0.000	336	-0.224	100.000
0.85	1.3760	0.000	357	-0.163	100.000
0.90	1.3763	0.610	378	-0.105	99.390
0.95	1.3783	4.676	399	-0.051	95.324
1.00	1.3916	31.719	420	0.000	68.281
1.05	1.3946	37.819	441	0.049	62.181
1.10	1.3960	40.665	462	0.095	59.335
1.15	1.3964	41.479	483	0.140	58.521
1.20	1.3960	40.665	504	0.183	59.335
1.25	1.3950	38.632	525	0.224	61.368
1.30	1.3927	33.955	546	0.263	66.045
1.35	1.3901	28.669	567	0.301	71.331
1.40	1.3889	26.229	588	0.338	73.771
1.45	1.3880	24.399	609	0.374	75.601
1.50	1.3870	22.366	630	0.408	77.634
1.55	1.3860	20.333	651	0.442	79.667
1.60	1.3855	19.316	672	0.474	80.684
1.65	1.3850	18.299	693	0.506	81.701
1.70	1.3843	16.876	714	0.537	83.124
1.75	1.3835	15.249	735	0.567	84.751
1.80	1.3833	14.843	756	0.596	85.157
1.85	1.3827	13.623	777	0.625	86.377
1.90	1.3817	11.590	798	0.653	88.410
1.95	1.3807	9.556	819	0.680	90.444
2.00	1.3801	8.336	840	0.707	91.664
2.05	1.3800	8.133	861	0.733	91.867
2.1	1.3800	8.133	882	0.759	91.867
2.15	1.3800	8.133	903	0.784	91.867
2.2	1.3791	6.303	924	0.809	93.697
2.25	1.3777	3.457	945	0.833	96.543
2.3	1.3777	3.457	966	0.857	96.543
2.35	1.3770	2.033	987	0.881	97.967
2.4	1.3770	2.033	1008	0.904	97.967
2.45	1.3770	2.033	1029	0.926	97.967
2.5	1.3770	2.033	1050	0.949	97.967
2.55	1.3770	2.033	1071	0.971	97.967
2.6	1.3767	1.423	1092	0.992	98.577
2.65	1.3767	1.423	1113	1.014	98.577
2.7	1.3765	1.017	1134	1.035	98.983
2.75	1.3765	1.017	1155	1.055	98.983
2.8	1.3763	0.610	1176	1.076	99.390
2.85	1.3760	0.000	1197	1.096	100.000
2.9	1.3760	0.000	1218	1.116	100.000
2.95	1.3760	0.000	1239	1.135	100.000
3	1.3760	0.000	1260	1.155	100.000

Table C-5: Experimental Effluent Concentration Data for Run 5

Pore Volume Injected	Refractive Index	Cyclohexane Concentration, %	Cumulative P.V. Injected, cc	Lambda	N-Hexane Concentration, %
0.05	1.4248	99.223	21	-4.249	0.777
0.10	1.4248	99.223	42	-2.846	0.777
0.15	1.4248	99.223	63	-2.195	0.777
0.20	1.4248	99.223	84	-1.789	0.777
0.25	1.4248	99.223	105	-1.500	0.777
0.30	1.4248	99.223	126	-1.278	0.777
0.35	1.4248	99.223	147	-1.099	0.777
0.40	1.4248	99.223	168	-0.949	0.777
0.45	1.4248	99.223	189	-0.820	0.777
0.50	1.4248	99.223	210	-0.707	0.777
0.55	1.4248	99.223	231	-0.607	0.777
0.60	1.4248	99.223	252	-0.516	0.777
0.65	1.4248	99.223	273	-0.434	0.777
0.70	1.4248	99.223	294	-0.359	0.777
0.75	1.4248	99.223	315	-0.289	0.777
0.80	1.4248	99.223	336	-0.224	0.777
0.85	1.4204	90.277	357	-0.163	9.723
0.90	1.4166	82.551	378	-0.105	17.449
0.95	1.4115	72.181	399	-0.051	27.819
1.00	1.4011	51.035	420	0.000	48.965
1.05	1.3886	25.619	441	0.049	74.381
1.10	1.3870	22.366	462	0.095	77.634
1.15	1.3950	38.632	483	0.140	61.368
1.20	1.4134	76.044	504	0.183	23.956
1.25	1.4222	93.937	525	0.224	6.063
1.30	1.4234	96.377	546	0.263	3.623
1.35	1.4238	97.190	567	0.301	2.810
1.40	1.4242	98.003	588	0.338	1.997
1.45	1.4244	98.410	609	0.374	1.590
1.50	1.4246	98.817	630	0.408	1.183
1.55	1.4248	99.223	651	0.442	0.777
1.60	1.4248	99.223	672	0.474	0.777
1.65	1.4248	99.223	693	0.506	0.777
1.70	1.4248	99.223	714	0.537	0.777
1.75	1.4248	99.223	735	0.567	0.777
1.80	1.4248	99.223	756	0.596	0.777
1.85	1.4248	99.223	777	0.625	0.777
1.90	1.4248	99.223	798	0.653	0.777
1.95	1.4248	99.223	819	0.680	0.777
2.00	1.4248	99.223	840	0.707	0.777

Table C-6: Experimental Effluent Concentration Data for Run 6

Pore Volume Injected	Refractive Index	Cyclohexane Concentration, %	Cumulative P.V. Injected, cc	Lambda	N-Hexane Concentration, %
0.05	1.4248	99.223	21	-4.249	0.777
0.10	1.4248	99.223	42	-2.846	0.777
0.15	1.4248	99.223	63	-2.195	0.777
0.20	1.4248	99.223	84	-1.789	0.777
0.25	1.4248	99.223	105	-1.500	0.777
0.30	1.4248	99.223	126	-1.278	0.777
0.35	1.4248	99.223	147	-1.099	0.777
0.40	1.4248	99.223	168	-0.949	0.777
0.45	1.4248	99.223	189	-0.820	0.777
0.50	1.4248	99.223	210	-0.707	0.777
0.55	1.4248	99.223	231	-0.607	0.777
0.60	1.4248	99.223	252	-0.516	0.777
0.65	1.4248	99.223	273	-0.434	0.777
0.70	1.4248	99.223	294	-0.359	0.777
0.75	1.4248	99.223	315	-0.289	0.777
0.80	1.4248	99.223	336	-0.224	0.777
0.85	1.4248	99.223	357	-0.163	0.777
0.90	1.4248	99.223	378	-0.105	0.777
0.95	1.4215	92.514	399	-0.051	7.486
1.00	1.4189	87.227	420	0.000	12.773
1.05	1.4130	75.231	441	0.049	24.769
1.10	1.4024	53.678	462	0.095	46.322
1.15	1.3910	30.499	483	0.140	69.501
1.20	1.3790	6.100	504	0.183	93.900
1.25	1.3811	10.370	525	0.224	89.630
1.30	1.3864	21.146	546	0.263	78.854
1.35	1.3994	47.578	567	0.301	52.422
1.40	1.4226	94.750	588	0.338	5.250
1.45	1.4242	98.003	609	0.374	1.997
1.50	1.4248	99.223	630	0.408	0.777
1.55	1.4248	99.223	651	0.442	0.777
1.60	1.4248	99.223	672	0.474	0.777
1.65	1.4248	99.223	693	0.506	0.777
1.70	1.4248	99.223	714	0.537	0.777
1.75	1.4248	99.223	735	0.567	0.777
1.80	1.4248	99.223	756	0.596	0.777
1.85	1.4248	99.223	777	0.625	0.777
1.90	1.4248	99.223	798	0.653	0.777
1.95	1.4248	99.223	819	0.680	0.777
2.00	1.4248	99.223	840	0.707	0.777

Table C-7: Experimental Effluent Concentration Data for Run 7

Pore Volume Injected	Refractive Index	10% Brine Concentration, %	Cumulative P.V. Injected, cc	Lambda	2% Brine Concentration, %
0.05	1.3362	0.000	20.0	-4.249	100.000
0.10	1.3362	0.000	40.0	-2.846	100.000
0.15	1.3362	0.000	60.0	-2.195	100.000
0.20	1.3362	0.000	80.0	-1.789	100.000
0.25	1.3362	0.000	100.0	-1.500	100.000
0.30	1.3362	0.000	120.0	-1.278	100.000
0.35	1.3362	0.000	140.0	-1.099	100.000
0.40	1.3362	0.000	160.0	-0.949	100.000
0.45	1.3362	0.000	180.0	-0.820	100.000
0.50	1.3362	0.000	200.0	-0.707	100.000
0.55	1.3362	0.000	220.0	-0.607	100.000
0.60	1.3362	0.000	240.0	-0.516	100.000
0.65	1.3362	0.000	260.0	-0.434	100.000
0.70	1.3362	0.000	280.0	-0.359	100.000
0.75	1.3362	0.000	300.0	-0.289	100.000
0.80	1.3362	0.000	320.0	-0.224	100.000
0.85	1.3362	0.000	340.0	-0.163	100.000
0.90	1.337	6.636	360.0	-0.105	93.364
0.95	1.3405	35.670	380.0	-0.051	64.330
1.00	1.3436	61.385	400.0	0.000	38.615
1.05	1.3455	77.146	420.0	0.049	22.854
1.10	1.3465	85.442	440.0	0.095	14.558
1.15	1.3469	88.760	460.0	0.140	11.240
1.20	1.3474	92.907	480.0	0.183	7.092
1.25	1.3475	93.737	500.0	0.224	6.263
1.30	1.3478	96.226	520.0	0.263	3.774
1.35	1.348	97.885	540.0	0.301	2.115
1.40	1.348	97.885	560.0	0.338	2.115
1.45	1.3482	99.544	580.0	0.374	0.456
1.50	1.3482	99.544	600.0	0.408	0.456
1.55	1.3482	99.544	620.0	0.442	0.456
1.60	1.3482	99.544	640.0	0.474	0.456
1.65	1.3482	99.544	660.0	0.506	0.456
1.70	1.3482	99.544	680.0	0.537	0.456
1.75	1.3482	99.544	700.0	0.567	0.456
1.80	1.3482	99.544	720.0	0.596	0.456
1.85	1.3482	99.544	740.0	0.625	0.456
1.90	1.3482	99.544	760.0	0.653	0.456
1.95	1.3482	99.544	780.0	0.680	0.456
2.00	1.3482	99.544	800.0	0.707	0.456

Table C-8: Experimental Effluent Concentration Data for Run 8

Pore Volume Injected	Refractive Index	10% Brine Concentration, %	Cumulative P.V. Injected, cc	Lambda	2% Brine Concentration, %
0.05	1.3482	99.544	20.0	-4.249	0.456
0.10	1.3482	99.544	40.0	-2.846	0.456
0.15	1.3482	99.544	60.0	-2.195	0.456
0.20	1.3482	99.544	80.0	-1.789	0.456
0.25	1.3482	99.544	100.0	-1.500	0.456
0.30	1.3482	99.544	120.0	-1.278	0.456
0.35	1.3482	99.544	140.0	-1.099	0.456
0.40	1.3482	99.544	160.0	-0.949	0.456
0.45	1.3482	99.544	180.0	-0.820	0.456
0.50	1.3482	99.544	200.0	-0.707	0.456
0.55	1.3482	99.544	220.0	-0.607	0.456
0.60	1.3482	99.544	240.0	-0.516	0.456
0.65	1.3482	99.544	260.0	-0.434	0.456
0.70	1.3482	99.544	280.0	-0.359	0.456
0.75	1.3482	99.544	300.0	-0.289	0.456
0.80	1.3452	74.658	320.0	-0.224	25.342
0.85	1.343	56.408	340.0	-0.163	43.592
0.90	1.3418	46.454	360.0	-0.105	53.546
0.95	1.34	31.522	380.0	-0.051	68.478
1.00	1.3386	19.909	400.0	0.000	80.091
1.05	1.3382	16.591	420.0	0.049	83.409
1.10	1.3378	13.272	440.0	0.095	86.727
1.15	1.3375	10.784	460.0	0.140	89.216
1.20	1.3373	9.125	480.0	0.183	90.875
1.25	1.337	6.636	500.0	0.224	93.364
1.30	1.3368	4.977	520.0	0.263	95.023
1.35	1.3366	3.318	540.0	0.301	96.682
1.40	1.3364	1.659	560.0	0.338	98.341
1.45	1.3362	0.000	580.0	0.374	100.000
1.50	1.3362	0.000	600.0	0.408	100.000
1.55	1.3362	0.000	620.0	0.442	100.000
1.60	1.3362	0.000	640.0	0.474	100.000
1.65	1.3362	0.000	660.0	0.506	100.000
1.70	1.3362	0.000	680.0	0.537	100.000
1.75	1.3362	0.000	700.0	0.567	100.000
1.80	1.3362	0.000	720.0	0.596	100.000
1.85	1.3362	0.000	740.0	0.625	100.000
1.90	1.3362	0.000	760.0	0.653	100.000
1.95	1.3362	0.000	780.0	0.680	100.000
2.00	1.3362	0.000	800.0	0.707	100.000

Table C-7.1: Effluent Data for Plot B-7.1

Pore Volume Injected	Refractive Index	10% Brine Concentration, %	Cumulative P.V. Injected, cc	Lambda	2% Brine Concentration, %
0.05	1.3362	0.000	20.0	-4.249	100.000
0.10	1.3362	0.000	40.0	-2.846	100.000
0.15	1.3362	0.000	60.0	-2.195	100.000
0.20	1.3362	0.000	80.0	-1.789	100.000
0.25	1.3362	0.000	100.0	-1.500	100.000
0.30	1.3362	0.000	120.0	-1.278	100.000
0.35	1.3362	0.000	140.0	-1.099	100.000
0.40	1.3362	0.000	160.0	-0.949	100.000
0.45	1.3362	0.000	180.0	-0.820	100.000
0.50	1.3362	0.000	200.0	-0.707	100.000
0.55	1.3362	0.000	220.0	-0.607	100.000
0.60	1.3362	0.000	240.0	-0.516	100.000
0.65	1.3362	0.000	260.0	-0.434	100.000
0.70	1.3362	0.000	280.0	-0.359	100.000
0.75	1.3362	0.000	300.0	-0.289	100.000
0.80	1.3362	0.000	320.0	-0.224	100.000
0.85	1.3362	0.000	340.0	-0.163	100.000
0.90	1.3370	6.636	360.0	-0.105	93.360
0.95	1.3405	35.670	380.0	-0.051	64.330
1.00	1.3436	61.390	400.0	0.000	38.610
1.05	1.3455	77.150	420.0	0.049	22.850
1.10	1.3465	85.440	440.0	0.095	14.560
1.15	1.3469	88.760	460.0	0.140	11.240
1.20	1.3474	92.910	480.0	0.183	7.093
1.25	1.3475	93.740	500.0	0.224	6.263
1.30	1.3478	96.230	520.0	0.263	3.774

Table C-8.1: Effluent Data for Plot B-8.1

Pore Volume Injected	Refractive Index	10% Brine Concentration, %	Cumulative P.V. Injected, cc	Lambda	2% Brine Concentration, %
0.75	1.3482	99.540	300.0	-0.289	0.456
0.80	1.3452	74.660	320.0	-0.224	25.340
0.85	1.3430	56.410	340.0	-0.163	43.590
0.90	1.3418	46.450	360.0	-0.105	53.550
0.95	1.3400	31.520	380.0	-0.051	68.480
1.00	1.3386	19.910	400.0	0.000	80.090
1.05	1.3382	16.590	420.0	0.049	83.410
1.10	1.3378	13.270	440.0	0.095	86.730
1.15	1.3375	10.780	460.0	0.140	89.220
1.20	1.3373	9.125	480.0	0.183	90.880
1.25	1.3370	6.636	500.0	0.224	93.360
1.30	1.3368	4.977	520.0	0.263	95.020
1.35	1.3366	3.318	540.0	0.301	96.680
1.40	1.3364	1.659	560.0	0.338	98.340
1.45	1.3362	0.000	580.0	0.374	99.990

Table C-9: Experimental Effluent Concentration Data for Run 9

Pore Volume Injected	Refractive Index	10% Brine Concentration, %	Cumulative P.V. Injected, cc	Lambda	2% Brine Concentration, %
0.05	1.3362	0.000	20.0	-4.249	100.000
0.10	1.3362	0.000	40.0	-2.846	100.000
0.15	1.3362	0.000	60.0	-2.195	100.000
0.20	1.3362	0.000	80.0	-1.789	100.000
0.25	1.3362	0.000	100.0	-1.500	100.000
0.30	1.3362	0.000	120.0	-1.278	100.000
0.35	1.3362	0.000	140.0	-1.099	100.000
0.40	1.3362	0.000	160.0	-0.949	100.000
0.45	1.3362	0.000	180.0	-0.820	100.000
0.50	1.3362	0.000	200.0	-0.707	100.000
0.55	1.3362	0.000	220.0	-0.607	100.000
0.60	1.3362	0.000	240.0	-0.516	100.000
0.65	1.3362	0.000	260.0	-0.434	100.000
0.70	1.3362	0.000	280.0	-0.359	100.000
0.75	1.3362	0.000	300.0	-0.289	100.000
0.80	1.3362	0.000	320.0	-0.224	100.000
0.85	1.3362	0.000	340.0	-0.163	100.000
0.90	1.3362	0.000	360.0	-0.105	100.000
0.95	1.3365	2.489	380.0	-0.051	97.511
1.00	1.3388	21.568	400.0	0.000	78.432
1.05	1.3452	74.658	420.0	0.049	25.342
1.10	1.3465	85.442	440.0	0.095	14.558
1.15	1.3436	61.385	460.0	0.140	38.615
1.20	1.3421	48.942	480.0	0.183	51.058
1.25	1.3411	40.647	500.0	0.224	59.353
1.30	1.3395	27.375	520.0	0.263	72.625
1.35	1.3382	16.591	540.0	0.301	83.409
1.40	1.338	14.932	560.0	0.338	85.068
1.45	1.3377	12.443	580.0	0.374	87.557
1.50	1.3376	11.613	600.0	0.408	88.387
1.55	1.3375	10.784	620.0	0.442	89.216
1.60	1.3372	8.295	640.0	0.474	91.705
1.65	1.337	6.636	660.0	0.506	93.364
1.70	1.3366	3.318	680.0	0.537	96.682
1.75	1.3365	2.489	700.0	0.567	97.511
1.80	1.3363	0.830	720.0	0.596	99.170
1.85	1.3362	0.000	740.0	0.625	100.000
1.90	1.3362	0.000	760.0	0.653	100.000
1.95	1.3362	0.000	780.0	0.680	100.000
2.00	1.3362	0.000	800.0	0.707	100.000

Table C-10: Experimental Effluent Concentration Data for Run 10

Pore Volume Injected	Refractive Index	10% Brine Concentration, %	Cumulative P.V. Injected, cc	Lambda	2% Brine Concentration, %
0.05	1.3362	0.000	20.0	-4.249	100.000
0.10	1.3362	0.000	40.0	-2.846	100.000
0.15	1.3362	0.000	60.0	-2.195	100.000
0.20	1.3362	0.000	80.0	-1.789	100.000
0.25	1.3362	0.000	100.0	-1.500	100.000
0.30	1.3362	0.000	120.0	-1.278	100.000
0.35	1.3362	0.000	140.0	-1.099	100.000
0.40	1.3362	0.000	160.0	-0.949	100.000
0.45	1.3362	0.000	180.0	-0.820	100.000
0.50	1.3362	0.000	200.0	-0.707	100.000
0.55	1.3362	0.000	220.0	-0.607	100.000
0.60	1.3362	0.000	240.0	-0.516	100.000
0.65	1.3362	0.000	260.0	-0.434	100.000
0.70	1.3362	0.000	280.0	-0.359	100.000
0.75	1.3362	0.000	300.0	-0.289	100.000
0.80	1.3362	0.000	320.0	-0.224	100.000
0.85	1.3362	0.000	340.0	-0.163	100.000
0.90	1.3363	0.830	360.0	-0.105	99.170
0.95	1.3379	14.102	380.0	-0.051	85.898
1.00	1.3419	47.283	400.0	0.000	52.717
1.05	1.3446	69.681	420.0	0.049	30.319
1.10	1.3456	77.976	440.0	0.095	22.024
1.15	1.3469	88.760	460.0	0.140	11.240
1.20	1.3465	85.442	480.0	0.183	14.558
1.25	1.3441	65.533	500.0	0.224	34.467
1.30	1.342	48.113	520.0	0.263	51.887
1.35	1.3405	35.670	540.0	0.301	64.330
1.40	1.339	23.227	560.0	0.338	76.773
1.45	1.3382	16.591	580.0	0.374	83.409
1.50	1.3376	11.613	600.0	0.408	88.387
1.55	1.3375	10.784	620.0	0.442	89.216
1.60	1.3372	8.295	640.0	0.474	91.705
1.65	1.3369	5.807	660.0	0.506	94.193
1.70	1.3367	4.148	680.0	0.537	95.852
1.75	1.3365	2.489	700.0	0.567	97.511
1.80	1.3364	1.659	720.0	0.596	98.341
1.85	1.3362	0.000	740.0	0.625	100.000
1.90	1.3362	0.000	760.0	0.653	100.000
1.95	1.3362	0.000	780.0	0.680	100.000
2.00	1.3362	0.000	800.0	0.707	100.000

Table C-11: Experimental Effluent Concentration Data for Run 11

Pore Volume Injected	Refractive Index	10% Brine Concentration, %	Cumulative P.V. Injected, cc	Lambda	2% Brine Concentration, %
0.05	1.3482	99.544	20.0	-4.249	0.456
0.10	1.3482	99.544	40.0	-2.846	0.456
0.15	1.3482	99.544	60.0	-2.195	0.456
0.20	1.3482	99.544	80.0	-1.789	0.456
0.25	1.3482	99.544	100.0	-1.500	0.456
0.30	1.3482	99.544	120.0	-1.278	0.456
0.35	1.3482	99.544	140.0	-1.099	0.456
0.40	1.3482	99.544	160.0	-0.949	0.456
0.45	1.3482	99.544	180.0	-0.820	0.456
0.50	1.3482	99.544	200.0	-0.707	0.456
0.55	1.3482	99.544	220.0	-0.607	0.456
0.60	1.3482	99.544	240.0	-0.516	0.456
0.65	1.3482	99.544	260.0	-0.434	0.456
0.70	1.3482	99.544	280.0	-0.359	0.456
0.75	1.3482	99.544	300.0	-0.289	0.456
0.80	1.348	97.885	320.0	-0.224	2.115
0.85	1.3455	77.146	340.0	-0.163	22.854
0.90	1.3427	53.920	360.0	-0.105	46.080
0.95	1.3405	35.670	380.0	-0.051	64.330
1.00	1.3395	27.375	400.0	0.000	72.625
1.05	1.3409	38.988	420.0	0.049	61.012
1.10	1.3436	61.385	440.0	0.095	38.615
1.15	1.3454	76.317	460.0	0.140	23.683
1.20	1.3464	84.612	480.0	0.183	15.388
1.25	1.3472	91.248	500.0	0.224	8.752
1.30	1.3475	93.737	520.0	0.263	6.263
1.35	1.3478	96.226	540.0	0.301	3.774
1.40	1.3479	97.055	560.0	0.338	2.945
1.45	1.348	97.885	580.0	0.374	2.115
1.50	1.3481	98.714	600.0	0.408	1.286
1.55	1.3482	99.544	620.0	0.442	0.456
1.60	1.3482	99.544	640.0	0.474	0.456
1.65	1.3482	99.544	660.0	0.506	0.456
1.70	1.3482	99.544	680.0	0.537	0.456
1.75	1.3482	99.544	700.0	0.567	0.456
1.80	1.3482	99.544	720.0	0.596	0.456
1.85	1.3482	99.544	740.0	0.625	0.456
1.90	1.3482	99.544	760.0	0.653	0.456
1.95	1.3482	99.544	780.0	0.680	0.456
2.00	1.3482	99.544	800.0	0.707	0.456

Table C-12: Experimental Effluent Concentration Data for Run 12

Pore Volume Injected	Refractive Index	10% Brine Concentration, %	Cumulative P.V. Injected, cc	Lambda	2% Brine Concentration, %
0.05	1.3482	99.544	20.0	-4.249	0.456
0.10	1.3482	99.544	40.0	-2.846	0.456
0.15	1.3482	99.544	60.0	-2.195	0.456
0.20	1.3482	99.544	80.0	-1.789	0.456
0.25	1.3482	99.544	100.0	-1.500	0.456
0.30	1.3482	99.544	120.0	-1.278	0.456
0.35	1.3482	99.544	140.0	-1.099	0.456
0.40	1.3482	99.544	160.0	-0.949	0.456
0.45	1.3482	99.544	180.0	-0.820	0.456
0.50	1.3482	99.544	200.0	-0.707	0.456
0.55	1.3482	99.544	220.0	-0.607	0.456
0.60	1.3482	99.544	240.0	-0.516	0.456
0.65	1.3482	99.544	260.0	-0.434	0.456
0.70	1.3482	99.544	280.0	-0.359	0.456
0.75	1.3482	99.544	300.0	-0.289	0.456
0.80	1.3482	99.544	320.0	-0.224	0.456
0.85	1.347	89.589	340.0	-0.163	10.411
0.90	1.3445	68.851	360.0	-0.105	31.149
0.95	1.3419	47.283	380.0	-0.051	52.717
1.00	1.3402	33.181	400.0	0.000	66.819
1.05	1.3388	21.568	420.0	0.049	78.432
1.10	1.338	14.932	440.0	0.095	85.068
1.15	1.3376	11.613	460.0	0.140	88.387
1.20	1.3394	26.545	480.0	0.183	73.455
1.25	1.3424	51.431	500.0	0.224	48.569
1.30	1.3446	69.681	520.0	0.263	30.319
1.35	1.3461	82.124	540.0	0.301	17.876
1.40	1.3468	87.930	560.0	0.338	12.070
1.45	1.3472	91.248	580.0	0.374	8.752
1.50	1.3475	93.737	600.0	0.408	6.263
1.55	1.3479	97.055	620.0	0.442	2.945
1.60	1.348	97.885	640.0	0.474	2.115
1.65	1.3482	99.544	660.0	0.506	0.456
1.70	1.3482	99.544	680.0	0.537	0.456
1.75	1.3482	99.544	700.0	0.567	0.456
1.80	1.3482	99.544	720.0	0.596	0.456
1.85	1.3482	99.544	740.0	0.625	0.456
1.90	1.3482	99.544	760.0	0.653	0.456
1.95	1.3482	99.544	780.0	0.680	0.456
2.00	1.3482	99.544	800.0	0.707	0.456

Table C-13: Experimental Effluent Concentration Data for Run 13

Pore Volume Injected	Refractive Index	Cyclohexane Concentration, %	Cumulative P.V. Injected, cc	Lambda	N-Hexane Concentration, %
0.05	1.3760	0.000	21	-4.249	100.000
0.10	1.3760	0.000	42	-2.846	100.000
0.15	1.3760	0.000	63	-2.195	100.000
0.20	1.3760	0.000	84	-1.789	100.000
0.25	1.3760	0.000	105	-1.500	100.000
0.30	1.3760	0.000	126	-1.278	100.000
0.35	1.3760	0.000	147	-1.099	100.000
0.40	1.3760	0.000	168	-0.949	100.000
0.45	1.3760	0.000	189	-0.820	100.000
0.50	1.3760	0.000	210	-0.707	100.000
0.55	1.3760	0.000	231	-0.607	100.000
0.60	1.3760	0.000	252	-0.516	100.000
0.65	1.3802	8.540	273	-0.434	91.460
0.70	1.3988	46.358	294	-0.359	53.642
0.75	1.4102	69.538	315	-0.289	30.462
0.80	1.4216	92.717	336	-0.224	7.283
0.85	1.4232	95.970	357	-0.163	4.030
0.90	1.4238	97.190	378	-0.105	2.810
0.95	1.4240	97.597	399	-0.051	2.403
1.00	1.4244	98.410	420	0.000	1.590
1.05	1.4246	98.817	441	0.049	1.183
1.10	1.4246	98.817	462	0.095	1.183
1.15	1.4248	99.223	483	0.140	0.777
1.20	1.4248	99.223	504	0.183	0.777
1.25	1.4248	99.223	525	0.224	0.777
1.30	1.4248	99.223	546	0.263	0.777
1.35	1.4248	99.223	567	0.301	0.777
1.40	1.4248	99.223	588	0.338	0.777
1.45	1.4248	99.223	609	0.374	0.777
1.50	1.4248	99.223	630	0.408	0.777
1.55	1.4248	99.223	651	0.442	0.777
1.60	1.4248	99.223	672	0.474	0.777
1.65	1.4248	99.223	693	0.506	0.777
1.70	1.4248	99.223	714	0.537	0.777
1.75	1.4248	99.223	735	0.567	0.777
1.80	1.4248	99.223	756	0.596	0.777
1.85	1.4248	99.223	777	0.625	0.777
1.90	1.4248	99.223	798	0.653	0.777
1.95	1.4248	99.223	819	0.680	0.777
2.00	1.4248	99.223	840	0.707	0.777

Table C-13R: Experimental Effluent Concentration Data for Run 13R

Pore Volume Injected	Refractive Index	Cyclohexane Concentration, %	Cumulative P.V. Injected, cc	Lambda	N-Hexane Concentration, %
0 05	1.3760	0.000	21	-4.249	100.000
0.10	1.3760	0.000	42	-2.846	100.000
0.15	1.3760	0.000	63	-2.195	100.000
0.20	1.3760	0.000	84	-1.789	100.000
0.25	1.3760	0.000	105	-1.500	100.000
0.30	1.3760	0.000	126	-1.278	100.000
0.35	1.3760	0.000	147	-1.099	100.000
0.40	1.3760	0.000	168	-0.949	100.000
0.45	1.3760	0.000	189	-0.820	100.000
0.50	1.3760	0.000	210	-0.707	100.000
0.55	1.3760	0.000	231	-0.607	100.000
0.60	1.3765	1.017	252	-0.516	98.983
0.65	1.3805	9.150	273	-0.434	90.850
0.70	1.3993	47.375	294	-0.359	52.625
0.75	1.4108	70.758	315	-0.289	29.242
0.80	1.4219	93.327	336	-0.224	6.673
0.85	1.4238	97.190	357	-0.163	2.810
0.90	1.4243	98.207	378	-0.105	1.793
0.95	1.4245	98.613	399	-0.051	1.387
1.00	1.4250	99.630	420	0.000	0.370
1.05	1.4250	99.630	441	0.049	0.370
1.10	1.4250	99.630	462	0.095	0.370
1.15	1.4250	99.630	483	0.140	0.370
1.20	1.4250	99.630	504	0.183	0.370
1.25	1.4250	99.630	525	0.224	0.370
1.30	1.4250	99.630	546	0.263	0.370
1.35	1.4250	99.630	567	0.301	0.370
1.40	1.4250	99.630	588	0.338	0.370
1.45	1.4250	99.630	609	0.374	0.370
1.50	1.4250	99.630	630	0.408	0.370
1.55	1.4250	99.630	651	0.442	0.370
1.60	1.4250	99.630	672	0.474	0.370
1.65	1.4250	99.630	693	0.506	0.370
1.70	1.4250	99.630	714	0.537	0.370
1.75	1.4250	99.630	735	0.567	0.370
1.80	1.4250	99.630	756	0.596	0.370
1.85	1.4250	99.630	777	0.625	0.370
1.90	1.4250	99.630	798	0.653	0.370
1.95	1.4250	99.630	819	0.680	0.370
2.00	1.4250	99.630	840	0.707	0.370

Table C-13.1: Effluent Data for Plot B-13.1

Pore Volume Injected	Refractive Index	Cyclohexane Concentration, %	Cumulative P.V. Injected, cc	Lambda	N-Hexane Concentration, %
0.05	1.3760	0.000	21.0	-4.249	100.000
0.10	1.3760	0.000	42.0	-2.846	100.000
0.15	1.3760	0.000	63.0	-2.195	100.000
0.20	1.3760	0.000	84.0	-1.789	100.000
0.25	1.3760	0.000	105.0	-1.500	100.000
0.30	1.3760	0.000	126.0	-1.278	100.000
0.35	1.3760	0.000	147.0	-1.099	100.000
0.40	1.3760	0.000	168.0	-0.949	100.000
0.45	1.3760	0.000	189.0	-0.820	100.000
0.50	1.3760	0.000	210.0	-0.707	100.000
0.55	1.3760	0.000	231.0	-0.607	100.000
0.60	1.3760	0.000	252.0	-0.516	100.000
0.65	1.3802	8.540	273.0	-0.434	91.460
0.70	1.3988	46.360	294.0	-0.359	53.642
0.75	1.4102	69.540	315.0	-0.289	30.462
0.80	1.4216	92.720	336.0	-0.224	7.283
0.85	1.4232	95.970	357.0	-0.163	4.030
0.90	1.4238	97.190	378.0	-0.105	2.810
0.95	1.4240	97.600	399.0	-0.051	2.403
1.00	1.4244	98.410	420.0	0.000	1.590
1.05	1.4246	98.820	441.0	0.049	1.183
1.10	1.4246	98.820	462.0	0.095	1.183
1.15	1.4248	99.220	483.0	0.140	0.777
1.20	1.4248	99.220	504.0	0.183	0.777
1.25	1.4248	99.220	525.0	0.224	0.777

Table C-13R.1: Effluent Data for Plot B-13R

Pore Volume Injected	Refractive Index	Cyclohexane Concentration, %	Cumulative P.V. Injected, cc	Lambda	N-Hexane Concentration, %
0.05	1.3760	0.000	21.0	-4.249	100.000
0.10	1.3760	0.000	42.0	-2.846	100.000
0.15	1.3760	0.000	63.0	-2.195	100.000
0.20	1.3760	0.000	84.0	-1.789	100.000
0.25	1.3760	0.000	105.0	-1.500	100.000
0.30	1.3760	0.000	126.0	-1.278	100.000
0.35	1.3760	0.000	147.0	-1.099	100.000
0.40	1.3760	0.000	168.0	-0.949	100.000
0.45	1.3760	0.000	189.0	-0.820	100.000
0.50	1.3760	0.000	210.0	-0.707	100.000
0.55	1.3760	0.000	231.0	-0.607	100.000
0.60	1.3765	1.017	252.0	-0.516	98.983
0.65	1.3805	9.150	273.0	-0.434	90.850
0.70	1.3993	47.370	294.0	-0.359	52.625
0.75	1.4108	70.760	315.0	-0.289	29.242
0.80	1.4219	93.330	336.0	-0.224	6.673
0.85	1.4238	97.190	357.0	-0.163	2.810
0.90	1.4243	98.210	378.0	-0.105	1.793
0.95	1.4245	98.610	399.0	-0.051	1.387
1.00	1.4250	99.630	420.0	0.000	0.370
1.05	1.4250	99.630	441.0	0.049	0.370
1.10	1.4250	99.630	462.0	0.095	0.370
1.15	1.4250	99.630	483.0	0.140	0.370
1.20	1.4250	99.630	504.0	0.183	0.370
1.25	1.4250	99.630	525.0	0.224	0.370

Table C-14: Experimental Effluent Concentration Data for Run 14

Pore Volume Injected	Refractive Index	Cyclohexane Concentration, %	Cumulative P.V. Injected, cc	Lambda	N-Hexane Concentration, %
0.05	1.4250	99.630	21	-4.249	0.370
0.10	1.4250	99.630	42	-2.846	0.370
0.15	1.4250	99.630	63	-2.195	0.370
0.20	1.4250	99.630	84	-1.789	0.370
0.25	1.4250	99.630	105	-1.500	0.370
0.30	1.4250	99.630	126	-1.278	0.370
0.35	1.4250	99.630	147	-1.099	0.370
0.40	1.4250	99.630	168	-0.949	0.370
0.45	1.4250	99.630	189	-0.820	0.370
0.50	1.4250	99.630	210	-0.707	0.370
0.55	1.4207	90.887	231	-0.607	9.113
0.60	1.4152	79.704	252	-0.516	20.296
0.65	1.4104	69.944	273	-0.434	30.056
0.70	1.4070	63.031	294	-0.359	36.969
0.75	1.4042	57.338	315	-0.289	42.662
0.80	1.4014	51.645	336	-0.224	48.355
0.85	1.3985	45.748	357	-0.163	54.252
0.90	1.3914	31.312	378	-0.105	68.688
0.95	1.3847	17.689	399	-0.051	82.311
1.00	1.3810	10.166	420	0.000	89.834
1.05	1.3774	2.847	441	0.049	97.153
1.10	1.3772	2.440	462	0.095	97.560
1.15	1.3770	2.033	483	0.140	97.967
1.20	1.3767	1.423	504	0.183	98.577
1.25	1.3767	1.423	525	0.224	98.577
1.30	1.3766	1.220	546	0.263	98.780
1.35	1.3766	1.220	567	0.301	98.780
1.40	1.3766	1.220	588	0.338	98.780
1.45	1.3766	1.220	609	0.374	98.780
1.50	1.3766	1.220	630	0.408	98.780
1.55	1.3764	0.813	651	0.442	99.187
1.60	1.3764	0.813	672	0.474	99.187
1.65	1.3764	0.813	693	0.506	99.187
1.70	1.3764	0.813	714	0.537	99.187
1.75	1.3762	0.407	735	0.567	99.593
1.80	1.3762	0.407	756	0.596	99.593
1.85	1.3762	0.407	777	0.625	99.593
1.90	1.3762	0.407	798	0.653	99.593
1.95	1.3762	0.407	819	0.680	99.593
2.00	1.3762	0.407	840	0.707	99.593

Table C-14.1: Effluent Data for Plot B-14.1

Pore Volume Injected	Refractive Index	Cyclohexane Concentration, %	Cumulative P.V. Injected, cc	Lambda	N-Hexane Concentration, %
0.50	1.4248	99.220	210.0	-0.707	0.777
0.55	1.4205	90.480	231.0	-0.607	9.520
0.60	1.4150	79.300	252.0	-0.516	20.703
0.65	1.4102	69.540	273.0	-0.434	30.462
0.70	1.4068	62.620	294.0	-0.359	37.375
0.75	1.4040	56.930	315.0	-0.289	43.069
0.80	1.4012	51.240	336.0	-0.224	48.762
0.85	1.3983	45.340	357.0	-0.163	54.658
0.90	1.3912	30.910	378.0	-0.105	69.094
0.95	1.3845	17.280	399.0	-0.051	82.717
1.00	1.3808	9.760	420.0	0.000	90.240
1.05	1.3772	2.440	441.0	0.049	97.560
1.10	1.3770	2.033	462.0	0.095	97.967
1.15	1.3768	1.627	483.0	0.140	98.373
1.20	1.3765	1.017	504.0	0.183	98.983
1.25	1.3765	1.017	525.0	0.224	98.983
1.30	1.3764	0.813	546.0	0.263	99.187
1.35	1.3764	0.813	567.0	0.301	99.187
1.40	1.3764	0.813	588.0	0.338	99.187
1.45	1.3764	0.813	609.0	0.374	99.187
1.50	1.3764	0.813	630.0	0.408	99.187
1.55	1.3762	0.407	651.0	0.442	99.593
1.60	1.3762	0.407	672.0	0.474	99.593
1.65	1.3762	0.407	693.0	0.506	99.593
1.70	1.3762	0.407	714.0	0.537	99.593
1.75	1.3760	0.000	735.0	0.567	99.999

Table C-15: Experimental Effluent Concentration Data for Run 15

Pore Volume Injected	Refractive Index	Cyclohexane Concentration, %	Cumulative P.V. Injected, cc	Lambda	N-Hexane Concentration, %
0.05	1.3760	0.000	21.0	-4.249	100.000
0.10	1.3760	0.000	42.0	-2.846	100.000
0.15	1.3760	0.000	63.0	-2.195	100.000
0.20	1.3760	0.000	84.0	-1.789	100.000
0.25	1.3760	0.000	105.0	-1.500	100.000
0.30	1.3760	0.000	126.0	-1.278	100.000
0.35	1.3760	0.000	147.0	-1.099	100.000
0.40	1.3760	0.000	168.0	-0.949	100.000
0.45	1.3760	0.000	189.0	-0.820	100.000
0.50	1.3765	1.017	210.0	-0.707	98.983
0.55	1.3820	12.200	231.0	-0.607	87.800
0.60	1.3959	40.462	252.0	-0.516	59.538
0.65	1.4076	64.251	273.0	-0.434	35.749
0.70	1.4100	69.131	294.0	-0.359	30.869
0.75	1.4070	63.031	315.0	-0.289	36.969
0.80	1.4054	59.778	336.0	-0.224	40.222
0.85	1.3970	42.699	357.0	-0.163	57.301
0.90	1.3886	25.619	378.0	-0.105	74.381
0.95	1.3818	11.793	399.0	-0.051	88.207
1.00	1.3775	3.050	420.0	0.000	96.950
1.05	1.3764	0.813	441.0	0.049	99.187
1.10	1.3760	0.000	462.0	0.095	100.000
1.15	1.3760	0.000	483.0	0.140	100.000
1.20	1.3760	0.000	504.0	0.183	100.000
1.25	1.3760	0.000	525.0	0.224	100.000
1.30	1.3760	0.000	546.0	0.263	100.000
1.35	1.3760	0.000	567.0	0.301	100.000
1.40	1.3760	0.000	588.0	0.338	100.000
1.45	1.3760	0.000	609.0	0.374	100.000
1.50	1.3760	0.000	630.0	0.408	100.000
1.55	1.3760	0.000	651.0	0.442	100.000
1.60	1.3760	0.000	672.0	0.474	100.000
1.65	1.3760	0.000	693.0	0.506	100.000
1.70	1.3760	0.000	714.0	0.537	100.000
1.75	1.3760	0.000	735.0	0.567	100.000
1.80	1.3760	0.000	756.0	0.596	100.000
1.85	1.3760	0.000	777.0	0.625	100.000
1.90	1.3760	0.000	798.0	0.653	100.000
1.95	1.3760	0.000	819.0	0.680	100.000
2.00	1.3760	0.000	840.0	0.707	100.000

Table C-16: Experimental Effluent Concentration Data for Run 16

Pore Volume Injected	Refractive Index	Cyclohexane Concentration, %	Cumulative P.V. Injected, cc	Lambda	N-Hexane Concentration, %
0.05	1.3760	0.000	21.0	-4.249	100.000
0.10	1.3760	0.000	42.0	-2.846	100.000
0.15	1.3760	0.000	63.0	-2.195	100.000
0.20	1.3760	0.000	84.0	-1.789	100.000
0.25	1.3760	0.000	105.0	-1.500	100.000
0.30	1.3760	0.000	126.0	-1.278	100.000
0.35	1.3760	0.000	147.0	-1.099	100.000
0.40	1.3760	0.000	168.0	-0.949	100.000
0.45	1.3768	1.627	189.0	-0.820	98.373
0.50	1.3822	12.606	210.0	-0.707	87.394
0.55	1.3905	29.482	231.0	-0.607	70.518
0.60	1.3972	43.105	252.0	-0.516	56.895
0.65	1.4024	53.678	273.0	-0.434	46.322
0.70	1.4104	69.944	294.0	-0.359	30.056
0.75	1.4145	78.281	315.0	-0.289	21.719
0.80	1.4096	68.318	336.0	-0.224	31.682
0.85	1.4025	53.881	357.0	-0.163	46.119
0.90	1.3985	45.748	378.0	-0.105	54.252
0.95	1.3944	37.412	399.0	-0.051	62.588
1.00	1.3878	23.992	420.0	0.000	76.008
1.05	1.3826	13.420	441.0	0.049	86.580
1.10	1.3772	2.440	462.0	0.095	97.560
1.15	1.3760	0.000	483.0	0.140	100.000
1.20	1.3760	0.000	504.0	0.183	100.000
1.25	1.3760	0.000	525.0	0.224	100.000
1.30	1.3760	0.000	546.0	0.263	100.000
1.35	1.3760	0.000	567.0	0.301	100.000
1.40	1.3760	0.000	588.0	0.338	100.000
1.45	1.3760	0.000	609.0	0.374	100.000
1.50	1.3760	0.000	630.0	0.408	100.000
1.55	1.3760	0.000	651.0	0.442	100.000
1.60	1.3760	0.000	672.0	0.474	100.000
1.65	1.3760	0.000	693.0	0.506	100.000
1.70	1.3760	0.000	714.0	0.537	100.000
1.75	1.3760	0.000	735.0	0.567	100.000
1.80	1.3760	0.000	756.0	0.596	100.000
1.85	1.3760	0.000	777.0	0.625	100.000
1.90	1.3760	0.000	798.0	0.653	100.000
1.95	1.3760	0.000	819.0	0.680	100.000
2.00	1.3760	0.000	840.0	0.707	100.000

Table C-17: Experimental Effluent Concentration Data for Run 17

Pore Volume Injected	Refractive Index	Cyclohexane Concentration, %	Cumulative P.V. Injected, cc	Lambda	N-Hexane Concentration, %
0.05	1.4250	99.630	21.0	-4.249	0.370
0.10	1.4250	99.630	42.0	-2.846	0.370
0.15	1.4250	99.630	63.0	-2.195	0.370
0.20	1.4250	99.630	84.0	-1.789	0.370
0.25	1.4250	99.630	105.0	-1.500	0.370
0.30	1.4250	99.630	126.0	-1.278	0.370
0.35	1.4250	99.630	147.0	-1.099	0.370
0.40	1.4250	99.630	168.0	-0.949	0.370
0.45	1.4250	99.630	189.0	-0.820	0.370
0.50	1.4237	96.987	210.0	-0.707	3.013
0.55	1.4152	79.704	231.0	-0.607	20.296
0.60	1.4112	71.571	252.0	-0.516	28.429
0.65	1.4032	55.305	273.0	-0.434	44.695
0.70	1.3977	44.122	294.0	-0.359	55.878
0.75	1.3936	35.785	315.0	-0.289	64.215
0.80	1.3952	39.039	336.0	-0.224	60.961
0.85	1.3970	42.699	357.0	-0.163	57.301
0.90	1.4024	53.678	378.0	-0.105	46.322
0.95	1.4120	73.197	399.0	-0.051	26.803
1.00	1.4188	87.024	420.0	0.000	12.976
1.05	1.4224	94.343	441.0	0.049	5.657
1.10	1.4237	96.987	462.0	0.095	3.013
1.15	1.4239	97.393	483.0	0.140	2.607
1.20	1.4241	97.800	504.0	0.183	2.200
1.25	1.4243	98.207	525.0	0.224	1.793
1.30	1.4244	98.410	546.0	0.263	1.590
1.35	1.4244	98.410	567.0	0.301	1.590
1.40	1.4244	98.410	588.0	0.338	1.590
1.45	1.4244	98.410	609.0	0.374	1.590
1.50	1.4247	99.020	630.0	0.408	0.980
1.55	1.4248	99.223	651.0	0.442	0.777
1.60	1.4248	99.223	672.0	0.474	0.777
1.65	1.4248	99.223	693.0	0.506	0.777
1.70	1.4248	99.223	714.0	0.537	0.777
1.75	1.4250	99.630	735.0	0.567	0.370
1.80	1.4250	99.630	756.0	0.596	0.370
1.85	1.4250	99.630	777.0	0.625	0.370
1.90	1.4250	99.630	798.0	0.653	0.370
1.95	1.4250	99.630	819.0	0.680	0.370
2.00	1.4250	99.630	840.0	0.707	0.370

Table C-18: Experimental Effluent Concentration Data for Run 18

Pore Volume Injected	Refractive Index	Cyclohexane Concentration, %	Cumulative P.V. Injected, cc	Lambda	N-Hexane Concentration, %
0.05	1.4250	99.630	21.0	-4.249	0.370
0.10	1.4250	99.630	42.0	-2.846	0.370
0.15	1.4250	99.630	63.0	-2.195	0.370
0.20	1.4250	99.630	84.0	-1.789	0.370
0.25	1.4250	99.630	105.0	-1.500	0.370
0.30	1.4250	99.630	126.0	-1.278	0.370
0.35	1.4250	99.630	147.0	-1.099	0.370
0.40	1.4250	99.630	168.0	-0.949	0.370
0.45	1.4250	99.630	189.0	-0.820	0.370
0.50	1.4250	99.630	210.0	-0.707	0.370
0.55	1.4234	96.377	231.0	-0.607	3.623
0.60	1.4144	78.077	252.0	-0.516	21.923
0.65	1.4084	65.878	273.0	-0.434	34.122
0.70	1.3983	45.342	294.0	-0.359	54.658
0.75	1.3938	36.192	315.0	-0.289	63.808
0.80	1.3920	32.532	336.0	-0.224	67.468
0.85	1.3912	30.906	357.0	-0.163	69.094
0.90	1.3888	26.026	378.0	-0.105	73.974
0.95	1.3879	24.196	399.0	-0.051	75.804
1.00	1.3924	33.346	420.0	0.000	66.654
1.05	1.4046	58.151	441.0	0.049	41.849
1.10	1.4202	89.870	462.0	0.095	10.130
1.15	1.4225	94.547	483.0	0.140	5.453
1.20	1.4230	95.563	504.0	0.183	4.437
1.25	1.4232	95.970	525.0	0.224	4.030
1.30	1.4234	96.377	546.0	0.263	3.623
1.35	1.4236	96.783	567.0	0.301	3.217
1.40	1.4238	97.190	588.0	0.338	2.810
1.45	1.4239	97.393	609.0	0.374	2.607
1.50	1.4239	97.393	630.0	0.408	2.607
1.55	1.4239	97.393	651.0	0.442	2.607
1.60	1.4239	97.393	672.0	0.474	2.607
1.65	1.4239	97.393	693.0	0.506	2.607
1.70	1.4239	97.393	714.0	0.537	2.607
1.75	1.4242	98.003	735.0	0.567	1.997
1.80	1.4242	98.003	756.0	0.596	1.997
1.85	1.4244	98.410	777.0	0.625	1.590
1.90	1.4244	98.410	798.0	0.653	1.590
1.95	1.4247	99.020	819.0	0.680	0.980
2.00	1.4247	99.020	840.0	0.707	0.980

Table C-19: Experimental Effluent Concentration Data for Run 19

Pore Volume Injected	Refractive Index	10% Brine Concentration, %	Cumulative P.V. Injected, cc	Lambda	2% Brine Concentration, %
0.05	1.3362	0.000	21.8	-4.249	100.000
0.10	1.3362	0.000	43.5	-2.846	100.000
0.15	1.3362	0.000	65.3	-2.195	100.000
0.20	1.3362	0.000	87.0	-1.789	100.000
0.25	1.3362	0.000	108.8	-1.500	100.000
0.30	1.3362	0.000	130.5	-1.278	100.000
0.35	1.3362	0.000	152.3	-1.099	100.000
0.40	1.3362	0.000	174.0	-0.949	100.000
0.45	1.3362	0.000	195.8	-0.820	100.000
0.50	1.3362	0.000	217.5	-0.707	100.000
0.55	1.3362	0.000	239.3	-0.607	100.000
0.60	1.3362	0.000	261.0	-0.516	100.000
0.65	1.3362	0.000	282.8	-0.434	100.000
0.70	1.3362	0.000	304.5	-0.359	100.000
0.75	1.3362	0.000	326.3	-0.289	100.000
0.80	1.339	23.227	348.0	-0.224	76.773
0.85	1.3448	71.340	369.8	-0.163	28.660
0.90	1.3474	92.907	391.5	-0.105	7.092
0.95	1.3478	96.226	413.3	-0.051	3.774
1.00	1.3482	99.544	435.0	0.000	0.456
1.05	1.3482	99.544	456.8	0.049	0.456
1.10	1.3482	99.544	478.5	0.095	0.456
1.15	1.3482	99.544	500.3	0.140	0.456
1.20	1.3482	99.544	522.0	0.183	0.456
1.25	1.3482	99.544	543.8	0.224	0.456
1.30	1.3482	99.544	565.5	0.263	0.456
1.35	1.3482	99.544	587.3	0.301	0.456
1.40	1.3482	99.544	609.0	0.338	0.456
1.45	1.3482	99.544	630.8	0.374	0.456
1.50	1.3482	99.544	652.5	0.408	0.456
1.55	1.3482	99.544	674.3	0.442	0.456
1.60	1.3482	99.544	696.0	0.474	0.456
1.65	1.3482	99.544	717.8	0.506	0.456
1.70	1.3482	99.544	739.5	0.537	0.456
1.75	1.3482	99.544	761.3	0.567	0.456
1.80	1.3482	99.544	783.0	0.596	0.456
1.85	1.3482	99.544	804.8	0.625	0.456
1.90	1.3482	99.544	826.5	0.653	0.456
1.95	1.3482	99.544	848.3	0.680	0.456
2.00	1.3482	99.544	870.0	0.707	0.456

Table C-20: Experimental Effluent Concentration Data for Run 20

Pore Volume Injected	Refractive Index	10% Brine Concentration, %	Cumulative P.V. Injected, cc	Lambda	2% Brine Concentration, %
0.05	1.3482	100.000	21.8	-4.249	0.000
0.10	1.3482	100.000	43.5	-2.846	0.000
0.15	1.3482	100.000	65.3	-2.195	0.000
0.20	1.3482	100.000	87.0	-1.789	0.000
0.25	1.3482	100.000	108.8	-1.500	0.000
0.30	1.3482	100.000	130.5	-1.278	0.000
0.35	1.3482	100.000	152.3	-1.099	0.000
0.40	1.3482	100.000	174.0	-0.949	0.000
0.45	1.3482	100.000	195.8	-0.820	0.000
0.50	1.3482	100.000	217.5	-0.707	0.000
0.55	1.3482	100.000	239.3	-0.607	0.000
0.60	1.3482	100.000	261.0	-0.516	0.000
0.65	1.3482	100.000	282.8	-0.434	0.000
0.70	1.3482	100.000	304.5	-0.359	0.000
0.75	1.3473	92.534	326.3	-0.289	7.466
0.80	1.343	56.864	348.0	-0.224	43.136
0.85	1.3392	25.342	369.8	-0.163	74.658
0.90	1.3379	14.558	391.5	-0.105	85.442
0.95	1.337	7.093	413.3	-0.051	92.907
1.00	1.3366	3.774	435.0	0.000	96.226
1.05	1.3365	2.945	456.8	0.049	97.055
1.10	1.3364	2.115	478.5	0.095	97.885
1.15	1.3364	2.115	500.3	0.140	97.885
1.20	1.3364	2.115	522.0	0.183	97.885
1.25	1.3362	0.456	543.8	0.224	99.544
1.30	1.3362	0.456	565.5	0.263	99.544
1.35	1.3362	0.456	587.3	0.301	99.544
1.40	1.3362	0.456	609.0	0.338	99.544
1.45	1.3362	0.456	630.8	0.374	99.544
1.50	1.3362	0.456	652.5	0.408	99.544
1.55	1.3362	0.456	674.3	0.442	99.544
1.60	1.3362	0.456	696.0	0.474	99.544
1.65	1.3362	0.456	717.8	0.506	99.544
1.70	1.3362	0.456	739.5	0.537	99.544
1.75	1.3362	0.456	761.3	0.567	99.544
1.80	1.3362	0.456	783.0	0.596	99.544
1.85	1.3362	0.456	804.8	0.625	99.544
1.90	1.3362	0.456	826.5	0.653	99.544
1.95	1.3362	0.456	848.3	0.680	99.544
2.00	1.3362	0.456	870.0	0.707	99.544

Table C-19.1: Effluent Data for Plot B-19.1

Pore Volume Injected	Refractive Index	10% Brine Concentration, %	Cumulative P.V. Injected, cc	Lambda	2% Brine Concentration, %
0.05	1.3362	-0.830	21.8	-4.249	100.000
0.10	1.3362	-0.830	43.5	-2.846	100.000
0.15	1.3362	-0.830	65.3	-2.195	100.000
0.20	1.3362	-0.830	87.0	-1.789	100.000
0.25	1.3362	-0.830	108.8	-1.500	100.000
0.30	1.3362	-0.830	130.5	-1.278	100.000
0.35	1.3362	-0.830	152.3	-1.099	100.000
0.40	1.3362	-0.830	174.0	-0.949	100.000
0.45	1.3362	-0.830	195.8	-0.820	100.000
0.50	1.3362	-0.830	217.5	-0.707	100.000
0.55	1.3362	-0.830	239.3	-0.607	100.000
0.60	1.3362	-0.830	261.0	-0.516	100.000
0.65	1.3362	-0.830	282.8	-0.434	100.000
0.70	1.3362	-0.830	304.5	-0.359	100.000
0.75	1.3362	-0.830	326.3	-0.289	100.000
0.80	1.3390	22.400	348.0	-0.224	76.770
0.85	1.3448	70.510	369.8	-0.163	28.660
0.90	1.3474	92.080	391.5	-0.105	7.093
0.95	1.3478	95.400	413.3	-0.051	3.774
1.00	1.3482	98.710	435.0	0.000	0.456
1.05	1.3482	98.710	456.8	0.049	0.456
1.10	1.3482	98.710	478.5	0.095	0.456
1.15	1.3482	98.710	500.3	0.140	0.456

Table C-20.1: Effluent Data for Plot B-20.1

Pore Volume Injected	Refractive Index	10% Brine Concentration, %	Cumulative P.V. Injected, cc	Lambda	2% Brine Concentration, %
0.75	1.3473	92.530	326.3	-0.289	7.466
0.80	1.3430	56.860	348.0	-0.224	43.140
0.85	1.3392	25.340	369.8	-0.163	74.660
0.90	1.3379	14.560	391.5	-0.105	85.440
0.95	1.3370	7.093	413.3	-0.051	92.910
1.00	1.3366	3.774	435.0	0.000	96.230

Table C-21: Experimental Effluent Concentration Data for Run 21

Pore Volume Injected	Refractive Index	10% Brine Concentration, %	Cumulative P.V. Injected, cc	Lambda	2% Brine Concentration, %
0.05	1.3362	0.000	21.8	-4.249	100.000
0.10	1.3362	0.000	43.5	-2.846	100.000
0.15	1.3362	0.000	65.3	-2.195	100.000
0.20	1.3362	0.000	87.0	-1.789	100.000
0.25	1.3362	0.000	108.8	-1.500	100.000
0.30	1.3362	0.000	130.5	-1.278	100.000
0.35	1.3362	0.000	152.3	-1.099	100.000
0.40	1.3362	0.000	174.0	-0.949	100.000
0.45	1.3362	0.000	195.8	-0.820	100.000
0.50	1.3362	0.000	217.5	-0.707	100.000
0.55	1.3362	0.000	239.3	-0.607	100.000
0.60	1.3362	0.000	261.0	-0.516	100.000
0.65	1.3362	0.000	282.8	-0.434	100.000
0.70	1.3376	11.613	304.5	-0.359	88.387
0.75	1.3402	33.181	326.3	-0.289	66.819
0.80	1.3438	63.044	348.0	-0.224	36.956
0.85	1.3463	83.783	369.8	-0.163	16.217
0.90	1.3462	82.953	391.5	-0.105	17.047
0.95	1.3444	68.022	413.3	-0.051	31.978
1.00	1.3415	43.965	435.0	0.000	56.035
1.05	1.3394	26.545	456.8	0.049	73.455
1.10	1.3376	11.613	478.5	0.095	88.387
1.15	1.3371	7.466	500.3	0.140	92.534
1.20	1.3369	5.807	522.0	0.183	94.193
1.25	1.3366	3.318	543.8	0.224	96.682
1.30	1.3365	2.489	565.5	0.263	97.511
1.35	1.3364	1.659	587.3	0.301	98.341
1.40	1.3363	0.830	609.0	0.338	99.170
1.45	1.3362	0.000	630.8	0.374	100.000
1.50	1.3362	0.000	652.5	0.408	100.000
1.55	1.3362	0.000	674.3	0.442	100.000
1.60	1.3362	0.000	696.0	0.474	100.000
1.65	1.3362	0.000	717.8	0.506	100.000
1.70	1.3362	0.000	739.5	0.537	100.000
1.75	1.3362	0.000	761.3	0.567	100.000
1.80	1.3362	0.000	783.0	0.596	100.000
1.85	1.3362	0.000	804.8	0.625	100.000
1.90	1.3362	0.000	826.5	0.653	100.000
1.95	1.3362	0.000	848.3	0.680	100.000
2.00	1.3362	0.000	870.0	0.707	100.000

Table C-21R: Experimental Effluent Concentration Data for Run 21R

Pore Volume Injected	Refractive Index	10% Brine Concentration, %	Cumulative P.V. Injected, cc	Lambda	2% Brine Concentration, %
0.05	1.3362	0.000	21.8	-4.249	100.000
0.10	1.3362	0.000	43.5	-2.846	100.000
0.15	1.3362	0.000	65.3	-2.195	100.000
0.20	1.3362	0.000	87.0	-1.789	100.000
0.25	1.3362	0.000	108.8	-1.500	100.000
0.30	1.3362	0.000	130.5	-1.278	100.000
0.35	1.3362	0.000	152.3	-1.099	100.000
0.40	1.3362	0.000	174.0	-0.949	100.000
0.45	1.3362	0.000	195.8	-0.820	100.000
0.50	1.3362	0.000	217.5	-0.707	100.000
0.55	1.3362	0.000	239.3	-0.607	100.000
0.60	1.3362	0.000	261.0	-0.516	100.000
0.65	1.3368	4.977	282.8	-0.434	95.023
0.70	1.3382	16.591	304.5	-0.359	83.409
0.75	1.3408	38.158	326.3	-0.289	61.842
0.80	1.3446	69.681	348.0	-0.224	30.319
0.85	1.3468	87.930	369.8	-0.163	12.070
0.90	1.3466	86.271	391.5	-0.105	13.729
0.95	1.345	72.999	413.3	-0.051	27.001
1.00	1.3421	48.942	435.0	0.000	51.058
1.05	1.3399	30.693	456.8	0.049	69.307
1.10	1.338	14.932	478.5	0.095	85.068
1.15	1.3375	10.784	500.3	0.140	89.216
1.20	1.3372	8.295	522.0	0.183	91.705
1.25	1.3369	5.807	543.8	0.224	94.193
1.30	1.3366	3.318	565.5	0.263	96.682
1.35	1.3365	2.489	587.3	0.301	97.511
1.40	1.3364	1.659	609.0	0.338	98.341
1.45	1.3363	0.830	630.8	0.374	99.170
1.50	1.3362	0.000	652.5	0.408	100.000
1.55	1.3362	0.000	674.3	0.442	100.000
1.60	1.3362	0.000	696.0	0.474	100.000
1.65	1.3362	0.000	717.8	0.506	100.000
1.70	1.3362	0.000	739.5	0.537	100.000
1.75	1.3362	0.000	761.3	0.567	100.000
1.80	1.3362	0.000	783.0	0.596	100.000
1.85	1.3362	0.000	804.8	0.625	100.000
1.90	1.3362	0.000	826.5	0.653	100.000
1.95	1.3362	0.000	848.3	0.680	100.000
2.00	1.3362	0.000	870.0	0.707	100.000

Table C-22: Experimental Effluent Concentration Data for Run 22

Pore Volume Injected	Refractive Index	10% Brine Concentration, %	Cumulative P.V. Injected, cc	Lambda	2% Brine Concentration, %
0.05	1.3362	0.000	21.8	-4.249	100.000
0.10	1.3362	0.000	43.5	-2.846	100.000
0.15	1.3362	0.000	65.3	-2.195	100.000
0.20	1.3362	0.000	87.0	-1.789	100.000
0.25	1.3362	0.000	108.8	-1.500	100.000
0.30	1.3362	0.000	130.5	-1.278	100.000
0.35	1.3362	0.000	152.3	-1.099	100.000
0.40	1.3362	0.000	174.0	-0.949	100.000
0.45	1.3362	0.000	195.8	-0.820	100.000
0.50	1.3362	0.000	217.5	-0.707	100.000
0.55	1.3362	0.000	239.3	-0.607	100.000
0.60	1.3362	0.000	261.0	-0.516	100.000
0.65	1.3362	0.000	282.8	-0.434	100.000
0.70	1.3375	10.784	304.5	-0.359	89.216
0.75	1.3406	36.499	326.3	-0.289	63.501
0.80	1.3442	66.362	348.0	-0.224	33.637
0.85	1.3464	84.612	369.8	-0.163	15.388
0.90	1.347	89.589	391.5	-0.105	10.411
0.95	1.3472	91.248	413.3	-0.051	8.752
1.00	1.3469	88.760	435.0	0.000	11.240
1.05	1.3445	68.851	456.8	0.049	31.149
1.10	1.3412	41.477	478.5	0.095	58.523
1.15	1.3391	24.056	500.3	0.140	75.944
1.20	1.3376	11.613	522.0	0.183	88.387
1.25	1.337	6.636	543.8	0.224	93.364
1.30	1.3366	3.318	565.5	0.263	96.682
1.35	1.3364	1.659	587.3	0.301	98.341
1.40	1.3363	0.830	609.0	0.338	99.170
1.45	1.3362	0.000	630.8	0.374	100.000
1.50	1.3362	0.000	652.5	0.408	100.000
1.55	1.3362	0.000	674.3	0.442	100.000
1.60	1.3362	0.000	696.0	0.474	100.000
1.65	1.3362	0.000	717.8	0.506	100.000
1.70	1.3362	0.000	739.5	0.537	100.000
1.75	1.3362	0.000	761.3	0.567	100.000
1.80	1.3362	0.000	783.0	0.596	100.000
1.85	1.3362	0.000	804.8	0.625	100.000
1.90	1.3362	0.000	826.5	0.653	100.000
1.95	1.3362	0.000	848.3	0.680	100.000
2.00	1.3362	0.000	870.0	0.707	100.000

Table C-23: Experimental Effluent Concentration Data for Run 23

Pore Volume Injected	Refractive Index	10% Brine Concentration, %	Cumulative P.V. Injected, cc	Lambda	2% Brine Concentration, %
0.05	1.3482	100.000	21.8	-4.249	0.000
0.10	1.3482	100.000	43.5	-2.846	0.000
0.15	1.3482	100.000	65.3	-2.195	0.000
0.20	1.3482	100.000	87.0	-1.789	0.000
0.25	1.3482	100.000	108.8	-1.500	0.000
0.30	1.3482	100.000	130.5	-1.278	0.000
0.35	1.3482	100.000	152.3	-1.099	0.000
0.40	1.3482	100.000	174.0	-0.949	0.000
0.45	1.3482	100.000	195.8	-0.820	0.000
0.50	1.3482	100.000	217.5	-0.707	0.000
0.55	1.3482	100.000	239.3	-0.607	0.000
0.60	1.3482	100.000	261.0	-0.516	0.000
0.65	1.3482	100.000	282.8	-0.434	0.000
0.70	1.3469	89.216	304.5	-0.359	10.784
0.75	1.345	73.455	326.3	-0.289	26.545
0.80	1.3425	52.717	348.0	-0.224	47.283
0.85	1.3406	36.956	369.8	-0.163	63.044
0.90	1.339	23.683	391.5	-0.105	76.317
0.95	1.341	40.274	413.3	-0.051	59.726
1.00	1.344	65.160	435.0	0.000	34.840
1.05	1.3465	85.898	456.8	0.049	14.102
1.10	1.3472	91.705	478.5	0.095	8.295
1.15	1.3479	97.511	500.3	0.140	2.489
1.20	1.3481	99.170	522.0	0.183	0.830
1.25	1.3482	100.000	543.8	0.224	0.000
1.30	1.3482	100.000	565.5	0.263	0.000
1.35	1.3482	100.000	587.3	0.301	0.000
1.40	1.3482	100.000	609.0	0.338	0.000
1.45	1.3482	100.000	630.8	0.374	0.000
1.50	1.3482	100.000	652.5	0.408	0.000
1.55	1.3482	100.000	674.3	0.442	0.000
1.60	1.3482	100.000	696.0	0.474	0.000
1.65	1.3482	100.000	717.8	0.506	0.000
1.70	1.3482	100.000	739.5	0.537	0.000
1.75	1.3482	100.000	761.3	0.567	0.000
1.80	1.3482	100.000	783.0	0.596	0.000
1.85	1.3482	100.000	804.8	0.625	0.000
1.90	1.3482	100.000	826.5	0.653	0.000
1.95	1.3482	100.000	848.3	0.680	0.000
2.00	1.3482	100.000	870.0	0.707	0.000

Table C-24: Experimental Effluent Concentration Data for Run 24

Pore Volume Injected	Refractive Index	10% Brine Concentration, %	Cumulative P.V. Injected, cc	Lambda	2% Brine Concentration, %
0.05	1.3482	100.000	21.8	-4.249	0.000
0.10	1.3482	100.000	43.5	-2.846	0.000
0.15	1.3482	100.000	65.3	-2.195	0.000
0.20	1.3482	100.000	87.0	-1.789	0.000
0.25	1.3482	100.000	108.8	-1.500	0.000
0.30	1.3482	100.000	130.5	-1.278	0.000
0.35	1.3482	100.000	152.3	-1.099	0.000
0.40	1.3482	100.000	174.0	-0.949	0.000
0.45	1.3482	100.000	195.8	-0.820	0.000
0.50	1.3482	100.000	217.5	-0.707	0.000
0.55	1.3482	100.000	239.3	-0.607	0.000
0.60	1.3482	100.000	261.0	-0.516	0.000
0.65	1.3482	100.000	282.8	-0.434	0.000
0.70	1.347	90.046	304.5	-0.359	9.954
0.75	1.3446	70.137	326.3	-0.289	29.863
0.80	1.3435	61.012	348.0	-0.224	38.988
0.85	1.3422	50.228	369.8	-0.163	49.772
0.90	1.3389	22.854	391.5	-0.105	77.146
0.95	1.3385	19.535	413.3	-0.051	80.465
1.00	1.3378	13.729	435.0	0.000	86.271
1.05	1.3371	7.922	456.8	0.049	92.078
1.10	1.339	23.683	478.5	0.095	76.317
1.15	1.3446	70.137	500.3	0.140	29.863
1.20	1.347	90.046	522.0	0.183	9.954
1.25	1.3479	97.511	543.8	0.224	2.489
1.30	1.3482	100.000	565.5	0.263	0.000
1.35	1.3482	100.000	587.3	0.301	0.000
1.40	1.3482	100.000	609.0	0.338	0.000
1.45	1.3482	100.000	630.8	0.374	0.000
1.50	1.3482	100.000	652.5	0.408	0.000
1.55	1.3482	100.000	674.3	0.442	0.000
1.60	1.3482	100.000	696.0	0.474	0.000
1.65	1.3482	100.000	717.8	0.506	0.000
1.70	1.3482	100.000	739.5	0.537	0.000
1.75	1.3482	100.000	761.3	0.567	0.000
1.80	1.3482	100.000	783.0	0.596	0.000
1.85	1.3482	100.000	804.8	0.625	0.000
1.90	1.3482	100.000	826.5	0.653	0.000
1.95	1.3482	100.000	848.3	0.680	0.000
2.00	1.3482	100.000	870.0	0.707	0.000

Table C-25: Experimental Effluent Concentration Data for Run 25

Pore Volume Injected	Refractive Index	Cyclohexane Concentration, %	Cumulative P.V. Injected, cc	Lambda	N-Hexane Concentration, %
0.05	1.3760	0.000	21.5	-4.249	100.000
0.10	1.3760	0.000	43.0	-2.846	100.000
0.15	1.3760	0.000	64.5	-2.195	100.000
0.20	1.3760	0.000	86.0	-1.789	100.000
0.25	1.3760	0.000	107.5	-1.500	100.000
0.30	1.3760	0.000	129.0	-1.278	100.000
0.35	1.3760	0.000	150.5	-1.099	100.000
0.40	1.3760	0.000	172.0	-0.949	100.000
0.45	1.3760	0.000	193.5	-0.820	100.000
0.50	1.3760	0.000	215.0	-0.707	100.000
0.55	1.3760	0.000	236.5	-0.607	100.000
0.60	1.3760	0.000	258.0	-0.516	100.000
0.65	1.3825	13.216	279.5	-0.434	86.784
0.70	1.4073	63.641	301.0	-0.359	36.359
0.75	1.4221	93.733	322.5	-0.289	6.267
0.80	1.4236	96.783	344.0	-0.224	3.217
0.85	1.4240	97.597	365.5	-0.163	2.403
0.90	1.4242	98.003	387.0	-0.105	1.997
0.95	1.4244	98.410	408.5	-0.051	1.590
1.00	1.4244	98.410	430.0	0.000	1.590
1.05	1.4245	98.613	451.5	0.049	1.387
1.10	1.4245	98.613	473.0	0.095	1.387
1.15	1.4246	98.817	494.5	0.140	1.183
1.20	1.4248	99.223	516.0	0.183	0.777
1.25	1.4248	99.223	537.5	0.224	0.777
1.30	1.4248	99.223	559.0	0.263	0.777
1.35	1.4248	99.223	580.5	0.301	0.777
1.40	1.4248	99.223	602.0	0.338	0.777
1.45	1.4248	99.223	623.5	0.374	0.777
1.50	1.4248	99.223	645.0	0.408	0.777
1.55	1.4248	99.223	666.5	0.442	0.777
1.60	1.4248	99.223	688.0	0.474	0.777
1.65	1.4248	99.223	709.5	0.506	0.777
1.70	1.4248	99.223	731.0	0.537	0.777
1.75	1.4248	99.223	752.5	0.567	0.777
1.80	1.4248	99.223	774.0	0.596	0.777
1.85	1.4248	99.223	795.5	0.625	0.777
1.90	1.4248	99.223	817.0	0.653	0.777
1.95	1.4248	99.223	838.5	0.680	0.777
2.00	1.4248	99.223	860.0	0.707	0.777

Table C-26: Experimental Effluent Concentration Data for Run 26

Pore Volume Injected	Refractive Index	Cyclohexane Concentration, %	Cumulative P.V. Injected, cc	Lambda	N-Hexane Concentration, %
0.05	1.4248	99.223	21.5	-4.249	0.777
0.10	1.4248	99.223	43.0	-2.846	0.777
0.15	1.4248	99.223	64.5	-2.195	0.777
0.20	1.4248	99.223	86.0	-1.789	0.777
0.25	1.4248	99.223	107.5	-1.500	0.777
0.30	1.4248	99.223	129.0	-1.278	0.777
0.35	1.4248	99.223	150.5	-1.099	0.777
0.40	1.4248	99.223	172.0	-0.949	0.777
0.45	1.4248	99.223	193.5	-0.820	0.777
0.50	1.4248	99.223	215.0	-0.707	0.777
0.55	1.4173	83.974	236.5	-0.607	16.026
0.60	1.4115	72.181	258.0	-0.516	27.819
0.65	1.4082	65.471	279.5	-0.434	34.529
0.70	1.4029	54.695	301.0	-0.359	45.305
0.75	1.3922	32.939	322.5	-0.289	67.061
0.80	1.3865	21.349	344.0	-0.224	78.651
0.85	1.3823	12.810	365.5	-0.163	87.190
0.90	1.3787	5.490	387.0	-0.105	94.510
0.95	1.3770	2.033	408.5	-0.051	97.967
1.00	1.3768	1.627	430.0	0.000	98.373
1.05	1.3766	1.220	451.5	0.049	98.780
1.10	1.3765	1.017	473.0	0.095	98.983
1.15	1.3767	1.423	494.5	0.140	98.577
1.20	1.3767	1.423	516.0	0.183	98.577
1.25	1.3765	1.017	537.5	0.224	98.983
1.30	1.3765	1.017	559.0	0.263	98.983
1.35	1.3768	1.627	580.5	0.301	98.373
1.40	1.3767	1.423	602.0	0.338	98.577
1.45	1.3766	1.220	623.5	0.374	98.780
1.50	1.3767	1.423	645.0	0.408	98.577
1.55	1.3767	1.423	666.5	0.442	98.577
1.60	1.3773	2.643	688.0	0.474	97.357
1.65	1.3767	1.423	709.5	0.506	98.577
1.70	1.3767	1.423	731.0	0.537	98.577
1.75	1.3765	1.017	752.5	0.567	98.983
1.80	1.3765	1.017	774.0	0.596	98.983
1.85	1.3765	1.017	795.5	0.625	98.983
1.90	1.3767	1.423	817.0	0.653	98.577
1.95	1.3763	0.610	838.5	0.680	99.390
2.00	1.3763	0.610	860.0	0.707	99.390

Table C-25.1: Effluent Data for Plot B-25.1

Pore Volume Injected	Refractive Index	Cyclohexane Concentration, %	Cumulative P.V. Injected, cc	Lambda	N-Hexane Concentration, %
0.05	1.3760	0.000	21.5	-4.249	100.000
0.10	1.3760	0.000	43.0	-2.846	100.000
0.15	1.3760	0.000	64.5	-2.195	100.000
0.20	1.3760	0.000	86.0	-1.789	100.000
0.25	1.3760	0.000	107.5	-1.500	100.000
0.30	1.3760	0.000	129.0	-1.278	100.000
0.35	1.3760	0.000	150.5	-1.099	100.000
0.40	1.3760	0.000	172.0	-0.949	100.000
0.45	1.3760	0.000	193.5	-0.820	100.000
0.50	1.3760	0.000	215.0	-0.707	100.000
0.55	1.3760	0.000	236.5	-0.607	100.000
0.60	1.3760	0.000	258.0	-0.516	100.000
0.65	1.3825	13.220	279.5	-0.434	86.784
0.70	1.4073	63.640	301.0	-0.359	36.359
0.75	1.4221	93.730	322.5	-0.289	6.266
0.80	1.4236	96.780	344.0	-0.224	3.217
0.85	1.4240	97.600	365.5	-0.163	2.403
0.90	1.4242	98.000	387.0	-0.105	1.997
0.95	1.4244	98.410	408.5	-0.051	1.590
1.00	1.4244	98.410	430.0	0.000	1.590
1.05	1.4245	98.610	451.5	0.049	1.387
1.10	1.4245	98.610	473.0	0.095	1.387
1.15	1.4246	98.820	494.5	0.140	1.183
1.20	1.4248	99.220	516.0	0.183	0.777
1.25	1.4248	99.220	537.5	0.224	0.777

Table C-26.1: Effluent Data for Plot B-26.1

Pore Volume Injected	Refractive Index	Cyclohexane Concentration, %	Cumulative P.V. Injected, cc	Lambda	N-Hexane Concentration, %
0.50	1.4248	99.220	215.0	-0.707	0.777
0.55	1.4173	83.970	236.5	-0.607	16.030
0.60	1.4115	72.180	258.0	-0.516	27.820
0.65	1.4082	65.470	279.5	-0.434	34.530
0.70	1.4029	54.690	301.0	-0.359	45.310
0.75	1.3922	32.940	322.5	-0.289	67.060
0.80	1.3865	21.350	344.0	-0.224	78.650
0.85	1.3823	12.810	365.5	-0.163	87.190
0.90	1.3787	5.490	387.0	-0.105	94.510
0.95	1.3770	2.033	408.5	-0.051	97.970
1.00	1.3768	1.627	430.0	0.000	98.370
1.05	1.3766	1.220	451.5	0.049	98.780
1.10	1.3765	1.017	473.0	0.095	98.980
1.15	1.3767	1.423	494.5	0.140	98.580
1.20	1.3767	1.423	516.0	0.183	98.580
1.25	1.3765	1.017	537.5	0.224	98.980
1.30	1.3765	1.017	559.0	0.263	98.980
1.35	1.3768	1.627	580.5	0.301	98.370
1.40	1.3767	1.423	602.0	0.338	98.580
1.45	1.3766	1.220	623.5	0.374	98.780
1.50	1.3767	1.423	645.0	0.408	98.580
1.55	1.3767	1.423	666.5	0.442	98.580
1.60	1.3773	2.643	688.0	0.474	97.360
1.65	1.3767	1.423	709.5	0.506	98.580
1.70	1.3767	1.423	731.0	0.537	98.580
1.75	1.3765	1.017	752.5	0.567	98.980

Table C-27: Experimental Effluent Concentration Data for Run 27

Pore Volume Injected	Refractive Index	Cyclohexane Concentration, %	Cumulative P.V. Injected, cc	Lambda	N-Hexane Concentration, %
0.05	1.3760	0.000	21.5	-4.249	100.000
0.10	1.3760	0.000	43.0	-2.846	100.000
0.15	1.3760	0.000	64.5	-2.195	100.000
0.20	1.3760	0.000	86.0	-1.789	100.000
0.25	1.3760	0.000	107.5	-1.500	100.000
0.30	1.3760	0.000	129.0	-1.278	100.000
0.35	1.3760	0.000	150.5	-1.099	100.000
0.40	1.3760	0.000	172.0	-0.949	100.000
0.45	1.3813	10.776	193.5	-0.820	89.224
0.50	1.3950	38.632	215.0	-0.707	61.368
0.55	1.4052	59.371	236.5	-0.607	40.629
0.60	1.4048	58.558	258.0	-0.516	41.442
0.65	1.4015	51.848	279.5	-0.434	48.152
0.70	1.4010	50.832	301.0	-0.359	49.168
0.75	1.3985	45.748	322.5	-0.289	54.252
0.80	1.3925	33.549	344.0	-0.224	66.451
0.85	1.3872	22.773	365.5	-0.163	77.227
0.90	1.3836	15.453	387.0	-0.105	84.547
0.95	1.3799	7.930	408.5	-0.051	92.070
1.00	1.3775	3.050	430.0	0.000	96.950
1.05	1.3767	1.423	451.5	0.049	98.577
1.10	1.3765	1.017	473.0	0.095	98.983
1.15	1.3765	1.017	494.5	0.140	98.983
1.20	1.3765	1.017	516.0	0.183	98.983
1.25	1.3765	1.017	537.5	0.224	98.983
1.30	1.3765	1.017	559.0	0.263	98.983
1.35	1.3765	1.017	580.5	0.301	98.983
1.40	1.3764	0.813	602.0	0.338	99.187
1.45	1.3762	0.407	623.5	0.374	99.593
1.50	1.3762	0.407	645.0	0.408	99.593
1.55	1.3762	0.407	666.5	0.442	99.593
1.60	1.3762	0.407	688.0	0.474	99.593
1.65	1.3762	0.407	709.5	0.506	99.593
1.70	1.3762	0.407	731.0	0.537	99.593
1.75	1.3762	0.407	752.5	0.567	99.593
1.80	1.3762	0.407	774.0	0.596	99.593
1.85	1.3762	0.407	795.5	0.625	99.593
1.90	1.3762	0.407	817.0	0.653	99.593
1.95	1.3762	0.407	838.5	0.680	99.593
2.00	1.3762	0.407	860.0	0.707	99.593

Table C-28: Experimental Effluent Concentration Data for Run 28

Pore Volume Injected	Refractive Index	Cyclohexane Concentration, %	Cumulative P.V. Injected, cc	Lambda	N-Hexane Concentration, %
0.05	1.3760	0.000	21.5	-4.249	100.000
0.10	1.3760	0.000	43.0	-2.846	100.000
0.15	1.3760	0.000	64.5	-2.195	100.000
0.20	1.3760	0.000	86.0	-1.789	100.000
0.25	1.3760	0.000	107.5	-1.500	100.000
0.30	1.3760	0.000	129.0	-1.278	100.000
0.35	1.3760	0.000	150.5	-1.099	100.000
0.40	1.3760	0.000	172.0	-0.949	100.000
0.45	1.3760	0.000	193.5	-0.820	100.000
0.50	1.3760	0.000	215.0	-0.707	100.000
0.55	1.3760	0.000	236.5	-0.607	100.000
0.60	1.3790	6.100	258.0	-0.516	93.900
0.65	1.3912	30.906	279.5	-0.434	69.094
0.70	1.4090	67.098	301.0	-0.359	32.902
0.75	1.4197	88.854	322.5	-0.289	11.146
0.80	1.4202	89.870	344.0	-0.224	10.130
0.85	1.4124	74.011	365.5	-0.163	25.989
0.90	1.4086	66.284	387.0	-0.105	33.716
0.95	1.4075	64.048	408.5	-0.051	35.952
1.00	1.4005	49.815	430.0	0.000	50.185
1.05	1.3925	33.549	451.5	0.049	66.451
1.10	1.3876	23.586	473.0	0.095	76.414
1.15	1.3812	10.573	494.5	0.140	89.427
1.20	1.3778	3.660	516.0	0.183	96.340
1.25	1.3770	2.033	537.5	0.224	97.967
1.30	1.3766	1.220	559.0	0.263	98.780
1.35	1.3765	1.017	580.5	0.301	98.983
1.40	1.3764	0.813	602.0	0.338	99.187
1.45	1.3765	1.017	623.5	0.374	98.983
1.50	1.3764	0.813	645.0	0.408	99.187
1.55	1.3765	1.017	666.5	0.442	98.983
1.60	1.3765	1.017	688.0	0.474	98.983
1.65	1.3765	1.017	709.5	0.506	98.983
1.70	1.3765	1.017	731.0	0.537	98.983
1.75	1.3765	1.017	752.5	0.567	98.983
1.80	1.3762	0.407	774.0	0.596	99.593
1.85	1.3764	0.813	795.5	0.625	99.187
1.90	1.3765	1.017	817.0	0.653	98.983
1.95	1.3764	0.813	838.5	0.680	99.187
2.00	1.3762	0.407	860.0	0.707	99.593

Table C-29: Experimental Effluent Concentration Data for Run 29

Pore Volume Injected	Refractive Index	Cyclohexane Concentration, %	Cumulative P.V. Injected, cc	Lambda	N-Hexane Concentration, %
0.05	1.4250	99.630	21.5	-4.249	0.370
0.10	1.4250	99.630	43.0	-2.846	0.370
0.15	1.4250	99.630	64.5	-2.195	0.370
0.20	1.4250	99.630	86.0	-1.789	0.370
0.25	1.4250	99.630	107.5	-1.500	0.370
0.30	1.4250	99.630	129.0	-1.278	0.370
0.35	1.4250	99.630	150.5	-1.099	0.370
0.40	1.4250	99.630	172.0	-0.949	0.370
0.45	1.4230	95.563	193.5	-0.820	4.437
0.50	1.4120	73.197	215.0	-0.707	26.803
0.55	1.4088	66.691	236.5	-0.607	33.309
0.60	1.4049	58.761	258.0	-0.516	41.239
0.65	1.4029	54.695	279.5	-0.434	45.305
0.70	1.4021	53.068	301.0	-0.359	46.932
0.75	1.4009	50.628	322.5	-0.289	49.372
0.80	1.4004	49.612	344.0	-0.224	50.388
0.85	1.4044	57.745	365.5	-0.163	42.255
0.90	1.4100	69.131	387.0	-0.105	30.869
0.95	1.4184	86.210	408.5	-0.051	13.790
1.00	1.4215	92.514	430.0	0.000	7.486
1.05	1.4231	95.767	451.5	0.049	4.233
1.10	1.4237	96.987	473.0	0.095	3.013
1.15	1.4240	97.597	494.5	0.140	2.403
1.20	1.4241	97.800	516.0	0.183	2.200
1.25	1.4241	97.800	537.5	0.224	2.200
1.30	1.4241	97.800	559.0	0.263	2.200
1.35	1.4241	97.800	580.5	0.301	2.200
1.40	1.4241	97.800	602.0	0.338	2.200
1.45	1.4241	97.800	623.5	0.374	2.200
1.50	1.4241	97.800	645.0	0.408	2.200
1.55	1.4241	97.800	666.5	0.442	2.200
1.60	1.4241	97.800	688.0	0.474	2.200
1.65	1.4242	98.003	709.5	0.506	1.997
1.70	1.4242	98.003	731.0	0.537	1.997
1.75	1.4244	98.410	752.5	0.567	1.590
1.80	1.4244	98.410	774.0	0.596	1.590
1.85	1.4244	98.410	795.5	0.625	1.590
1.90	1.4244	98.410	817.0	0.653	1.590
1.95	1.4244	98.410	838.5	0.680	1.590
2.00	1.4245	98.613	860.0	0.707	1.387

Table C-30: Experimental Effluent Concentration Data for Run 30

Pore Volume Injected	Refractive Index	Cyclohexane Concentration, %	Cumulative P.V. Injected, cc	Lambda	N-Hexane Concentration, %
0.05	1.4250	99.630	21.5	-4.249	0.370
0.10	1.4250	99.630	43.0	-2.846	0.370
0.15	1.4250	99.630	64.5	-2.195	0.370
0.20	1.4250	99.630	86.0	-1.789	0.370
0.25	1.4250	99.630	107.5	-1.500	0.370
0.30	1.4250	99.630	129.0	-1.278	0.370
0.35	1.4250	99.630	150.5	-1.099	0.370
0.40	1.4250	99.630	172.0	-0.949	0.370
0.45	1.4235	96.580	193.5	-0.820	3.420
0.50	1.4179	85.194	215.0	-0.707	14.806
0.55	1.4081	65.268	236.5	-0.607	34.732
0.60	1.4067	62.421	258.0	-0.516	37.579
0.65	1.4020	52.865	279.5	-0.434	47.135
0.70	1.3995	47.782	301.0	-0.359	52.218
0.75	1.3940	36.599	322.5	-0.289	63.401
0.80	1.3915	31.516	344.0	-0.224	68.484
0.85	1.3899	28.262	365.5	-0.163	71.738
0.90	1.3905	29.482	387.0	-0.105	70.518
0.95	1.3945	37.615	408.5	-0.051	62.385
1.00	1.4021	53.068	430.0	0.000	46.932
1.05	1.4113	71.774	451.5	0.049	28.226
1.10	1.4201	89.667	473.0	0.095	10.333
1.15	1.4225	94.547	494.5	0.140	5.453
1.20	1.4225	94.547	516.0	0.183	5.453
1.25	1.4225	94.547	537.5	0.224	5.453
1.30	1.4229	95.360	559.0	0.263	4.640
1.35	1.4231	95.767	580.5	0.301	4.233
1.40	1.4220	93.530	602.0	0.338	6.470
1.45	1.4225	94.547	623.5	0.374	5.453
1.50	1.4225	94.547	645.0	0.408	5.453
1.55	1.4232	95.970	666.5	0.442	4.030
1.60	1.4240	97.597	688.0	0.474	2.403
1.65	1.4248	99.223	709.5	0.506	0.777
1.70	1.4250	99.630	731.0	0.537	0.370
1.75	1.4250	99.630	752.5	0.567	0.370
1.80	1.4250	99.630	774.0	0.596	0.370
1.85	1.4250	99.630	795.5	0.625	0.370
1.90	1.4250	99.630	817.0	0.653	0.370
1.95	1.4250	99.630	838.5	0.680	0.370
2.00	1.4250	99.630	860.0	0.707	0.370

Table C-31: Experimental Effluent Concentration Data for Run 31

Pore Volume Injected	Refractive Index	10% Brine Concentration, %	Cumulative P.V. Injected, cc	Lambda	2% Brine Concentration, %
0.05	1.3362	0.000	20.0	-4.249	100.000
0.10	1.3362	0.000	40.0	-2.846	100.000
0.15	1.3362	0.000	60.0	-2.195	100.000
0.20	1.3362	0.000	80.0	-1.789	100.000
0.25	1.3362	0.000	100.0	-1.500	100.000
0.30	1.3362	0.000	120.0	-1.278	100.000
0.35	1.3362	0.000	140.0	-1.099	100.000
0.40	1.3362	0.000	160.0	-0.949	100.000
0.45	1.3362	0.000	180.0	-0.820	100.000
0.50	1.3362	0.000	200.0	-0.707	100.000
0.55	1.3362	0.000	220.0	-0.607	100.000
0.60	1.3362	0.000	240.0	-0.516	100.000
0.65	1.3362	0.000	260.0	-0.434	100.000
0.70	1.3362	0.000	280.0	-0.359	100.000
0.75	1.3362	0.000	300.0	-0.289	100.000
0.80	1.3372	8.295	320.0	-0.224	91.705
0.85	1.3414	43.136	340.0	-0.163	56.864
0.90	1.3455	77.146	360.0	-0.105	22.854
0.95	1.347	89.589	380.0	-0.051	10.411
1.00	1.3476	94.567	400.0	0.000	5.433
1.05	1.3478	96.226	420.0	0.049	3.774
1.10	1.3481	98.714	440.0	0.095	1.286
1.15	1.3482	99.544	460.0	0.140	0.456
1.20	1.3482	99.544	480.0	0.183	0.456
1.25	1.3482	99.544	500.0	0.224	0.456
1.30	1.3482	99.544	520.0	0.263	0.456
1.35	1.3482	99.544	540.0	0.301	0.456
1.40	1.3482	99.544	560.0	0.338	0.456
1.45	1.3482	99.544	580.0	0.374	0.456
1.50	1.3482	99.544	600.0	0.408	0.456
1.55	1.3482	99.544	620.0	0.442	0.456
1.60	1.3482	99.544	640.0	0.474	0.456
1.65	1.3482	99.544	660.0	0.506	0.456
1.70	1.3482	99.544	680.0	0.537	0.456
1.75	1.3482	99.544	700.0	0.567	0.456
1.80	1.3482	99.544	720.0	0.596	0.456
1.85	1.3482	99.544	740.0	0.625	0.456
1.90	1.3482	99.544	760.0	0.653	0.456
1.95	1.3482	99.544	780.0	0.680	0.456
2.00	1.3482	99.544	800.0	0.707	0.456

Table C-32: Experimental Effluent Concentration Data for Run 32

Pore Volume Injected	Refractive Index	10% Brine Concentration, %	Cumulative P.V. Injected, cc	Lambda	2% Brine Concentration, %
0.05	1.3482	99.544	20.0	-4.249	0.456
0.10	1.3482	99.544	40.0	-2.846	0.456
0.15	1.3482	99.544	60.0	-2.195	0.456
0.20	1.3482	99.544	80.0	-1.789	0.456
0.25	1.3482	99.544	100.0	-1.500	0.456
0.30	1.3482	99.544	120.0	-1.278	0.456
0.35	1.3482	99.544	140.0	-1.099	0.456
0.40	1.3482	99.544	160.0	-0.949	0.456
0.45	1.3482	99.544	180.0	-0.820	0.456
0.50	1.3482	99.544	200.0	-0.707	0.456
0.55	1.3482	99.544	220.0	-0.607	0.456
0.60	1.3482	99.544	240.0	-0.516	0.456
0.65	1.3482	99.544	260.0	-0.434	0.456
0.70	1.3482	99.544	280.0	-0.359	0.456
0.75	1.3475	93.737	300.0	-0.289	6.263
0.80	1.3435	60.556	320.0	-0.224	39.444
0.85	1.3415	43.965	340.0	-0.163	56.035
0.90	1.3395	27.375	360.0	-0.105	72.625
0.95	1.3385	19.079	380.0	-0.051	80.921
1.00	1.3375	10.784	400.0	0.000	89.216
1.05	1.3375	10.784	420.0	0.049	89.216
1.10	1.3372	8.295	440.0	0.095	91.705
1.15	1.3369	5.807	460.0	0.140	94.193
1.20	1.3369	5.807	480.0	0.183	94.193
1.25	1.3365	2.489	500.0	0.224	97.511
1.30	1.3365	2.489	520.0	0.263	97.511
1.35	1.3365	2.489	540.0	0.301	97.511
1.40	1.3365	2.489	560.0	0.338	97.511
1.45	1.3362	0.000	580.0	0.374	100.000
1.50	1.3362	0.000	600.0	0.408	100.000
1.55	1.3362	0.000	620.0	0.442	100.000
1.60	1.3362	0.000	640.0	0.474	100.000
1.65	1.3362	0.000	660.0	0.506	100.000
1.70	1.3362	0.000	680.0	0.537	100.000
1.75	1.3362	0.000	700.0	0.567	100.000
1.80	1.3362	0.000	720.0	0.596	100.000
1.85	1.3362	0.000	740.0	0.625	100.000
1.90	1.3362	0.000	760.0	0.653	100.000
1.95	1.3362	0.000	780.0	0.680	100.000
2.00	1.3362	0.000	800.0	0.707	100.000

Table C-31.1: Effluent Data for Plot B-31.1

Pore Volume Injected	Refractive Index	10% Brine Concentration, %	Cumulative P.V. Injected, cc	Lambda	2% Brine Concentration, %
0.05	1.3362	0.000	20.0	-4.249	100.000
0.10	1.3362	0.000	40.0	-2.846	100.000
0.15	1.3362	0.000	60.0	-2.195	100.000
0.20	1.3362	0.000	80.0	-1.789	100.000
0.25	1.3362	0.000	100.0	-1.500	100.000
0.30	1.3362	0.000	120.0	-1.278	100.000
0.35	1.3362	0.000	140.0	-1.099	100.000
0.40	1.3362	0.000	160.0	-0.949	100.000
0.45	1.3362	0.000	180.0	-0.820	100.000
0.50	1.3362	0.000	200.0	-0.707	100.000
0.55	1.3362	0.000	220.0	-0.607	100.000
0.60	1.3362	0.000	240.0	-0.516	100.000
0.65	1.3362	0.000	260.0	-0.434	100.000
0.70	1.3362	0.000	280.0	-0.359	100.000
0.75	1.3362	0.000	300.0	-0.289	100.000
0.80	1.3372	8.295	320.0	-0.224	91.700
0.85	1.3414	43.140	340.0	-0.163	56.860
0.90	1.3455	77.150	360.0	-0.105	22.850
0.95	1.3470	89.590	380.0	-0.051	10.410
1.00	1.3476	94.570	400.0	0.000	5.433
1.05	1.3478	96.230	420.0	0.049	3.774
1.10	1.3481	98.710	440.0	0.095	1.286
1.15	1.3482	99.540	460.0	0.140	0.456

Table C-32.1: Effluent Data for Plot B-32.1

Pore Volume Injected	Refractive Index	10% Brine Concentration, %	Cumulative P.V. Injected, cc	Lambda	2% Brine Concentration, %
0.75	1.3475	93.740	300.0	-0.289	6.263
0.80	1.3435	60.560	320.0	-0.224	39.440
0.85	1.3415	43.970	340.0	-0.163	56.030
0.90	1.3395	27.370	360.0	-0.105	72.630
0.95	1.3385	19.080	380.0	-0.051	80.920
1.00	1.3375	10.780	400.0	0.000	89.220

Table C-33: Experimental Effluent Concentration Data for Run 33

Pore Volume Injected	Refractive Index	10% Brine Concentration, %	Cumulative P.V. Injected, cc	Lambda	2% Brine Concentration, %
0.05	1.3362	0.000	20.0	-4.249	100.000
0.10	1.3362	0.000	40.0	-2.846	100.000
0.15	1.3362	0.000	60.0	-2.195	100.000
0.20	1.3362	0.000	80.0	-1.789	100.000
0.25	1.3362	0.000	100.0	-1.500	100.000
0.30	1.3362	0.000	120.0	-1.278	100.000
0.35	1.3362	0.000	140.0	-1.099	100.000
0.40	1.3362	0.000	160.0	-0.949	100.000
0.45	1.3362	0.000	180.0	-0.820	100.000
0.50	1.3362	0.000	200.0	-0.707	100.000
0.55	1.3362	0.000	220.0	-0.607	100.000
0.60	1.3362	0.000	240.0	-0.516	100.000
0.65	1.3362	0.000	260.0	-0.434	100.000
0.70	1.3362	0.000	280.0	-0.359	100.000
0.75	1.3362	0.000	300.0	-0.289	100.000
0.80	1.3362	0.000	320.0	-0.224	100.000
0.85	1.3362	0.000	340.0	-0.163	100.000
0.90	1.3362	0.000	360.0	-0.105	100.000
0.95	1.3372	8.295	380.0	-0.051	91.705
1.00	1.3432	58.067	400.0	0.000	41.933
1.05	1.3469	88.760	420.0	0.049	11.240
1.10	1.3465	85.442	440.0	0.095	14.558
1.15	1.343	56.408	460.0	0.140	43.592
1.20	1.3415	43.965	480.0	0.183	56.035
1.25	1.34	31.522	500.0	0.224	68.478
1.30	1.3385	19.079	520.0	0.263	80.921
1.35	1.3374	9.954	540.0	0.301	90.046
1.40	1.337	6.636	560.0	0.338	93.364
1.45	1.3368	4.977	580.0	0.374	95.023
1.50	1.3365	2.489	600.0	0.408	97.511
1.55	1.3365	2.489	620.0	0.442	97.511
1.60	1.3365	2.489	640.0	0.474	97.511
1.65	1.3365	2.489	660.0	0.506	97.511
1.70	1.3365	2.489	680.0	0.537	97.511
1.75	1.3365	2.489	700.0	0.567	97.511
1.80	1.3365	2.489	720.0	0.596	97.511
1.85	1.3365	2.489	740.0	0.625	97.511
1.90	1.3365	2.489	760.0	0.653	97.511
1.95	1.3365	2.489	780.0	0.680	97.511
2.00	1.3365	2.489	800.0	0.707	97.511

Table C-34: Experimental Effluent Concentration Data for Run 34

Pore Volume Injected	Refractive Index	10% Brine Concentration, %	Cumulative P.V. Injected, cc	Lambda	2% Brine Concentration, %
0.05	1.3362	0.000	20.0	-4.249	100.000
0.10	1.3362	0.000	40.0	-2.846	100.000
0.15	1.3362	0.000	60.0	-2.195	100.000
0.20	1.3362	0.000	80.0	-1.789	100.000
0.25	1.3362	0.000	100.0	-1.500	100.000
0.30	1.3362	0.000	120.0	-1.278	100.000
0.35	1.3362	0.000	140.0	-1.099	100.000
0.40	1.3362	0.000	160.0	-0.949	100.000
0.45	1.3362	0.000	180.0	-0.820	100.000
0.50	1.3362	0.000	200.0	-0.707	100.000
0.55	1.3362	0.000	220.0	-0.607	100.000
0.60	1.3362	0.000	240.0	-0.516	100.000
0.65	1.3362	0.000	260.0	-0.434	100.000
0.70	1.3362	0.000	280.0	-0.359	100.000
0.75	1.3362	0.000	300.0	-0.289	100.000
0.80	1.3362	0.000	320.0	-0.224	100.000
0.85	1.3362	0.000	340.0	-0.163	100.000
0.90	1.3362	0.000	360.0	-0.105	100.000
0.95	1.338	14.932	380.0	-0.051	85.068
1.00	1.3445	68.851	400.0	0.000	31.149
1.05	1.347	89.589	420.0	0.049	10.411
1.10	1.3475	93.737	440.0	0.095	6.263
1.15	1.3476	94.567	460.0	0.140	5.433
1.20	1.3445	68.851	480.0	0.183	31.149
1.25	1.3425	52.260	500.0	0.224	47.740
1.30	1.3405	35.670	520.0	0.263	64.330
1.35	1.3392	24.886	540.0	0.301	75.114
1.40	1.3382	16.591	560.0	0.338	83.409
1.45	1.3375	10.784	580.0	0.374	89.216
1.50	1.3374	9.954	600.0	0.408	90.046
1.55	1.3371	7.466	620.0	0.442	92.534
1.60	1.337	6.636	640.0	0.474	93.364
1.65	1.3368	4.977	660.0	0.506	95.023
1.70	1.3368	4.977	680.0	0.537	95.023
1.75	1.3366	3.318	700.0	0.567	96.682
1.80	1.3364	1.659	720.0	0.596	98.341
1.85	1.3364	1.659	740.0	0.625	98.341
1.90	1.3362	0.000	760.0	0.653	100.000
1.95	1.3362	0.000	780.0	0.680	100.000
2.00	1.3362	0.000	800.0	0.707	100.000

Table C-35: Experimental Effluent Concentration Data for Run 35

Pore Volume Injected	Refractive Index	10% Brine Concentration, %	Cumulative P.V. Injected, cc	Lambda	2% Brine Concentration, %
0.05	1.3482	99.544	20.0	-4.249	0.456
0.10	1.3482	99.544	40.0	-2.846	0.456
0.15	1.3482	99.544	60.0	-2.195	0.456
0.20	1.3482	99.544	80.0	-1.789	0.456
0.25	1.3482	99.544	100.0	-1.500	0.456
0.30	1.3482	99.544	120.0	-1.278	0.456
0.35	1.3482	99.544	140.0	-1.099	0.456
0.40	1.3482	99.544	160.0	-0.949	0.456
0.45	1.3482	99.544	180.0	-0.820	0.456
0.50	1.3482	99.544	200.0	-0.707	0.456
0.55	1.3482	99.544	220.0	-0.607	0.456
0.60	1.3482	99.544	240.0	-0.516	0.456
0.65	1.3482	99.544	260.0	-0.434	0.456
0.70	1.3482	99.544	280.0	-0.359	0.456
0.75	1.3482	99.544	300.0	-0.289	0.456
0.80	1.3482	99.544	320.0	-0.224	0.456
0.85	1.3479	97.055	340.0	-0.163	2.945
0.90	1.3465	85.442	360.0	-0.105	14.558
0.95	1.3426	53.090	380.0	-0.051	46.910
1.00	1.34	31.522	400.0	0.000	68.478
1.05	1.3386	19.909	420.0	0.049	80.091
1.10	1.3398	29.863	440.0	0.095	70.137
1.15	1.3438	63.044	460.0	0.140	36.956
1.20	1.3464	84.612	480.0	0.183	15.388
1.25	1.3475	93.737	500.0	0.224	6.263
1.30	1.3479	97.055	520.0	0.263	2.945
1.35	1.348	97.885	540.0	0.301	2.115
1.40	1.348	97.885	560.0	0.338	2.115
1.45	1.348	97.885	580.0	0.374	2.115
1.50	1.3482	99.544	600.0	0.408	0.456
1.55	1.3482	99.544	620.0	0.442	0.456
1.60	1.3482	99.544	640.0	0.474	0.456
1.65	1.3482	99.544	660.0	0.506	0.456
1.70	1.3482	99.544	680.0	0.537	0.456
1.75	1.3482	99.544	700.0	0.567	0.456
1.80	1.3482	99.544	720.0	0.596	0.456
1.85	1.3482	99.544	740.0	0.625	0.456
1.90	1.3482	99.544	760.0	0.653	0.456
1.95	1.3482	99.544	780.0	0.680	0.456
2.00	1.3482	99.544	800.0	0.707	0.456

Table C-36: Experimental Effluent Concentration Data for Run 36

Pore Volume Injected	Refractive Index	10% Brine Concentration, %	Cumulative P.V. Injected, cc	Lambda	2% Brine Concentration, %
0.05	1.3482	99.544	20.0	-4.249	0.456
0.10	1.3482	99.544	40.0	-2.846	0.456
0.15	1.3482	99.544	60.0	-2.195	0.456
0.20	1.3482	99.544	80.0	-1.789	0.456
0.25	1.3482	99.544	100.0	-1.500	0.456
0.30	1.3482	99.544	120.0	-1.278	0.456
0.35	1.3482	99.544	140.0	-1.099	0.456
0.40	1.3482	99.544	160.0	-0.949	0.456
0.45	1.3482	99.544	180.0	-0.820	0.456
0.50	1.3482	99.544	200.0	-0.707	0.456
0.55	1.3482	99.544	220.0	-0.607	0.456
0.60	1.3482	99.544	240.0	-0.516	0.456
0.65	1.3482	99.544	260.0	-0.434	0.456
0.70	1.3482	99.544	280.0	-0.359	0.456
0.75	1.3482	99.544	300.0	-0.289	0.456
0.80	1.3482	99.544	320.0	-0.224	0.456
0.85	1.3475	93.737	340.0	-0.163	6.263
0.90	1.3436	61.385	360.0	-0.105	38.615
0.95	1.34	31.522	380.0	-0.051	68.478
1.00	1.3388	21.568	400.0	0.000	78.432
1.05	1.3382	16.591	420.0	0.049	83.409
1.10	1.3376	11.613	440.0	0.095	88.387
1.15	1.3379	14.102	460.0	0.140	85.898
1.20	1.3412	41.477	480.0	0.183	58.523
1.25	1.3449	72.169	500.0	0.224	27.831
1.30	1.3466	86.271	520.0	0.263	13.729
1.35	1.3472	91.248	540.0	0.301	8.752
1.40	1.3476	94.567	560.0	0.338	5.433
1.45	1.3478	96.226	580.0	0.374	3.774
1.50	1.348	97.885	600.0	0.408	2.115
1.55	1.348	97.885	620.0	0.442	2.115
1.60	1.3481	98.714	640.0	0.474	1.286
1.65	1.3482	99.544	660.0	0.506	0.456
1.70	1.3482	99.544	680.0	0.537	0.456
1.75	1.3482	99.544	700.0	0.567	0.456
1.80	1.3482	99.544	720.0	0.596	0.456
1.85	1.3482	99.544	740.0	0.625	0.456
1.90	1.3482	99.544	760.0	0.653	0.456
1.95	1.3482	99.544	780.0	0.680	0.456
2.00	1.3482	99.544	800.0	0.707	0.456

Table C-36R: Experimental Effluent Concentration Data for Run 36R

Pore Volume Injected	Refractive Index	10% Brine Concentration, %	Cumulative P.V. Injected, cc	Lambda	2% Brine Concentration, %
0.05	1.3482	99.544	20.0	-4.249	0.456
0.10	1.3482	99.544	40.0	-2.846	0.456
0.15	1.3482	99.544	60.0	-2.195	0.456
0.20	1.3482	99.544	80.0	-1.789	0.456
0.25	1.3482	99.544	100.0	-1.500	0.456
0.30	1.3482	99.544	120.0	-1.278	0.456
0.35	1.3482	99.544	140.0	-1.099	0.456
0.40	1.3482	99.544	160.0	-0.949	0.456
0.45	1.3482	99.544	180.0	-0.820	0.456
0.50	1.3482	99.544	200.0	-0.707	0.456
0.55	1.3482	99.544	220.0	-0.607	0.456
0.60	1.3482	99.544	240.0	-0.516	0.456
0.65	1.3482	99.544	260.0	-0.434	0.456
0.70	1.3482	99.544	280.0	-0.359	0.456
0.75	1.3482	99.544	300.0	-0.289	0.456
0.80	1.348	97.885	320.0	-0.224	2.115
0.85	1.344	64.703	340.0	-0.163	35.297
0.90	1.3402	33.181	360.0	-0.105	66.819
0.95	1.339	23.227	380.0	-0.051	76.773
1.00	1.3384	18.250	400.0	0.000	81.750
1.05	1.3378	13.272	420.0	0.049	86.727
1.10	1.3375	10.784	440.0	0.095	89.216
1.15	1.3374	9.954	460.0	0.140	90.046
1.20	1.3379	14.102	480.0	0.183	85.898
1.25	1.3401	32.352	500.0	0.224	67.648
1.30	1.3439	63.874	520.0	0.263	36.126
1.35	1.346	81.294	540.0	0.301	18.706
1.40	1.3472	91.248	560.0	0.338	8.752
1.45	1.3477	95.396	580.0	0.374	4.604
1.50	1.3479	97.055	600.0	0.408	2.945
1.55	1.348	97.885	620.0	0.442	2.115
1.60	1.3481	98.714	640.0	0.474	1.286
1.65	1.3481	98.714	660.0	0.506	1.286
1.70	1.3482	99.544	680.0	0.537	0.456
1.75	1.3482	99.544	700.0	0.567	0.456
1.80	1.3482	99.544	720.0	0.596	0.456
1.85	1.3482	99.544	740.0	0.625	0.456
1.90	1.3482	99.544	760.0	0.653	0.456
1.95	1.3482	99.544	780.0	0.680	0.456
2.00	1.3482	99.544	800.0	0.707	0.456